

# Diverse Functions of Astroglial Cells – The Role of Molecular Pathways Regulating Polarity

Dissertation

der Fakultät der Biologie

der Ludwig-Maximilian-Universität München



prepared at the Institute of Physiology, LMU München

and at the Institute of Stem Cell Research, Helmholtz Zentrum München

submitted by

Stefanie Robel

April 2010

## **Gutachter**

1. Prof. Dr. Benedikt Grothe (1. Votum informativum)
2. Prof. Dr. Hans Straka (2. Votum informativum)
3. Prof. Dr. Rainer Uhl (Disputation)
4. Prof. Dr. Angelika Böttger (Disputation)
5. Prof. Dr. Thomas Cremer (Umlauf)
6. Prof. Dr. George Boyan (Umlauf)
7. Prof Dr Magdalena Götz (Sondervotum)

**Die Arbeit wurde am 29.04.2010 eingereicht.**

**Die Disputation hat am 12.08.2010 stattgefunden.**

*Nichts ist verblüffender als die einfache Wahrheit, nichts ist exotischer als unsere Umwelt, nichts ist phantasievoller als die Sachlichkeit. Und nichts Sensationelleres gibt es in der Welt als die Zeit, in der man lebt.*

*E.E. Kisch*



# Content

<b>1</b>	<b><i>Abstract</i></b>	<b>1</b>
<b>2</b>	<b><i>Introduction</i></b>	<b>3</b>
2.1	<b>Neuroglial cells in the adult brain – A brief historical view about the term astroglia</b>	<b>3</b>
2.2	<b>Astrocyte subtypes</b>	<b>5</b>
2.2.1	Protoplasmic astrocytes of the gray matter	8
2.2.2	Fibrous astrocytes of the white matter	9
2.2.3	Subependymal zone stem cell astrocytes	10
2.3	<b>Diversity of astroglial functions</b>	<b>12</b>
2.3.1	Functions in the intact adult brain	12
2.3.2	Astrocytes respond to brain injury	13
2.3.3	Signaling after brain injury	16
2.4	<b>Polarity cues as candidates for defining astrocytic properties</b>	<b>33</b>
2.4.1	The astrocytic basal site is major part of the neurovascular unit	35
2.4.2	Small RhoGTPases at the apical side and after injury	43
<b>3</b>	<b><i>Aims of this study</i></b>	<b>47</b>
<b>4</b>	<b><i>Abbreviations</i></b>	<b>49</b>
<b>5</b>	<b><i>Material</i></b>	<b>55</b>
5.1.1	Equipment	55
<b>5.2</b>	<b>Consumables</b>	<b>56</b>
<b>5.3</b>	<b>Chemicals</b>	<b>57</b>
<b>5.4</b>	<b>Plasmids</b>	<b>61</b>
<b>5.5</b>	<b>Solutions and Media</b>	<b>61</b>
5.5.1	DNA preparation and genotyping PCR	61
5.5.2	tissue preparation	63
5.5.3	Immuno-histochemistry/ cytochemistry	65
5.5.4	Western blot	66
5.5.5	Electron microscopy	66
5.5.6	Cell culture media and supplements	68

---

<b>6</b>	<b>Methods</b>	<b>72</b>
<b>6.1</b>	<b>Animals</b>	<b>72</b>
6.1.1	Mouse strains	72
6.1.2	Genotyping of transgenic animals	73
6.1.3	Tamoxifen administration	78
6.1.4	Stereotactic operations	78
6.1.5	BrdU labeling	79
<b>6.2</b>	<b>Histology</b>	<b>80</b>
6.2.1	Immunohistochemistry	80
<b>6.3</b>	<b>Western Blot analysis</b>	<b>84</b>
6.3.1	Tissue lysis	84
6.3.2	Photometric quantification of protein amounts with Bicinchoninic acid	84
6.3.3	Sample preparation for Western gel loading	84
6.3.4	Western blot and signal detection	85
<b>6.4</b>	<b>Electron Microscopy</b>	<b>85</b>
<b>6.5</b>	<b>Cell Culture</b>	<b>87</b>
6.5.1	Primary astrocyte cultures and in vitro scratch wound assay	87
6.5.2	Tissue dissociation and culturing of primary astrocytes	87
6.5.3	Maintenance and splitting of the astrocyte culture	88
6.5.4	Transduction of astrocyte cultures with lentiviruses	88
6.5.5	In vitro scratch wound assay	88
6.5.6	Dissection and dissociation of adult mouse brains for culturing neurospheres from the SEZ	89
6.5.7	Dissection and dissociation of adult mouse brains for culturing neurospheres from the stab wound injury	90
6.5.8	Passaging Neurospheres	90
6.5.9	Paraformaldehyde fixation of cultured cells	90
6.5.10	Immunocytochemistry	91
<b>6.6</b>	<b>Virus production</b>	<b>92</b>
6.6.1	Viral vector design	92
6.6.2	DNA preparation for virus production (CsCl-Gradient)	93
6.6.3	Lentiviral preparations	96
<b>6.7</b>	<b>Data analysis</b>	<b>100</b>
6.7.1	Cell numbers per area and marker coexpression	100
6.7.2	Reorientation of centrosomes	100

---

6.7.3	Quantification of astrocyte protrusions	101
6.7.4	Analysis of the lesion size	101
<b>7</b>	<b>Results</b>	<b>103</b>
<b>7.1</b>	<b>The influence of <math>\beta</math>1-integrins on gray matter astrocytes</b>	<b>103</b>
7.1.1	Deletion of $\beta$ 1-integrin by the use of hGFAP-Cre causes partial reactive gliosis	103
7.1.2	Deletion of $\beta$ 1-integrin by Nex::Cre	110
7.1.3	Loss of $\beta$ 1-integrins leads to a secondary partial microglia activation	111
7.1.4	Could the gliosis phenotype be induced by non cell autonomous side effects of $\beta$ 1-integrin deletion?	116
7.1.5	The basement membrane is not primarily affected after loss of $\beta$ 1-integrins at postnatal stages	117
7.1.6	The astrocyte endfeet polarity is disturbed after deletion of $\beta$ 1-integrin	120
7.1.7	Reactive astrocytes in $\beta$ 1-integrin-deficient cortices do not proliferate or regain stem cell properties	120
<b>7.2</b>	<b>The influence of <math>\beta</math>1-integrins on astroglial-like stem cells</b>	<b>124</b>
7.2.1	$\beta$ 1-integrins are dispensable for the proliferation of adult SEZ stem cells	124
7.2.2	$\beta$ 1-integrins are important for neuroblast migration	125
<b>7.3</b>	<b>Polarity of astrocytes after brain injury</b>	<b>128</b>
7.3.1	Small RhoGTPases influence astrocyte polarization and migration in vitro	131
7.3.2	Astrocyte polarization upon injury leads to their subsequent migration in vitro	140
7.3.3	Conditional Cdc42 deletion influences morphology changes of astrocytes after cortical stab wound injury	142
7.3.4	Deletion of Cdc42 in virtually all astrocytes lead to an increased injury size after stab wound injury in vivo	145
7.3.5	Are astrocytes migrating after acute brain trauma in vivo?	146
<b>7.4</b>	<b>The influence of Cdc42 on astroglial-like stem cells and their progeny</b>	<b>150</b>
<b>8</b>	<b>Discussion</b>	<b>153</b>
<b>8.1</b>	<b><math>\beta</math>1-Integrin functions in astroglial cells</b>	<b>153</b>
<b>8.2</b>	<b><math>\beta</math>1-integrins in reactive gliosis</b>	<b>154</b>
<b>8.3</b>	<b>Deletion of <math>\beta</math>1-Integrins in astrocytes leads to polarity defects</b>	<b>156</b>
<b>8.4</b>	<b>Basement membrane defects occur only secondary to reactive gliosis phenotype</b>	<b>157</b>

---

<b>8.5</b>	<b>The BBB is not affected by loss of <math>\beta</math>1-Integrins from astrocytes at postnatal stages</b>	<b>158</b>
<b>8.6</b>	<b>Loss of b1-integrins caused misrouting of neuroblasts</b>	<b>159</b>
<b>8.7</b>	<b>Misrouted neuroblasts mature in the striatum after loss of <math>\beta</math>1-integrins</b>	<b>161</b>
<b>8.8</b>	<b>The role of polarity cues in astrocytes and their stem cell potential</b>	<b>162</b>
8.8.1	Basal polarity mediated by b1-integrins	162
8.8.2	Apical polarity mediated by Cdc42	164
<b>8.9</b>	<b>Polarity of astrocytes after injury and their dedifferentiation</b>	<b>165</b>
<b>8.10</b>	<b>The role of Cdc42 in astrocyte migration and wound healing</b>	<b>167</b>
<b>8.11</b>	<b>The impact of astrocytes for brain repair</b>	<b>168</b>
<b>9</b>	<b><i>References</i></b>	<b>171</b>
<b>10</b>	<b><i>Acknowledgments</i></b>	<b>189</b>
<b>11</b>	<b><i>Curriculum vitae</i></b>	<b>191</b>

# Figures

Figure 2-1 Drawing of “Nervenkitt” by Rudolf Virchow	5
Figure 2-2 Progenitor cells in the SVZ/ SEZ during ontogenesis	7
Figure 2-3 Gray and white matter astrocytes	9
Figure 2-4 Stem cell astrocytes of the subependymal zone	11
Figure 2-5 Changes in astrocytes after brain injury	15
Figure 2-6 Mitogen-activated protein kinase/ extracellular signal-regulated kinase cascade	22
Figure 2-7 Triggers and molecular regulators of reactive gliosis	27
Figure 2-8 The Cre/ loxP systems allows cell type specific gene deletion	30
Figure 2-9 Polarity of radial glia and adult neural stem cells	35
Figure 2-10 The neurovascular unit is characterized by the interplay of astrocytes, endothelial cells and neurons	36
Figure 2-11 Epithelial and astrocytic basement membranes contain distinct laminin isoforms	38
Figure 2-12 The dystrophin-associated glycoprotein complex at the blood-brain interface	39
Figure 2-13 The laminin receptors integrin, dystroglycan and Lutheran blood group glycoprotein	42
Figure 2-14 Regulation of small RhoGTPases by GAPs, GEFs and GDIs	43
Figure 6-1 Map of the <i>Cre-IRES-GFP</i> lentiviral construct	93
Figure 7-1 Western Blot analysis of $\beta 1$ -integrin protein levels	105
Figure 7-2 Gross analysis showed no differences in WT and $\beta 1^{-/-}$ cerebral cortex	107
Figure 7-3 Partial gliosis in the cerebral cortex of $\beta 1^{-/-}$ mice	109
Figure 7-4 Neuron specific deletion of the $\beta 1$ -integrin gene did not lead to gliosis	111
Figure 7-5 Microglia activation shortly after a stab wound injury	112
Figure 7-6 Iba1 positive microglia were not recombined by hGFAP-Cre	113
Figure 7-7 Microglia were activated after loss of $\beta 1$ -integrins	114
Figure 7-8 Microglia are proliferating in WT and in $\beta 1^{-/-}$ cerebral cortex	115
Figure 7-9 The blood-brain barrier is not impaired after deletion of $\beta 1$ -integrins	117
Figure 7-10 Basement membrane changes only at later stages in $\beta 1^{-/-}$ cortices	118
Figure 7-11 Analysis of the basement membrane at the ultrastructural level	119
Figure 7-12 Astrocyte endfeet polarity is disturbed after deletion of $\beta 1$ -integrin	121
Figure 7-13 Astrocytes do not re-enter the cell-cycle after loss of $\beta 1$ -integrins	123
Figure 7-14 Proliferation capacity of SEZ stem cells after deletion of $\beta 1$ -integrins	125
Figure 7-15 $\beta 1$ -integrins influence neuroblast migration	127
Figure 7-16 Astrocytes change their morphology after acute injury in vivo	129

---

<b>Figure 7-17 Astrocytes in vitro react to injury by polarization and migration</b>	<b>130</b>
<b>Figure 7-18 Cdc42 is re-localized after scratch wound in vitro</b>	<b>131</b>
<b>Figure 7-19 Conditional alleles for Cdc42, Rac1, and RhoA and lentiviral constructs</b>	<b>132</b>
<b>Figure 7-20 Loss of Cdc42 protein after deletion of the gene</b>	<b>133</b>
<b>Figure 7-21 Cdc42 is involved in establishment of astrocyte polarity after injury in vitro</b>	<b>135</b>
<b>Figure 7-22 The role of Rac1 after scratch wound injury in vitro</b>	<b>137</b>
<b>Figure 7-23 The role of RhoA after scratch wound injury in vitro</b>	<b>139</b>
<b>Figure 7-24 The role of Cdc42 for the reaction of astrocytes to injury in vivo</b>	<b>144</b>
<b>Figure 7-25 Consequences of Cdc42 deletion in virtually all astrocytes</b>	<b>146</b>
<b>Figure 7-26 Intravital imaging of astrocytes after an injury</b>	<b>149</b>
<b>Figure 7-27 The role of Cdc42 in SEZ stem cells and their progeny</b>	<b>151</b>

## Tables

<b>Table 2-1 Marker expression in neuroepithelial cells and various astrocyte subtypes</b>	<b>12</b>
<b>Table 2-2 Molecular changes in reactive astrocytes</b>	<b>16</b>
<b>Table 2-3 Pathways mediating certain components of reactive gliosis</b>	<b>31</b>
<b>Table 5-1 Equipment</b>	<b>56</b>
<b>Table 5-2 Consumables</b>	<b>57</b>
<b>Table 5-3 Chemicals</b>	<b>60</b>
<b>Table 5-4 Cell culture reagents</b>	<b>68</b>
<b>Table 6-1 Primer sequences for genotyping of transgenic animals</b>	<b>75</b>
<b>Table 6-2 PCR reactions</b>	<b>76</b>
<b>Table 6-3 Cycling conditions</b>	<b>77</b>
<b>Table 6-4 First antibodies immunohistochemistry</b>	<b>81</b>
<b>Table 6-5 Secondary antibodies immunohistochemistry</b>	<b>82</b>
<b>Table 6-6 First antibodies immunocytochemistry</b>	<b>91</b>
<b>Table 6-7 Secondary antibodies immunocytochemistry</b>	<b>91</b>



# 1 Abstract

Astrocytes perform many functions in the adult brain and even act as neural stem cells after brain injury (Buffo et al., 2008) or in regions where neurogenesis persists, e.g. in the subependymal zone of the lateral ventricle. The stem cell astrocytes possess an apicobasal polarity as they are coupled by adherens junctions to neighbouring ependymal cells and possess an apical membrane domain with CD133 and Par complex proteins and a basolateral membrane domain including contact of processes to the basement membrane (BM). This is notably different from parenchymal astrocytes that only have contacts to the BM under physiological conditions. The major underlying question is how differences between neural stem cells and 'normal' astrocytes are generated and how polarity mechanisms may be involved in generating this difference. Here, I set out to determine the role of BM contact and the Par complex for astrocyte function in the normal brain parenchyma as well as in the neurogenic niche.

First, I examined the influence of BM-mediated signaling by conditional deletion of  $\beta$ 1-integrin, one of the major BM receptors in the CNS. The use of specific Cre lines resulted in a loss of  $\beta$ 1-integrin protein only at postnatal stages either in both glia and neurons or specifically in neurons. Strikingly, only the former resulted in reactive gliosis, with the hallmarks of reactive astrocytes comprising astrocyte hypertrophy and upregulation of the intermediate filaments GFAP and Vimentin as well as pericellular components, such Tenascin-C and the 473HD proteoglycan. This reaction to the loss of  $\beta$ 1-integrin was further accompanied by non-cell autonomous activation of microglial cells. However, neither reactive astrocytes nor microglia divided, suggesting that the loss of  $\beta$ 1-integrin-mediated signaling is not sufficient to elicit proliferation of these cells. Interestingly, this partial reactive gliosis appeared in the absence of cell death and blood-brain barrier disturbances. As these effects did not appear after neuron-specific deletion of  $\beta$ 1-integrin, we conclude that  $\beta$ 1-integrin-mediated signaling in astrocytes is required to promote their acquisition of a mature, non-reactive state. Interestingly, neural stem cell astrocytes in the SEZ were not

affected in their proliferation and fate, suggesting that  $\beta$ 1-integrins are not involved in the regulation of these stem cell properties. However, loss of  $\beta$ 1-integrins interfered with the normal dedifferentiation of astrocytes into stem cells after brain injury.

Next, I examined the role of Cdc42, a key activator of the Par complex, but also a mediator of  $\beta$ 1-integrin signalling in adult stem cell astrocytes. Therefore, I genetically deleted this small RhoGTPase in astroglia at adult stages. In contrast to what has been observed during development, loss of Cdc42 had no influence on proliferation or fate of subependymal zone astrocytes. These effects on adult astroglia-like stem cells differ profoundly from effects on parenchymal astrocytes upon injury. Here, deletion of Cdc42 resulted in severe defects of astrocyte polarity as measured by centrosome reorientation and oriented process extension in the scratch assay in vitro. In vivo, astrocytes could still orient towards the injury site suggesting the existence of compensating signaling pathways. However, the increase of astrocyte numbers around the injury site was reduced. Impaired proliferation certainly contributes to this phenotype. Most importantly, loss of Cdc42 resulted in a significantly increased size of brain injury enlightening the importance of this pathway in the wound reaction towards brain injury. Conversely, no effects were seen by Cdc42 deletion in astrocytes in the absence of injury, suggesting that integrin-mediated signaling from the BM maintains the hallmarks of mature non-reactive astrocytes while Cdc42, most likely via activation of the Par complex, regulates polarity and dedifferentiation after injury.

Taken together, this work elucidated for the first time specific signaling pathways regulating the role of astrocytes as stem cells during wound reaction of the injured brain.

## 2 Introduction

Astrocytes are a class of cells comprising various different cell types with diverse functions. As the topic of this thesis is how the diversity of types and functions is influenced by polarity I will first introduce the term “astroglia”, relevant astrocyte types and their functions.

### 2.1 Neuroglial cells in the adult brain – A brief historical view about the term astroglia

For the most of the 19<sup>th</sup> century researchers argued about the organization of the nervous system. Two opposing concepts existed at this time: The reticularists thought of the nervous system as a large network of tissue, or reticulum, formed by the fused processes of nerve elements. The neuronists, on the other hand argued that the nervous system consisted of distinct elements (E. Clarke and O'Malley, 1996). In 1838 Theodore Schwann and Matthias Schleiden proposed that the cell was the basic functional unit of all living things. The cell theory was not, however, believed to apply to the nervous system, and it was not until the end of the 19<sup>th</sup> century that it became generally accepted that the brain, too, consisted of cells. The term and concept ‘neuroglia’ (Nervenkit) has been introduced by the pathologist Rudolf Virchow in a German medical journal in 1856 actually before the establishment of the cell concept and was therefore also rather addressing an interstitial substance (Figure 2-1):

*“...According to my investigations, the ependyma [of the cerebral ventricles] consists not only of an epithelium, but essentially a layer of connective tissue covered with epithelium. Although it can be separated without difficulty from the surface, yet it does not constitute an isolated membrane...but only a layer of interstitial connective tissue of the brain substance which is prominent on the surface. This connective substance, which is in the brain, the spinal cord, and the special sense nerves, is a kind of glue (neuroglia) in which the nervous elements are embedded.”* (Virchow, 1856; Kettenmann and Ransom, 2005)

When Virchow gave a lecture in 1858 he mentioned that neuroglia contains a certain number of cellular elements, but was not referring to a “glial cell” yet.

Rather, Heinrich Müller's Müller Cells in the retina were the first depicted glial cells and soon after Otto Deiters described stellate cells in the cortical white and gray matter as component parts of the connective tissue. At the end of the 19<sup>th</sup> century neuroglia could be further classified into astrocytes, oligodendrocytes and microglia by the use of different silver staining methods developed by Camillo Golgi, Santiago Ramón y Cajal, Carl Weigert and Pío del Río Hortega on the basis of their morphology (Somjen, 1988).

Finally, the term astrocyte was coined by Michael von Lenhossek in 1893 to refer to star-shaped neuroglial cells:

*"...Astrocytes are the small elements, which form the supportive system of the spinal cord. They are star shaped and indeed no other comparison describes their form so clearly. While the term spider cell introduced by Jastrowitz has become popular and gives a proper impression of the cells, one should regard Gierke's note, namely that nobody has seen a spider with so many feet as these cells have processes."* (Lenhossék, 1893; Kettenmann and Ransom, 2005).

Although the human brain contains 3 times more astroglial than nerve cells the stigma of being just brain glue stuck to these cells and astrocytes were regarded as passive participants as they are not electrically excitable as neurons. However, in the late 1980s it has been shown that astrocytes express voltage-gated channels and neurotransmitter receptors pointing to a participation of these cells in intercellular communication (for review see Ritchie, 1992; Oh, 1997; Kettenmann and Ransom, 2005). In recent years, exciting discoveries unraveling the miscellaneous functions, including the control of synapse formation and function, as well as the regulation of the vascular tone and their role as adult neural stem cells (NSCs) led to a decisive rethinking about astroglial cells.

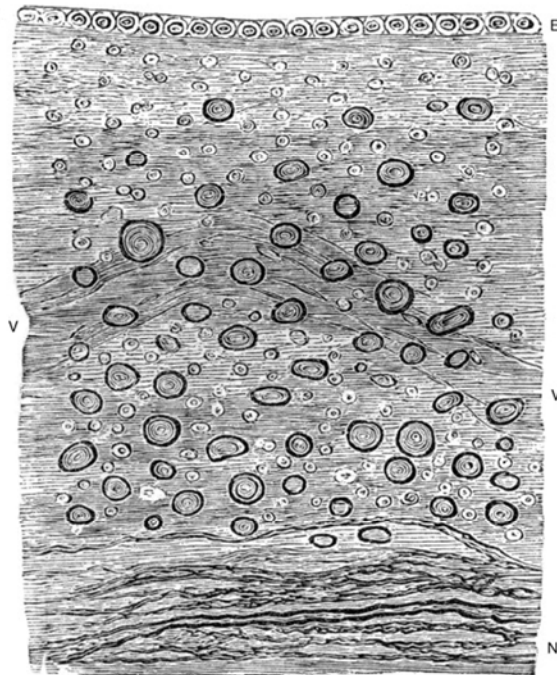


**Figure 2-1 Drawing of “Nervenkitt” by Rudolf Virchow**

**Between Ependyma and nerve fibers “the free portion of the neuroglia with numerous connective tissue corpuscles and nuclei” is illustrated. E ependymal epithelium, V blood vessel, N nerve fibers (Virchow, 1858).**

## 2.2 Astrocyte subtypes

The term astrocyte is an umbrella term for a heterogeneous population of cells that are highly adapted to their local environment and to the developmental stage. During development radial glia (RG) function not only as a scaffold for neuroblast migration, but are indeed progenitor cells giving rise to neurons and glial cells (Figure 2-2 and Malatesta et al., 2000). In the adult brain various astrocyte subtypes have been described comprising the more familiar protoplasmic astrocytes of the gray matter (Figure 2-3 A) and the fibrous astrocytes of the white matter (Figure 2-3 B), but also the bipolar shaped stem cell astrocytes at the lateral wall of the lateral ventricle (Figure 2-4 A, B) that show strong similarities to RG, the radial astrocytes of the retina and cerebellum, the velate astrocytes with their processes ensheathing cerebellar glomeruli (Chan-Palay and Palay, 1972) or dendritic segments and

periglomerular cells in the olfactory bulb (Valverde and Lopez-Mascaraque, 1991), and the interlaminar astrocytes that have a long process that projects through several cortical layers in primates (Oberheim et al., 2009). These types of astrocytes do not only differ in their morphological appearance and territorial organization across brain regions and species but also in their marker expression (see Table 2-1) and functional properties (for an overview see Kettenmann and Ransom, 2005). In the cerebral cortex astrocytes seem to have various sources of origin including RG and glial restricted progenitors in the subventricular zone (SVZ) and within the parenchyma. Interestingly, it has also been suggested that some progenitors could be generated directly from neuroepithelial cells, which are the progenitors of RG (Figure 2-2 and Levison et al., 1993; Levison and Goldman, 1993; Hartfuss et al., 2001). Recently, NG2-positive glia or polydendrocytes, a fourth glial cell type besides the well known astrocytes, oligodendrocytes and microglia, came into focus as glial progenitors. They have intriguingly been demonstrated to be a source of exclusively ventral gray matter astrocytes, although otherwise it is entirely unclear how the differences between astrocyte subtypes are generated and whether a certain origin is associated with a defined astrocytic morphology or function. As postnatal development proceeds radial glia cells transform into ependymal cells and type B stem cell astrocytes that can give rise to neurons, oligodendrocytes and astrocytes throughout adulthood (Figure 2-2). Again, it is still unsolved, which signals allow this particular astrocytic subpopulation to escape maturation and keep their stem cell potential throughout adulthood.

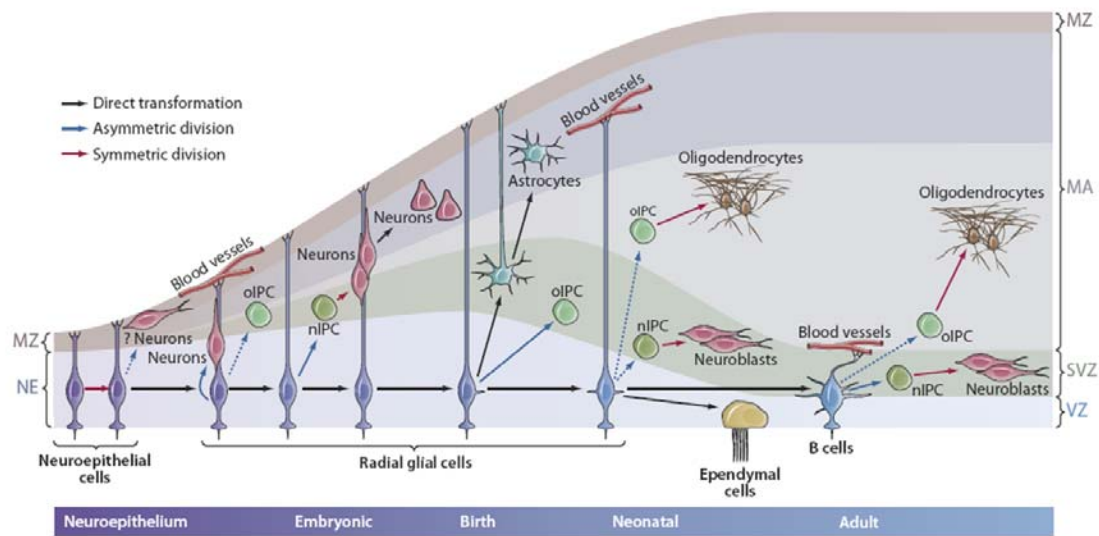


Figure 2-2 Progenitor cells in the SVZ/ SEZ during ontogenesis

Neuroepithelial cells in early development divide symmetrically to generate more neuroepithelial cells, some may also generate early neurons. As embryogenesis proceeds neuroepithelial cells convert into radial glial (RG) cells. RG divide asymmetrically to generate neurons directly or indirectly through intermediate progenitor cells/basal progenitors (nIPCs). Radial glia have an apical-basal polarity: apically (down), RG contact the ventricle, where they project a single primary cilium; basally (up), RG contact the meninges, basal lamina, and blood vessels. At the end of embryonic development, most RG begin to detach from the apical side and convert into astrocytes. Production of astrocytes may also include some IPCs (not illustrated here). A subpopulation of RG retains apical contact and continues functioning as NSCs in the neonate. These neonatal RG continue to generate neurons; some convert into ependymal cells, whereas others convert into adult SVZ astrocytes (type B cells) that continue to function as NSCs in the adult. B cells maintain an epithelial organization with apical contact at the ventricle and basal endings in blood vessels. B cells continue to generate neurons and oligodendrocytes. Neither the generation of oligodendrocytes via oIPCs has been finally proven, nor the generation of oligodendrocytes from adult NSCs in vivo (taken from A. Kriegstein and A. Alvarez-Buylla, 2009).

IPC intermediate progenitor cell, MA mantle, MZ marginal zone, NE neuroepithelium, nIPC neurogenic progenitor cell, oIPC oligodendrocytic progenitor cell, RG radial glia, SVZ subventricular zone, VZ ventricular zone

### **2.2.1 Protoplasmic astrocytes of the gray matter**

Protoplasmic astrocytes are scattered through all layers of the cortical gray matter and throughout the brain parenchyma. Rodent gray matter astrocytes have three to four main processes emanating more or less radially from the cell body and extend thousands of finer branches resulting in a high surface to volume ratio (Figure 2-3 A). Although the volume of astroglia accounts for only 10% to 20% of the total gray matter volume, astrocyte processes contact most of the available neuronal surfaces (Volterra et al., 2002). Gray matter astrocytes extend two types of processes: fine perisynaptic processes covering synapses and large diameter vascular endfeet that are closely ensheathing blood vessels (Iadecola and Nedergaard, 2007). These astrocytes have a high density, but show a surprisingly low overlap of less than 5% and thus occupy separate anatomical domains (Bushong et al., 2002; Oberheim et al., 2008). At the sites of contact protoplasmic astrocytes are interconnected with each other through gap junctions. Gap junctions are distributed evenly along astrocytic processes and therefore do not only couple neighboring cells, but also neighboring processes derived from the same cell minimizing the differences between individual processes by mediating the sharing of all molecules with molecular weights of less than 1000 kDa (Nedergaard et al., 2003). Fascinatingly, the glia-to-neuron index, which is largely determined by the number of protoplasmic astrocytes, increases as a function of brain size. Indeed, the human brain has a higher glia-to-neuron ratio than most other species although the astrocyte size disproportionally increased from rodents to humans pointing to the intriguing hypothesis that enlargement of the astroglial domain and glial numbers are associated with an increase in intellectual capacity during phylogeny (Oberheim et al., 2006; Oberheim et al., 2009).

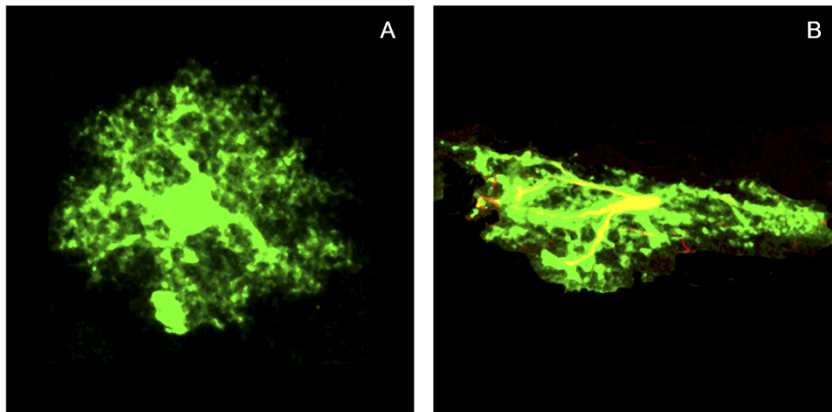


**Figure 2-3 Gray and white matter astrocytes**

**Astrocytes of the gray (A) and white matter (B) are labeled with green fluorescent protein (green). White matter astrocytes are additionally positive for GFAP (red).**

### **2.2.2 Fibrous astrocytes of the white matter**

Fibrous astrocytes are found in white matter tracts, in optic nerve, and in the nerve fiber layer of the mammalian vascularized retinae. They are less complex than protoplasmic astrocytes extending straighter and less branched fibers that run frequently in parallel to nerve fibers (Figure 2-3 B). The surface to volume ratio is less pronounced than in gray matter astrocytes. Often their cell bodies lie in rows between axon bundles. They are not organized in domains; instead processes of adjacent astrocytes intermingle and overlap frequently, although the cells are found equidistant from one another. The less complex appearance and relative uniformity of fibrous astrocytes points to a mainly supportive function (for review see Kettenmann and Ransom, 2005; Oberheim et al., 2006). Nevertheless, white matter astrocyte processes have been shown to contact the nodes of Ranvier where they play a role in signal transduction (D. D. Wang and Bordey, 2008). In adult rodents fibrous astrocytes are characterized by high expression levels of the intermediate filament glial fibrillary acidic protein (GFAP), whereas GFAP protein is not detected in most astrocytes in the brain parenchyma or only to a low extent in some layer I astrocytes in the cortical gray matter (Table 2-1).

### **2.2.3 Subependymal zone stem cell astrocytes**

The maybe most amazing role of astrocytes in the adult brain is their function as stem cells throughout adulthood. It was traditionally believed that the brain loses its capacity of regeneration during maturation. However, NSCs were found to reside in two regions of the adult brain, the subgranular zone (SGZ) of the hippocampus and the subependymal zone (SEZ) at the lateral ventricle (Altman and Das, 1965; Altman, 1969; Reynolds and Weiss, 1992; Doetsch et al., 1997; Eriksson et al., 1998; Doetsch et al., 1999). These cells fulfill all characteristics of stem cells as they self-renew and are pluripotent giving rise to the three major CNS cell types, neurons, astrocytes and oligodendrocytes (for review see Mori et al., 2005). In the SEZ the slow proliferating astroglia-like stem cells, also called type-B cells, give rise to fast proliferating transit amplifying precursors (type-C cells), which further specify to type-A neuroblasts (for review see (Ihrie and Alvarez-Buylla, 2008). These newborn neurons migrate through the rostral migratory stream (RMS) towards the olfactory bulb (OB), where they differentiate into interneurons (for review see Lledo et al., 2006). Interestingly, neuroblasts have been observed to leave their conserved path after brain injury and migrate into the site of brain damage, thus possibly displaying an intrinsic source for brain repair (Shin et al., 2000; Kokaia and Lindvall, 2003; Lindvall and Kokaia, 2004; Lindvall et al., 2004; Brill et al., 2009). However, most of these neuroblasts do not further mature and subsequently die; only a very small proportion of migrating neuroblast are able to integrate upon targeted projection neuron degeneration, an injury paradigm largely devoid of glial reactivity (Shin et al., 2000; Brill et al., 2009).

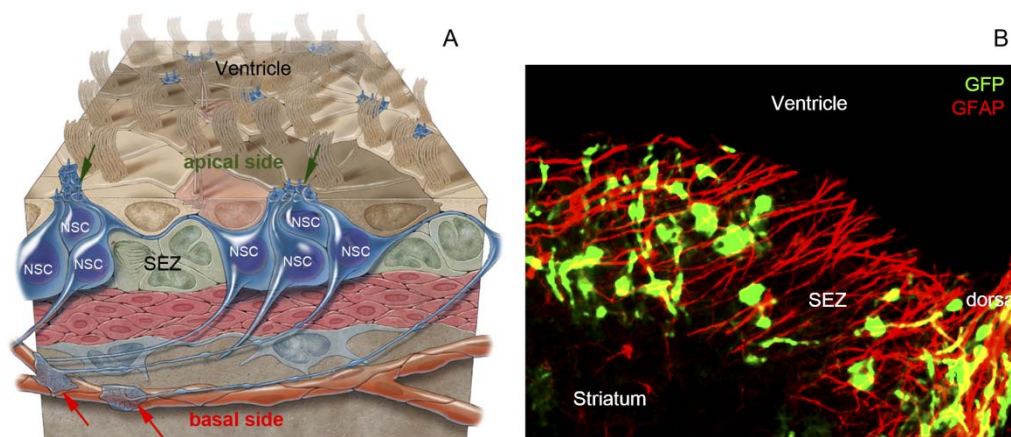


**Figure 2-4 Stem cell astrocytes of the subependymal zone**

**Schematic drawing modified from Z. Mirzadeh et al., 2008 depicting the polarized appearance of SCA with an apical membrane site at the ventricular surface and a basal membrane domain where a process makes contact with the basement membrane surrounding blood vessels (A). Astrocytes at the SEZ can be labeled with GFAP and GFP expressed in GLAST-positive NSCs (B). NSC Neural stem cell, SEZ subependymal zone, GFP green fluorescent protein, GFAP glial fibrillary acidic protein.**

What does capacitate astroglia-like stem cells in the SEZ to preserve their stem cell potential that is otherwise lost in maturing astrocytes as development proceeds? Are these cells more closely related to parenchymal astrocytes, which are of the same RG origin, or to ependymal cells with which they share the niche in addition? The niche is the microenvironment that may regulate stem cell survival, self-renewal and differentiation. Key niche components and interactions include growth factors, cell-cell contacts and cell matrix adhesions (Discher et al., 2009). Comparative transcriptome analysis of parenchymal astrocytes, NSCs and ependymal cells revealed that NSCs share characteristics of astrocytes and ependymal cells and that NSC are intermediate between those two (P. Tripathi et al., 2010), which was surprising as their marker expression and morphology rather resembles their RG progenitors. In contrast to ependymal cells that have a cuboids shape, they have a unique bipolar morphology with one cilium-bearing process that has access to the lateral ventricle and thus possess an apical membrane domain (Mirzadeh et al., 2008). Their second process contacts the basement membrane (BM) enwrapping blood vessels within the SEZ (Figure 2-4 A).

Lately, this basal membrane component has been discussed to be especially important for the stemness of NSCs (Shen et al., 2008; Tavazoie et al., 2008). Like RG, they express the marker brain lipid-binding protein (BLBP), the intermediate filaments Nestin, Vimentin and GFAP, as well as the extracellular matrix molecule Tenascin-C (ECM TN-C; see Table 2-1). This marker profile is rather characteristic for immature cells during development and differs profoundly from the one of mature astrocytes (Table 2-1). Interestingly, it largely overlaps, though, with protein expression in reactive astrocytes after acute or chronic brain injury, which will be discussed in more detail below.

**Table 2-1 Marker expression in neuroepithelial cells and various astrocyte subtypes**

	Neuroepithelial Cell	Radial Glia	Neural Stem Cell	adult white matter Astrocytes	adult gray matter Astrocytes	Reactive Astrocytes
Glycogen granules	-	+	+	+	+	+
GLAST	-	+	+	+	+	+
Glutamine synthetase	-	+	+	+	+	+
S100 $\beta$	-	+	+	+	+	+
GFAP	-	not in rodents	+	+	-	+
Vimentin	-	+	+	-	-	+
Nestin/ RC2	+	+	+	-	-	+
TN-C	-	+	+	-	-	+
BLBP	+	+	+	-	-	+

modified from Mori et al., 2005; Pinto and Gotz, 2007

## 2.3 Diversity of astroglial functions

### 2.3.1 Functions in the intact adult brain

Astrocytes, the most abundant glial cell type in the brain, are possibly as heterogeneous as nerve cells in regard to their morphology and function. Astrocytic tasks in the healthy brain can be subdivided in three groups; those that provide housekeeping functions to keep neurons healthy, those that are involved in shaping synaptic function (D. D. Wang and Bordey, 2008) and their

role as stem cells in the adult brain (see above). In regard to their housekeeping functions, astrocytes are involved in fostering neurons by buffering potassium and neurotransmitters like glutamate, providing nutrient and structural support around synapses, and enhancing neuronal survival and neurite function by secretion of growth factors including nerve growth factor (NGF), brain-derived neurotrophic factor (BDNF), neurotrophin-3 (NT-3), and fibroblast growth factor (FGF) in all brain regions (Ojeda et al., 2000). They are not only the major source of the ECM, but also secrete proteolytic enzymes, in particular the metalloproteinases (MMPs) that play a role in ECM degradation and remodeling (Shapiro, 1998; Yong et al., 1998; Rosenberg, 2009). More recently, astrocytes have been shown to transmit signals to neurons that directly modulate synaptic strength or even contribute to synaptic transmission by release of transmitters that directly stimulate postsynaptic neurons (for review see Haydon, 2001; Newman, 2003). But not only that, changes in intracellular calcium in astrocytes reflect a mode of astrocyte excitability. Astrocytes can sense neuronal activity through activation of ion channels, transporters and receptors reacting with fast depolarization and/ or increase in intracellular calcium (D. D. Wang and Bordey, 2008) that can be communicated to neighboring cells via gap junctions. Nevertheless, the overlap of processes of adjacent astrocytes is minimal. The functional consequence of their domain organization is not fully understood, but one could imagine that all synapses lying within a given volumetrically defined compartment might be under the influence of a single astrocyte, which would then provide a higher integrative order (Nedergaard et al., 2003). Furthermore, through their contact to blood vessels astrocyte domains might provide the unique structure to fine tune the cerebral blood flow according to synaptic activity and coherent metabolic demands within this functional unit of the brain (Iadecola and Nedergaard, 2007).

### **2.3.2 Astrocytes respond to brain injury**

Astrocytes, together with microglia cells and NG2 glia, mediate the reaction to every kind of brain injury including trauma, infection, ischemia and

neurodegeneration with a process called 'reactive gliosis'. Reactive gliosis starts when trigger molecules at the injury site drive astrocytes to become activated. During this process astrocytes gradually change their morphology and biochemical profile (see Figure 2-5 and Table 2-2) dependent on the severity of the injury. They also release factors that mediate or enhance an inflammatory response and tissue remodeling (Figure 2-5 b). In severe cases a tight glial scar is formed that is inhibitory for neuronal regeneration (Figure 2-5 e). Early morphological and molecular changes in astrocytes comprise hypertrophy, upregulation of intermediate filament proteins, such as GFAP, Vimentin, Synemin and Nestin and secretion of ECM components, e.g. Tenascin-C and chondroitin sulfate proteoglycans (CSPGs) (Mathewson and Berry, 1985; Dobbertin et al., 2003; Jing et al., 2007; Pekny et al., 2007; Buffo et al., 2008). Despite the protection from secondary damage by isolation of the injured region from other brain parts and sealing of the blood-brain barrier (BBB), another potentially beneficial aspect of astrogliosis derives from the finding that a subset of reactive astrocytes can recapitulate stem cell/ progenitor features in response to brain damage (Buffo et al., 2005; Buffo et al., 2008). Thus, 7 days after cortical stab wound injury around half of all GFAP-positive astrocytes incorporated the thymidin base analogue Bromodeoxyuridin (BrdU) (Buffo et al., 2005; Buffo et al., 2008). In vivo, however, these proliferating cells do not switch fate, but give rise to astrocytes only. Nevertheless, if the injured tissue is dissociated and cells are cultured as neurospheres in vitro, reactive astrocytes are able to differentiate into all three major neural cell types, astrocytes, oligodendrocytes and neurons (Buffo et al., 2008). These findings indicate that astrocytes after injury possess the intrinsic capacity to dedifferentiate towards a stem cell like cell. However, the inhospitable environment may not allow or even inhibit astrocytes to evolve their full stem cell-like potential.

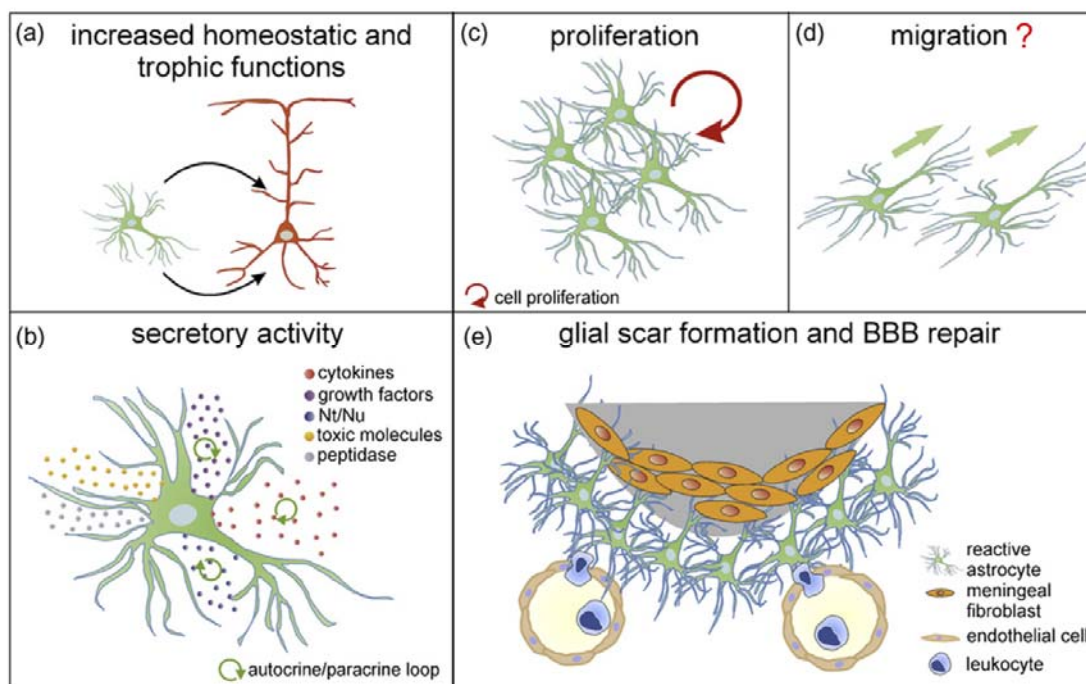


**Figure 2-5 Changes in astrocytes after brain injury**

Upon CNS injury, activated astrocytes increase their homeostatic and trophic functions (a), the production of growth factors and cytokines, as well as the release of nucleotides and toxic compounds (b). Their secretion is regulated via complex autocrine and paracrine loops (b). Astrogliosis includes cell proliferation (c) and possibly migration towards the lesion site (d). Reactive astrocytes participate in glial scar formation, and contribute to the resealing of the damaged blood–brain barrier, thus excluding infiltrating leukocytes and meningeal fibroblasts from the injured tissue (e) (modified from Buffo et al., 2010).

Nt/ Nu nucleotides/ nucleosides, BBB blood–brain barrier.

Despite the fact that astrocyte reactivity has long been known to accompany brain pathology and many molecules have been shown to be differentially regulated after different injury paradigms (see Table 2-2), the molecular signals dissecting beneficial and detrimental effects are poorly understood (for review see Sofroniew, 2009; Buffo et al., 2010). Nonetheless, it becomes more and more clear that it is the reaction of glia, which determines initiation, course and outcome of the majority of brain insults and the glial performance decides upon the balance of neuroprotection, neuroregeneration and neural death, thus controlling the pathology of the brain. Therefore, it is of great interest to

examine the molecular pathways regulating and differentiating between the various nuances of the glial reaction (see also Table 2-3).

**Table 2-2 Molecular changes in reactive astrocytes**

Functional categories	Molecular changes in reactive astrocytes
Structural	GFAP, Vimentin, Nestin, Synemin
transcriptional regulators	NF-kappaB, Stat3 , cAMP, Olig2, mTOR, Sox9
ECM and cell-cell interactions	CSPGs, integrins, collagens, cadherins laminins, ephrins, metalloproteases
Inflammatory cell regulators	cytokines, growth factors, glutathione
fluid and ion homeostasis	Aqp4, Na/K transporters
extracellular transmitter clearance	glutamate transporters
vascular regulators	NO, PGE
Purines, pyrimidines and receptors	P2Y, P2X, P1; ATP, ADP, UTD, UDP, Ado
oxidative stress and protection	NO, NOS, SOD, glutathione
gap junctions proteins	Cx43
energy provision	lactate
synapse formation and remodeling	Thrombospondin, complement C1q

modified from Sofroniew, 2009; Buffo et al., 2010

### **2.3.3 Signaling after brain injury**

Numerous molecules and pathways have been implicated in mediating the response of astrocytes towards brain injury (for review see Sofroniew, 2009; Buffo et al., 2010) and Table 2-3). Obvious candidates for initiating the astrocytic response to injury are purine (ATP, ADP) and pyrimidine (UTP, UDP, and UDP-sugars) nucleotides, because they are released in massive amounts from damaged cells at early stages after brain injury. This is a consequence of cytoplasm leakage of dying cells and increased excitotoxic transmission or astrocyte exposure to plasma components like thrombin (Melani et al., 2005; Kreda et al., 2008; Lecca and Ceruti, 2008). Astrocytes are able to sense changes in nucleotide levels as they express all known G-protein coupled metabotropic P2Y-receptors and 7 ionotropic P2X subtypes (Fumagalli et al., 2003; Di Virgilio et al., 2009). Indeed, astrocytic proliferation, the extension of long branched astrocytic processes and cytoskeleton dynamics through integrin

interactions, as well as cyclooxygenase-2 (COX-2) upregulation and secretion of arachidonic acid seem to be triggered by P2Y receptors activation (for review see Buffo et al., 2010). The P2X7 receptor has recently been shown to modulate the synthesis of cytokines and inflammatory mediators and is predominantly activated by pathological high ATP levels (for review see Cotrina and Nedergaard, 2009). Upon activation it leads to the opening of a membrane pore that allows cytokine release and promotes cell death (Di Virgilio, 2007). Systemically administration of the P2X7 receptor antagonist Brilliant blue G after spinal cord injury in rats reduced local activation of astrocytes and microglia, as well as neutrophil infiltration (Peng et al., 2009).

After injury, purinergic factors promote the release of cytokines (Cotrina and Nedergaard, 2009; Di Virgilio et al., 2009), which are a family of low molecular weight proteins and include, but are not limited to, interleukins (ILs), chemokines, interferons (INF- $\alpha$ ,  $\beta$  and  $\gamma$ ), tumor necrosis factor (TNF- $\alpha$  and TNF- $\beta$ ), colony stimulating factors (CSFs, IL-3 and some other ILs), and growth factors (Transforming growth factor, TGF  $\alpha$  and  $\beta$ , EGF, FGF, PDGF, LIF, CNTF, IL-6) (Ebadi et al., 1997). Cytokines participate in a wide range of biological responses, including growth, development and modulation of inflammation, immune responses and regulation of homeostasis.

Acute brain injury leads to the release of pro-inflammatory cytokines such as TNF- $\alpha$ , IL1 $\beta$ , IL-6, and INF $\gamma$  mainly from microglia (for review see Kim and de Vellis, 2005). Nonetheless, astrocytes do not only possess a large variety of cytokine receptors enabling them to sense microglial signals, but also release proinflammatory and immunomodulatory cytokines themselves, giving rise to an autocrine/ paracrine loop of glial cell activation (Figure 2-7 and Hauwel et al., 2005; Farina et al., 2007; Kahn et al., 1995; Levison et al., 2000). IL-1 $\beta$  as well as IL-1 receptor knockout mice show a delay in GFAP-upregulation, whereas in the latter induction of CSPGs, S-100 $\beta$ , GLAST and glutamate transporter-1 (GLT-1), and glutamine synthetase (GS) were not affected (Herx and Yong, 2001; Lin et al., 2006). Conversely, IL1 $\beta$  and TNF- $\gamma$  seem to mediate GFAP upregulation in Creutzfeldt Jacob Disease, a neurodegenerative disorder (Kordek et al., 1996). On the contrary, immunomodulatory cytokines such as IL-

10, INF $\gamma$  and Epo attenuate gliosis after spinal cord injury or ischemia respectively (Vitellaro-Zuccarello et al., 2008; de Bilbao et al., 2009; Ito et al., 2009).

Upon injury, also growth factors such as ciliary neurotrophic factor (CNTF), vascular endothelial growth factor (VEGF), epidermal growth factor (EGF), and basic fibroblast growth factor (bFGF) are released (Buffo et al., 2010). They trophically support damaged neurons and oligodendrocytes, promote revascularization, and may play a role in activating progenitors in some injury paradigms (Buffo et al., 2008; Sirko et al., 2009).

These primary mediators then lead to a secretion of secondary mediators like arachidonic acid metabolites, nitric oxide (NO), and enzymes including MMPs that can contribute to the long-lasting astrocytic response to injury for example in chronic neurodegenerative diseases. In addition, they trigger intracellular signaling pathways. The molecular pathways mediating between injury-derived signals and astroglia reactivity are numerous and their intracellular interactions are largely unclear. Intracellular cascades can either mediate changes at the cytoplasmic level including cytoskeletal rearrangements or translational modifications, or gene expression can be modified through activation of intracellular cascades leading to nuclear responses. Below three main pathways will be discussed that regulate proliferation, hypertrophy and GFAP upregulation in astrocytes.

### Pathways triggering a proliferative response of astrocytes after brain injury

In vitro, exposure of astrocytes to a number of growth factors including EGF and bFGF, or VEGF induced typical features of reactive astrocytes like cell proliferation, upregulation of GFAP, as well as emission of long and branched processes (Buffo et al., 2010). In addition, microarray analysis revealed that treating astrocytes in culture with EGF leads to the upregulation of various genes related to brain injury including CSPG 2 (Versican), Tenascin C, MMPs,

tissue inhibitor of metalloproteinase, some collagens, Syndecan, Nestin, Endothelin A receptor, FGF, LIF, TGF- $\beta$ 1 and TGF- $\beta$ 1-receptor, whereas GS, Vimentin, IL-6, laminin, and PTEN seems to be regulated via EGF-R-independent pathways (Liu et al., 2006).

After injury in vivo, astrocytes strongly upregulate the expression of these cytokines or their receptors (Sun et al., 2010; Nieto-Sampedro et al., 1988; Leadbeater et al., 2006; Krum et al., 2008; R. B. Tripathi and McTigue, 2008). The absence of the potent mitogen FGF-2 in knockout mice revealed a baseline decrease in GFAP immunoreactivity in cortical gray and white matter and the striatum and a reduction of proliferating cells after traumatic brain injury (Reuss et al., 2003; Yoshimura et al., 2003). After blocking of VEGF-mediated signaling with neutralizing antibodies against VEGF receptor-1 (flt-1) administered by a minipump, less astrocytes were expressing FGF-2 and the number of proliferating astrocytes was dramatically reduced (Krum et al., 2008). Furthermore, rapid upregulation of EGF-R (ErbB-1-4) and its ligands (TGF $\alpha$ , and EGF are ErbB-1 ligands) in astrocytes has been demonstrated after acute brain injury and neurodegenerative diseases (Nieto-Sampedro, 1988; Nieto-Sampedro et al., 1988; Liu and Neufeld, 2007). Upon activation, EGF-R signaling modulates the ECM composition by upregulation of CSPG proteins including phosphacan and neurocan via the EGF-R ErbB1 (McKeon et al., 1999; G. M. Smith and Strunz, 2005) and induces astrocyte proliferation. Stimulation of the EGF-R cascade by TGF $\alpha$  and EGF induces astrocyte proliferation in vitro (Liu and Neufeld, 2004; Sharif et al., 2006). Conversely, astrocyte proliferation is impaired in EGF-R deficient mice in vivo (Sibilia et al., 1998). Overexpression of TGF- $\alpha$  in vivo triggers an increase of the expression of its receptor (EGF-R) (Rabchevsky et al., 1998; White et al., 2008), upregulation of intermediate filaments and hypertrophy of GFAP-positive cells. However, astrocytes did not re-enter the cell cycle in this particular study (Rabchevsky et al., 1998). On the contrary, the TGF- $\alpha$  deficient mouse mutant waved-1 shows a reduction in GFAP expressing postnatal astrocytes (Weickert and Blum, 1995).

Taken together, the growth factors EGF, FGF, and VEGF trigger mainly the proliferative response of astrocytes to brain injury (Sibilia et al., 1998; Levison et al., 2000; Yoshimura et al., 2003; Liu and Neufeld, 2004; Sharif et al., 2006; Krum et al., 2008). How these extracellular stimuli are then translated into this specific biological response in the cell?

#### *Rheb-mTOR pathway and phosphatase tensin homolog (PTEN)*

The serine/threonine kinase mTOR (mammalian target of rapamycin) is a key regulator of cell size and proliferation downstream of growth factor receptors and has a role in mediating cell responses to nutrients at the translational level (for review see Chiang and Abraham, 2007; Ma and Blenis, 2009). In cultures of adult spinal cord astrocytes EGF activates the mTOR pathway through Akt-mediated phosphorylation of the GTPase activating protein Tuberin. In its phosphorylated form Tuberin is unable to inactivate the small GTPase Rheb, which is required for EGF-dependent mTOR activation. In an ischemic model of spinal cord injury elevated mTOR signaling was detected in reactive astrocytes. Treating injured rats with the mTOR inhibitor rapamycin leads to an overall decrease of GFAP and Vimentin levels (Codeluppi et al., 2009). Conversely, deletion of the mTOR negative regulator phosphatase tensin homolog (PTEN) and thus pronounced mTOR signaling promotes astrocyte hypertrophy and proliferation (Fraser et al., 2004).

#### *The mitogen-activated protein kinase/ extracellular signal-regulated kinase pathway*

Mitogen-activated protein kinases (MAPK) are proline-directed serine/threonine-specific protein kinases responsible for most cellular responses to cytokines and external stress signals and crucial for regulation of the production of inflammation mediators. Increased activity of MAPKs in activated microglia and astrocytes is regulating intracellular events including gene expression, proliferation, differentiation, cell apoptosis and survival respectively (Pearson et al., 2001). The signaling cascade involves a MAP kinase kinase kinase (MAP3K), e.g. EGF-R or FGF-R (Sundaram, 2006; Neary et al., 2008). The MAP3K is sensing the extracellular stimuli, which subsequently phosphorylates

a MAP kinase kinase (MAP2K). MAP2K likewise phosphorylates a MAPK at its serine and threonine residues leading to specific biological responses (Figure 2-6). Six different groups of MAPKs have been characterized in mammals. In signaling after brain injury the classical MAP kinase ERK1 and ERK2, the c-JUN N-terminal kinases/ stress activated protein kinases (JNK/ SAPK), and p38 pathways have been implicated.

The extracellular signal-regulated kinase (ERK)/ MAPK pathway mediates the effects of extracellular nucleotides, growth factors including NGF, EGF, and FGF-2, as well as the vasoactive factor endothelin, which are released after brain injury (Brambilla et al., 2002; Irving and Bamford, 2002; Carbonell and Mandell, 2003; Neary et al., 2004; Gadea et al., 2008; Neary et al., 2008). Shortly after stab wound injury the ERK/ MAPK pathway is activated in a subset of GFAP-positive astrocytes, suggesting a specific functional activation of these cells. Furthermore, a downstream target of the ERK/ MAPK cascade, cAMP response element-binding (CREB) protein, has been shown to be phosphorylated in perilesional astrocytes with a peak at 7 days after the injury (Carbonell and Mandell, 2003). Endothelin-1 (ET-1), a potent vasoactive neuropeptide, and the endothelin receptors (ET(A)R and ET(B)R), expressed in astrocytes during development and in the adult brain, are strongly upregulated in astrocytes after brain injury (Nie and Olsson, 1996; Barnes and Turner, 1997; Schinelli, 2006). Infusion of ET(B)R agonists induced hypertrophy of astrocytes even in the intact brain (Rogers et al., 2003). Conversely, infusion or injection of ET(B)R antagonists were associated with a reduction in GFAP-upregulation and hypertrophy in different injury paradigms (Baba, 1998; Peters et al., 2003; Rogers et al., 2003). ET-1 can activate all three MAPK pathways inducing transcription or phosphorylation of the transcriptional regulators CREB, and the AP1 complex components c-fos and c-jun (Schinelli et al., 2001; Schinelli, 2006; Gadea et al., 2008). The induction of CREB in astrocytes is induced via an ERK and p38-dependent MAPK pathway after Endothelin-1 (ET-1) stimulation (Schinelli et al., 2001). Interestingly, the Rap1/ PKC/ ERK-dependent pathway induces the phosphorylation of activating transcription factor-1 (ATF-1), CREB and Elk-1, whereas the p38MAPK pathway only induces phosphorylation of

CREB. ET-1 induced transcription of the immediate early gene c-fos requires the concomitant activation of both pathways (Schinelli et al., 2001). Recently, another study showed that ET-1 induces a combined activation of ERK and JNK-dependent MAPK pathways that synergistically act to phosphorylate c-fos and c-jun, which subsequently modulate astrocyte proliferation and GFAP expression (Gadea et al., 2008). Conversely, it has been shown that Interferon- $\gamma$  (INF- $\gamma$ ) attenuates GFAP-upregulation and astrocyte proliferation by reduction of mitogen-activated ERK-regulating kinase (MEK)/ ERK phosphorylation (Figure 2-6) after spinal cord injury, which is correlated to a better functional outcome (Ito et al., 2009).

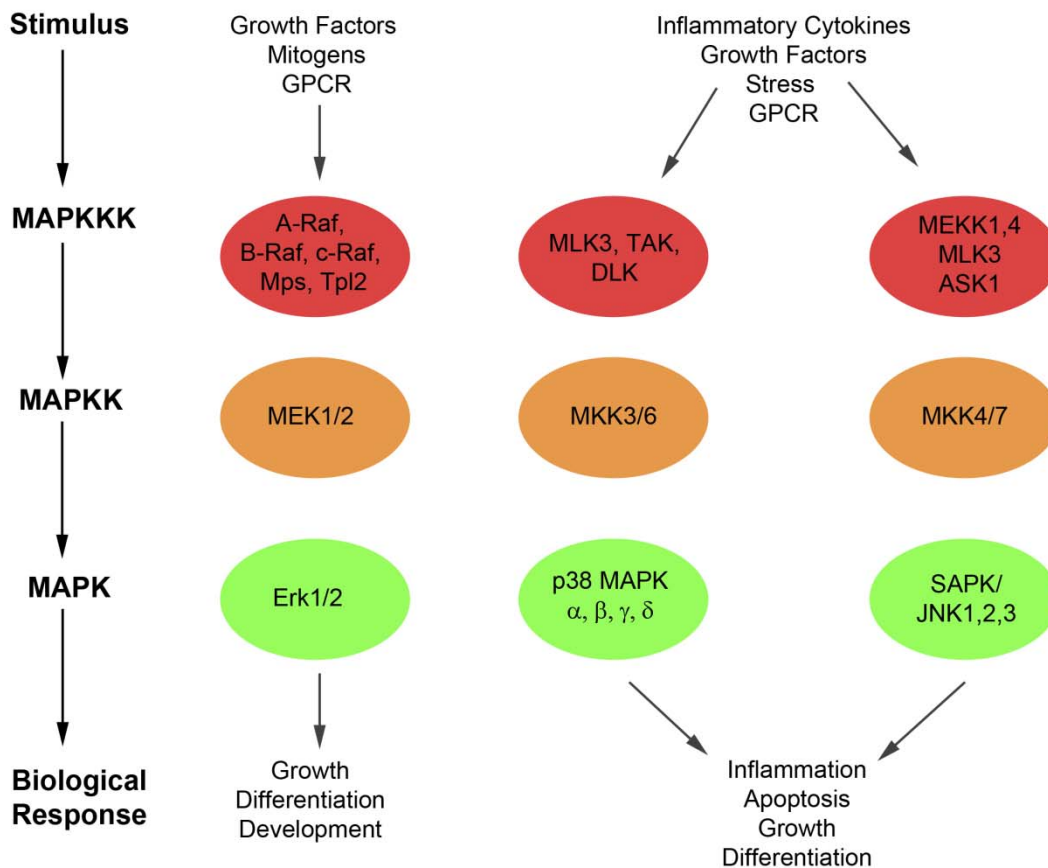


**Figure 2-6 Mitogen-activated protein kinase/ extracellular signal-regulated kinase cascade**

Upon sensing an extracellular stimulus a mitogen-activated protein (MAP) kinase kinase kinase phosphorylates a MAP kinase kinase, which subsequently phosphorylates a MAP kinase leading to a specific biological response (adapted from Cell Signaling Technology®).

### CNTF triggers JAK/STAT mediated signaling leading to hypertrophy and upregulation of GFAP

Astrogliosis is directly initiated by the pro-inflammatory cytokines IL-6 and CNTF (Fattori et al., 1995; Kahn et al., 1997; Klein et al., 1997; Okada et al., 2004), which belong to a cytokine family involved in astrocyte fate specification during development. The interleukin (IL)-6 family of cytokines, which includes IL-6 itself, leukemia inhibitory factor (LIF), cardiotrophin-1 (CT-1) and ciliary neurotrophic factor (CNTF) are able to activate the CNTF receptor that promotes differentiation of cerebral cortical precursor cells into astrocytes and at the same time inhibits the differentiation along the neuronal lineage in culture (Bonni et al., 1997). Ligand binding at the corresponding receptor induces homo- or heterodimerization of the co-receptor Gp130 that is shared by several receptor complexes as a critical component for signal transduction. Neither Gp130 nor its dimer partners possess an intrinsic tyrosine kinase domain. However, dimerization of Gp130 leads to an activation of the Janus Tyrosine Kinase/ Signal Transducers and Activators of Transcription (JAK/ STAT) pathway (Stahl et al., 1994; Taga and Kishimoto, 1997; Levy and Darnell, 2002). The activated transcription factors STAT1 and/ or 3 dimerize and translocate to the nucleus where they bind specific sites in the DNA. Furthermore, STATs can bind cofactors of the p300/ CREB-binding protein group (CBP). These cofactors bridge between STAT1/ 3 and the RNA-Polymerase II leading to an increase in transcription. STATs have been shown to bind to the promoter region of genes encoding astrocytic proteins (e.g. GFAP and S100 $\beta$ ) after stimulation of precursor cells with IL-6, CT-1, LIF or CNTF, promote the transcription of astrocytic genes and thus astrocytic fate specification or re-expression of GFAP after injury (Bonni et al., 1997; Namihira et al., 2004; He et al., 2005). Among the genes activated by STAT1/ 3 are components of the JAK/ STAT signaling cascade itself, including Gp130, JAK1, STAT1 and STAT3 suggesting that STAT signaling induces an autoregulatory loop that reinforces itself and stabilizes the astrocytic phenotype (Kessaris et al., 2008). As most of these studies are done in culture, the question arises whether all of the cytokines are of relevance after brain injury in vivo. Genetic

ablation of IL-6 in mice as well as pharmacological blocking of the IL-6 receptor leads to less phosphorylation of STAT3, a less pronounced GFAP upregulation, a lower number of proliferating astrocytes and to a reduction in microglia activation and proliferation (Klein et al., 1997; Swartz et al., 2001; Okada et al., 2004). Conversely, neuron-specific overexpression of human IL-6 mediated upregulation of GFAP and an increase in microglial numbers most likely due to IL-6 secretion from neurons. Neuronal damage, however, has not been excluded (Fattori et al., 1995) and could also be the cause for astrocyte and microglia activation in this model. These mice displayed strongly elevated levels of proinflammatory cytokines including murine IL-6, IL-1 $\beta$ , and TNF after intracerebroventricular injection of lipopolysaccharide (Di Santo et al., 1996), suggesting a faster and amplified production of these cytokines after an inflammatory stimuli either because of the elevated baseline of human IL-6, or due to already activated astrocytes and microglia. Similarly, CNTF levels are elevated after CNS injury (Kahn et al., 1995; Krum et al., 2008; R. B. Tripathi and McTigue, 2008) and CNTF-injection into the intact brain promotes GFAP-upregulation but not astrocyte proliferation (Kahn et al., 1995; Kahn et al., 1997).

IL-6 and CNTF are well known activators of the JAK/ STAT pathway and indeed, activation of the JAK2/ STAT3 pathway in astrocytes could be shown to precede GFAP upregulation in vivo after 1-Methyl-4-phenyl-1,2,3,6-tetrahydropyridine (MPTP) induced neurodegeneration. After MPTP-induced damage of striatal dopaminergic nerve terminals phosphorylation of STAT3 and translocation to the nucleus was observed in astrocytes. Pharmacological inhibition of Janus kinase-2 (JAK2) attenuated both, STAT3 phosphorylation and GFAP upregulation (Sriram et al., 2004). Conditional deletion of STAT3 by either using Nestin-Cre or mGFAP-Cre led to attenuated upregulation of GFAP, reduced hypertrophy of astrocytes after spinal cord injury, limited migration of astrocytes into the injury site and more widespread infiltration of inflammatory cells. This resulted in an increase in injury volume and impaired recovery of motor functions several weeks after the injury (Okada et al., 2006; Herrmann et al., 2008). Conversely, conditional knockout of the protein suppressor of

cytokine signaling 3 (Socs3) is associated with higher levels of phospho-STAT3, an increase in astrocytic migration into a lesion and enhanced contraction of the lesioned area, as well as improvement of functional recovery after spinal cord injury (Okada et al., 2006).

Thus, IL-6 or CNTF induced activation of the JAK/ STAT pathway mediates the expression of GFAP and induces hypertrophy in astrocytes after brain injury.

#### Bone morphogenic protein/ TGF- $\beta$ signaling through Smads leads to the acquisition of an astrocytic cell fate

Cytokines of the transforming growth factor- $\beta$  (TGF- $\beta$ ) superfamily, including TGF- $\beta$ s and bone morphogenetic proteins (BMPs) are upregulated in response to different injury paradigms in brain and spinal cord (Ebadi et al., 1997; Setoguchi et al., 2001; Buisson et al., 2003; Vivien and Ali, 2006; Z. Zhang et al., 2006; Hampton et al., 2007). This is in particular of interest as during development BMP signaling promotes acquisition of an astrocytic fate and may explain why proliferating astrocytes after brain injury stay within their lineage and do not efficiently acquire a neuronal fate in vivo, even upon forced expression of neurogenic transcription factors (Buffo et al., 2005; Berninger et al., 2007; Buffo et al., 2008; Heinrich et al., in press). Cytokines of the TGF- $\beta$  family bind to specific serine/ threonine kinase type II receptor, which recruits a type I receptor and allows the transphosphorylation-mediated activation of this receptor. Subsequently, signaling molecules against decapentaplegic peptides (Smads), intracellular nuclear effectors of transforming growth factor-beta (TGF- $\beta$ ) family members, are activated. Whereas Smad2 and Smad3 are phosphorylated by TGF- $\beta$  type I receptors, and activin type I receptors, Smad1, Smad5 and Smad8 act downstream of BMP type I receptors (BMPRI). Activated receptor-regulated Smads (R-Smads) form heteromeric complexes with common-partner Smads (Co-Smads), e.g. Smad4, which translocate efficiently to the nucleus. In the nucleus they regulate, in co-operation with other transcription factors, coactivators and corepressors, the transcription of target genes (for review see (Itoh et al., 2000; Miyazono, 2000)).

Interfering with BMP-signaling by astrocyte-specific deletion of BMPRI $\alpha$  or full knockout of BMPRI $\beta$  followed by spinal cord injury, leads to opposing effects on astrogliosis (Sahni et al., 2010). Whereas loss of BMPRI $\alpha$  is attended by a less tight glial scar and reduced GFAP levels accompanied by increased inflammatory infiltration and lower functional recovery, GFAP-levels were elevated in BMPRI $\beta$  KOs leading to reduced lesion areas shortly after injury (Sahni et al., 2010). Interestingly, astrocytes do not only upregulate BMPs, but also the BMP inhibitor noggin after cortical stab wound and spinal cord injury (Hampton et al., 2007). Infusion of a noggin-blocking antibody directly after injury leads to an increase of GFAP-positive cells and also the number of BrdU-incorporating GFAP cells is increased. The authors, however, suggest that this is due to an upregulation of GFAP in anyway proliferating astrocytes rather than an increase in astrocyte proliferation as total numbers of BrdU-positive cells are not elevated (Hampton et al., 2007).

Partial deletion of TGF- $\beta$  signaling by the use of Smad3 null mice results in a reduction in GFAP-positive cells, as well as microglia and NG2-positive cells after cortical stab wound injury (Y. Wang et al., 2007). Surprisingly, the authors could not detect any proliferating astrocytes in wildtype and in Smad3 KO mice. This is in sharp contrast to many other studies describing a proliferative response after astrocytes after brain injury (for review see Costa et al., 2010; Buffo et al., 2008). However, the reduction in the inflammatory response in Smad3 null brains leads to a reduced wound cavity size 3 and 7 days after injury (Y. Wang et al., 2007). This is in contrast to the above mentioned study, where higher GFAP levels are indicative for smaller lesion areas, whereas lower GFAP levels lead to an increase in infiltration or activation of microglia and more damage (Sahni et al., 2010). This controversial outcome may be due to regional differences of the astrocytic reaction to injury, as one study is performed in spinal cord and the other one in the cerebral cortex.

So far, it is not fully clear whether TGF- $\beta$ / BMP-signaling is involved in upregulation of GFAP in already existing astrocytes or whether it is involved in defining the fate of newly generated cells after brain injury in vivo.

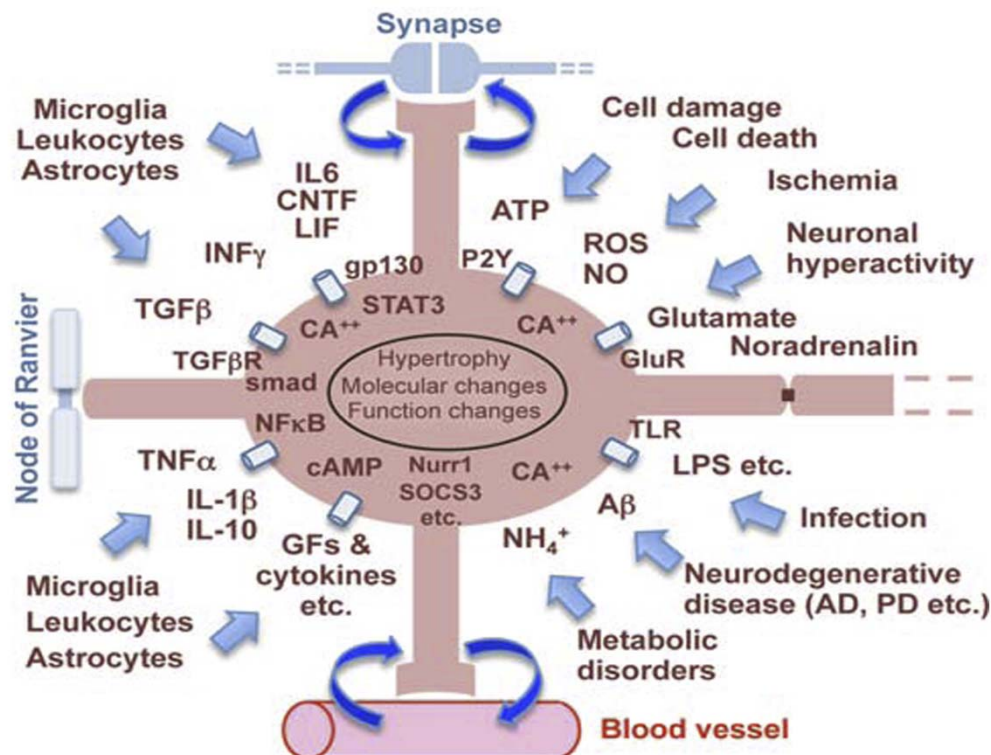


Figure 2-7 Triggers and molecular regulators of reactive gliosis

A huge variety of factors trigger astrogliosis by activation of molecular pathways that are numerous as well (taken from Sofroniew and Vinters).

### Interaction of signaling cascades

Above three major pathways regulating different aspects of astrogliosis, namely proliferation, upregulation of GFAP and hypertrophy, and acquisition of an astrocytic cell fate, have been discussed. These pathways are mainly activated by growth factors and cytokines. Given the multitude of cytokines and growth factors, which are released after injury and the various effects and pathways that are initiated by these factors, the level of astrogliosis may be regulated by the interplay of multiple factors. Thus, one factor is able to activate several pathways and there is a cross-talk between different pathways, which regulates and fine tunes the biological response. For example, IL-6-type cytokines are not capable to promote astrocyte proliferation alone, but enhance EGF-stimulated astrocyte proliferation suggesting an interaction of the EGF-R/ MAPK and JAK/ STAT pathway (Kahn et al., 1995; Levison et al., 2000). Also P2 purinergic

receptors seem to signal via the MAPK pathway to STAT3 in astrocytes. Both, P2Y and P2X receptors can stimulate STAT3 phosphorylation not directly, but via the interaction with the ERK/ MAPK pathway. Activation of P2Y and P2X receptors can stimulate Tyrosin-705 STAT3 phosphorylation, whereas only P2Y mediates additional Serin-727 STAT3 phosphorylation. As described above, purinergic signaling via P2 receptors activates ERK signaling. If this pathway was inhibited by U0126, a potent and selective inhibitor of MEK1, the upstream activator of ERK, phosphorylation of Ser727-STAT3 was blocked. Thus, specific phosphorylation of STAT3 at Ser727 is a possible mechanism of cross-talk between ERK/ MAPK and the STAT pathway (Washburn and Neary, 2006). Interestingly, extracellular ATP acting via P2Y receptors has been shown to synergistically enhance the ability of FGF2, a mitogen upregulated after injury, to induce proliferative effects, whereas P2X receptors inhibit the ability of FGF2 to stimulate DNA synthesis in rat cortical astrocyte cultures (Neary et al., 1994; Neary and Kang, 2005). One difference between these two pathways may be the different phosphorylation state of STAT3. Furthermore, P2 receptors can couple to extracellular signal-regulated protein kinases (ERK) and blocking ERK signaling is preventing Serin-727 STAT3 phosphorylation showing that signaling pathways modulating astrogliosis are strongly interconnected (Figure 2-7 and (Washburn and Neary, 2006). One well established function of STAT3 upon activation is to bind to the GFAP promoter and enhance transcription. Interestingly, the GFAP promoter contains non-overlapping binding sites for STAT3 and Smad1 with the co-factor p300 bridging between the both, thus providing a mechanism for the synergistic effect of the JAK/ STAT and BMP/ Smad signaling pathway (for review see Kessaris et al., 2008).

### Interpretation of these studies

These were only few examples showing the complexity of signaling pathways and their interaction after brain injury, which is only partially understood. For the most part, these data were achieved in vitro through biochemical and immunocytochemical analysis of postnatal astrocyte cultures treated with different

cytokines or growth factors and agonists or antagonists of different pathways. Whether this indeed resembles the reaction of adult and mature astrocytes is disputable, as culturing astrocytes from the adult brain has so far not been successful. Thus, *in vivo* studies of genetic mouse models are preferable. However, to investigate the role of a certain gene mostly full knockout mice were used. In these models a gene of interest is deleted from the genome and protein expression is therefore missing throughout ontogenesis in all cell types and tissues. This makes the study of widely expressed genes, e.g. genes encoding cytokines, growth factor and their receptors, difficult or even impossible, if gene deletion is fatal at early developmental stages. Furthermore, astrogliosis is a common secondary effect due to developmental abnormalities or impairment of other neural cell types. Accordingly, analysis of GFAP-expression and microglia activation alone may be misleading and does not cover the entire range of the gliotic reaction, especially as the functional outcome in terms of wound healing or locomotor recovery cannot be predicted from these parameters and can even be opposed dependent on the injury paradigm (see above).

To circumvent some of these problems, in this study I took advantage of the Cre/ loxP system allowing cell type specific gene deletion. This is achieved by genetically manipulating the sequence of a certain gene by inserting loxP sites in non-coding regions of the gene (floxed allele). LoxP sites are recognition sequences for the Cre recombinase that is a cyclization recombination protein of the P1 bacteriophage, normally not encoded in the mammalian genome. However, Cre can be expressed in transgenic or knock-in mouse lines under the control of cell type-specific promoters. In order to delete genes containing loxP sites, mice containing floxed alleles were mated to lines encoding the Cre-recombinase under a specific promoter (Figure 2-8 A), e.g. hGFAP-Cre or Nex::Cre with the former expressing Cre in radial glia with an onset at E13.5 (Zhuo et al., 2001) and the latter expressing Cre in neurons from E11.5 (Goebbels et al., 2006). After translation in the cytoplasm, the Cre-recombinase shuttles to the nucleus, where it recognizes and cuts the sequence in between two loxP sites from the genome (Figure 2-8 B). Thus gene deletion occurs from

the time point of promoter expression. To be able to delete a gene in astrocytes at a chosen time point, I took advantage of the *Glast::CreERT2* mouse line (Mori et al., 2006). In this line the Cre recombinase is under control of the astrocyte specific *Glast* promoter and the Cre recombinase is fused to a modified estrogen receptor that allows translocation to the nucleus only upon administration of the estrogen analogue Tamoxifen (Figure 2-8 C). Thus, gene deletion takes place in specific cell types at a given time point and does not interfere with general development.

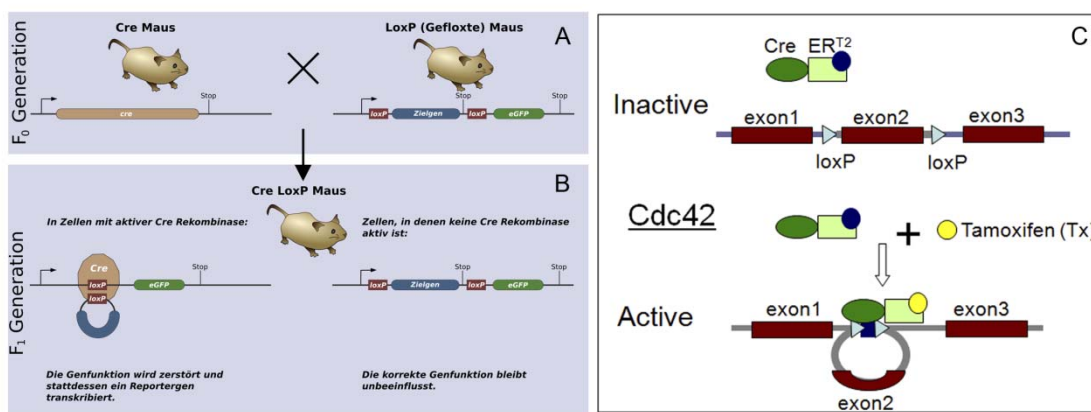


**Figure 2-8** The Cre/ loxP systems allows cell type specific gene deletion

Mice expressing Cre under a specific promoter were mated to mice containing floxed alleles (A). In the offspring gene deletion occurs in cell types expressing this promoter by recombination of the sequence in between loxP sites (B). To be able to specify the time point of recombination, the Cre recombinase was fused to a modified estrogen receptor allowing translocation to the nucleus only upon administration of Tamoxifen (C) (A and B taken from <http://de.wikipedia.org/wiki/Cre/loxP-System> and C modified from Mori et al., 2006).

**Table 2-3 Pathways mediating certain components of reactive gliosis**

pathway	IMF	hypertrophy	proliferation	ECM	microglia	references
purinergic signaling	P2Y P2X7	P2Y P2X7	P2Y	not investigated	P2Y P2X7	(Franke et al., 2001; Neary and Kang, 2005; Bianco et al., 2006; Peng et al., 2009)
cytokines	IL-6, IL6-R, CNTF, TNF- $\alpha$ , IL-1 $\alpha$ , IL-1 $\beta$ , IL-1R1 Epo, IFN- $\beta$	IL-6, IL6-R, CNTF, TNF- $\alpha$	VEGF no effect (IL-6, IL6-R, CNTF, TNF- $\alpha$ ) IFN- $\beta$	no effect (IL1-R1) Epo	IL-6, IL6-R, CNTF, TNF- $\alpha$ , IL-1 $\alpha$ , IL-1 $\beta$ , IL-1R1	(Fattori et al., 1995; Kahn et al., 1995; Di Santo et al., 1996; Kordek et al., 1996; Kahn et al., 1997; Klein et al., 1997; Herx and Yong, 2001; Okada et al., 2004; Lin et al., 2006; Krum et al., 2008; Vitellaro-Zuccarello et al., 2008; Ito et al., 2009)
EGF-R	EGF-R, EGF, TGF- $\alpha$	TGF- $\alpha$	EGF-R, EGF, TGF- $\alpha$	EGF-R, EGF, TGF- $\alpha$ , TGF- $\beta$ 1	no effect	(Nieto-Sampedro et al., 1988; Weickert and Blum, 1995; Rabchevsky et al., 1998; Levison et al., 2000; Liu and Neufeld, 2004; G. M. Smith and Strunz, 2005; Liu et al., 2006; Sharif et al., 2006; Liu and Neufeld, 2007; White et al., 2008)
MAPK/ERK	ET-1 INF- $\beta$	ET-1	ET-1 INF- $\beta$	not investigated	not investigated	(Baba, 1998; Peters et al., 2003; Rogers et al., 2003; Gadea et al., 2008; Ito et al., 2009)
BMP/Smad	BMP-2/4, 7, Smad3, BMPRI $\alpha$ BMPRI $\beta$	no effect	(Smad3?)	Smad3	Smad3	(Sahni et al., ; Hampton et al., 2007; Y. Wang et al., 2007; Sabo et al., 2009)
Rheb/mTOR	Pten	Pten	Pten	not investigated	not investigated	(Fraser et al., 2004; Codeluppi et al., 2009)
JAK/STAT	CNTF STAT3 Socs3	CNTF STAT3 Socs3	FGF	not investigated	CNTF STAT3 Socs3	(Neary et al., 1994; Neary and Kang, 2005; Okada et al., 2006; Herrmann et al., 2008)



## **2.4 Polarity cues as candidates for defining astrocytic properties**

One still unresolved question is which mechanisms drive parenchymal astrocytes towards a quiescent, non-proliferative state, whereas a subset of astroglial-like cells in the subependymal zone preserves its ability to self-renew. Along these lines it is highly debated whether cell intrinsic or environmental factors play a major role in keeping the stemness of some astrocytes in defined regions. After injury, environmental factors trigger signaling pathways known from development in parenchymal astrocytes, which consequently lead to expression of more immature marker in reactive astrocytes that are characteristic as well for adult NSCs (Table 2-1). Strikingly, some of these astrocytes at the injury site even re-enter the cell cycle and regain stem cell properties, self-renewal and multipotency in vitro. Given the fact that after acute brain trauma, as well as in neurodegenerative diseases massive neuronal loss occurs, the idea of an intrinsic source of cells able to generate new neurons is intriguing. However, in vivo the proliferating astrocytes stay within their lineage and do not reprogram towards a neuronal cell fate or with a very low efficiency even after forced expression of transcription factors promoting neurogenesis (Buffo et al., 2005). On the contrary, astrocytes contribute to the generation of a very tight glial scar and an inhospitable environment not only for newly generated neurons, but also for axonal regeneration of neurons from surrounding regions. Identifying molecular pathways differentiating between the beneficial and detrimental role of astrocytes after brain insult is thus of great value. While many studies examined the role of growth factors and cytokines after injury, virtually nothing is known about the role of cell polarity for astrocyte function in the normal and injured brain. Cell polarity is involved in processes such as cell division, cell migration and signaling and is defined as asymmetry in cell shape, protein distributions or cell functions (Nelson, 2003). A hallmark of mature astrocytes in the adult brain is the contact of their endfeet to the basement membrane surrounding blood vessels, which they share with stem cell astrocytes and which are characterized by a polarized protein distribution

towards this endfeet. The astrocyte-BM contact is mediated by integrins and dystroglycan, both of them acting as receptors for various ECM molecules including laminin. Stem cell astrocytes are further polarized and possess - similar to radial glia cells during development - not only a basal membrane domain (Figure 2-9 A and B), but also an apical membrane domain delineated by their junctions to the ependymal cells (Figure 2-9 B). At this site, proteins of the Par complex, such as Par6, the atypical protein kinase and the small RhoGTPase Cdc42 are localized. Interestingly, also astrocytes in an in vitro injury model develop a rather bipolar shape and localize the Par complex to the tip of their leading process (Etienne-Manneville and Hall, 2001, 2003; Etienne-Manneville et al., 2005). After injury in vivo, a subpopulation of the astrocytes at the injury site re-enters the cell cycle dedifferentiating to a more immature state possibly in between a multipotent stem-cell astrocyte and a mature astrocytic cell. Polarity molecules from the basal or apical site are possible candidates mediating changes in the potential of different astrocyte subtypes. Therefore, I examined the here both sets of molecules, integrins at the basal site of astrocytes and Cdc42, a major regulator of the Par complex activity.

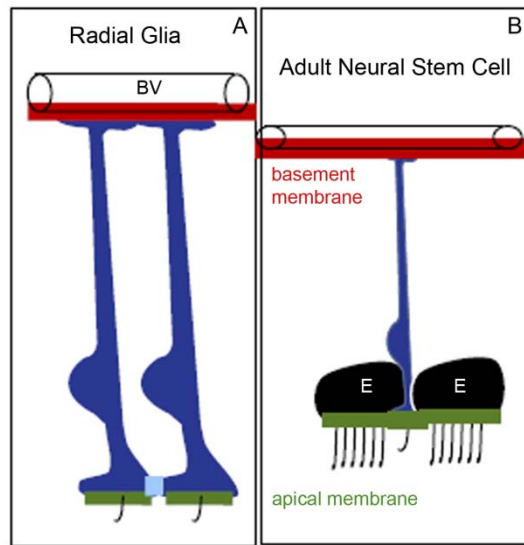


**Figure 2-9 Polarity of radial glia and adult neural stem cells**

Radial glia (A, blue) and adult neural stem cells (B, blue) have both contact to the basement membrane (red) at the pial or blood vessel (BV) surface. At the ventricular surface they possess an apical membrane domain (green). In the adult brain ependymal cells (E) are lining the ventricle and neural stem cells extend their process through the ependyma layer (B) (drawing provided by Magdalena Götz).

### **2.4.1 The astrocytic basal site is major part of the neurovascular unit**

A hallmark of parenchymal astrocytes is their contact to the BM surrounding the vasculature, which is thoroughly covered by astrocyte endfeet. Therefore, astrocytes can be understood as mediators between neurons and the vasculature as they are capable of regulating the local blood flow in response to energy demands of the neurons. To fulfill this function an asymmetric intracellular organization of astrocytes is required. A functional neurovascular unit consists of neurons with their associated astrocytes, which interact with endothelial and smooth muscle cells on the microvessels (Figure 2-10 and Abbott et al., 2006).

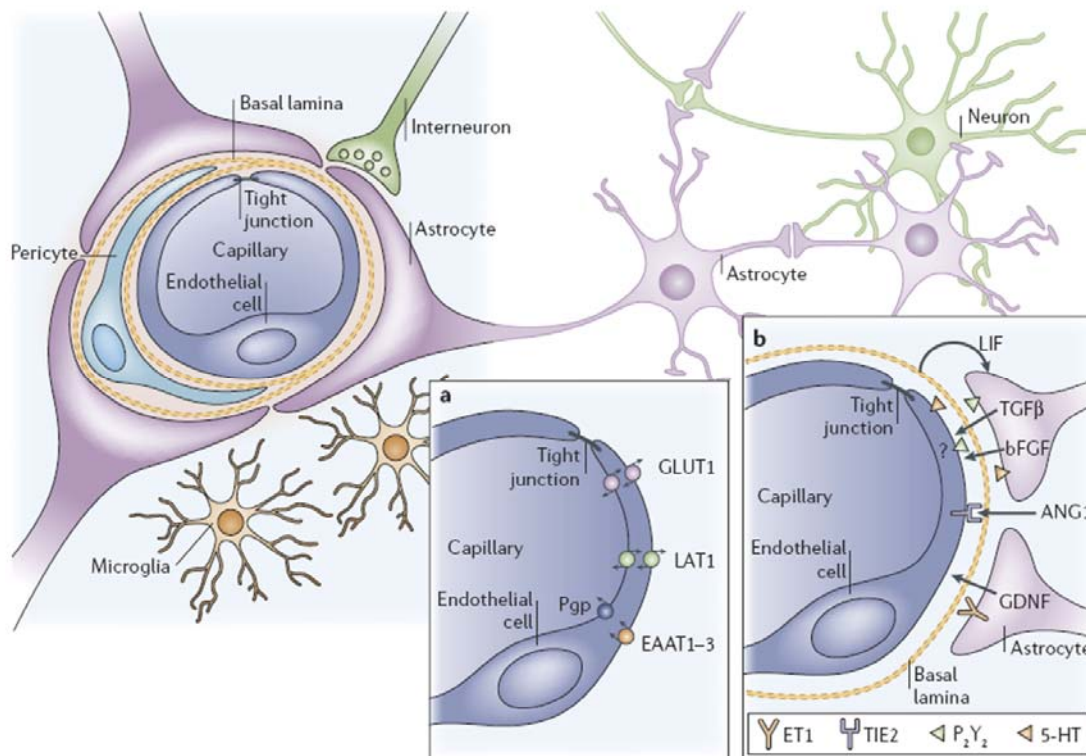


**Figure 2-10** The neurovascular unit is characterized by the interplay of astrocytes, endothelial cells and neurons

Endothelial cells are responsible to reduce the paracellular flux of substances to the brain by forming tight junctions. The endothelial cells are surrounded by a basement membrane and astrocytic perivascular endfeet with the entire complex and embedded pericytes forming the blood-brain barrier (b). Astrocytes provide a link between the vasculature and neurons ensuring brain energy and transmitter metabolism through a specialized transporter system (for endothelial part of transporter system see a) (taken from (Abbott et al., 2006).

The vascular supply of the brain is provided by four large arteries, the carotid and vertebral arteries, which merge to form the circle of Willis at the base of the brain. The arteries which arise from the circle of Willis run along the brain surface giving rise to pial arteries. These arteries branch into smaller vessels penetrating the brain parenchyma and are separated from the brain tissue by an extension of the subarachnoidal space, which is called Virchow-Robin space (Iadecola and Nedergaard, 2007). The Virchow-Robin space includes leptomeningeal cells, macrophages and other antigen-presenting cells and is bordered by two basement membranes on one side towards the endothelial

compartment and on the other side towards the glia limitans (Figure 2-11). The inner basement membrane is formed by endothelial cells and pericytes, whereas the outer basement membrane is generated by astrocytes. Around smaller vessels the outer vascular membrane fuses with the membrane of the glia limitans (fused gliovascular membrane) thereby excluding the Virchow-Robin space (Krueger and Bechmann). Basement membranes are thin, specialized extracellular matrices surrounding most metazoan tissues. One function of BMs is to provide structural support for cells, to separate tissue compartments and form a barrier, for example against T cell invasion into the brain parenchyma (Sixt et al., 2001). Furthermore they are high capacity binders of growth factors and other ECM molecules and the individual ECM composition provides distinct spatial and molecular information influencing cell migration, proliferation, differentiation and survival. Neural BMs are composed mainly of laminin, type IV collagen, nidogen, and the heparan sulfate proteoglycan perlecan. Different isoforms of these components expressed in temporal and spatial different patterns define structurally and functionally distinct basement membranes (for review see Hallmann et al., 2005). Thus, it is possible to differentiate between the inner endothelial and the outer astrocytic BM around larger vessels on the basis of their laminin isoforms. The endothelial BM contains laminin 8 composed of the laminin chains  $\alpha 4$ ,  $\beta 1$ , and  $\gamma 1$  and laminin 10 ( $\alpha 5\beta 1\gamma 1$ ), whereas the parenchymal BM generated by astrocytes contains laminin 1 ( $\alpha 1\beta 1\gamma 1$ ) and 2 ( $\alpha 2\beta 1\gamma 1$ ) (Sixt et al., 2001). The BM around microvessels consists of laminin 2, 8 and 10 and hence combines both, astrocytic derived and endothelial derived BM (Figure 2-11 and Sixt et al., 2001).

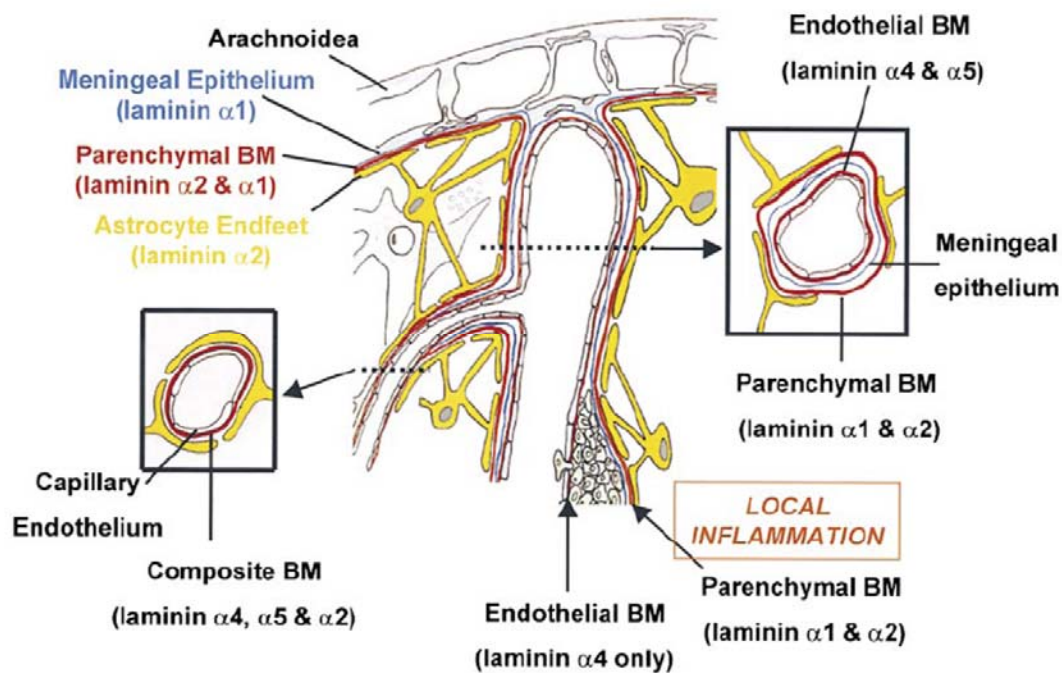
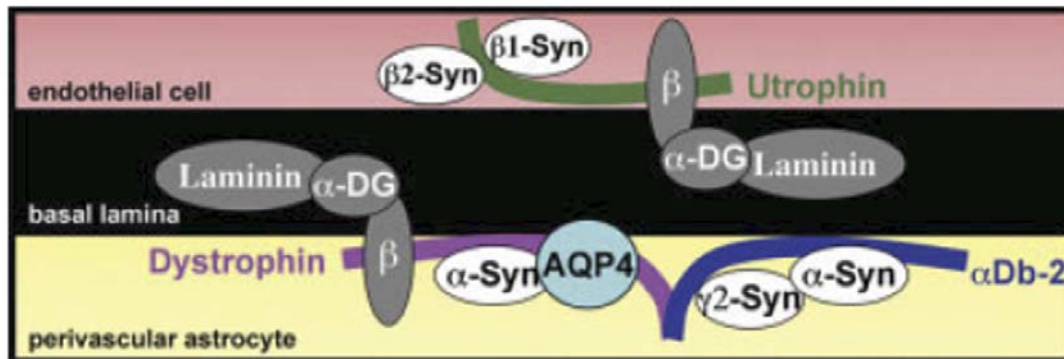


Figure 2-11 Epithelial and astrocytic basement membranes contain distinct laminin isoforms

Larger blood vessels consist of an inner endothelial cell layer with basement membrane (containing the laminin subunits  $\alpha 4$  and  $\alpha 5$ ), bordered by the meningeal epithelium and its basement membrane (containing the laminin subunit  $\alpha 1$ ), and an outer astroglial basement membrane (containing the laminin subunit  $\alpha 2$ ) and astrocyte endfeet. The meningeal and astroglial basement membranes are collectively termed the parenchymal basement membranes as they delineate the border to the brain parenchyma. Only at sites of local inflammation are the endothelial and parenchymal basement membranes clearly distinguishable and define the inner and outer limits of the perivascular space where leukocytes accumulate before infiltrating the brain parenchyma. Microvessels where no epithelial meningeal contribution occurs appear to have a composite basement membrane containing the endothelial cell laminins ( $\alpha 4$  and  $\alpha 5$ ), and laminin subunit  $\alpha 2$  produced by the astrocytes and deposited at their endfeet (taken from Sixt et al., 2001).

At the contact points of astrocyte endfeet with the BM, parenchymal astrocytes possess a highly specialized membrane domain characterized by enrichment of proteins of the dystrophin associated glycoprotein complex (DAG), the water channel Aquaporin4 (Aqp4), and the potassium channel Kir4.1 (Figure 2-12 and for review see Wolburg et al., 2009a; Wolburg et al., 2009b) displaying a special kind of basal polarity in mature astrocytes. The DAG links the BM with the

astrocytic cytoskeleton and is furthermore needed for localization of Aqp4 and Kir4.1 at the astrocyte endfeet (Figure 2-12 and Bragg et al., 2006).



**Figure 2-12 The dystrophin-associated glycoprotein complex at the blood-brain interface**

The illustration displays the interaction of proteins of the dystrophin-associated glycoprotein complex (DAG) in astrocyte endfeet, which is necessary to properly localize the water channel Aquaporin4 (Aqp4). In endothelial cells the DAG is composed slightly different excluding the proteins  $\alpha$ -Syntrophin,  $\alpha$ -Dystrobrevin-2 and Dystrophin (taken from Bragg et al., 2006).

Interestingly, this polarity has been reported to be interconnected with BBB integrity (Wolburg et al., 2009b). The BBB is a biological barrier between blood and brain tissue located within the epithelium and formed by tight junctions between endothelial cells that restrict the paracellular flux protecting the brain tissue from neurotoxic substances that circulate in the blood (Figure 2-10). Furthermore, it consists of a specialized transporter system that ensures the brain energy and transmitter metabolism (for review see Wolburg et al., 2009a). The tightness of this barrier depends not only on endothelial cells, but also on the surrounding BM and the cells in close proximity to the endothelium including pericytes and astrocytes. Pericytes do not only provide physical support for endothelial cells; together with astrocytes they also secrete soluble factors, such as Angiopoietin-1, TGF- $\beta$ , and Src-suppressed C kinase substrate protein that regulate the expression of tight junction proteins like occludin (for review see Lee et al., 2009). Astrocytes have been implicated in the formation of the BBB during development and in BBB maintenance in the adult brain. During

development angiogenesis precedes barrierogenesis in the brain and this process is tightly regulated by the complex coordination of various extracellular factors, e.g. VEGF, TGF- $\beta$  and Angiopoietin. Until now it is not fully understood whether astrocytes, pericytes or both secrete these factors and a dialogue between several cell populations of the neurovascular unit and possible compensatory mechanisms have been suggested (for review see Krueger and Bechmann, 2010; Lee et al., 2009). In addition, most of these results have been obtained in vitro in co-culture models of endothelial cells and astrocytes and/or pericytes and in vivo evidence is still lacking. Interestingly, development of the BBB and maturation of astrocytes as defined by the basal polarization of astrocytes, seem to be closely correlated during development (Nico et al., 2001). Also after brain injury a correlation between BBB disruptions, loss of polarized protein distribution towards the endfeet and astrocytic reactivity could be observed (Dobbertin et al., 2003; Wolburg-Buchholz et al., 2009), although the causality is not yet clear. It is well known that reactive astrocytes also contribute to remodeling of the ECM by upregulation of ECM molecules including the glycoprotein Tenascin C and the chondroitin proteoglycan phosphacan/ DSD-1 (Laywell et al., 1992; Garwood et al., 2001; Joester and Faissner, 2001; Sirko et al., 2007). Interestingly, these molecules are also expressed in high amounts during development and in adult neurogenic niches and degrading CSPGs in vivo by injecting the enzyme chondroitinase ABC interferes with progenitor proliferation (Sirko et al., 2007). However, the signaling at the gliovascular interface and from the ECM/ BM has not been addressed in regard to its influence on parenchymal astrocytes so far; especially relatively little is known about the precise effects of signals from the BM to glial cells in regard to CNS pathology. ECM-mediated signaling is clearly of major importance in wound reactions in other systems like skin or kidney (Brakebusch et al., 2000; Kagami and Kondo, 2004; Tran et al., 2004), but ECM-glia signals have so far been difficult to study in the CNS in vivo. Therefore, I aimed here to examine the effects of  $\beta$ 1-integrin deletion in astrocytes in vivo, as integrins are receptors for various ECM molecules.

### Integrins are basement membrane receptors

Indeed, a possible role of ECM-mediated signaling to astrocytes is particularly relevant as astrocyte endfeet of parenchymal astrocytes as well as stem cell astrocytes in the neurogenic niches are in close contact to the basement membrane (BM) surrounding blood vessels in the intact, uninjured brain (Brightman, 1968; Brightman and Kaya, 2000; Sixt et al., 2001; Bragg et al., 2006). This contact is obviously interrupted after invasive injury, such as a trauma or stab wound injury, but it is not known to which extent the possible loss of BM-contact may contribute to the changes seen in reactive gliosis. The major receptors for BM proteins are members of the integrin family and dystroglycan (Figure 2-13), which is a central component of the DGC (del Zoppo and Milner, 2006). Interestingly, conditional deletion of dystroglycan resulted in GFAP upregulation, suggesting a possible role of signaling via this complex in astroglia activation (Moore et al., 2002). However, dystroglycan was already lost at early developmental stages in these conditional knock-out mice, resulting in defects in neuronal migration and midline fusion as well as severe disruptions of the glia limitans (Moore et al., 2002), suggesting that either developmental aberrations or abnormal cell contacts to the subarachnoidal space may be involved in this phenotype. As the DGC has been implicated in targeting the water channel Aqp4 and the inward-directed potassium channel Kir4.1 to astroglial endfeet (Sievers et al., 1994b, a; Bragg et al., 2006). These channels are redistributed after injury and may contribute to the glial reactivity, in particular the astrocyte swelling (Iandiev et al., 2006; Nestic et al., 2006; Ulbricht et al., 2008). Taken together, these data raise the possibility that alterations in BM-astrocyte signaling may play a crucial role in the reaction to brain injury.

In order to better understand the role of ECM-mediated signaling to astrocytes, I focused here on the role of the  $\beta$ 1-integrin subunit that is part of most integrin receptors in the CNS (Takada et al., 2007). Integrins are transmembrane receptors, which link the ECM to the intracellular actin cytoskeleton. They form heterodimers consisting of an  $\alpha$  and a  $\beta$  subunit. Depending on their subunit

composition, they bind different ligands in the ECM and perform distinct functions (Reichardt and Tomaselli, 1991; Brakebusch and Fassler, 2005; Takada et al., 2007). Conditional deletion of  $\beta 1$ -integrin containing heterodimers during brain development led to defects in axonal guidance and synaptogenesis, as well as in glial differentiation and cell migration (Reichardt and Tomaselli, 1991; Graus-Porta et al., 2001; Blaess et al., 2004; Belvindrah et al., 2006; Huang et al., 2006; Belvindrah et al., 2007a). However, virtually nothing is known about the role of  $\beta 1$ -integrins after later deletion in the postnatal brain.

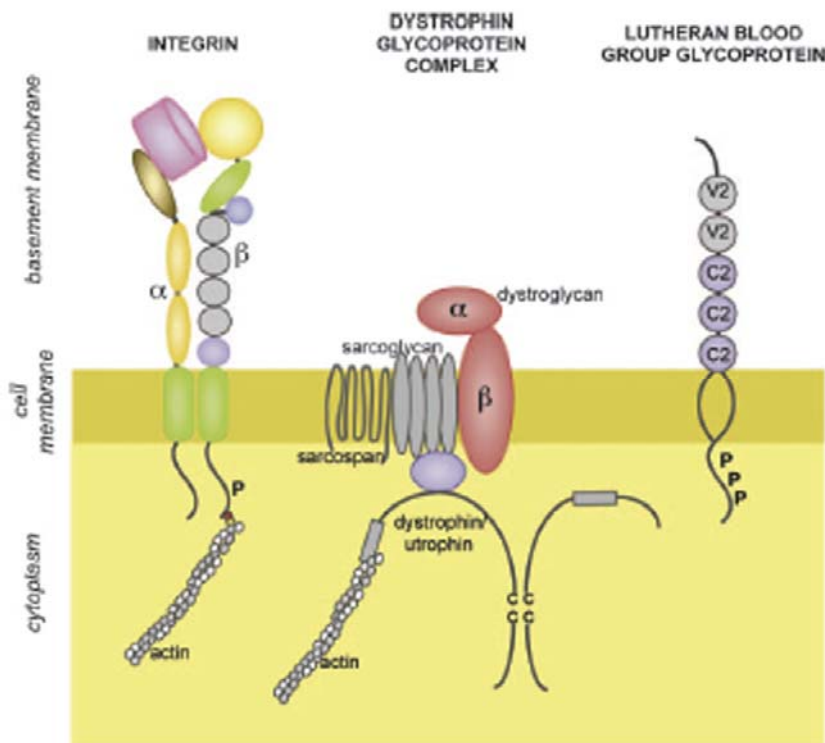


**Figure 2-13 The laminin receptors integrin, dystroglycan and Lutheran blood group glycoprotein**

Three major transmembrane receptor types are responsible for cell binding to laminins: the integrins (principally  $\beta 1$ - and  $\beta 3$ -integrins),  $\alpha$ -dystroglycan of the dystrophin-glycoprotein complex (DGC), and the Lutheran blood group glycoprotein with the latter not expressed in astrocytes (taken from Hallmann et al., 2005).

### 2.4.2 Small RhoGTPases at the apical side and after injury

The small RhoGTPases Rac1, RhoA and Cdc42 are downstream effectors of integrins (Schwartz and Shattil, 2000), as these molecules control signal transduction pathways linking membrane receptors to the cytoskeleton and thereby influencing cell polarity, morphological plasticity, cell migration and cell fate decisions (for review see Hall, 2005). The activity of RhoGTPases is regulated by signals from different classes of surface receptors like G protein coupled receptors, tyrosine kinase receptors, cytokine receptors, and adhesion receptors such as integrins. RhoGTPases function as tightly regulated molecular switches cycling between an inactive GDP-bound state and an active GTP-bound state (Figure 2-14) (Heasman and Ridley, 2008).

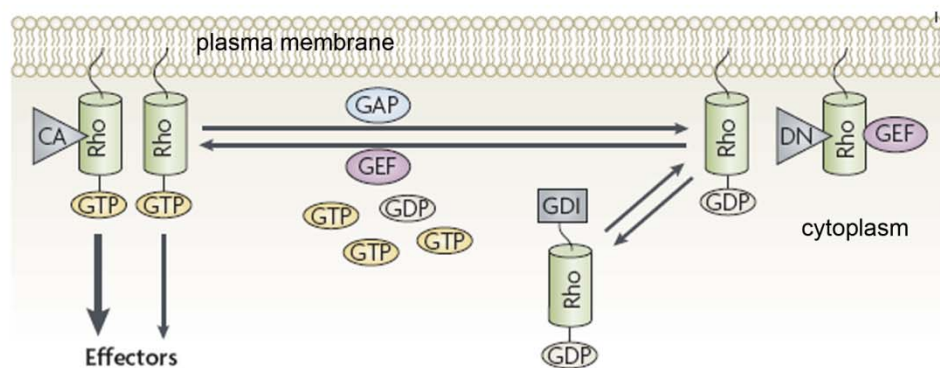


**Figure 2-14 Regulation of small RhoGTPases by GAPs, GEFs and GDIs**

Guanine nucleotide-exchange factors (GEFs) activate RhoGTPases by promoting the release of GDP and the binding of GTP. GTPase-activating proteins (GAPs) inactivate RhoGTPases by increasing the intrinsic GTPase activity of Rho proteins. Guanine nucleotide-dissociation inhibitors (GDIs) bind to C-terminal phenyl groups on some Rho proteins, sequestering them in the cytoplasm away from their regulators and targets (modified from Heasman and Ridley, 2008).

The small G-proteins, Cdc42, Rac and Rho, seem to mediate the initial signals leading to the polarization of migrating cells. The balance of activities of the three RhoGTPases must be tightly controlled between the front and the rear of the cell. A simplistic view is that Cdc42 and Rac are gradually activated toward

the front edge where they control actin and microtubule re-arrangements to promote protrusive activity, whereas Rho is rather active at the rear of the cells where, by inducing actomyosin contractility, it controls rear-end retraction and allows forward movement (for review see Etienne-Manneville, 2008).

Besides acting downstream of  $\beta$ 1-integrins, Cdc42 functions also with the Par complex (PAR6-PAR3-aPKC) that has been proposed to mediate the capture and stabilization of microtubules at the front of the cell and to orientate golgi and microtubule organizing center (MTOC) during the establishment of migratory polarity in astrocytes and other cell types (Etienne-Manneville and Hall, 2003; Pegtel et al., 2007).

Small RhoGTPases have been implicated in establishment of this astrocyte polarity in vitro by the use of dominant negative or constitutively active constructs (Etienne-Manneville and Hall, 2001; Cau and Hall, 2005). However, often these constructs are directed against guanine exchange factors (GEFs) or guanine nucleotide dissociation inhibitors (GIDs), which are known to be not specific for a single RhoGTPase but rather act on several members of the family. To overcome this limitation and to examine the specific role of certain small RhoGTPases, but particularly to investigate their role on astrocyte polarity and migration in vivo, I took advantage of transgenic mice carrying Cre-recombinase recognition sequences (loxP sites) within the genes for the small RhoGTPases Cdc42, Rac1 or RhoA allowing deletion of these genes in astrocytes in vitro and in vivo.

Whereas mechanisms controlling cell migration in vitro are relatively well understood in some experimental models (Lauffenburger and Horwitz, 1996; Ridley et al., 2003; Puklin-Faucher and Sheetz, 2009), less is known about the mechanisms and molecules promoting the motility of individual cells in vivo, for example after brain injury. Although it is widely assumed that astrocytes migrate after CNS injury and, indeed, they do so in in-vitro assays, that has not been shown in vivo so far.

Besides its effect on cytoskeletal rearrangements and migration, Cdc42 has been implicated in cell fate determination following cell division by regulating

cell polarity in different cell types (Cappello et al., 2006; Chen et al., 2006; X. Wu et al., 2006; Yang et al., 2007). For instance, genetic deletion of Cdc42 from radial glia cells during development interferes with proper recruitment of the Par complex and localization of adherens junctions at the apical site of VZ stem cells causing a failure in stem cell self-renewal and premature neurogenic differentiation (Cappello et al., 2006). Accordingly, downregulation of Par3 using siRNA leads to premature cell-cycle exit and neurogenic differentiation, whereas overexpression of Par3 or Par6 promoted the generation of self-renewing progenitors (Costa et al., 2008). The influence of Cdc42 on adult astroglia-like stem cells has not been investigated so far.



### **3 Aims of this study**

Main objective of this thesis is to unravel the role of two major polarity signaling molecules in astrocytes in the healthy and injured brain. Conditional deletion of  $\beta$ 1-integrin and the small RhoGTPase Cdc42 aim to identify the function of these pathways in astrocytes. The consequences of early postnatal deletion of  $\beta$ 1-integrin in the progeny of radial glia cells will be analyzed in regard to morphology, marker expression, and proliferation of gray matter astrocytes in vivo in the intact adult brain and after stab wound injury. The impact of  $\beta$ 1-integrins on stem cell astrocytes will be investigated with respect to proliferation and self-renewing capacity in the same genetic mouse model. Cell type specific deletion of Cdc42 in the adult brain allows exploring the functions of this molecule on parenchymal astrocytes and astroglia-like stem cells. Proliferation of adult NSCs and parenchymal astrocytes after stab wound injury will be also investigated in this model. Moreover, in vitro and in vivo analysis of cell polarity after injury will be conducted and the influence of Cdc42 on wound healing after injury will be examined by determining the lesion size in mice deficient for Cdc42.



## 4 Abbreviations

<b>aPKC</b>	atypical protein kinase C
<b>APS</b>	Ammonium persulfate
<b>Aqp4</b>	Aquaporin-4
<b>ATF-1</b>	Activating transcription factor-1
<b>BBB</b>	Blood-brain barrier
<b>BDNF</b>	Brain-derived neurotrophic factor
<b>bHLH</b>	basic helix-loop-helix
<b>BLBP</b>	Brain lipid-binding protein
<b>BM</b>	Basement membrane
<b>BMP</b>	Bone morphogenic protein
<b>BMPR</b>	Bone morphogenic protein receptor
<b>Bp</b>	Base pairs
<b>BrdU</b>	5-bromo-2-desoxy-uridine
<b>CB</b>	Citrate buffer
<b>cDNA</b>	complementary DNA
<b>CL</b>	Contralateral
<b>CNS</b>	Central nervous system
<b>CNTF</b>	Ciliary neurotrophic factor
<b>Cre</b>	Cyclization recombination protein of the P1 bacteriophage
<b>CREB</b>	cAMP response element binding (protein)
<b>CsCl</b>	Cesium chloride
<b>CSPG</b>	Chondroitin sulfate proteoglycan
<b>CSPG-2</b>	Versican
<b>CTX</b>	Cortex
<b>Da</b>	Dalton
<b>DAG</b>	Dystrophin associated glycoprotein complex
<b>DAPI</b>	4, 6-damindino-2-phenyl-indol

---

<b>Dcx</b>	Doublecortin
<b>DIV</b>	Days in vitro
<b>DNA</b>	Desoxyribonucleic acid
<b>DPL</b>	Days post lesion
<b>dNTP</b>	Deoxynucleotidetriphosphate
<b>E</b>	Embryonic day
<b>EAE</b>	Experimental autoimmune encephalomyelitis
<b>ECM</b>	Extracellular matrix
<b>EDTA</b>	Ethylendiamine tetraacetate
<b>EGF</b>	Epidermal growth factor
<b>EGF-R</b>	Epidermal growth factor receptor
<b>ERK</b>	Extracellular signal-regulated kinase
<b>Epo</b>	Erythropoietin
<b>ET</b>	Endothelin
<b>ET-1</b>	Endothelin-1
<b>ET(A/ B)R</b>	Endothelin (A/ B) receptor
<b>EtBr</b>	Ethidium bromide
<b>EtOH</b>	Ethanol
<b>FACS</b>	Fluorescent activated cell sorting
<b>FBS</b>	Fetal bovine serum
<b>FCS</b>	Fetal calf serum
<b>(b)FGF</b>	(basic) FGF
<b>Fig.</b>	Figure
<b>GAPDH</b>	Glyceraldehyde-3-phosphate dehydrogenase
<b>GDNF</b>	Glial cell-line derived neurotrophic factor
<b>GEF</b>	Guanine exchange factor
<b>GFAP</b>	glial fibrillary acidic protein
<b>(e)GFP</b>	(enhanced) GFP

---

<b>GID</b>	Guanine nucleotide dissociation inhibitors
<b>GLAST</b>	Glutamate-aspartate transporter
<b>GLT-1</b>	Glutamate transporter-1
<b>GM</b>	Gray matter
<b>GPCR</b>	G-protein coupled receptor
<b>GS</b>	Glutamine synthetase
<b>HBSS</b>	Hank's buffered salt solution
<b>Hepes</b>	4-(2-hydroxyethyl)-1-piperazineethanesulfonic acid
<b>hGFAP</b>	human glial fibrillary acidic protein
<b>HPI</b>	Hours after injury
<b>HRP</b>	Horse radish peroxidase
<b>IFN</b>	Interferon
<b>Ig</b>	Immunoglobulin
<b>IGF-1</b>	Insulin growth factor-1
<b>IL</b>	Interleucine
<b>IMF</b>	Intermediate filaments
<b>IP</b>	Intraperitoneal
<b>(n/ o) IPC</b>	(neurogenic/ oligodendrogenic) Intermediate progenitor cell
<b>IRES</b>	Internal ribosomal entry site
<b>JAK</b>	Janus kinase
<b>JNK</b>	c-Jun N-terminal kinase
<b>kDa</b>	Kilo Dalton
<b>KO</b>	Knockout
<b>LIF</b>	Leucemia inhibitory factor
<b>loxP</b>	originally: locus of crossing-over on P1 bacteriophage DNA recognition sequence for Cre recombinase
<b>LTR</b>	Long terminal repeat
<b>LV</b>	Lateral ventricle

---

<b>MA</b>	Mantle
<b>MAG</b>	Myelin associated glycoprotein
<b>MAPK</b>	Mitogen-activated protein kinase
<b>MAP2K</b>	Mitogen-activated protein kinase kinase
<b>MAP3K</b>	Mitogen-activated protein kinase kinase kinase
<b>MBP</b>	Myelin basic protein
<b>MEK</b>	Mitogen-activated ERK regulating kinase
<b>mGFAP</b>	mouse glial fibrillary acidic protein
<b>MMP</b>	Metalloproteinases
<b>mRNA</b>	messenger ribonucleic acid
<b>MTOC</b>	Microtubule organization center
<b>mTOR</b>	mammalian target of rapamycin
<b>n</b>	number of samples
<b>NE</b>	Neuroepithelium
<b>NeuN</b>	Neuronal nuclei
<b>NF</b>	Neurofilament
<b>NGF</b>	Nerve growth factor
<b>Ngn</b>	Neurogenin
<b>NGS</b>	Normal goat serum
<b>NO</b>	Nitric oxide
<b>NSC(s)</b>	Neural stem cell(s)
<b>Nt</b>	Nucleotides
<b>NT-3</b>	Neurotrophin-3
<b>Nu</b>	Nucleosides
<b>OB</b>	Olfactory bulb
<b>ON</b>	Overnight
<b>OPC</b>	Oligodendrocyte precursor cell
<b>P</b>	Postnatal day

---

<b>p</b>	p-value – observed significance level
<b>PBS</b>	Phosphate buffered saline
<b>PCR</b>	Polymerase chain reaction
<b>PDGF</b>	Platelet-derived growth factor
<b>PLO</b>	poly-L-ornithine
<b>PFA</b>	Paraformaldehyde
<b>PTEN</b>	Phosphatase and tensin homolog
<b>RFP</b>	Red fluorescent protein
<b>RG</b>	Radial glia
<b>RMS</b>	Rostral migratory stream
<b>RNA</b>	Ribonucleic acid
<b>ROS</b>	Reactive oxygen species
<b>Rpm</b>	Rounds per minute
<b>RT</b>	Room temperature
<b>SD</b>	Standard deviation
<b>SDS</b>	Sodium dodecylsulfate
<b>SDS-PAGE</b>	SDS-polyacrylamid gel electrophoresis
<b>SEM</b>	Standard error of the mean
<b>SEZ</b>	Subependymal zone
<b>SGZ</b>	Subgranular zone
<b>Shh</b>	Sonic hedgehog
<b>Smad</b>	Signaling mother against decapentaplegic peptide
<b>Socs3</b>	Suppressor of cytokine signaling 3
<b>STAT</b>	Signal transducer and activator of transcription
<b>SVZ</b>	Subventricular zone
<b>TAP</b>	Transit-amplifying precursor
<b>Taq</b>	DNA polymerase of bacterium <i>Thermus aquaticus</i>
<b>TBS</b>	Tris buffered saline

<b>TEMED</b>	N, N, N', N'-tetramethylethylenediamine
<b>TF</b>	Transcription factor
<b>TN-C</b>	Tenascin-C
<b>TGF</b>	Transforming growth factor
<b>TNF</b>	Tumor necrosis factor
<b>TSA</b>	Tyramide signal amplification
<b>Tx</b>	Tamoxifen
<b>TX</b>	TritonX
<b>UTR</b>	Untranslated region
<b>VEGF</b>	Vascular endothelial growth factor
<b>VZ</b>	Ventricular zone
<b>WM</b>	White matter
<b>WT</b>	Wildtype

## 5 Material

### 5.1.1 Equipment

<b>description</b>	<b>company</b>
Binocular MZ6	Leica
Cell culture incubator	Binder
Centrifuge 5430	Eppendorf
Centrifuge 5810R	Eppendorf
Centrifuge Mikro22R	Hettich
Centrifuge Rotofix32 (cell culture)	Hettich
Centrifuge Sorvall Evolution RC	Thermo Fisher
Centrifuge (table centrifuge)	neolab
Centrifuge Optima™ LE-80K (Ultracentrifuge)	Beckman Coulter
Cold-light source KL1500LCD	Leica
Cryostate CM 3050	Leica
Dounce tissue grinder (1 ml)	Wheaton
Freezer	Privileg, Liebherr
Geldoc™ XR	BIO-RAD
Laminar flow	Bdk
Magnetic stirrer IKAMAG® RCT	Bachofer
Microscope Axiovert 40CFL with fluolamp HXP120 (Kübler) and camera A640 (Canon)	Zeiss
Microscope SPE (confocal microscope)	Leica
Microscope SP5 (confocal microscope)	Leica
Microscope LSM700 (confocal microscope)	Zeiss
Microscope Fluo Olympus BX61 (fluorescence microscope)	Olympus
Microscope Observer.Z1 (timelapse microscope)	Zeiss
Microwave	Privileg
Odyssey Scanner	LI-COR
Perfusion pump	Gilson
pH meter	WTW
Picopump PV 820 connected to Jun-Air compressor (Condor)	WPI
Pipette grinder EG-44	Narishige
Power supply Power Pac 200	BIO-RAD
Power supply ST606	Gibco BRL

description	company
Pulse/delay generator PDG 204	Scientific Instruments
Refrigerators	Privileg, Liebherr
Scale	Scaltec
Scale analytic (precision scale)	Sartorius
Semi-Dry Transfer Cell Trans-Blot® SD	BIO-RAD
Shaker IKA-Vibrax-VXR	electronic
Shaker RM5 (rotary shaker)	Assistant
Shaker Duomax 1030	Heidolph
Shaker Vortemp56EVC	Uniequip
Spectral photometer Prim advanced	Secoman
Stereotactic apparatus	Stoelting
Thermocycler 3000	Biometra
Thermomixer comfort	Eppendorf
Ultrasonic bath 2510	Branson
Ultrathorax Sonopuls	Bandelin
Vertical pipette puller 720	David Kopf Instruments
Vibratome VT1000S	Leica
Vortex IKA MS 3	Basic
Vortex-Genie	Bender & Hobein AG
Water bath (cell culture)	Memmert

**Table 5-1 Equipment**

## 5.2 Consumables

description	company
Augen- und Nasensalbe	Bepanthen
BC assay reagent A	Uptima
BC assay reagent B	Uptima
Cell culture flask with filter lid Cellstar® (T25, T75, T175), PS red	greiner bio-one
Drill	Foredom
filaments (Vicryl, 4-0, SH-1 plus, 21.8 mm ½c, 70 cm)	Ethicon
filter/strainer 70 µm	BD Transduction Laboratory
gloves (latex)	Diana Baronin von Schaezler
gloves Nitra-Tex® (nitrile)	Ansell

description	company
insulin needles, U-100, 1 ml	BD Micro Fine (PZN: 324870)
Kwik-Fil Borosilicate glass capillaries	WPI (1B150F-4)
Millex HV low protein binding PVDF, 0.45 µm syringe filters, yellow rim, 33 mm diameter (SLHV033RS) for viral supernatants	Millipore
OptiSeal tube (11.2 ml)	Beckmann
Parafilm PM-996	Parafilm
pipette tips	
Phase Lock Heavy 50 ml tube	
Reaction tube( 0.5 ml, 1.5 ml, 2 ml)	Plastibrand
Reaction tube (15 ml, 50 ml)	greiner
Serological pipettes (5 ml, 10 ml, 25 ml)	Sarstedt
Steritop filter (250 ml, 500 ml)	Millipore
Sugi	Kettenbach GmbH (REF 31603)
Syringes 30 ml	Sarstedt
V-Lance™ Knife, 19 Gauge	Alcon® Surgical (8065 911901)

Table 5-2 Consumables

## 5.3 Chemicals

Chemical		M in g/mol	company	catalogue number
Acetone	C <sub>3</sub> H <sub>6</sub> O	58.08	Roth	9372.4
Acetic acid glacial	C <sub>2</sub> H <sub>4</sub> O <sub>2</sub>	60.05	Roth	3738.4
Acetic anhydride	(CH <sub>3</sub> CO) <sub>2</sub> O	102.09	Sigma	32,010-2
Agarose			Serva	11404
Ammonium bicarbonate	NH <sub>4</sub> HCO <sub>3</sub>	79.06	Roth	A-6141
Ammonium chloride	NH <sub>4</sub> Cl	53.49	Sigma	A-9434
Ammonium nitrate	NH <sub>4</sub> NO <sub>3</sub>	80.04	Sigma	256064-25g
Ammonium peroxodisulfate	(NH <sub>4</sub> ) <sub>2</sub> S <sub>2</sub> O <sub>8</sub>	228.28	Roth	9592.3
Brilliant blue R	C <sub>45</sub> H <sub>44</sub> N <sub>3</sub> O <sub>7</sub> S <sub>2</sub> Na	826	Sigma	B-7920
Bromophenol blue	C <sub>19</sub> H <sub>9</sub> Br <sub>4</sub> O <sub>5</sub> SNa	691.9	Sigma	B-8026
5-Bromo-2'-Deoxy-Uridine	BrdU	307.1	Sigma	B5002-5g

Chemical		M in g/mol	company	catalogue number
Calcium chloride dihydrate	$\text{CaCl}_2 \times 2\text{H}_2\text{O}$	147.0	Sigma	C-7902
Cesium chloride	CsCl	168.36	Roth	8627.2
Chloral hydrate	$\text{C}_2\text{H}_3\text{Cl}_3\text{O}_2$	165.4	Sigma	C-8383
4',6-diamidino-2-phenylindole, dilactate (DAPI)		457.5	Invitrogen	D-3571
Corn oil			Sigma	C-8267
Diethyl ether	$(\text{C}_2\text{H}_5)_2\text{O}$	74.12	Merck	K37257821 729
Dimethylarsinic acid sodium salt trihydrate	$\text{C}_2\text{H}_6\text{AsNaO}_2 \times 3\text{H}_2\text{O}$	214.05	Merck	8.20670.0100
Ethanol	$\text{C}_2\text{H}_6\text{O}$	46.07	Roth	9065.4
70% Ethanol	$\text{C}_2\text{H}_6\text{O}$	46.07	Roth	T913.3
Ethanolamine	$\text{C}_2\text{H}_7\text{NO}$	61.08	Sigma	E0135-100ML
Ethylene glycol	$\text{HOCH}_2\text{CH}_2\text{OH}$	62.07	Sigma	10,246-6
Ethylene glycol-bis-N,N,N',N', Tetraacetic acid (EGTA)	$\text{C}_{14}\text{H}_{20}\text{N}_2\text{O}_{10}\text{Na}_4$	468.3	Sigma	E-8145
Ethylenediamine-tetraacetic acid (EDTA)	$\text{C}_{10}\text{H}_{14}\text{N}_2\text{O}_8\text{Na}_2 \times 2\text{H}_2\text{O}$	372.2	Sigma	E-5134
Formaldehyde	$\text{CH}_2\text{O}$	30.03	Roth	4979.1
Formamide	$\text{CH}_3\text{NO}$	45.04	Roth	6749.1
D(+)-Glucose-Monohydrat	$\text{C}_6\text{H}_{12}\text{O}_6 \times \text{H}_2\text{O}$	198.17	Merck	1.08342.1000
Glutaraldehyde 25% solution in water	$\text{C}_5\text{H}_8\text{O}_2$		Serva	23115
Glycerol	$\text{C}_3\text{H}_8\text{O}_3$	92.09	Sigma	G6279-1L
Glycine	$\text{C}_2\text{H}_5\text{NO}_2$	75.07	Sigma	G8790-1KG
HEPES	$\text{C}_8\text{H}_{18}\text{N}_2\text{O}_4\text{S}$	238.31	Sigma	H3375-1KG
Hydrochloric acid	HCl	36.46	Merck	1-13386.2500
Igepal CA-630	$(\text{C}_2\text{H}_4\text{O})_n \times \text{C}_{14}\text{H}_{22}\text{O}$		Sigma	I3021-50ML
Isoamyl alcohol	$\text{C}_5\text{H}_{12}\text{O}$	88.15	Sigma	I-9392
10% Ketamin			cp-pharma	
Lead(II)nitrate	$\text{Pb}(\text{NO}_3)_2$		Sigma	22,862-1
Magnesium sulphate heptahydrate	$\text{MgSO}_4 \times 7\text{H}_2\text{O}$	246.5	Sigma	M-1880
Magnesium sulphate	$\text{MgSO}_4 \times 6\text{H}_2\text{O}$	203.3	Merck	1.05833.0250

Chemical		M in g/mol	company	catalogue number
hexahydrate				
2-Mercaptoethanol	C <sub>2</sub> H <sub>6</sub> OS	78.13	Sigma	M7522-100ML
0,9% NaCl solution	NaCl		Braun	
Osmium tetroxide solution, 4 %	OsO <sub>4</sub>	254,23	Sigma	75632
Paraformaldehyde			Sigma	P6148
2-Propanol	C <sub>3</sub> H <sub>8</sub> O	60.1	Roth	6752.5
Polyethylene glycol 6000	HO (C <sub>2</sub> H <sub>4</sub> O) <sub>n</sub> H		Merck	12033.0100
Polyvinyl alcohol 4-88			Fluka	81381
Potassium acetate	C <sub>2</sub> H <sub>3</sub> KO <sub>2</sub>	98.15	Roth	T874.2
Potassium chloride	KCl	74.56	Sigma	P-9541
Potassium dihydrogen phosphate	KH <sub>2</sub> PO <sub>4</sub>	136.09	Merck	1.04873.1000
Potassium phosphate	K <sub>2</sub> HPO <sub>4</sub>	174.2	Sigma	P-3786-500G
Potassium hydroxide	KOH	56.11	Sigma	P-5958
Potassium permanganate	KmnO <sub>4</sub>	158.04	Fluka	60459
Potassium phosphate	KH <sub>2</sub> PO <sub>4</sub>	136.1	Sigma	P-0662
Putrescine dihydrochloride	C <sub>4</sub> H <sub>12</sub> N <sub>2</sub> x 2H <sub>2</sub> O	161.1	Sigma	P-5780
Pyridine	C <sub>5</sub> H <sub>5</sub> N	79.1	Sigma	49,441-0
Saccharose	C <sub>12</sub> H <sub>22</sub> O <sub>11</sub>	342.3	Merck	1.07651.1000
Silver nitrate	AgNO <sub>3</sub>	169.88	Sigma	20,913-9
Sodium acetate trihydrate	C <sub>2</sub> H <sub>3</sub> NaO <sub>2</sub> x 3H <sub>2</sub> O	136.08	Roth	6779.1
Sodium cacodylate trihydrate	C <sub>2</sub> H <sub>6</sub> AsNaO <sub>2</sub> x 3H <sub>2</sub> O	214.0	Sigma	C0250-100G
Sodium bicarbonate	NaHCO <sub>3</sub>	84.01	Sigma	S-5761
Sodium carbonate	Cna <sub>2</sub> O <sub>3</sub>	105.99	Fluka	71345
Sodium chloride	NaCl	58.44	Sigma	S-3014
Sodium citrate dehydrate	C <sub>6</sub> H <sub>5</sub> Na <sub>3</sub> O <sub>7</sub> x 2H <sub>2</sub> O	294.1	Sigma	S-4641
Sodium dodecyl sulphate	C <sub>12</sub> H <sub>25</sub> O <sub>4</sub> SNa	288.4	Sigma	L-4509
di-Sodium hydrogen phosphate dihydrate	Na <sub>2</sub> HPO <sub>4</sub> x 2H <sub>2</sub> O	177.99	Merck	1.06580.1000
Sodium hydroxide	NaOH	40	Fluka	71690
Sodium hydroxide pellets	NaOH	40	Sigma	S-5881

Chemical		M in g/mol	company	catalogue number
Sodium nitrite	$\text{NNaO}_2$	69.0	Fluka	71759
Sodium phosphate	$\text{NaH}_2\text{PO}_4 \times \text{H}_2\text{O}$	138	Sigma	S-9638
Sodium pyrophosphate decahydrate	$\text{Na}_4\text{P}_2\text{O}_7 \times 10\text{H}_2\text{O}$	446.1	Sigma	S-6422
di-Sodium tetraborate	$\text{Na}_2\text{B}_4\text{O}_7$	201.22	Merck	1.06306.0250
Sodium thiosulfate	$\text{Na}_2\text{S}_2\text{O}_3$	158.11	Sigma	S7026-250G
Sudan black B	$\text{C}_{29}\text{H}_{24}\text{N}_6$	456.54	Sigma	19,966-4
5-Sulfosalicylic acid dihydrate	$\text{C}_7\text{H}_6\text{O}_6\text{S} \times 2\text{H}_2\text{O}$	254.22	Roth	4119.1
Tamoxifen	$\text{C}_{26}\text{H}_{29}\text{NO}$	371.52	Sigma	T-5648
TO-PRO-3			Invitrogen	T-3605
Triethanolamine Hydrochloride	$\text{C}_6\text{H}_{15}\text{NO}_3 \times \text{HCl}$	185.7	Sigma	T-1502
Triton X-100	$(\text{C}_2\text{H}_4\text{O})_n \times \text{C}_{14}\text{H}_{22}\text{O}$		Sigma	X100-1L
Trizma base	$\text{C}_4\text{H}_{11}\text{NO}_3$	121.14	Sigma	T-1503-1KG
Urea	$\text{CH}_4\text{N}_2\text{O}$	60.06	Roth	2317.1
2% Xylazinhydrochlorid			Bayer	
Xylene cyanole	$\text{C}_{25}\text{H}_{27}\text{N}_2\text{O}_6\text{S}_2\text{Na}_2$	538.6	Sigma	X-4126

Table 5-3 Chemicals

## 5.4 Plasmids

For packaging of viral vectors by 293T cells for lentiviral production the following plasmids were used:

pCMVΔR8.9 packaging vector (2<sup>nd</sup> generation; Naldini L., Trono D.): expressing HIV structural proteins, HIV reverse transcriptase, and the HIV transactivator TAT.

Lentiviral expression plasmid (Pfeifer et al., 2001): containing the insert of interest under an internal promoter, a self-inactivating 3'LTR and retroviral regulatory sequences for efficient processing of viral genomic RNA and proviral DNA.

pVSVG envelope vector: expressing a pseudotyping viral envelope glycoprotein, here vesicular stomatitis virus glycoprotein under the CMV promoter.

## 5.5 Solutions and Media

### 5.5.1 DNA preparation and genotyping PCR

#### Lysis buffer

1 M	NaCl
1 M	Tris/HCl pH 8.5
10 %	SDS
0.5 M	EDTA
10 mg/ ml	Proteinase K
in H <sub>2</sub> O <sub>dd</sub>	

10 mM Tris buffer to solve DNA

1.211g                      Tris base

ad 1000 ml H<sub>2</sub>O<sub>dd</sub>, pH 8.0

10 x PCR buffer (A)

500 mM                      KCl

100 mM                      Tris/ HCl

pH 8.7

10 x PCR buffer (B)

500 mM                      KCl

100 mM                      Tris base

150 mM                      (NH<sub>4</sub>)<sub>2</sub>SO<sub>4</sub>

15 mM                        MgCl<sub>2</sub> x 6 H<sub>2</sub>O

dNTP mix

2.5 mM each                dATP, dTTP, dGTP, dCTP

in H<sub>2</sub>O<sub>dd</sub>

50 x TAE

242 g                        Tris

32.2 g                        Na<sub>2</sub>EDTA

57.1 mg                      acetic acid (100 %)

ad 1000 ml H<sub>2</sub>O<sub>dd</sub> , pH 8.0

4 x DNA loading buffer

20 ml                    100% Glycerin  
1 ml                     50 x TAE  
200 µl                  Bromophenol blue  
500 µl                  Xylene cyanol solution  
ad 50 ml H<sub>2</sub>O<sub>dd</sub>

**5.5.2 tissue preparation**Tamoxifen

40 mg/ ml              Tamoxifen  
10 %                    Ethanol  
in corn oil  
to solve shake at 37 °C 3-4 h

BrdU – drinking water

1 mg/ ml                5-Bromo-2-desoxyuridin  
10 mg/ ml              Saccharose  
in Aqua

20 % Paraformaldehyd (PFA) stock

67 g                     Na<sub>2</sub>HPO<sub>4</sub> x 2 H<sub>2</sub>O in 800 ml H<sub>2</sub>O<sub>dd</sub>  
heat to 60 °C  
200 g                    PFA  
ca. 10 ml                NaOH  
filtrate by the use of paper filters  
ad 2 l H<sub>2</sub>O<sub>dd</sub>, pH 7.4  
freeze 50ml aliquots at -20 °C

2 % Paraformaldehyd

50ml                      PFA 20 %  
ad 500 ml H<sub>2</sub>O<sub>dd</sub>

4% Paraformaldehyd

100ml                     PFA 20 %  
ad 500 ml H<sub>2</sub>O<sub>dd</sub>

Phosphate buffer 0.25M, pH 7.2-7.4

0.025 N                  HCl  
1 M                        NaOH  
0.85 M                  NaH<sub>2</sub>PO<sub>4</sub>

30 % Saccharose solution for cryoprotection

15 g                        Saccharose  
ad 50 ml 1 x PBS

Storing solution for floating sections

4 M                        Glycerol  
5.4 M                     Ethylenglycol  
25 mM                   phosphate buffer, pH 7.2 - 7.4

### **5.5.3 Immuno-histochemistry/ cytochemistry**

#### 10 x phosphate buffered saline (PBS) (1,5 M)

1.5 M                    NaCl  
0.03 M                 KCl  
0.080 M               Na<sub>2</sub>HPO<sub>4</sub> x 2 H<sub>2</sub>O  
0.010 M               KH<sub>2</sub>PO<sub>4</sub> pH 7.5  
in H<sub>2</sub>O<sub>dd</sub>, pH 7.4

#### blocking/ dilution buffer (sections)

0.5 %                   TritonX100  
10 %                    goat or donkey serum  
in 1 x PBS

#### blocking/ dilution buffer (cells)

0.1 %                   TritonX100  
10 %                    goat or donkey serum  
in 1 x PBS

#### 4',6-Diamidino-2-phenylindol (DAPI) stock

10.9 mM                DAPI, dilactate in H<sub>2</sub>O<sub>dd</sub>

#### Sodium citrate buffer 0,1 M

29.41 g                 sodium citrate  
ad 1000 ml H<sub>2</sub>O<sub>dd</sub>, pH 6.0

TO-PRO-3 Iodide stock

1 mM in DMSO

**5.5.4 Western blot**Lysis buffer (total lysates)

50 mM Tris-HCl, pH 7.4

0.15 M NaCl

1% TritonX 100

10% Glycerin

5 mM EDTA

Protease inhibitors: 4.2  $\mu$ M leupeptin, 100 nM aprotinin, 5.8  $\mu$ M pepstatin, 1.7 mM pefabloc

4x loading dye

2 ml 1M Tris HCl pH 8.5

8 ml 20 % SDS

5 ml Glycerin

1.6 ml  $\beta$ -Mercaptoethanol

3.4 ml H<sub>2</sub>O<sub>dd</sub>

50 mg Bromphenol blue

**5.5.5 Electron microscopy**Cacodylat solution

0.2 M Cacodylate

21.4 g Dimethylarsinic acid sodium salt trihydrate

0.22 g CaCl dehydrate

ad 500 ml H<sub>2</sub>O<sub>dd</sub>, pH 7.2



### 5.5.6 Cell culture media and supplements

description	company	catalog number
B27	Gibco	17504-044
basic fibroblast growth factor (FGF)	Gibco	13256029
Bovine serum albumin (BSA)	Sigma	A4503
D-Glucose 45%	Sigma	G8769
Dulbecco's Modified Eagle Medium (DMEM) + GlutaMAX™ low glucose for astrocytes	Gibco	21885
DMEM + GlutaMAX™ high glucose	Gibco	61965
DMEM + GlutaMAX™ high glucose, 25mM HEPES	Gibco	32430
DMEM/ F12 + GlutaMAX™ for neurospheres	Gibco	31331
DMEM/ F12	Gibco	21331
Earle's Balanced Salt Solution (EBSS)	Life Technologies	24010-043
Fetal bovine serum	Gibco	10106169
Geneticin (G418)	Invitrogen	ant-gn-1
Hank's Balanced Salt Solution (HBSS)	Gibco	24020
HEPES 1M	Gibco	15630
human epidermal growth factor (EGF)	Gibco	13247051
Hyaluronidase	Sigma	H3884
L-Glutamine 200mM	Gibco	25030
Lipofectamine	Invitrogen	11668-019
Neurobasal A	Gibco	10888022
OPTI-MEM® + GlutaMAX™	Gibco	51985
Penicillin/Streptomycin 100x	Gibco	15070063
poly-L-ornithine	Sigma	P4957
Sucrose	Sigma	S1888
Trypsin/EDTA 0.05%	Gibco	25300054
Trypsin	Sigma	T4665

**Table 5-4 Cell culture reagents**

Astrocyte medium

DMEM, GlutaMAX™, low glucose (1 g/ L)

10 %            Fetal bovine serum

10                mM Hepes

1x                Penicillin/ Streptomycin

Filter through 0.2 µm 500 ml Steritop filter to remove particles

Aliquote into 50 ml reaction tubes

Solution 1 (HBSS-Glucose)

50 ml            HBSS

9 ml             D-Glucose

7.5 ml          Hepes (1 M)

ad 500 ml H<sub>2</sub>O<sub>dd</sub>, pH 7.5

Solution 2 (Sucrose-HBSS)

25 ml            HBSS

154 g            Sucrose

475 ml          H<sub>2</sub>O<sub>dd</sub>, pH 7.5

Solution 3 (BSA-EBSS-Hepes)

20 g             BSA

10 ml            Hepes

490 ml          EBSS, pH 7.5

Neurosphere medium

48 ml        DMEM/ F12 + GlutaMAX™  
1 ml         B27  
8 mM        Hepes  
100 units/ ml Penicillin/Streptomycin  
10 µg/ ml    EGF  
10 µg/ ml    FGF

Neurosphere differentiation medium

48 ml        Neurobasal A  
500 µl       Glutamate  
500 µl       Penicillin/Streptomycin  
1 ml         B27

Dissociation medium

10 ml        Solution 1  
13,3 mg     Trypsin (Sigma)  
7 mg        Hyaluronidase

Stock medium for propagation of 293T cells

DMEM high glucose, GlutaMAX™, Hepes  
10 %        FCS  
500 µg/ ml    Geneticin (G418)

Transfection medium (lentivirus production)

Opti-MEM, GlutaMAX™  
(10%        FCS)

Packaging medium (lentivirus production)

DMEM high glucose, GlutaMAX™, Hepes

10% FCS

No G418 or any other antibiotic!

TBS-5 buffer for viral vector re-suspension

5 ml 1 M Tris-HCl, pH 7.8 (final concentration: 50 mM)

2.6 ml 5 M NaCl (130 mM)

1 ml 1 M KCl (10mM)

0.5 ml 1 M MgCl<sub>2</sub> (5 mM)

ad 100 ml tissue culture grade water

storage at 4 °C

## 6 Methods

### 6.1 Animals

All animal procedures were performed in accordance with the policies of the use of Animals and Humans in Neuroscience Research, revised and approved by the Society of Neuroscience and the state of Bavaria under licence number 55.2-1-54-2531-23/04 and 55.2-1-54-2531-144/07.

#### 6.1.1 Mouse strains

129/Sv- $\beta$ 1-integrin, carrying floxed alleles of  $\beta$ 1-integrin (Potocnik et al., 2000)

C57Bl/6//129/Sv- $\beta$ 1-integrin, carrying loxP sites flanking exon2 of the  $\beta$ 1-integrin gene (unpublished)

C57Bl/6//129/Sv- $\beta$ 1-integrin null, carrying one  $\beta$ 1-integrin knockout allele (Fassler and Meyer, 1995)

C57Bl/6J//129/Sv-Cdc42, carrying floxed alleles of Cdc42 (X. Wu et al., 2006)

C57Bl/6J//129/Sv-Rac1, carrying floxed alleles of Rac1 (Chrostek et al., 2006)

C57Bl/6J//129/Sv-RhoA, carrying floxed alleles of RhoA (unpublished)

C57Bl/6J-Dystroglycan, carrying floxed alleles of Dystroglycan (Moore et al., 2002)

C57Bl/6//129/Sv-GFAP null, carrying a deletion of the GFAP gene (Pekny et al., 1995)

C57Bl/6//129/Sv-vimentin null, carrying a null mutation of the vimentin gene (Colucci-Guyon et al., 1994)

hGFAP-Cre, expressing Cre recombinase from the human GFAP promoter (Zhuo et al., 2001)

hGFAP-eGFP, expressing enhanced GFP under the human GFAP promoter (Nolte et al., 2001)

Nex::Cre, expressing Cre recombinase in the Nex locus (Goebbels et al., 2006)

GLAST::CreERT2, expressing a Cre recombinase estrogen receptor fusion protein in the GLAST locus (Mori et al., 2006)

Z/EG reporter mouse line, expressing enhanced green fluorescent protein (EGFP) behind a Stop cassette flanked by loxP sites (Novak et al., 2000)

CAG-CAT-EGFP reporter mouse line, expressing the CMV- $\beta$ -actin promoter and the loxP flanked chloramphenicol acetyl-transferase (CAT) gene upstream of the EGFP cassette (Nakamura et al., 2006)

The  $\beta$ 1-integrin floxed and full knockout lines were kindly provided by Dr. R. Fässler, MPI for Biochemistry, Martinsried, the lines C57Bl/6J//129/Sv-Cdc42, C57Bl/6J//129/Sv-Rac1 and C57Bl/6J//129/Sv-RhoA by Dr. C. Brakebusch, University of Copenhagen, the C57Bl/6J-Dystroglycan mice by Dr. K. Campbell, Howard Hughes Medical Institute, the hGFAP-Cre line by Dr. R. Klein, MPI for Neurobiology, Martinsried, the Nex::Cre line by Dr. S. Göbbels, MPI for Experimental Medicine, Göttingen, and the GFAP Vimentin full KO line by Dr. Milos Pekny, University of Gothenburg, Gothenburg.

### **6.1.2 Genotyping of transgenic animals**

Genotyping by polymerase chain reaction (PCR) was performed on genomic DNA extracted from mouse tails.

To identify and genotype individual animals, ears were clipped with numbered tags and tail biopsies of less than 5 mm length were taken. The tails were transferred to 1.5 ml reaction tubes and incubated in 0.5 ml lysis buffer (see solutions) at 55°C in a shaker at 100 rpm until the tails were dissolved (at least 2h). After lysis hairs and tissue residues were re-moved by centrifugation at 14,000 rpm for approximately 5 minutes. The supernatant was transferred to a new 1.5 ml tube and DNA was precipitated by adding 0.5 ml Isopropanol, followed by another centrifugation step (14,000 rpm, 10 minutes). The

supernatant was removed from the pellet and tubes were dried upside down for 30 minutes at room temperature until the DNA was completely dry. The dry DNA was dissolved in 200  $\mu$ l 10 mM Tris Buffer pH 8, followed by 30 minutes shaking at 55°C.

The DNA was kept at 4°C until polymerase chain reactions (PCRs) were run. PCR reactions using the DNA primers listed in table 5 were pipetted on ice according to table 6 and cycled as described in table 7.

Table 6-1 Primer sequences for genotyping of transgenic animals

line	primer sequence
$\beta$ 1-integrin	5'-AGG TGC CCT TCC CTC TAG A-3' 5'-GTG AAG TAG GTG AAA GGT AAC-3'
$\beta$ 1 full KO	5'-AGG TGC CCT TCC CTC TAG A-3' 5'-TAA AAA GAC AGA ATA AAA CGC AC-3'
Cdc42	5'-TTG TAA TGT AGT GTC TGT CCA TTG G-3' 5'-TGT CCT CTG CCA TCT ACA CAT ACA C-3'
Rac1	5'-GTC TTG AGT TAC ATC TCT GG-3' 5'-CTG ACG CCA ACA ACT ATG C-3'
RhoA	5'-AGC CAG CCT CTT GAC CGA TTT A-3' 5'-TGT GGG ATA CCG TTT GAG CAT-3' 5'-ATG TCA AAG AGG AAA TAC TGC-3'
Dystroglycan	5'-GGA GAG GAT CAA TCA TGG-3' 5'-CAA CTG CTG CAT CTC TAC-3'
GFAP full KO	5'-TGT TCT CCT CTT CCT CAT CTC C-3' 5'-ATT GTC TGT TGT GCC CAG TC-3' 5'-GTC CAG CCG CAG CCG CAG-3' 5'-CTC CGA GAC GGT GGT CAG G-3'
Vimentin full KO	5'-AGC TGC TCG AGC TCA GCC AGC-3' (vas) 5'-TGT CCT CGT CCT CCT ACC GC-3' (vs) 5'-CTG TTC GCC AGG CTC AAG GC-3' (ns)
hGFAP-Cre	5'-ACT CCT TCA TAA AGC CCT CG-3' 5'-ATC ACT CGT TGC ATC GAC CG-3'
Nex::Cre	5'-CCG CAT AAC CAG TGA AAC AG-3' 5'-AGA ATG TGG AGT AGG CTG AC-3' 5'-GAG TCC TGG AAT CAG TCT TTT TC-3'
GLAST::CreERT2	5'-GAG GCA CTT GGC TAG GCT CTG AGG A-3' 5'-GAG GAG ATC CTG ACC GAT CAG TTG G-3' 5'-GGT GTA CGG TCA GTA AAT TGG ACA T-3'
Z/EG and hGFAP-eGFP	5'-TTC ACC TTG ATG CCG TTC T-3' 5'-GCC GCT ACC CCG ACC AC-3'
CAG-CAT-EGFP	5'-CTG CTA ACC ATG TTC ATG CC-3' 5'-GGT ACA TTG AGC AAC TGA CTG-3'

Table 6-2 PCR reactions

line	10x buffer	MgCl (25mM)	primers	dNTPs	Taq	Q-solution	DNA	H <sub>2</sub> O
β1-integrin	3 μl (A)	3 μl	1.5 μl each	0.6 μl	1 μl		1 μl	18.4 μl
β1 full KO	3 μl (B)		1.2 μl each	0.6 μl	1 μl	6 μl	1 μl	16 μl
Cdc42	2.5 μl (B)		1 μl each	0.5 μl	0.5 μl		2 μl	17.5 μl
Rac1	2 (B)		1 μl each	0.5 μl	0.5 μl		2 μl	13 μl
RhoA	2 μl (B)		0.2 μl each	0.4 μl	1 μl		2 μl	14.2 μl
Dystroglycan	2.5 μl (B)		0.5 μl each	0.5 μl	1 μl		1 μl	19.5 μl
GFAP full KO	2.5 μl (B)		0.75 μl each	0.5 μl	0.5 μl	0.25 μl 10% Tween20	1 μl	17.3 μl
Vimentin full KO	2.5 μl (A)	2.6 μl	1 μl (ns, vs) 3 μl (vas)	0.5 μl	0.5 μl		2 μl	11.9 μl
hGFAP-Cre	3 μl (A)	3 μl	1 μl each	0.6 μl	1 μl	6 μl	1 μl	13.5 μl
Nex::Cre	2 μl (NEB)		0.5 μl each	0.5 μl	0.2 μl (NEB)		1 μl	14.8 μl
GLAST::CreERT 2	2.5 μl (A)	2.5 μl	1 μl each	0.5 μl	1 μl	5 μl	1 μl	9.5 μl
Z/EG	.5 μl (A)	0.5 μl	1 μl each	0.5 μl		4 μl	1 μl	14 μl
CAG-CAT-EGFP	2.5 μl	1.5 μl	1 μl each	0.5 μl	0.5 μl	5 μl	1 μl	12 μl

Table 6-3 Cycling conditions

line	annealing temperature	annealing time	elongation time	cycles	fragment size
$\beta$ 1-integrin	55°C	30 sec	30 sec	35	wt: 350bp fl: 500bp
$\beta$ 1 full KO	63°C 53°C	30 sec 30 sec	30 sec 30 sec	10 35	null allele: 210 bp
Cdc42	53°C	30 sec	45 sec	35	wt: 200 bp fl: 300 bp
Rac1	63°C 53°C	30 sec 30 sec	30 sec 30 sec	10 35	wt: 200bp fl: 280bp
RhoA	55°C	30 sec	30sec	35	wt: 297 bp fl: 393 bp
Dystroglycan	55°C	60 sec	60 sec	36	wt: 509 bp fl: 615 bp
GFAP full KO	65°C 65°C	30 sec 30 sec	30 sec 20 sec	5 35	wt: 350 bp KO: 140 bp
Vimentin full KO	65°C	60 sec	60 sec	35	wt: 396 bp KO: 533 bp
hGFAP-Cre	60°C	60 sec	60 sec	30	tg: 200 bp
Nex::Cre	53°C	30 sec	60 sec	40	wt: 770 bp tg: 520 bp
GLAST::CreERT2	55°C	20 sec	30 sec	35	wt: 700 bp tg: 400 bp
Z/EG	59°C	30 sec	20 sec	30	tg: 400 bp
CAG-CAT-EGFP	55°C	30 sec	60 sec	30 sec	tg: 350 bp

### **6.1.3 Tamoxifen administration**

Mice older than 2 months received tamoxifen (250 µl; 10 mg) orally three times: once a day every second day for five days or by injection twice a day for five consecutive days (100µl; 1mg per injection). Neonatal pups gathered Tamoxifen via the milk of their mothers. Mothers received 12 mg tamoxifen orally once.

### **6.1.4 Stereotactic operations**

Microsurgery for stab wound injuries and/or viral injections into different regions of the adult murine brain were performed according to the following protocol.

#### **Anesthesia**

Mice were deeply anaesthetized with around 100 µl up to 180 µl (depending on the body weight) using the following mix: 1.0 ml Ketamin 10 %, (injected at approximately 100 mg/kg), 0.25 ml 2% Xylazin Hydrochloride (injected at 5 mg/kg body weight) and 2.5 ml 0.9 % NaCl solution. For injection of the anesthesia insulin needles were the most suitable device because of their very short and thin cannula. After injection mice were checked for fading pain reactions, i.e. pinching the tail or toes, and reflexes. If reflexes persisted additional 20 – 50 µl anesthetics were injected.

#### **Injection**

Mice were fixed in the stereotactic apparatus and eyes were kept wet using Bepanthen Augen- und Nasensalbe. The fur on top of the head was disinfected with 70 % EtOH and a small midline incision was performed. The skull was dried with a Sugi and bregma was searched by pressing gently on the skull with forceps. The digital display of the stereotactic apparatus was set to zero after an empty glass capillary was set onto bregma and a very small dot with a pen was

put on the skull under the glass capillary to find the zero point for the following injections easier. The capillary was set to the coordinates and a dot was put on the skull at the position of the coordinates. A drill was used to open the skull cautiously at the position of the dots so that the meninges stayed intact. Coordinates were re-checked, using again the empty glass capillary. A new capillary was inserted containing now viral suspension and set again onto bregma. The digital display was adjusted to zero again and 0.5 – 1 µl viral suspension was injected at the coordinates very slowly (5 – 10 min) using an air system. A pulse generator gave a pulse every 5 or 10 seconds and pulses were given at the lowest possible pressure and pulse length. After finishing the injection the capillary was retracted 2 minutes up to 5 minutes. The skin covering the skull was sewed by filaments with 3 stitches. For recovery from anesthesia mice were put in an airing cupboard at 37°C and checked every 5 – 10 minutes.

#### Stab wound injury

Mice were fixed in the stereotactic apparatus and prepared as described above. For stab wound injuries a V-lance knife, instead of a glass capillary was inserted into the stereotactic apparatus. After trepanation a 1.5 mm long/ 0.6 mm deep cut was positioned usually in the right sensorimotor cortex avoiding large meningeal vessels to circumvent extensive bleeding.

#### **6.1.5 BrdU labeling**

For labeling dividing cells the DNA base analogue 5-Bromo-2'-deoxy-Uridine (BrdU) was injected Intraperitoneal (50 mg/kg body weight) one to two hours before perfusion to label fast proliferating cells (short pulse). BrdU was dissolved at a concentration of 5 mg/ml in sterile 0.9 % NaCl solution. Complete solution of BrdU could only be reached by shaking the solution for 2 hours at 37 °C. Aliquots were stored at -20 °C. For marking slow and fast dividing cells BrdU was given into the drinking water at a concentration of 1 mg/ml (1 %

sucrose was added for better acceptance) and stirred for at least 1 hour at room temperature. 50 ml of BrdU-water was sufficient for 2 - 3 mice per cage for 2 - 3 days and was exchanged two times per week. BrdU drinking water containing sucrose was stored in the fridge up to one week.

## 6.2 Histology

Adult animals were deeply anaesthetized by intraperitoneal injection of Ketamin/Xylacine and, as soon as respiratory depression began, transcardially perfused with phosphate buffered saline (PBS) followed by 2 % or 4 % paraformaldehyde (PFA) in PBS (100 ml/ animal). Brains were post-fixed in the same fixative for at least 2 hours to maximal overnight at 4 °C and either cryoprotected in 30 % sucrose for cutting 30 µm floating sections at the cryostat (chamber temperature: 4 °C; temperature of object head: -35 °C for freezing the brain, -10 °C for cutting) or stored in PBS for later embedding in 4 % agarose and cutting 60 µm vibratome sections. Sections were kept in storing solution at -20 °C.

### 6.2.1 Immunohistochemistry

For immuno-labeling sections were incubated over night at 4 °C in a solution containing the first antibody, 0.5 % Triton 100 (TX) and 10 % normal goat serum (NGS).

Distinct pre-treatments were used to increase the specificity of different antibodies:

#### Citrate-buffer pre-treatment (CB)

Sections were boiled 20-60 minutes in 0.01 M sodium citrate (pH6) at 95 °C.

#### HCl-pre-treatment (HCl)

Sections were incubated in 2 N HCl for 30 minutes and afterwards 2 times for 15 minutes in 0.1 M Sodium-tetraborate (pH 8.5).

Signal amplification by Thyramid-Kit (TK)

Secondary antibody incubation was preceded by 30 minutes of incubation in 0.3 % H<sub>2</sub>O<sub>2</sub> in PBS and the secondary, biotinylated antibody was detected with the Thyramid detection kit (Perkin Elmar Life Science).

Secondary antibodies were applied in conditions according to the first antibody and incubated for 1-3 hours at room-temperature. Nuclei were visualized by staining with either 4,6-diamidino-2-phenylindol (DAPI, 1:1000) or TO-PRO 3 Iodide (1:10000) in the secondary antibody solution. Specimens were mounted with Aqua Poly-Mount and analyzed using confocal or light microscopy.

**Table 6-4 First antibodies immunohistochemistry**

recognized antigen	host-animal/ Ig subtype	pre-treatment incubation conditions*	company
Aquaporin4	rabbit	1:200, CB citrate-buffer treatment	Millipore (AB2218)
Aquaporin4	rabbit	1:800 no pre-treatment	Sigma (A5971)
CollagenIV	rabbit	1:100, CB citrate-buffer treatment	Millipore (AB756P)
BrdU	rat IgG2a	1:200, HCl or CB citrate-buffer treatment	Biozol/AbDSeroTec (OBT0030)
GLT-1	guinea pig	1:100 or 1:500 (TK)	Millipore (AB1783)
Glutamine- Synthetase	mouse IgG2a	1:200	BD Bioscience (610517)
Isolectin B4 (GSA)	lectin-biotinyliert	1:50 blocking not with NGS	Sigma (L2140)
β-Dystroglycan	mouse IgG2a	1:200, CB citrate-buffer treatment	A. Menarini (NCL-b-DG)
Fibronectin	rabbit	1:40, CB citrate-buffer treatment	Millipore (AB2047)
GFAP	mouse IgG1	1:1000	Sigma (G3898)
GFAP	rabbit	1:500	Dako/Invitrogen (Z0334)
GFP	mouse IgG1	1:1000	Millipore (MAB3580)
GFP	rabbit	1:1000	Invitrogen (A6455)

recognized antigen	host-animal/ Ig subtype	pre-treatment incubation conditions*	company
GFP	chick	1:1000	Aves Lab (GFP-1020)
Laminin	rat	1:1000, CB No PFA perfusion!	Millipore (MAB1904)
NeuN	mouse IgG1	1:100	Millipore (MAB377)
Neurofilament-70	mouse IgG1	1:100	Millipore (MAB1615)
$\gamma$ -tubulin	mouse IgG1	1:100	Sigma (T5326)
S100	rabbit	1:100	Sigma (S2644)
S100 $\beta$	mouse IgG1	1:500	Sigma (S2532)
Vimentin	goat	1:20 amplification with biotinylated secondary AB	Millipore AB(1620)

\* if different from general descriptions

**Table 6-5 Secondary antibodies immunohistochemistry**

antibody	host species	label	dilutions	company
$\alpha$ -guinea pig	goat	Cy3	1:500	Dianova (106166003)
$\alpha$ -chick	goat	Alexa488	1:500	Invitrogen (A11039)
$\alpha$ -chick	donkey	FITC	1:200	Dianova (703095155)
$\alpha$ -rat	donkey	Alexa488	1:500	Invitrogen (A21208)
		Alexa594	1:500	Invitrogen (A21209)
	goat	Cy3	1:500	Dianova (112165167)
	rabbit	biotinylated	1:200	Vector (BA-4001)
$\alpha$ -rabbit	donkey	Alexa488	1:500	Invitrogen (A21206)
		Cy3	1:500	Dianova

antibody	host species	label	dilutions	company
				(711165152)
		Alexa594	1:500	Invitrogen (A21207)
	goat	Cy3	1:500	Dianova (111165144)
		biotinylated	1:200	Vector (BA-1000)
$\alpha$ -mouse IgG1	goat	Alexa488	1:500	Invitrogen (A21121)
		Alexa594	1:500	Invitrogen (A21125)
		biotinylated	1:200	South.B. (1070-08)
$\alpha$ -mouse IgG2a	goat	Alexa488	1:500	Invitrogen (A-21131)
		Alexa594	1:500	Invitrogen (A-21135)
$\alpha$ -mouse IgG3	goat	Alexa488	1:500	Invitrogen (MG320)
$\alpha$ -mouse IgG	goat	Alexa488	1:500	Invitrogen (A11029)
		Cy3	1:500	Dianova (115165166)
		Cy5	1:500	Dianova (115176072)
	donkey	Alexa594	1:500	Invitrogen (A-21203)

## **6.3 Western Blot analysis**

### **6.3.1 Tissue lysis**

Brain tissue was dissected in HBSS medium, transferred to an empty reaction tube, frozen in liquid nitrogen and stored at -80 °C until further processing. Dependent on the tissue size 100 µl up to 1 ml lysis buffer (see solutions western blot) was added. Tissue and lysis buffer were transferred to a 1 ml dounce tissue grinder and grinded with the tight pestle 10-15 x. The homogenate was pulse sonified for 5 seconds at 10% intensity and kept on ice for 15 minutes. The lysate was centrifuged at 10000 g for 15 minutes at 4 °C. The total protein lysate containing supernatant was transferred to a new reaction tube and stored at -80 °C.

### **6.3.2 Photometric quantification of protein amounts with Bicinchoninic acid**

Protein samples were quantified using the BCA assay (Uptima) according to the manufacturer protocol. The assay is based on the fact that proteins reduce alkaline copper (II) ions to copper (I) ions. Bicinchoninic acid (BCA) reacts with copper (I) ions to a violet colored complex with an absorption maximum at 562 nm. The absorption is proportional to the protein concentration in a range from 20 - 2000 µg/ ml and was measured using a spectral photometer. Samples with ascending bovine serum albumin (BSA) amounts (50 µg, 250 µg, 375 µg, 500 µg, 750 µg, 1000 µg and 1500 µg) were measured for a standard curve before detection of the absorption of specific protein samples.

### **6.3.3 Sample preparation for Western gel loading**

Protein samples were adjusted with Aqua bidest to a certain protein amount (20 to 30 µg) depending on the specific Western Blot, 4x loading buffer was added and samples were boiled at 95 °C for 5 minutes. For western blots against b1-

integrin better results could be obtained under less reduced conditions (loading buffer without  $\beta$ -Mercaptoethanol).

#### **6.3.4 Western blot and signal detection**

Sodium dodecylsulfate (SDS) polyacrylamide gels (resolving gel: 8–10%; stacking gel: 4%) were run in SDS-PAGE running buffer. Proteins were transferred to a PVDF membrane by semi dry blotting. Membranes were blocked for one hour with 5% milk powder in TBS and probed with rabbit  $\beta$ 1-integrin antibody (Wennerberg et al., 2000) over night at 4 °C. For protein loading control, membranes were probed with mouse anti-GAPDH antibody (abcam). Secondary antibodies were coupled to near infrared fluorescent dyes for detection with the Licor scanning system and the Odyssey V3.0 software. Membranes were incubated with secondary antibodies (1:15000 in TBST) for 2 hours at room temperature. Western Blots were replicated at least three times for quantification.

## **6.4 Electron Microscopy**

The electron microscopy experiments concerning the basement membrane integrity of  $\beta$ 1-integrin mutant mice were performed in collaboration with Dr. Saida Zouba, Helmholtz Zentrum München, Institute for Pathology: The animals were deeply anesthetized and perfused with a 0.1 M phosphate buffered 4 % paraformaldehyde / 2.5 % glutaraldehyde fixative. The brain was removed and post-fixed in the same solution for 4 hours at 4 °C. Coronal sections of 2 mm thickness were cut at the vibratome. The sections were rinsed in 0.1 M sodium phosphate buffer, post-fixed in buffered 1.0 % osmium tetroxide, dehydrated in a graded series of ethanol to 100%, transitioned to propylene oxide, and embedded in Epon. Semi-thin sections were stained with toluidine blue to determine areas of interest; the grids were stained sequentially with uranyl acetate and lead citrate. The ultrastructure was examined by a transmission electron microscope.

The electron microscopy study examining myelin defects in  $\beta$ 1-integrin mutant were done in collaboration with Dr. Leda Dimou, Munich University LMU, Physiological Genomics: Animals were deeply anesthetized and transcardially perfused using freshly prepared Karnovski fixative. Brains were taken out and post-fixed for 3 hours in the same solution. Then brains were transferred to the post-fix and storing solution and kept at 4 °C until further processing.

Brains were washed in washing solution for 2 – 4 hours before 400 – 500  $\mu$ m vibratome sections were cut and washed again before osmication. As a strong oxidant, osmium cross-links lipids mainly by reacting with unsaturated carbon-carbon bonds, thereby fixing and labeling biological membranes and other lipid rich structures like myelin sheets for transmission electron microscopy, since osmium atoms are extremely electron dense. Sections were transferred to opaque glass vials filled with osmication solution standing on a pre-cooled metal plate. Osmication took place for 1.5 – 2 hours while slow warming of the solution at room temperature. The sections were washed in a 24-well plate in 0.1 M Cacodylat for 20 minutes and dehydrated in a graded series of EtOH to 100 % (70 %, 80 %, 90 %, 96 %, 100 %, 100 %, 20 minutes each). Sections were transferred to glass vials for the final 30 minutes washing step with propylenoxide (propylenoxide disintegrated plastic), before sections were incubated in a propylenoxide : araldit (1:1) mixture over night at 4 °C. Sections were embedded using an araldit epoxy embedding kit following the manufacturer's protocol.

The araldit blocks were sent to the LMU anatomic institute for contrasting and cutting semi-and ultra-thin sections. Grids were then analyzed at a transmission electron microscope.

## 6.5 Cell Culture

### 6.5.1 Primary astrocyte cultures and in vitro scratch wound assay

Primary astrocytes cultures were prepared from cortices of mice at postnatal day 5 – 7. Therefore, 3 – 4 pups were decapitated and heads were washed in 70 % EtOH. Brains were taken out and transferred to Hank's Buffered Salt Solution (HBSS) supplemented with HEPES (final concentration: 10mM) to stabilize the pH-value. Meninges were removed and hemispheres were separated using 2 forceps (size 5), then cortical gray and white matter was dissected from the underlying striatum. Finally the hippocampi which are located under each cortical hemisphere were removed and this cortical tissue was then transferred into a 15 ml Falcon tube filled with HBSS and kept on ice until further processing.

### 6.5.2 Tissue dissociation and culturing of primary astrocytes

All further steps were carried out at room temperature under sterile conditions in a laminar flow. Media and supplements are listed in chapter 5.5.6 *Cell Culture media and supplements*. The tissue was chopped into smaller pieces using a 10 ml serologic pipette. Tissue pieces were collected at the bottom of the 15 ml reaction tube by centrifugation for 5 minutes at 1000 rpm. The supernatant was removed and 10 ml astrocyte medium was added. The tissue was further dissociated using first a 5 ml serologic and then a glass Pasteur pipette. The cell suspension was centrifuged for 5 minutes at 1000 rpm, the supernatant was drawn off and 10 ml fresh astrocyte medium was added. Cells were gently resuspended with a 10 ml serologic pipette and transferred to a poly-L-ornithine (PLO) coated T75 cell culture flask and incubated in a cell culture incubator ventilated with 5 % CO<sub>2</sub>.

### **6.5.3 Maintenance and splitting of the astrocyte culture**

The culture medium was completely exchanged each 2 - 3 days for 1 week after 100 % confluence was reached (2-3 weeks after preparation). At this time point, almost all oligodendrocyte progenitors, which are the round cells located on top of the astrocyte monolayer, already disappeared. In case they were still present, the medium was replaced by PBS and oligodendrocyte precursors were removed by sound shaking of the flask. After washing with PBS 2 ml Trypsin/EDTA was added and the flask was placed back into the incubator for maximum 5 minutes. Astrocytes that had remained attached were loosened by shaking the flask, and then the trypsination was stopped by addition of 3 volumes of astrocyte medium. The cell suspension was transferred to a 15 ml reaction tube and centrifuged for 5 minutes at 1000 rpm. The supernatant was removed, 1 ml fresh astrocyte medium was added and cells were re-suspended by pipetting the suspension up and down. 10  $\mu$ l of the cell suspension was transferred to an improved Neubauer chamber and living cells were counted. Cells were seeded on PLO-coated 14 mm glass coverslips in a 24-well plate or directly into a PLO-coated 24-well plate (Falcon!) for timelapse imaging at a density of 70000 – 100000 cells per well. The medium was changed 24 hours after plating and each 2 – 3 days thereafter.

### **6.5.4 Transduction of astrocyte cultures with lentiviruses**

Astrocyte cultures were transduced during the splitting step after re-suspension of the cells by adding 0.8  $\mu$ l lentivirus per 500  $\mu$ l cell suspension and well. Cells were then plated and plates were placed into the incubator for 24 hours, before the medium was changed again.

### **6.5.5 In vitro scratch wound assay**

At the earliest two weeks after viral transduction and one week after confluence on the coverslips had been reached experiments were started: A short 10 $\mu$ l

pipette tip was used to scratch the astrocyte monolayer once or twice across the entire width of the well. The medium was changed immediately to remove detached cells and the plate was either placed back into the cell culture incubator until fixation of the cells or into the timelapse imaging setup.

### **6.5.6 Dissection and dissociation of adult mouse brains for culturing neurospheres from the SEZ**

For culturing neurosphere cells from the adult subependyma the protocol described by (Johansson et al., 1999) was followed. Media and supplements are listed in chapter 5.5.6 *Cell culture*. At least 3 mice per genotype were used for one preparation. Mice were killed by cervical dislocation and whole brains were isolated and kept in HBSS containing 10 mM Hepes until dissection. Brains were cut at the midline between the two hemispheres and in the middle. The medial wall of the ventricle was removed and the lateral wall was isolated by cutting beneath the wall with scissors. These tissue pieces were kept in HBSS/Hepes. At the end of the preparation the dissociation medium was freshly prepared and filter sterilized. Tissue was incubated in this dissociation medium for 15 min at 37°C, thoroughly triturated with a 5 ml pipette for at least 10 times up-and-down and again incubated for 15 min at 37°C. The enzyme activity was stopped by adding 1 volume ice cold solution 3 and cells were passed through a 70 µm strainer into a 50 ml reaction tube to remove bigger pieces of tissue, followed by a centrifugation step at 1300 rpm for 5 minutes in a 15 ml reaction tube. The supernatant was removed and the pellet was re-suspended in 10 ml ice cold solution 2 and centrifuged at 2000 rpm for 10 minutes. This centrifugation step is similar to a sucrose gradient and gets rid of dead cells which are very small in size and hence fail to pellet. The supernatant was drawn off and cells in the pellet were re-suspended in 2 ml ice cold solution 3. A new 15 ml tube was filled with 10 ml ice cold solution 3 and 2 ml of the cell suspension was added on top of the new tube, followed by another centrifugation step at 1500 rpm for 7 minutes. The supernatant was removed; cells were re-suspended in 7 ml neurosphere media and seeded in a small cell

culture flask. Cells were cultured in the presence of 20 ng/ ml EGF and 10 ng/ ml FGF2 (added each 2 – 3 days) under non-adherent conditions to allow for the formation of neurospheres.

### **6.5.7 Dissection and dissociation of adult mouse brains for culturing neurospheres from the stab wound injury**

For culturing neurospheres from reactive astroglial cells from a stab wound injured cortex at least 3 mice per genotype were used 3 days after the operation. Animals were sacrificed by cervical dislocation and brains were isolated and kept in HBSS/ Hepes for dissection. A thin slice of approximately 500 µm of the injured area was cut using a scalpel thereby strictly avoiding hitting the white matter. It may be advantageous to cut a 1 – 2 mm coronal slice first before dissecting the injured tissue. The dissociation of the tissue was performed as described above. Cells from the stab wound tissue were cultured with double the amount of growth factors (40 ng/ ml EGF and 20 ng/ ml FGF).

### **6.5.8 Passaging Neurospheres**

For passaging the neurospheres were collected in their medium in a 15 ml tube and centrifuged at 800 rpm for 5 minutes. Most of the supernatant was removed spearing 500 µl in which cells were then dissociated mechanically. Cells were counted in an improved Neubauer chamber after the first split and seeded in 24-well plates at a density of 1 cell / µl.

### **6.5.9 Paraformaldehyde fixation of cultured cells**

Cells were fixed with 4 % paraformaldehyde (heated to 37 °C) for 15 minutes at 37 °C and washed with 2 ml PBS twice afterwards. Coverslips were stored covered with PBS in 24-well plates at 4 °C until stainings were performed.

### 6.5.10 Immunocytochemistry

F-actin was detected using fluorescent labeled Phalloidin in the secondary antibody solution.

**Table 6-6 First antibodies immunocytochemistry**

recognized antigen	host-animal/Ig subtype	pre-treatment & incubating conditions*	obtained from
$\beta$ -catenin	mouse IgG1	1:50	BD Biosciences (610153)
Cdc42	mouse IgG3	1:100	Santa Cruz (8401)
$\beta$ 1-Integrin	rat	1:100	Millipore (MAB1997)
GFAP	mouse IgG1	1:1000	Sigma (G3898)
GFAP	rabbit	1:4000	Dako/Invitrogen (Z0334)
GFP	mouse IgG1	1:2000	Millipore (MAB3580)
GFP	rabbit	1:2000	Invitrogen (A6455)
GFP	chick	1:2000	Aves Lab (GFP-1020)
$\gamma$ -tubulin	mouse IgG1	1:1000	Sigma (T5326)
RFP	rabbit	1:500	Millipore (AB3216)

**Table 6-7 Secondary antibodies immunocytochemistry**

antibody	host species	label	dilutions	supply
$\alpha$ -chick	donkey	FITC	1:1000	Dianova (703095155)
$\alpha$ -rat	donkey	TRITC	1:1000	Dianova (712025153)
	rabbit	biotinylated	1:200	Vector (BA-4001)
$\alpha$ -rabbit	goat	FITC	1:1000	Dianova (111095003)
		TRITC	1:1000	Dianova (111025144)

antibody	host species	label	dilutions	supply
$\alpha$ -mouse IgG1	goat	FITC	1:1000	South.Biot (1070-02)
		TRITC	1:1000	South.Biot (1070-03)

In addition see secondary antibodies in 6.2.1. The antibodies listed there were diluted 1:2000.

## 6.6 Virus production

In this study mostly lentiviruses have been used. Lentiviral constructs for expression of the Cre recombinase (*Cre-IRES-GFP*, Figure 6-1) and the corresponding green fluorescent protein (*GFP*) control construct were kindly provided by Dr. A. Pfeiffer, University of Bonn. Lentiviruses were designed and produced with the help and according to the protocol of Dr. Alexandra Lepier in the department of Cellular Physiology.

### 6.6.1 Viral vector design

The GFP-expression behind an internal ribosome entry site (IRES) is weaker than GFP expression directly driven from the internal CMV-promoter (Figure 6-1). Therefore GFP levels in cells transduced with GFP control virus were significantly higher than in cells transduced with Cre-IRES-GFP virus. As this has been disadvantageous for timelapse imaging, constructs were designed encoding the red fluorescent protein *tomato* directly behind the promoter followed by an IRES and the sequence for Cre recombinase (*tomato-IRES-Cre*) or carrying tomato alone (*tomato*). To ascertain that expression of Cre recombinase behind IRES is sufficient, double stainings for RFP and Cre were performed after transfection of HEK cells with the *tomato-IRES-Cre* construct and after transduction of HEK cells or astrocytes with *tomato-IRES-Cre* virus. RFP-positive Cre-negative cells were neither detected after transfection or

transduction of HEK cells, nor after viral transduction of astrocytes indicating high levels of expression of both proteins.

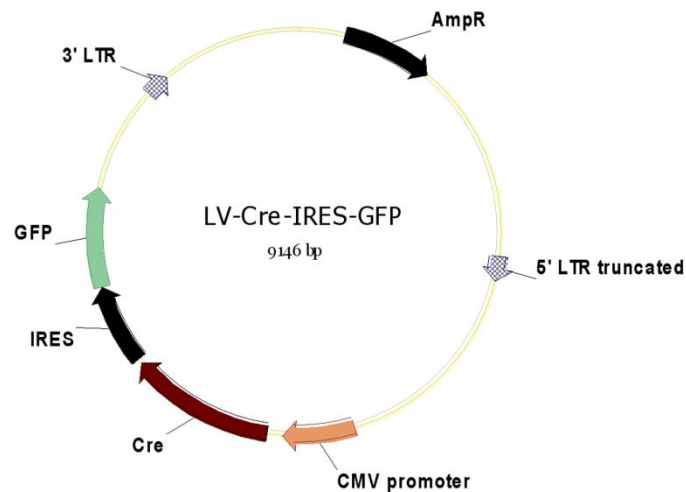


Figure 6-1 Map of the *Cre-IRES-GFP* lentiviral construct

*Cre* is expressed under the CMV promoter followed by an internal ribosomal entry site in front of the GFP sequence. *Cre* and *tomato* are switched in the *tomato-IRES-Cre* lentiviral vector.

### 6.6.2 DNA preparation for virus production (CsCl-Gradient)

This method provides very pure supercoiled plasmid DNA, while nicked (relaxed circled) DNA is separated and all proteins are removed, as non-covalent binding sites are eliminated due to the cesium ions absorbing remaining water molecules. Thus, the pure DNA is free of endotoxins and its amount can be defined in a reproducible way by measuring the absorbance without varying disturbances from damaged DNA or protein contaminations.

#### Harvest and DNA extraction

A 250 ml bacterial culture was used. Notably, care was taken that the culture was not overgrown with an optimum at around 90 % confluence. Bacteria were

spun down at 5000 x g for 20 minutes and drained off the supernatant. The pellet was re-suspended in 10 ml Qiagen buffer 1 with RNase. After complete re-suspension, 10 ml Qiagen buffer 2 for lysis was added. The tube was shaken gently and incubated for exactly 5 minutes. 10 ml of ice-cold Qiagen buffer 3 was added, and mixed well. The mixture was filtered through a folded paper filter pre-wetted with clean water into a 50 ml tube (volume around 25 ml, some rest may stay in the filter).

DNA was precipitated by adding 20 ml Isopropanol to the filtrate (1:1), mixing of the solution, and followed by a centrifugation step at 8000 x g for 1 hour at 4°C. The supernatant was removed; the white pellet was washed carefully with 70 % EtOH and spun again for 10 minutes. After draining off EtOH the wet pellet was dissolved in 15 ml TE, pH 8.0. The pH of the solution should be around pH 8 (otherwise adjust pH).

#### Phenol extraction

This purification step may be omitted, but then more precipitates are formed during cesium chloride extraction. The pure DNA solution was poured into a Phase Lock Heavy 50 ml tube, 7.5 ml of phenol equilibrated with TE and 7.5 ml Chloroform were added and shaken well. The solution was spun at 1500 x g at RT for 20 min in a swing out rotor. The upper, aqueous phase was transferred into a new 50 ml tube, 1.5 ml of 3 M Sodium Acetate pH 5.2 and 15 ml Isopropanol were added for DNA precipitation, mixed well and centrifuged at 8000 x g for 1 hour at 4°C. The supernatant was removed and the pellet was washed with 70 % EtOH and spun again for 10 minutes. Rests of EtOH were removed; the DNA pellet was air-dried until it appeared transparent. Dry pellets may be stored at -20°C.

#### Cesium Chloride (CsCl) - gradient preparation and ultracentrifugation

The dry pellet was dissolved completely in 8.0 ml TE. The DNA solution (8.0 ml) was added to 8.80 g CsCl in a 50 ml tube and the salt was dissolved completely

(solution will get cold). 800 µl of saturated ethidium bromide (EtBr) was added and the solution was mixed until a fine precipitate was formed. Samples were warmed up to 37°C for 15 minutes in the water bath and centrifuged at full speed in a swing out rotor for 10 minutes so that the precipitate was clung to the surface and the wall of the Falcon tube. Less precipitates were formed, when The DNA solution was purified by phenol extraction. The supernatant was filled into an 11.2 ml OptiSeal tube (Beckmann) until the meniscus touched the basis of the tube's neck. Tubes were balanced precisely to 0.0 g and sealed for the following ultracentrifugation step: 65.000 rpm for 5 hours and 30 minutes at 20°C at maximum acceleration and slow brake settings. Start of the centrifuge was delayed so that the spin ended at the next working day. After centrifugation finished visible DNA bands were immediately extracted.

#### Extraction of the ethidium bromide from the rotor tube

For harvest of the DNA band, a UV lamp in vertical direction and a dark room are required, as well as skin protection (i.e. e. lab coat, nitrile gloves and face protection).

When the centrifuge stopped, tubes were removed from the rotor as soon as possible, and the tube was fixed in front of the UV-lamp in a holder. The tube's shoulder was pierced with a canula (around 22 Gauge) for ventilation of the tube when DNA-band was withdrawn. The tube was put in a fitting clamp, so that the band was visible halfway down the tube. Now the second needle (also 22 Gauge) was put into the tube shortly under the DNA band. The UV-lamp was used to check the height of the DNA band (upper band: nicked DNA, lower band: super-coiled DNA). The needle was connected to a 2 ml syringe and as much as possible DNA was collected into the syringe by moving the syringe up and down. Content of the syringe was transferred into a 15 ml tube. DNA can be stored at that stage at room temperature overnight under light protection.

### Removal of ethidium bromide from the DNA

An equal volume of n-Butanol saturated with TE was added to the DNA + EtBr solution, shaken well and spun briefly in a swing out rotor after which the upper organic phase was removed. The extraction was repeated until the lower aqueous phase was completely colorless (around 5 – 6 times). An equal volume of Diethyl ether was added, the solution was mixed and the upper, organic phase was removed to separate rests of n-Butanol from the water phase. At room temperature the ether will evaporate during the next steps. DNA solutions were transferred into 50 ml tubes and diluted with 2 volumes of sterile TE. 1/10 new volume of 3 M Sodium-Acetate pH 5.2 and another 2 volumes of cold 100 % EtOH (stored at -20°C) were added, the solution was mixed and incubated on ice for 1 – 2 hours or overnight at 4°C, followed by a centrifugation step 10000 x g for 1 hour at 4°C. The supernatant was removed and washed with 10 ml cold 100 % EtOH, spun again at 10000 x g for 10 minutes and again rests of EtOH were removed. The pellet was air-dried and appeared transparent then. DNA was dissolved under a tissue culture hood in 500 µl of sterile 10 mM Tris-HCl pH 8. Vigorous shaking was avoided! DNA solution was transferred into a 1.5 ml reaction tube, eventually followed by another spin at full speed for 5 minutes to further remove insoluble particles. The average yield was around 1 mg of pure DNA.

### **6.6.3 Lentiviral preparations**

Lentiviruses are a subclass within the large group of retroviruses, which stably integrate into the genome of the target cell. The lentiviral pre-integration complex recruits components of the cellular nuclear import machinery, which actively transport the complex through the nuclear pore. Therefore the integration of the lentiviral genome is - in contrast to all other retroviruses - independent of the cell cycle of the host cell and takes also place in post-mitotic, non-cycling cells.

For security reasons retroviral vector systems have been depleted of replicative and pathogenic viral genes and their remaining genome has been splitted into different plasmids resulting in replication-incompetent vectors.

#### Propagation of 293T cells

Media and medium supplements are listed in chapter 5.5.6. 293T cells were cultured in stock medium in T175 flasks and splitted 2 – 3 times a week when confluence reached 80 – 90 %. Trypsin-EDTA for detachment and dissociation of the cells was diluted 1:5 in PBS. After 20 – 30 passages cultures were discarded and fresh 293T cells were thawed. For packaging cells were expanded to 3 T175 flasks per reaction seeded in a density that would lead to 60 % confluence 3 days later.

#### Transfection (day 1, evening)

The stock and transfection medium were heated to room temperature. Per packaging reaction one 50 ml tube containing 9 ml Opti-MEM without serum, 45 µg packaging vector Δ8.9, 30 µg VSVG-pseudotyping vector and 18 µg expression plasmid and one tube containing 9 ml Opti-MEM without serum and 216 µl Lipofectamin 2000 were prepared. Especially important was the ratio of the 3 plasmids rather than the total DNA amount. The tubes were incubated for 5 minutes before the transfection reagent was added to the DNA, gently mixed and incubated for another 20 minutes at room temperature. During the incubation 293T cells were harvested and cells from 3 flasks were pooled into one pellet per reaction. From a fraction of these cells new 293T stock flasks were seeded in stock medium. The cell pellet was re-suspended in 30 ml Opti-MEM with 10 % FCS. The transfection mix was added to the cell suspension and gently mixed. Then 6 10 cm dishes were seeded with 8 ml cell suspension each. The confluence should be at 60 – 70 % after attachment of the cells. Dishes were placed into the incubator overnight.

### Washing and changing medium (day 2, morning)

The packaging medium was heated to 37 °C and 50 ml were filled to a reaction tube to avoid contamination of the stock. The supernatant from one dish was drawn off and immediately replaced by cautious addition of 5 ml of packaging medium thereby avoiding that cells fell dry or detach from the plate. The procedure was repeated one by one for the other 5 dishes. Then the supernatant from the first dish was replaced by 12 ml of fresh packaging medium and subsequently the other 5 dishes were washed as well. Dishes were placed back into the incubator.

### Preparation of the ultracentrifuge run

The screw lids of the SW 28 ultracentrifuge rotor buckets were sterilized with 70 % EtOH and dried in the laminar air flow. Rotor and buckets were assembled then and pre-cooled to 4 °C in the refrigerator. The rotor chamber of the ultracentrifuge was cooled to 4 °C as well. Ultracentrifugation tubes (2 per reaction) were sterilized by filling them to the rim with non-toxic 70 % EtOH (made from absolute EtOH and tissue-culture grade water) and letting them stand in the flow for a couple of minutes. The 70 % EtOH was recycled; tubes were dried and labeled with an EtOH-resistant marker. A working aliquot of TBS-5 was placed on ice. Packaging medium was pre-warmed and aliquoted as described before.

### Ultracentrifuge run and harvest (day 3, 4, 5, 6)

The first harvest was conducted when cells were confluent and the medium turned light orange. The supernatant of one after the other dish was transferred to 50 ml tube and immediately replaced with 12 ml of fresh packaging medium and plates were put back into the incubator. The viral supernatant of 3 plates was pooled into one 50 ml tube. After the second harvest supernatant was removed and cells were discarded.

Supernatants were centrifuged for 15 minutes in a cell culture centrifuge to remove detached cells and debris. Meanwhile Millex 0.45  $\mu\text{m}$  filters were pre-wetted to avoid sticking of the virus to the filter. Therefore the plunger from a 30 ml syringe was removed and filters were mounted onto syringes (one per 50 ml tube with viral supernatant). A few drops of packaging medium were filled onto filters from inside of the syringes. Viral supernatant was transferred into new tubes thereby avoiding any carry-over of debris and then filtered through the pre-wetted Millex filters by decanting the supernatant into the syringes. The plunger was carefully replaced and gentle pressure was applied. Exactly 30 ml of each supernatant was transferred into the earlier prepared ultracentrifuge tubes and the SW 28 rotor was assembled and centrifuged for 90 minutes at 25000 rpm at 4 °C. The supernatant was removed revealing a brownish glassy viral pellet. 1 ml of ice-cold TBS-5 was added; tubes were closed with 2 layers of Parafilm and placed on ice for 4 hours or overnight in a cold room. For a viral preparation with only one ultracentrifuge run only 100  $\mu\text{l}$  of TBS-5 were added and viral suspension was directly aliquoted and frozen after incubation on ice.

In case problems with toxicity of the viral batches occurred or if viral preparations were used for injections into the brain, a second ultracentrifuge run was advantageous to further purify the viral particles from components of packaging medium. For the second run the virus was dissociated by pipetting up and down with a serological plastic pipette while minimizing the formation of air bubbles. The viral suspension was filled up to 30 ml with ice-cold TBS-5 and the rotor was assembled for another centrifugation for 90 minutes at 25000 rpm and 4 °C. The supernatant was removed and the viral pellet appeared colorless and translucent. 100  $\mu\text{l}$  of TBS-5 were added, tubes were covered with Parafilm and placed on ice for 4 hours or overnight.

#### Aliquoting and freezing of the virus

The viral supernatant was transferred from the ultracentrifuge tube to a 1.5 ml reaction tube before re-suspension. The bottom of the ultracentrifuge tube was rinsed with another 50  $\mu\text{l}$  of TBS-5 that were added the viral supernatant. The

supernatant was re-suspended by pipetting up and down with a 200  $\mu\text{l}$  pipette set to 150  $\mu\text{l}$ . To remove remaining debris and aggregates tubes were spun at 5000 rpm for 30 seconds in a benchtop centrifuge. The supernatant was transferred to a new tube and spins were repeated until no white pellet was formed anymore. The viral supernatant was aliquoted into 0.5  $\mu\text{l}$  tubes; 10  $\mu\text{l}$  aliquots were frozen and stored at  $-80\text{ }^{\circ}\text{C}$ .

## 6.7 Data analysis

### 6.7.1 Cell numbers per area and marker coexpression

For quantification of cell numbers per  $\text{mm}^2$  and marker coexpression the NeuroLucida software was used in combination with an Olympus BX50 microscope. The analysis was performed on coronal or sagittal sections in at least 3 pairs of WT and mutant mice. For all data sets, the arithmetic average, standard deviations and standard errors of the mean (SEM) were calculated. The error bars in the diagrams are showing the SEM. To test the data for significance the unpaired student's T-test was used in the in vivo studies. The p-value (p) of these tests declares the probability of the conclusion being correct. There is a 95% chance of the means to be significant different if  $p = 0.05$  (indicated in graphs as \*), a 99% chance of the means to be highly significant different for  $p = 0.01$  (\*\*) and a 99.9% (\*\*\*) chance of the means to be very highly significant different for  $p = 0.001$ .

### 6.7.2 Reorientation of centrosomes

Reorientation of the centrosome in wounded astrocyte cultures was quantified by separating the space in 4 equal quadrants joining in the center of the nucleus of interest and placed so that one of the quadrants is facing the scratch (the median of each  $90^{\circ}$  angle being either perpendicular or parallel to the scratch). Centrosomes are scored as reoriented when the centrosome is located in the quadrant facing the scratch. The data were obtained from 3 independent

preparations of different litters. For each preparation and time point 2 different coverslips, each with at least 100 transduced cells in the first row at the scratch, were counted. The significance of the data was tested using the Mann-Whitney test. The calculations and constructions of the diagrams were carried out with Excel and GraphPadPrism 3.0. Means were considered significantly different for  $p \leq 0.01$  (\*\*) and  $p \leq 0.001$  (\*\*\*).

### **6.7.3 Quantification of astrocyte protrusions**

Scratched astrocyte cultures stained for microtubules were observed under the fluorescence microscope (Olympus, BX61) using a 60x objective. Transduced cells in the first row at the scratch with one major protrusion, which appeared at least three times longer than wide, were scored as “protruding” cells. The significance of the data was tested using the Mann-Whitney test. The calculations and constructions of the diagrams were done with Excel and GraphPadPrism 3.0. Means were considered significantly different for  $p \leq 0.01$  (\*\*) and  $p \leq 0.001$  (\*\*\*).

For analysis of protrusion formation of astrocytes after a stab wound injury in vivo confocal images were taken. Length and width of GFP<sup>+</sup> cells as well as the longest process towards the stab wound was measured in the ZEN 2008 software from Zeiss. The measurements of the cell length and width were done together with Sophia Bardehle (Institute of Stem Cell Research, HelmholtzZentrum München). To test the data for significance the unpaired student's T-test was used and calculations and statistical analysis were done with Excel and GraphPadPrism 3.0. Means were considered significantly different for  $p \leq 0.05$  (\*),  $p \leq 0.01$  (\*\*) and  $p \leq 0.001$  (\*\*\*).

### **6.7.4 Analysis of the lesion size**

To analyze the lesion size after stab wound injury confocal pictures were taken. The area free of DAPI-positive nuclei within the injury, the area covered by

reactive astrocytes and microglia was measured in at least 3 sections from 3 animals using the ZEN 2008 software from Zeiss. To test the data for significance the unpaired student's T-test or the Mann-Whitney test was used and calculations and statistical analysis were done with Excel and GraphPadPrism 3.0. Means were considered significantly different for  $p \leq 0.05$  (\*),  $p \leq 0.01$  (\*\*) and  $p \leq 0.001$  (\*\*\*).

## 7 Results

### 7.1 The influence of $\beta$ 1-integrins on gray matter astrocytes

To examine the impact of signaling between the basement membrane (BM) surrounding blood vessels and astrocytes that contact the BM by their endfeet,  $\beta$ 1-integrins were conditionally deleted. Towards this aim, mice carrying alleles for the  $\beta$ 1-integrin gene that were flanked by loxP sites were crossed to mice expressing the Cre-recombinase under the human GFAP (hGFAP) promoter. Cre-expression driven from the hGFAP promoter leads to recombination from embryonic day (E) 13 in radial glia cells that give rise to astrocytes, oligodendocytes and neurons in the forebrain (Malatesta et al., 2003). Therefore all progeny of recombined radial glia cells carry a deletion of the complete coding and 3 prime uncoding sequence of the  $\beta$ 1-integrin gene.

#### 7.1.1 Deletion of $\beta$ 1-integrin by the use of hGFAP-Cre causes partial reactive gliosis

##### $\beta$ 1-integrin protein levels are reduced at postnatal stages

As there is  $\beta$ 1-integrin protein expressed before the time point of gene deletion the stability of the protein determines the duration until a knockout on the protein level is achieved. Thus,  $\beta$ 1-integrin protein expression was examined by western blot analysis in conditional knockout mice (from now on referred to as  $\beta$ 1-/-) and wildtype littermates (WT) with WT protein levels set to 100%. At the day of birth (postnatal day 0) the amount of  $\beta$ 1-integrin protein had already decreased to  $65 \pm 14$  % in  $\beta$ 1-/- cortices (Figure 7-1 A, C) and was further reduced to  $37 \pm 3$ % at postnatal day (P) 7 (Figure 7-1 B, C). Consistent with Cre-expression in radial glia in almost all brain regions (Malatesta et al., 2003)  $\beta$ 1-integrin protein levels in the adult brain were reduced to  $57.7$  %  $\pm$   $10.7$  % in the  $\beta$ 1-/- cortex and to  $56.7$  %  $\pm$   $7$  % in the hindbrain (Figure 7-1 D, E). As  $\beta$ 1-

integrin is ubiquitously expressed the remaining  $\beta 1$ -integrin levels are most likely due to not-recombined cell types like endothelial cells and mesenchymal derived microglia. Even in the spinal cord, where hGFAP-Cre mediated recombination occurs at relatively late stages in radial glia, when mainly astrocytes and less neurons are generated (Barry and McDermott, 2005; Mori et al., 2005; McMahon and McDermott, 2007; Pinto et al., 2008)  $\beta 1$ -integrin protein levels were decreased to  $41.7 \pm 7.3$  (Figure 7-1 D, E). However, in the midbrain protein amounts were similar in  $\beta 1^{-/-}$  ( $109.3 \% \pm 18.6 \%$ ) and WT brains (Figure 7-1 D, E), correlating with the lower Cre expression in this region that has been reported previously (Zhuo et al., 2001).

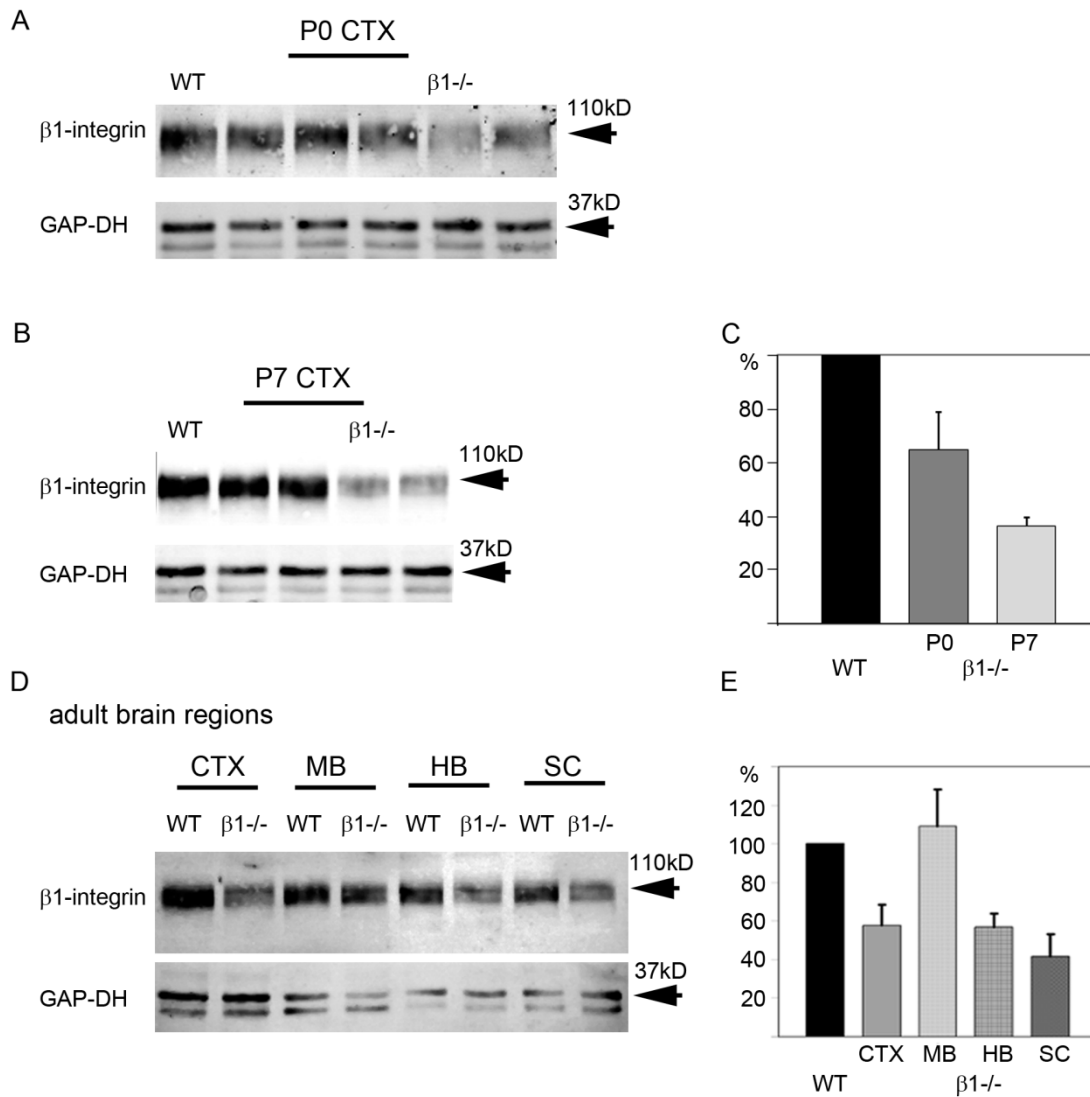


**Figure 7-1 Western Blot analysis of  $\beta 1$ -integrin protein levels**

Western blot analysis against  $\beta 1$ -integrin revealed lower levels of the protein at the day of birth in total lysates of  $\beta 1^{-/-}$  cerebral cortices compared to WT controls (A, C) and was further reduced one week later (B, C). In  $\beta 1^{-/-}$  brains of adult animals  $\beta 1$ -integrin protein levels were reduced not only in the cerebral cortex, but also in hindbrain and spinal cord (D; E). In the midbrain protein levels were comparable to WT controls (D, E).

### Loss of $\beta 1$ -integrins at postnatal stages does not cause major abnormalities

Consistent with preceding reports of CNS-specific deletion of  $\beta 1$ -integrins (Graus-Porta et al., 2001; Blaess et al., 2004; Huang et al., 2006; Belvindrah et al., 2007b) knockout animals were born at normal mendelian ratios, survived into adult stages, had a body weight similar to WT littermates and did not show obvious behavioral abnormalities. In addition, no gross differences in brain morphology in  $\beta 1^{-/-}$  compared to WT brains were observed, except from the cerebellum, which was smaller and contained fused folia in  $\beta 1^{-/-}$  mice (Figure 7-2 A, B; see also Graus-Porta et al., 2001). During forebrain development newborn neurons migrate along radial glia from the ventricular zone towards the basal lamina thereby forming six cortical layers in an inside out way (Gaiano, 2008). Interestingly, neuronal ectopia in cortical layer I were not detected in  $\beta 1$ -integrin mutant cortices in contrast to previous reports of deletion of  $\beta 1$ -integrins at an earlier time point (Figure 7-2 C, D and Graus-Porta et al., 2001; Belvindrah et al., 2007b). The cortical layering was indistinguishable in  $\beta 1^{-/-}$  and WT brains as examined by 4',6-diamidino-2-phenylindole (DAPI) and Nissl staining. The density of cells quantified by counting DAPI-positive nuclei per area, as well as the number of neuronal nuclei (NeuN)-positive neurons was comparable in mutant (Fig. 4.2 D and  $5334 \pm 314$  DAPI-positive nuclei/  $\text{mm}^2$ ,  $n = 3$ ;  $2741 \pm 864$  NeuN-positive neurons,  $n = 8$ ) and WT cortices (Fig. 4.2 C,  $6109 \pm 450$  DAPI-positive nuclei/  $\text{mm}^2$ ,  $n = 3$ ,  $p = 0.15$ ;  $3158 \pm 335$  NeuN-positive cells /  $\text{mm}^2$ ,  $n = 5$ ,  $p = 0.91$ ). Furthermore, there were no apparent differences in the intensity of neurofilament-70 or myelin associated glycoprotein (MAG) immunofluorescence in WT and  $\beta 1^{-/-}$  brains suggesting that neither axons nor myelin are affected by the deletion of  $\beta 1$ -integrins in almost all forebrain cells. Additionally, astrocytes were labeled by immunofluorescence staining against the astrocytic marker S100 $\beta$ . Quantification of S100 $\beta^+$  astrocytes per area showed similar numbers in WT and  $\beta 1^{-/-}$  cortices. However, there were obvious morphological changes of the S100 $\beta^+$  cells, which were then analyzed in more detail.

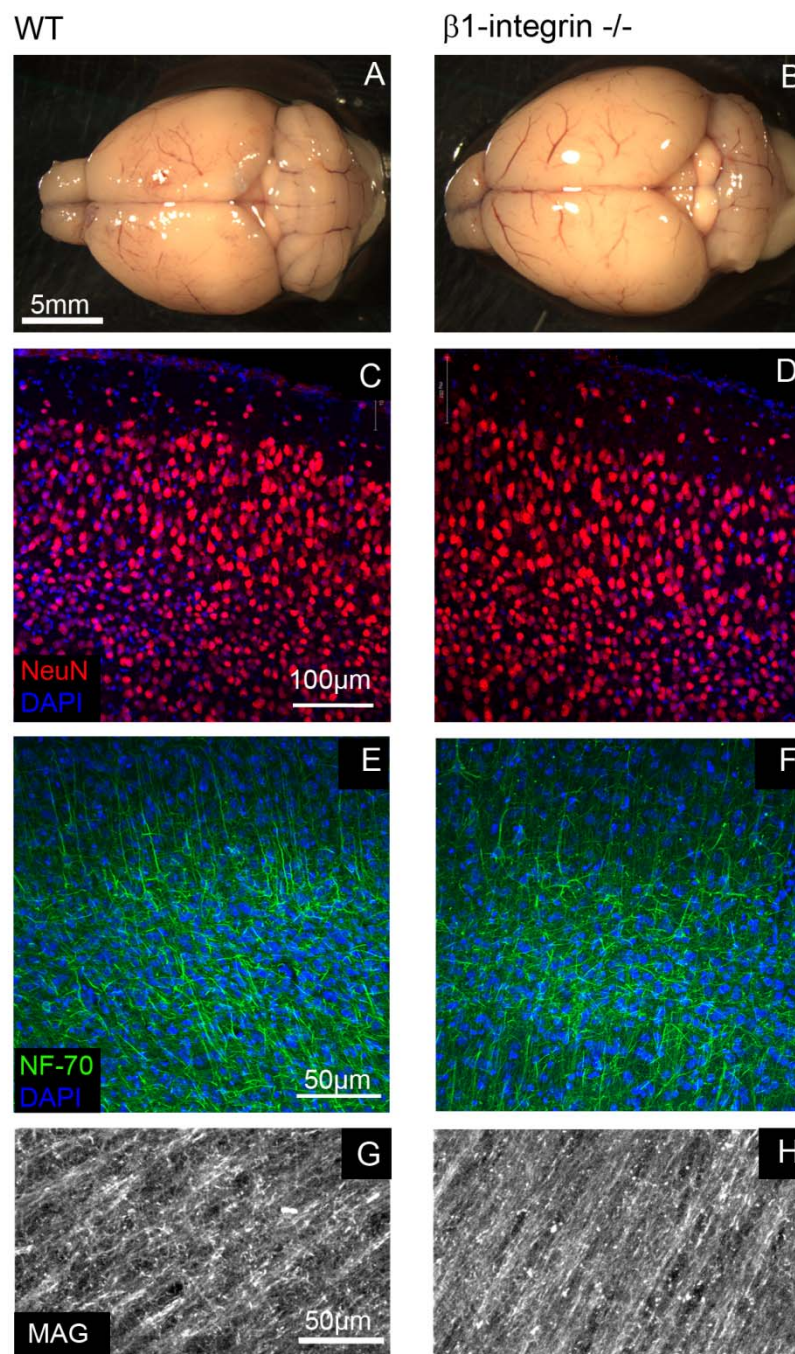
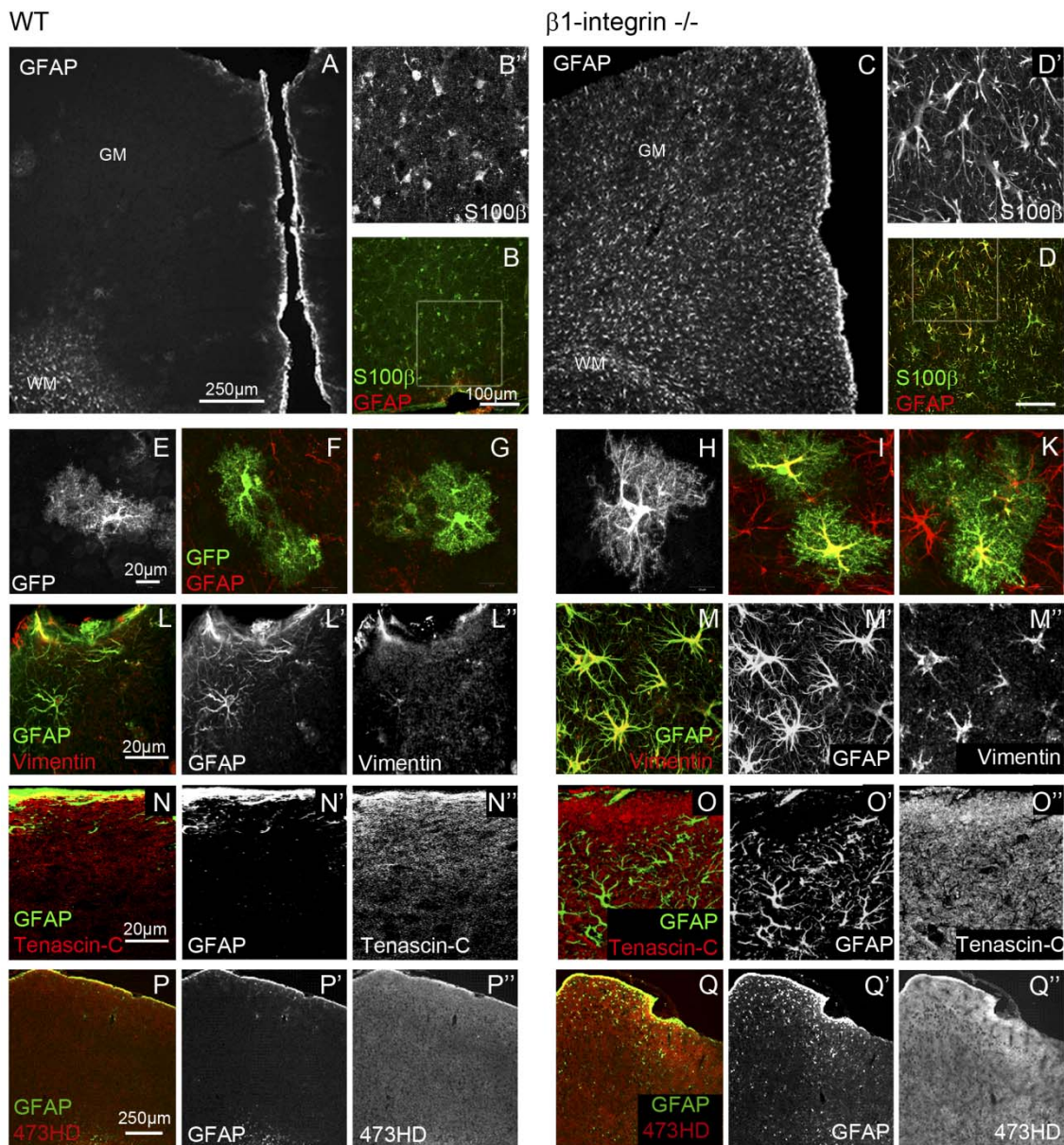


Figure 7-2 Gross analysis showed no differences in WT and  $\beta$ 1 $-/-$  cerebral cortex

Although  $\beta$ 1 $-/-$  brains appeared to be larger in size, the layered structure of the cerebral cortex seemed to be normal and there were no obvious differences in cell or neuronal densities judged by DAPI and NeuN staining (C, D). In addition, immunofluorescent stainings of axons (E, F) and myelin (G, H) was comparable in the gray matter of the cerebral cortex of  $\beta$ 1 $-/-$  and WT brains.

### Loss of $\beta$ 1-integrins in the postnatal forebrain leads to a transition of mature gray matter astrocytes towards reactive astrocytes

Single astrocytes were labeled using the Z/EG eGFP-reporter mouse line. Although almost all forebrain cells have been expected to be GFP-positive, I noticed in some animals that the Z/EG reporter activity was limited to single astrocytes in the cortical gray matter of adult mice (Figure 7-3 E-K). GFP-expressing astrocytes in  $\beta$ 1<sup>-/-</sup> brains seemed to be larger than WT astrocytes (Figure 7-3 E-K) and their main processes were clearly swollen (Figure 7-3 B, B', C, C' and Figure 7-3 E-K). As astrocytes have been shown to be hypertrophic after brain injury and these reactive astrocytes typically re-express the intermediate filaments GFAP and Vimentin, their expression was analyzed after deletion of  $\beta$ 1-integrins. As expected there were only low numbers of GFAP<sup>+</sup> astrocytes in the cortical gray matter of WT brains ( $13.2 \pm 23.8$  GFAP<sup>+</sup> cells/ mm<sup>2</sup> and Figure 7-3 A). In contrast, the number of GFAP<sup>+</sup> cells increased dramatically in the  $\beta$ 1<sup>-/-</sup> cortex ( $383 \pm 4.5$  GFAP<sup>+</sup> cells/ mm<sup>2</sup> and Figure 7-3 C) and all over the mutant telencephalon. Almost all S100 $\beta$ <sup>+</sup> cells now expressed GFAP in the mutant cortex ( $97.9 \% \pm 1.4 \%$  S100 $\beta$ <sup>+</sup> astrocytes also contain GFAP), whereas only  $6.9 \% \pm 2.7 \%$  of the S100 $\beta$ <sup>+</sup> astrocytes in the WT are co-expressing GFAP. Additionally, a subset of the GFAP-expressing astrocytes also expressed Vimentin throughout the  $\beta$ 1<sup>-/-</sup> cortex (Figure 7-3 M-M''), whereas this was rarely seen in WT astrocytes, only in a few cells underneath the pia mater (Figure 7-3 L-L''). It has been shown that upon brain trauma reactive astrocytes secrete extracellular matrix molecules like chondroitin sulfate proteoglycans (CSPG). Two members of this ECM-molecule family, Tenascin-C and the DSD-1 epitope recognized by the 473HD antibody were examined by Svetlana Sirko in WT (Figure 7-3 N-N'' and P-P'') and mutant cortices. Strikingly, these proteins were also upregulated after deletion of  $\beta$ 1-integrins (Figure 7-3 O-O'' and Q-Q''). Therefore it can be concluded that the loss of  $\beta$ 1-integrins at postnatal stages elicits several properties of reactive astrocytes after brain injury and integrin signaling is crucial for gray matter astrocytes to acquire a mature non-reactive state.



**Figure 7-3 Partial gliosis in the cerebral cortex of  $\beta 1^{-/-}$  mice**

In the cortical gray matter astrocytes are negative for the intermediate filament (IMF) GFAP (A), but can be labeled with S100 $\beta$  (B, B'). After deletion of  $\beta 1$ -integrins a strong upregulation of GFAP (C) in S100 $\beta$ -positive astrocytes (D, D') was observed. By using a GFP-reporter and thus visualizing an entire cell including all processes, astrocytes appeared larger in size with clearly swollen main processes in  $\beta 1^{-/-}$  brains (H-K) compared to the WT (E-G). Another IMF, Vimentin, normally not expressed in the gray matter of the cerebral cortex (L-L'') was upregulated after deletion of  $\beta 1$ -integrins (M-M''). The extracellular matrix molecules Tenascin C (N-O'') and DSD-1 labeled with an antibody against the epitope 473HD (P-Q'') were upregulated after loss of  $\beta 1$ -integrins.

### **7.1.2 Deletion of $\beta$ 1-integrin by Nex::Cre**

To further elucidate in which cell types the loss of  $\beta$ 1-integrins has to occur to elicit this phenotype, the  $\beta$ 1-integrin gene was deleted by the use Cre-recombinase under the control of the Nex-promoter. The basic helix-loop-helix transcription factor Nex is a member of the NeuroD family and is expressed from embryonic day E11.5 in most neocortical and hippocampal pyramidal neurons and their immediate progenitors, but not in astrocytes (Schwab et al., 1998; Beggs et al., 2003; Blaess et al., 2004; S. X. Wu et al., 2005; Belvindrah et al., 2007b). As expected astrocytes in the white matter were positive for GFAP (Figure 7-4 B, insert). However, even in 6 months old animals an upregulation of GFAP could not be observed in the gray matter of the cerebral cortex in Nex::Cre, fl $\beta$ 1/ fl $\beta$ 1 or WT animals (Figure 7-4 A, B) suggesting that the deletion of  $\beta$ 1-integrin in neurons only is not sufficient to cause the gliosis phenotype. Interestingly, the amount of myelin basic protein (MBP) and myelin associated glycoprotein (MAG) was massively reduced in the mutant gray matter (Figure 7-4 E, F) when compared to WT cortices (Figure 7-4 C, D) demonstrating that  $\beta$ 1-integrins were successfully deleted in mutant cortices. These data suggest that deletion of  $\beta$ 1-integrin at early stages in cortical neurons has severe effects on the interaction with myelinating oligodendrocytes, but does not affect astrocyte reactivity.

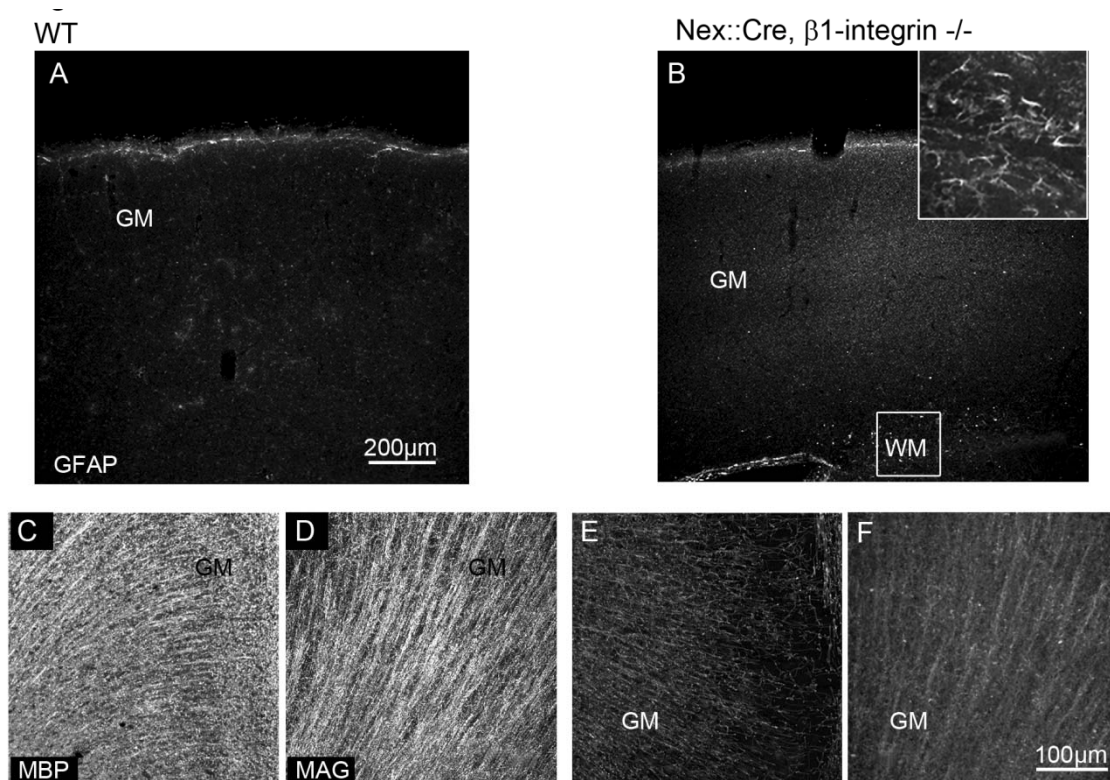


**Figure 7-4 Neuron specific deletion of the  $\beta$ 1-integrin gene did not lead to gliosis**

No signal for GFAP could be detected after immunofluorescent staining in the gray matter of the cerebral cortex of WT animals (A) and animals with a neuron specific deletion of  $\beta$ 1-integrins (B). However, another phenotype was observed confirming the successful deletion of the  $\beta$ 1-integrin gene; levels of the myelin proteins MBP and MAG were reduced after loss of  $\beta$ 1-integrins in neurons (E, F) when compared to the gray matter of the cerebral cortex in WT brains (C, D).

### **7.1.3 Loss of $\beta$ 1-integrins leads to a secondary partial microglia activation**

Upon acute brain trauma microglial cells are thought to be the first cell type reacting to the injury by change of their morphology, increase in motility and directed migration into the lesioned area, proliferation and upregulation of certain molecules, for example lectins or CD11b (Figure 7-5 A-A’’).

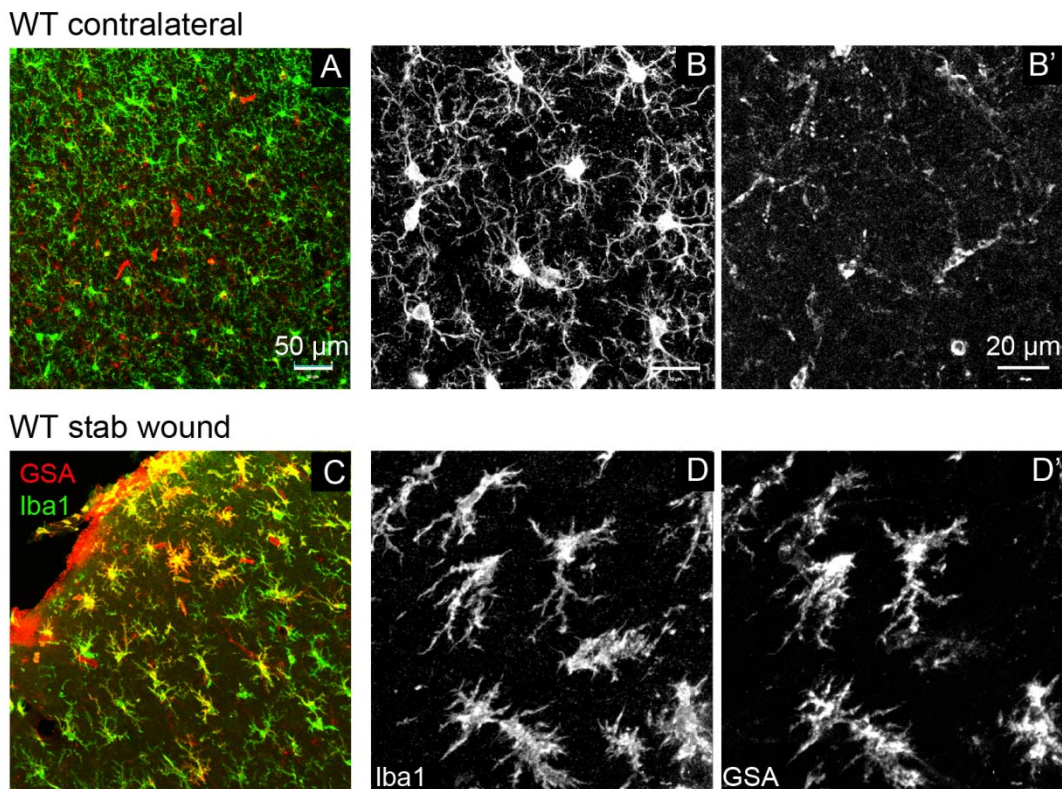


**Figure 7-5 Microglia activation shortly after a stab wound injury**

Microglia were labeled with Iba1 in uninjured WT brains (A) and after stab wound injury (C). Iba1-positive cells in the uninjured contralateral hemisphere are ramified with lots of fine processes (B). After stab wound injury microglia became hypertrophy with swollen cell bodies and main processes, whereas finer branches disappeared (D). In addition, activated microglia upregulated GSA-lectin (D'), which is also expressed in endothelial cells of blood vessels, but not in resting microglia (B').

However, this cell type was not expected to respond in the  $\beta 1^{-/-}$  animals, as microglia are of mesodermal origin (Chan et al., 2007) and should therefore not be recombined by hGFAP-Cre. This was confirmed by immunofluorescent staining for the general microglia marker Iba1 in reporter-positive WT and  $\beta 1^{-/-}$  brains. GFP-positive cells were in close proximity to Iba1<sup>+</sup> microglia, but GFP was not contained within Iba1<sup>+</sup> cells in WT or  $\beta 1^{-/-}$  brains (Figure 7-6 A-D).

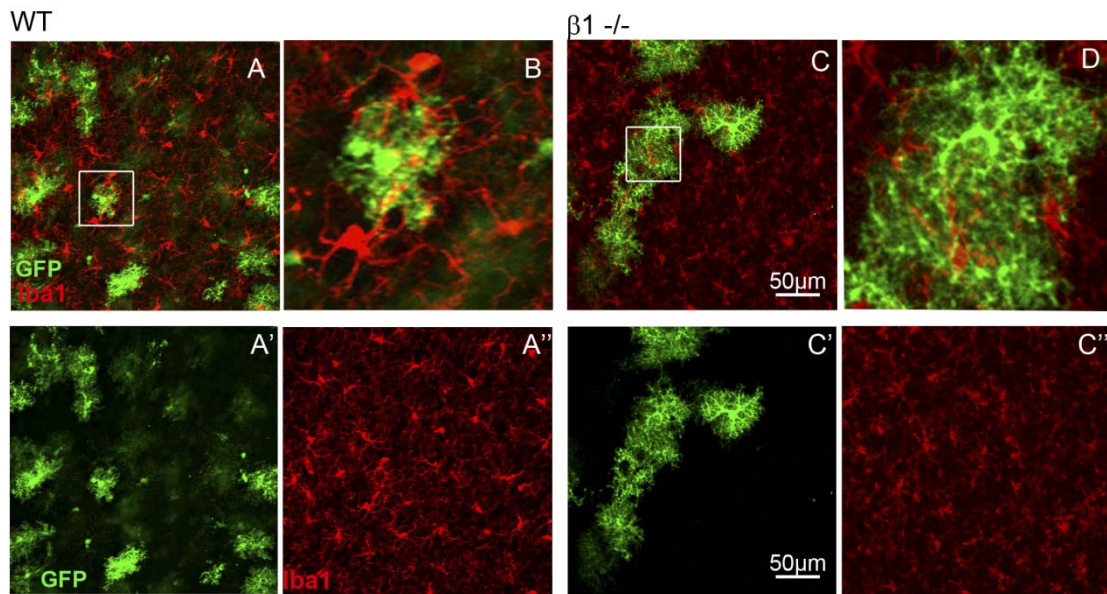


**Figure 7-6 Iba1 positive microglia were not recombined by hGFAP-Cre**

**A** GFP-reporter was used to examine whether hGFAP-Cre was also recombining microglia cells. In the gray matter of the cerebral cortex reporter-positive cells were in close proximity to each other, but no double positive cells could be detected in WT (A, A', A'', B) or  $\beta 1^{-/-}$  brains (C, C', C'', D).

Surprisingly, immunofluorescent staining against Iba1 revealed differences in the morphology of microglia in WT and  $\beta 1^{-/-}$  cortices as finer processes seemed to be reduced and main processes showed hypertrophy in mutant brains when compared to WT littermates (Figure 7-6 A'' and C'', Figure 7-7 A, A' and B, B'). Both, GSA-lectin and Cd11b were clearly upregulated in  $\beta 1^{-/-}$  brains (Figure 7-7 B'', D, D'), whereas in WT CD11b protein was at basic levels (Figure 7-7 C, C') and GSA-lectin was detected in endothelial cells only (Figure 7-7 A', A''). After an injury microglia migrate towards the injury site and start to proliferate to increase their cell numbers. Quantification of Iba1-positive microglial cells in cortical layers I to III, where reactive gliosis seemed to be strongest, showed a significant increase in numbers in  $\beta 1^{-/-}$  cortices ( $654.5 \pm 30.7$  Iba1<sup>+</sup>/mm<sup>2</sup>, n = 3) when compared to WT cortices ( $536.1 \pm 41.5$  Iba1<sup>+</sup>/mm<sup>2</sup>, n = 3,  $p \leq 0.039$ ).

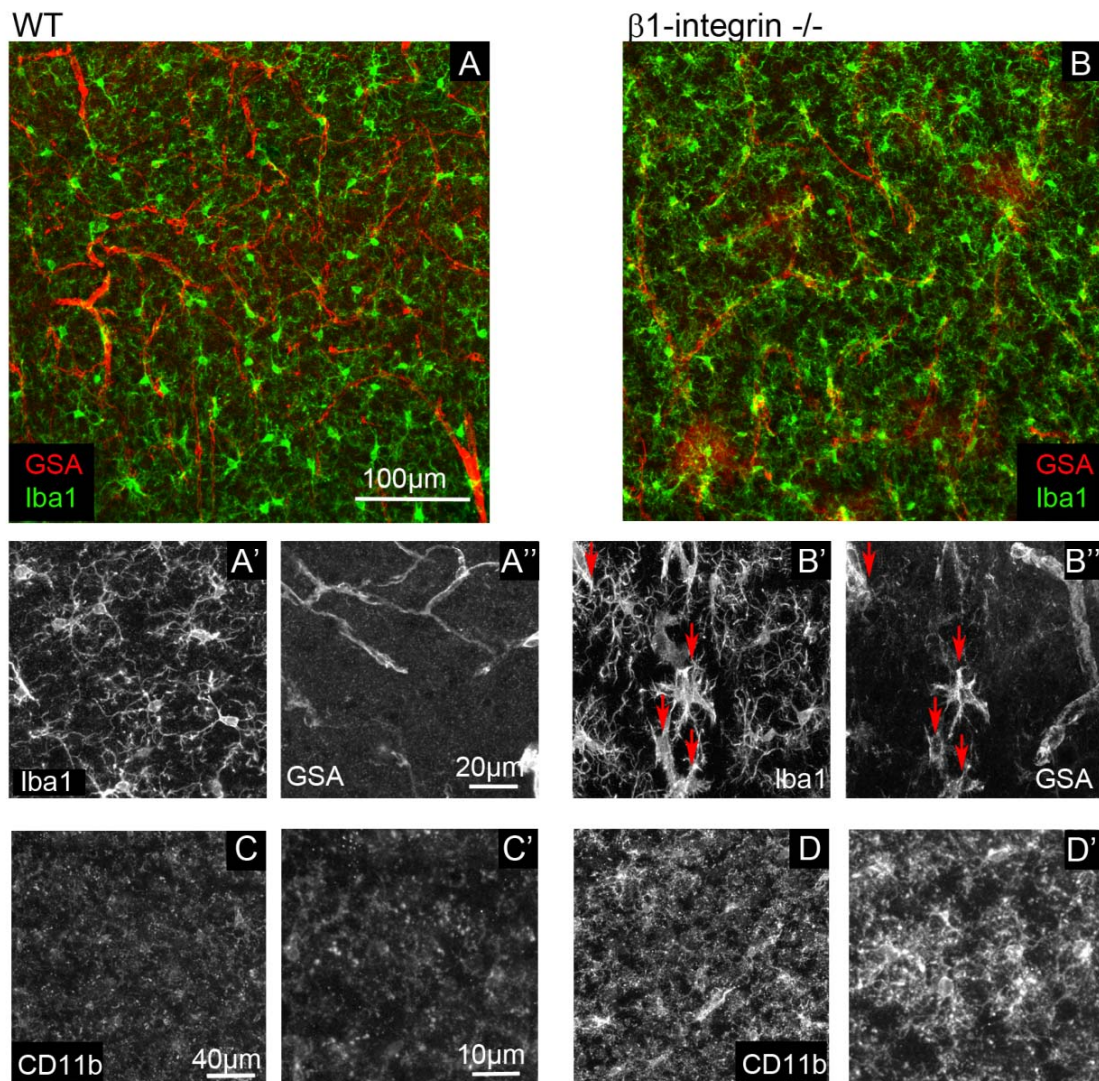


**Figure 7-7 Microglia were activated after loss of  $\beta$ 1-integrins**

In WT brains microglia stained for Iba1 (A) had lots of fine and often branched processes (A, A'), but were negative for GSA-lectin (A'') or Cd11b (C, C''), both markers for activated microglia. After loss of  $\beta$ 1-integrins overall less fine processes were seen (B). Instead some microglial cells had hypertrophy cell bodies and processes (B') and were positive for GSA-lectin (B''). Overall higher levels of Cd11b were detected in  $\beta$ 1-/- cortices (D, D').

To examine whether proliferation contributes to the increase in microglia numbers BrdU was administered for 14 days via the drinking water to label all fast and slow dividing cells. As described before (Kettenmann and Ransom, 2005), a low proportion of microglia proliferated in the non-injured WT cortices ( $1.6 \% \pm 0,4 \% \text{ Iba1}^+ \text{ BrdU}^+ / \text{ Iba1}^+$ ,  $n = 4$  and Figure 7-8 A, A'). Even though the

overall proliferation was not significantly increased in  $\beta$ 1<sup>-/-</sup> cortices (9.1 %  $\pm$  6.6 %, n = 5, p = 0.14 and Figure 7-8 B, B'), a difference between animals with 3 of 5 showing an increase in microglia proliferation (14.5 %  $\pm$  5 %, n = 3, p  $\leq$  0.02) suggesting an incomplete penetration of this phenotype. In conclusion, also microglia were activated after deletion of  $\beta$ 1-integrin showing hypertrophy, upregulation of GSA-lectin and CD11b and an incomplete increase in proliferation. As microglia are not recombined by hGFAP-Cre this activation seems to be rather indirect and due to a non-cell-autonomous mechanism

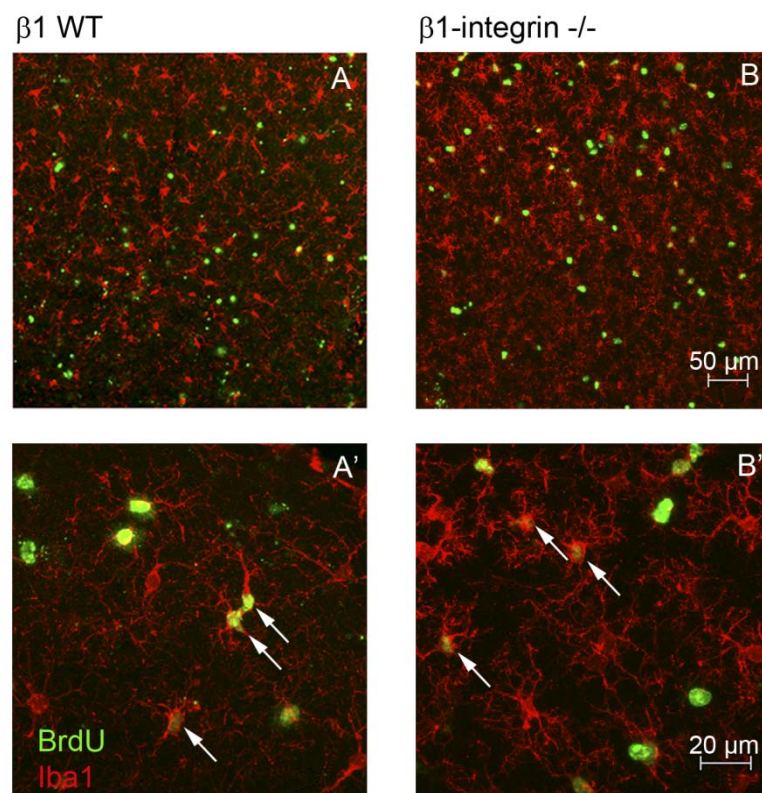


**Figure 7-8 Microglia are proliferating in WT and in  $\beta$ 1<sup>-/-</sup> cerebral cortex**

Immunofluorescent staining for Iba1 and BrdU revealed that not only activated microglia after loss of  $\beta$ 1-integrins were proliferating (B, B'), but also resting microglia in uninjured WT cortices (A, A').

#### **7.1.4 Could the gliosis phenotype be induced by non cell autonomous side effects of $\beta$ 1-integrin deletion?**

Given the fact that not only astrocytes but also microglia were activated after deletion of  $\beta$ 1-integrin the question arose whether indirect effects like cell death or disruptions of the BBB could account for these effects. Integrins have been implicated in the regulation of cell survival (Stupack, 2005) and dying cells could cause astrocytes and microglia to get reactive. For necrosis Tetsuji Mori used Cresyl violet- and DAPI staining, for apoptosis by staining against activated caspase 3. Comparable low numbers of pyknotic nuclei or caspase 3 positive cells were found in WT and  $\beta$ 1-/- cortices demonstrating that reactive astrocytes and neurons survive well after the deletion of  $\beta$ 1-integrins and that increase in cell death is unlikely to induce reactive gliosis in these animals. Astrocytes are thought to be important for the integrity and maintenance of the BBB as their endfeet cover the majority of the cerebral surface of the endothelium (Wolburg et al., 1994; Abbott et al., 2006). After brain injury the BBB is either mechanically disrupted or possibly also affected indirectly as a consequence of loss of astrocyte polarity observed in experimental autoimmune encephalomyelinitis (EAE) (Wolburg-Buchholz et al., 2009; Wolburg et al., 2009b). Additionally, in brain tumors the BBB has been reported to be leaky and this correlates with a loss in astrocyte polarity (Wolburg et al., 2003; Wolburg-Buchholz et al., 2009). The integrity of the BBB was examined by intraperitoneal injection of one of the smallest tracers for BBB leakage, Fluoresceine-Dextran with a molecular weight of 3000 Da. As expected the tracer diffused into the brain parenchyma after stab wound injury in  $\beta$ 1-/- animals (Figure 7-9 A). However, fluorescence was restricted to brain capillaries (Figure 7-9 B) and did not diffuse any further at the contralateral non-injured hemisphere in mutant animals (Figure 7-9 C) showing that the BBB is functionally intact even after loss of  $\beta$ 1-integrins. Thus, one can conclude that the gliosis phenotype is not secondary to the above described events, cell-death or BBB disruption.

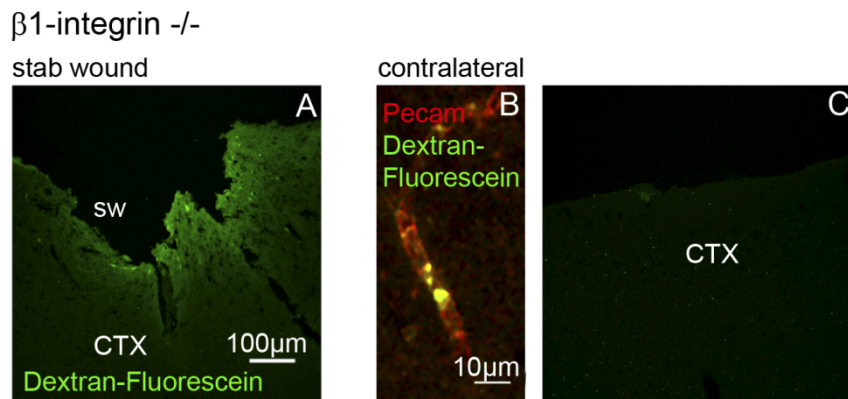


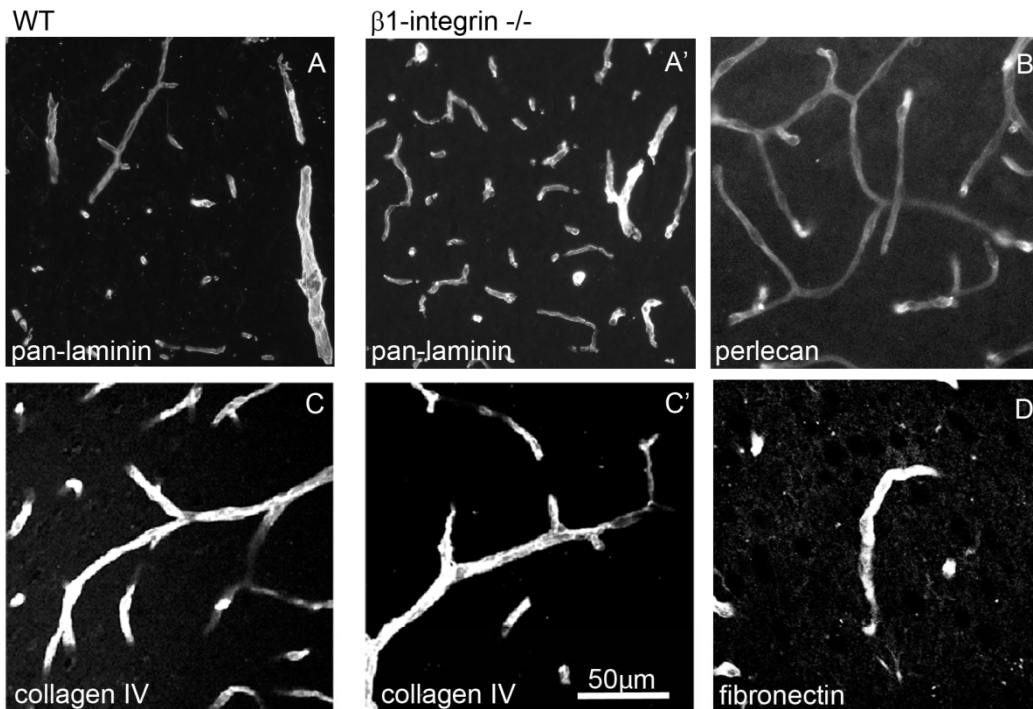
**Figure 7-9** The blood-brain barrier is not impaired after deletion of  $\beta$ 1-integrins

The integrity of the blood-brain barrier (BBB) was tested by injecting a dextran coupled to a fluorescent dye intraperitoneal. After stab wound injury to destroy the BBB as control for successful injection the dye diffused into the parenchyma in  $\beta$ 1-/- cerebral cortices (A). In the uninjured contralateral hemisphere the dye was restricted to the lumen of blood vessels (B) and did not diffuse into the brain parenchyma (C).

### **7.1.5 The basement membrane is not primarily affected after loss of $\beta$ 1-integrins at postnatal stages**

It has been demonstrated before that  $\beta$ 1-integrins are required for cells contacting the basement membrane (e.g. endothelial cells and radial glia) to maintain BM integrity (Graus-Porta et al., 2001; Brakebusch and Fassler, 2005; Belvindrah et al., 2006). Thus, the condition of the BM was examined by staining for their three major components laminin, collagen IV and perlecan. In two month old animals the immunostaining for these components nicely outlined blood vessels for all three constituents in both, WT (Figure 7-10 A, C) and mutant cortices (Figure 7-10 A', B, C') at the lightmicroscopic level. The same was true for fibronectin (Figure 7-10 D), another protein present in the ECM. At six month of age, however, an irregular distribution of collagen IV was observed along the vessels in  $\beta$ 1-/- cortices, especially at larger vessels and underneath the pia, where it seemed to be disrupted and sometimes punctuated (Figure 7-10 E'). The BM around smaller vessels seemed still to be intact.

2 month of age



6 month of age

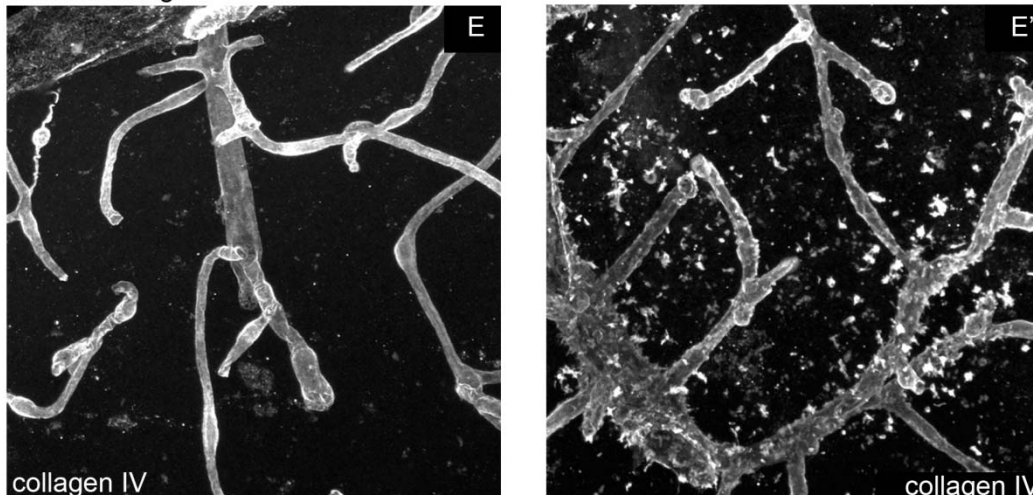


**Figure 7-10** Basement membrane changes only at later stages in  $\beta 1$ -/- cortices

Immunofluorescent staining of the basement membrane components laminin, perlecan, collagen IV and fibronectin were comparable in WT (A) and  $\beta 1$ -/- (A'-D) cerebral cortices of 2 months old mice. In 6 months old mice collagen IV staining smoothly outlined blood vessels in WT cerebral cortices (E). After deletion of  $\beta 1$ -integrin collagen IV was not only localized to the basement membrane surrounding blood vessels, but was also deposited in high amounts in the extracellular matrix close by (E').

To elucidate whether the zipper-like structure of the BM is changed already at younger ages leading to an obvious defect at the lightmicroscopy level only later on, an ultrastructural analysis of WT and  $\beta 1^{-/-}$  cortices was conducted at 2 and 6 month of age in collaboration with Saida Zoouba (Institute for Pathology, HelmholtzZentrum München). The leptomeningeal BM displayed some abnormalities already in 2 months old animals after loss of  $\beta 1$ -integrins seen as bright spots separating the two BM sheets. These aberrations were observed also in 6 months old mutant brains (Figure 7-11 B-B'), but never occurred in WT brains (Figure 7-11 A-A'). In contrast, the perivascular BM around intracerebral vessels appeared normal in 2 months and even in 6 months old WT and mutant animals (Figure 7-11 C-D'). Astrocyte endfeet appeared frequently swollen not only in  $\beta 1^{-/-}$  but also in WT brains most likely due to a fixation artifact. Otherwise endfeet were morphologically normal and in close contact to the BM surrounding intracerebral capillaries (Figure 7-11 C-D'). To summarize, perivascular BM defects appeared only at later stages and are neither correlated to, nor causing the gliosis phenotype.

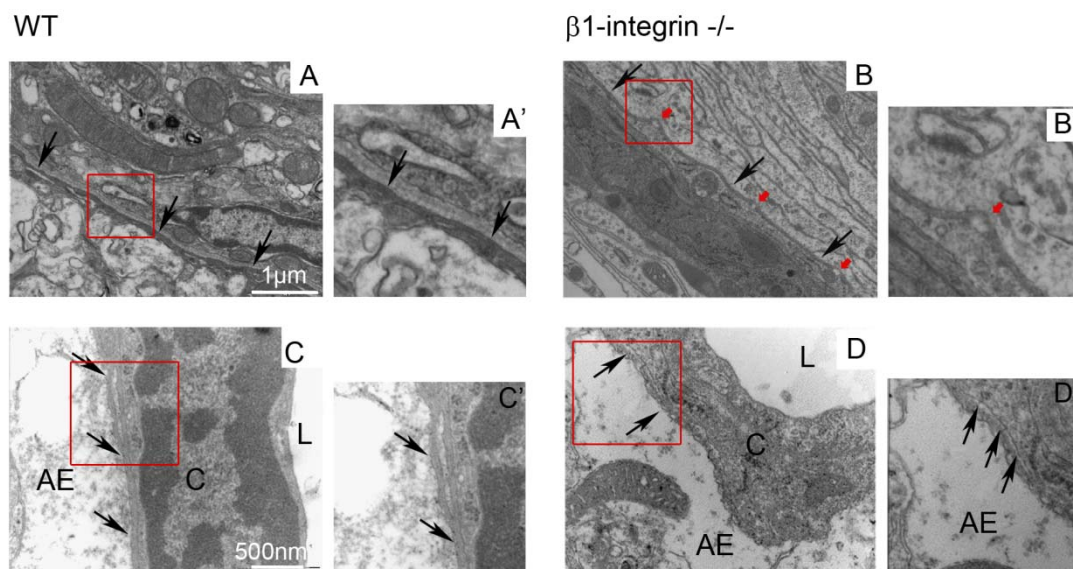


**Figure 7-11 Analysis of the basement membrane at the ultrastructural level**

**At the ultrastructural level the basement membranes (BM) can be identified as two dark parallel lines. The leptomeningeal BM (A, A') displayed irregularities in mutant cortices (B, B'). However, perivascular BMs were normal in WT (C, C') and  $\beta 1^{-/-}$  cortices (D, D') of 6 months old animals.**

### **7.1.6 The astrocyte endfeet polarity is disturbed after deletion of $\beta$ 1-integrin**

Not only any indirect effects like cell death, disruptions of the BBB or aberrations in the BM could be excluded as a cause for the gliosis, but also the loss of  $\beta$ 1-integrins in neurons is not sufficient to elicit this phenotype. Thus, disturbances in astrocyte polarity itself caused by the loss of signaling from the BM could account for the reactivity of astrocytes. To test this hypothesis, proteins that are specifically localized at astrocyte endfeet, e.g. Aqp4 and members of the DAG complex, were examined. As expected, staining for Aqp4, dystrophin,  $\beta$ -dystroglycan and  $\alpha$ -dystrobrevin outlined blood vessels in WT cortices as capillaries are almost completely covered by astrocyte endfeet (Figure 7-12 A, A', C, C', E, E', G, G'). Strikingly, this staining pattern was punctuated for all examined astrocyte endfeet proteins in  $\beta$ 1<sup>-/-</sup> cortices (Figure 7-12 B, B', D, D', F, F', H, H'). This is indicating that at least part of the astrocytes lost their endfeet polarity rather than their contact to the BM as no endfeet retraction was observed at the ultrastructural level. In conclusion,  $\beta$ 1-integrins are necessary to maintain the endfeet polarity of gray matter astrocytes enabling them to acquire a mature non-reactive state.

### **7.1.7 Reactive astrocytes in $\beta$ 1-integrin-deficient cortices do not proliferate or regain stem cell properties**

After brain injury, some reactive astrocytes dedifferentiate, re-enter the cell cycle and even regain stem cell properties in vitro (Buffo et al., 2005; Buffo et al., 2008). To test, whether reactive astrocytes in  $\beta$ 1<sup>-/-</sup> cerebral cortices proliferate, BrdU was administered for 2 weeks via the drinking water. BrdU-positive cells were found scattered throughout the brain parenchyma in comparable numbers in WT ( $131.1 \pm 21.5$  BrdU/ mm<sup>2</sup>, n = 4) and  $\beta$ 1<sup>-/-</sup> cerebral cortices ( $147.4 \pm 53.4$  BrdU/ mm<sup>2</sup>, n = 7, p = 0.65). The vast majority of these BrdU-incorporating cells are Olig2-positive progenitors in a normal, non-injured WT brain and are giving rise mainly to NG2-glia (Buffo et al., 2005; Dimou et al., 2008). In line with the observations in WT controls only a low proportion of these proliferating cells are positive for GFAP (0.2 %  $\pm$  0.7 % BrdU+ GFAP+)

GFAP<sup>+</sup> cells in WT,  $n = 4$  and Figure 7-13 D). Unexpectedly, there was no significant increase in proliferating astrocytes in  $\beta$ 1<sup>-/-</sup> cortices ( $3 \% \pm 1.8 \%$  BrdU<sup>+</sup> GFAP<sup>+</sup>/ GFAP<sup>+</sup>,  $n = 4$ ,  $p = 0.06$  and Figure 7-13 C, C', D). Similar results have been obtained using S100 $\beta$  to label astrocytes (Figure 7-13 A, B', D).

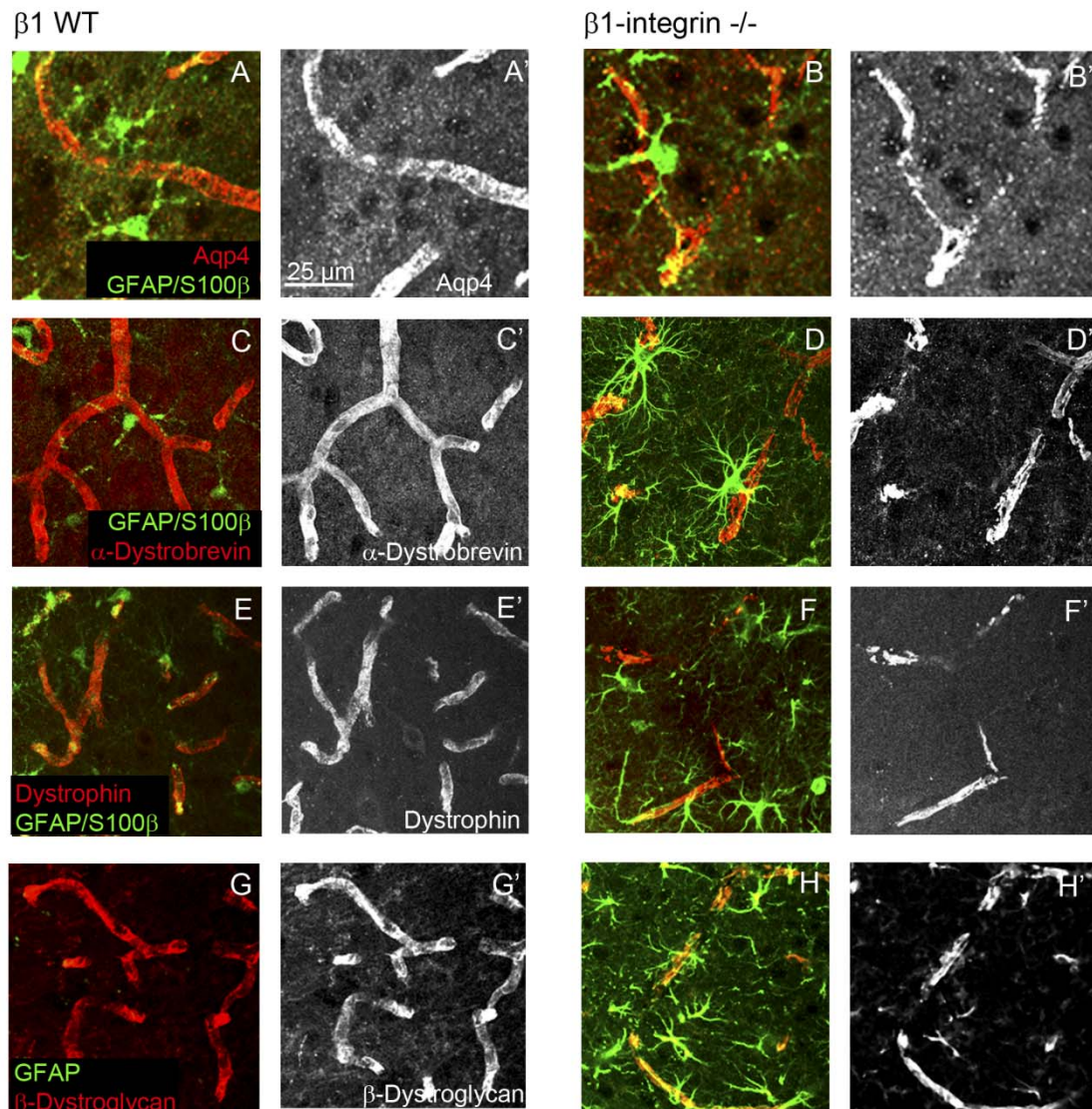


**Figure 7-12 Astrocyte endfeet polarity is disturbed after deletion of  $\beta$ 1-integrin**

In the cortical gray matter of WT animals immunofluorescent stainings for proteins localized in astrocyte endfeet, like the water channel Aqp4 (A, A') or members of Dystrophin-associated glycoprotein complex including  $\alpha$ -Dystrobrevin (C, C'), Dystrophin (E, E') and  $\beta$ -Dystroglycan (G, G') outline blood vessels as the latter are completely covered by astrocyte endfeet. After loss of  $\beta$ 1-integrins these stainings were disrupted and punctated (B, B', D, D'; F, F', H, H').

However, astrocytes in  $\beta 1^{-/-}$  cortices acquired several characteristics of reactive astrocytes after an injury and could be therefore prone to dedifferentiate under supporting conditions. The self-renewing and multipotency capacity of reactive astroglia can be tested using the in vitro neurosphere assay (Buffo et al., 2008). Towards this aim, tissue from uninjured WT and  $\beta 1^{-/-}$  cerebral cortices was dissociated and cultured in neurosphere medium. As expected, no neurospheres could be grown from WT uninjured gray matter even after 3 weeks in culture (Figure 7-13 E). Likewise, under physiological conditions astrocytes from  $\beta 1^{-/-}$  cortices never gave rise to any neurosphere (Figure 7-13 E), leading to the conclusion that loss of  $\beta 1$ -integrins mediated signaling in the uninjured brain is not sufficient to induce dedifferentiation of astrocytes towards a stem cell stage. A related question is whether deletion of  $\beta 1$ -integrin would even interfere with regaining a self-renewal capacity after brain injury. To tackle this possibility WT and  $\beta 1^{-/-}$  animals were injured using a V-lance knife and sacrificed 3 days later. Tissue around the lesion site and from the corresponding brain region at the contralateral hemisphere was dissected and dissociated according to the neurospheres culture protocol. As described before, neither from WT, nor from  $\beta 1^{-/-}$  contralateral hemispheres neurospheres could be generated. Comparable to (Buffo et al., 2008) a low number of plated cells gave rise to neurospheres in cultures from WT injured brain tissue (Figure 7-13 E). Interestingly, preliminary data suggest that this neurosphere-forming capacity is reduced after deletion of  $\beta 1$ -integrin (Figure 7-13 E). Taken together, although elsewhere all hallmarks of reactive astrocytes can be observed in  $\beta 1^{-/-}$  cortices, the proliferative response is not elicited or may be even inhibited upon deletion of  $\beta 1$ -integrins.

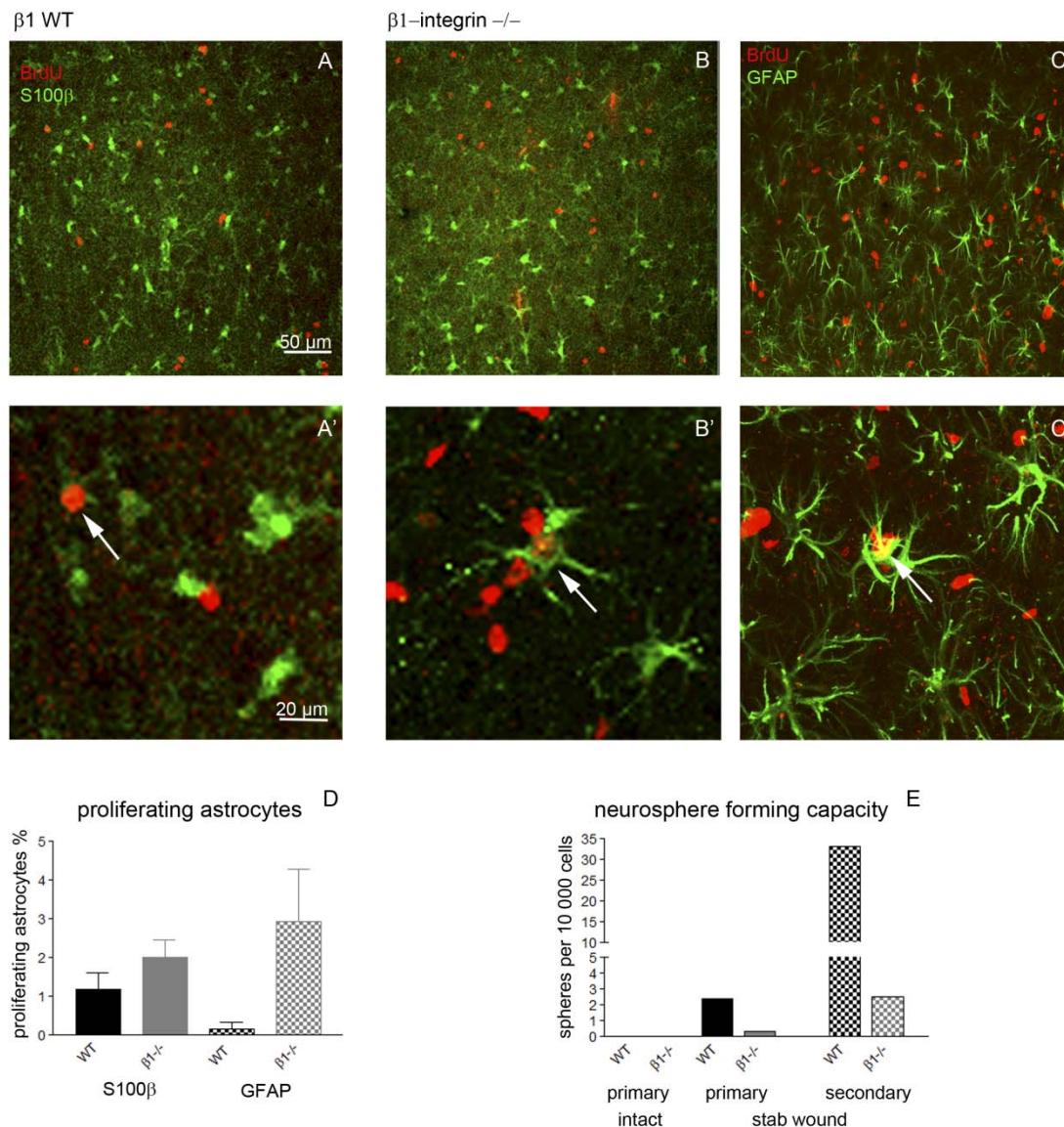


**Figure 7-13 Astrocytes do not re-enter the cell-cycle after loss of  $\beta 1$ -integrins**

After 2 weeks of BrdU administration hardly any BrdU S100 $\beta$  double positive astrocyte could be seen in WT (A, A') and  $\beta 1^{-/-}$  (B, B') cerebral cortices. The same held true for counter labeling with GFAP in  $\beta 1^{-/-}$  cortices (C, C'). D shows that numbers of BrdU-positive cells counterlabeled with S100 $\beta$  or GFAP do not differ between intact WT and  $\beta 1^{-/-}$  cortices. No neurospheres were formed from WT and  $\beta 1^{-/-}$  dissociated uninjured cortices (E). The formation of primary, as well as secondary neurospheres from the injured cerebral cortex was impaired in  $\beta 1^{-/-}$  mice (E).

## 7.2 The influence of $\beta$ 1-integrins on astroglial-like stem cells

Astroglial-like stem cells in the subependymal zone make contact to and are in close proximity to the BM surrounding blood vessels. It has been proposed that this close contact is a special and essential feature of the stem cell niche (Shen et al., 2008).

### 7.2.1 $\beta$ 1-integrins are dispensable for the proliferation of adult SEZ stem cells

To examine the role of  $\beta$ 1-integrins mediated signaling from the basement membrane, slow dividing cells were marked using a label retaining BrdU pulse. Therefore, BrdU was administered for two weeks via the drinking water followed by a two weeks chase to dilute the label in fast proliferating cells. In the SEZ of WT mice 40.4 % of the cells that incorporated and kept the BrdU label were GFAP<sup>+</sup> stem cells (Figure 7-14 A, n = 2). Similarly, 41.9 % of the cells were double positive for BrdU and GFAP in the SEZ of  $\beta$ 1<sup>-/-</sup> brains. Only a small proportion of the BrdU<sup>+</sup> cells stained for Dcx in WT (14.5 %) and  $\beta$ 1<sup>-/-</sup> (9.7 %) SEZs suggesting that 2 weeks chase are sufficient to dilute the label in most of the fast proliferating progeny of SEZ stem cells, the type C cells that then give rise to Dcx<sup>+</sup> neuroblasts. Almost half of the BrdU<sup>+</sup> cells were neither positive for GFAP nor for Dcx in WT (45.1 %) and  $\beta$ 1<sup>-/-</sup> (48.5 %) and Figure 7-14 A) brains and could be slow-proliferating NG2 or Olig2 cells, endothelial cells, ependymal or postmitotic progeny of the astroglial-like stem cells. To investigate the self renewing capacity of stem cells after loss of  $\beta$ 1-integrins neurospheres were cultured from the adult SEZ. In order to do so, the SEZ of WT and  $\beta$ 1<sup>-/-</sup> mice was dissected, the tissue was dissociated and cells were seeded in neurosphere medium containing the growth factors EGF and FGF under non-adherent conditions in cell culture flasks. Under these conditions, one single stem cell can divide giving rise to daughter cells that stick together forming a neurosphere. Thus, one neurosphere is a clone derived from a single cell. In line with the results obtained in vivo, primary neurospheres were similar in number in WT and  $\beta$ 1<sup>-/-</sup> cultures (Figure 7-14 B, n = 2). To test self-renewal,

primary neurospheres were dissociated to single cells and plated at clonal density (1 cell per  $\mu\text{l}$ ). The number of secondary spheres was quantified and preliminary results obtained from 2 independent cultures indicated no significant differences between WT and  $\beta 1^{-/-}$  cultures (Figure 7-14 B). Taken together, deletion of  $\beta 1$ -integrins did not interfere with the proliferative capacity of adult SEZ stem cells.

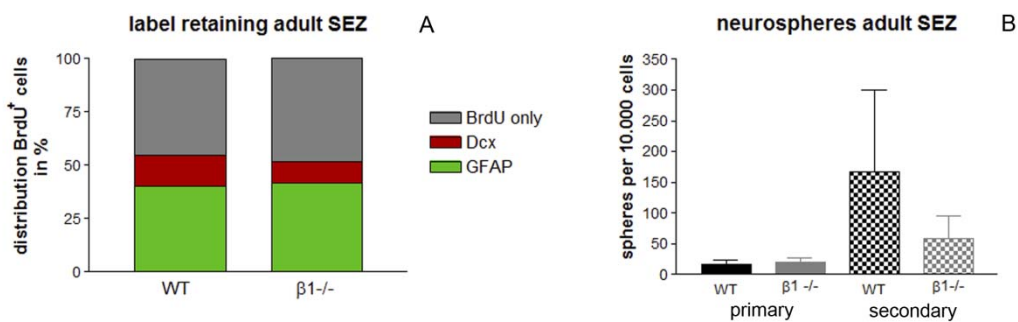


**Figure 7-14 Proliferation capacity of SEZ stem cells after deletion of  $\beta 1$ -integrins**

**A** label retention BrdU pulse was used to mark slow dividing and postmitotic cells. SEZ stem cells were quantified after immunofluorescent staining for BrdU and GFAP in WT and  $\beta 1^{-/-}$  brains (A). Neurospheres were cultured from the adult SEZ of WT and  $\beta 1^{-/-}$  brains and the number of primary and secondary spheres was quantified (B).

### **7.2.2 $\beta 1$ -integrins are important for neuroblast migration**

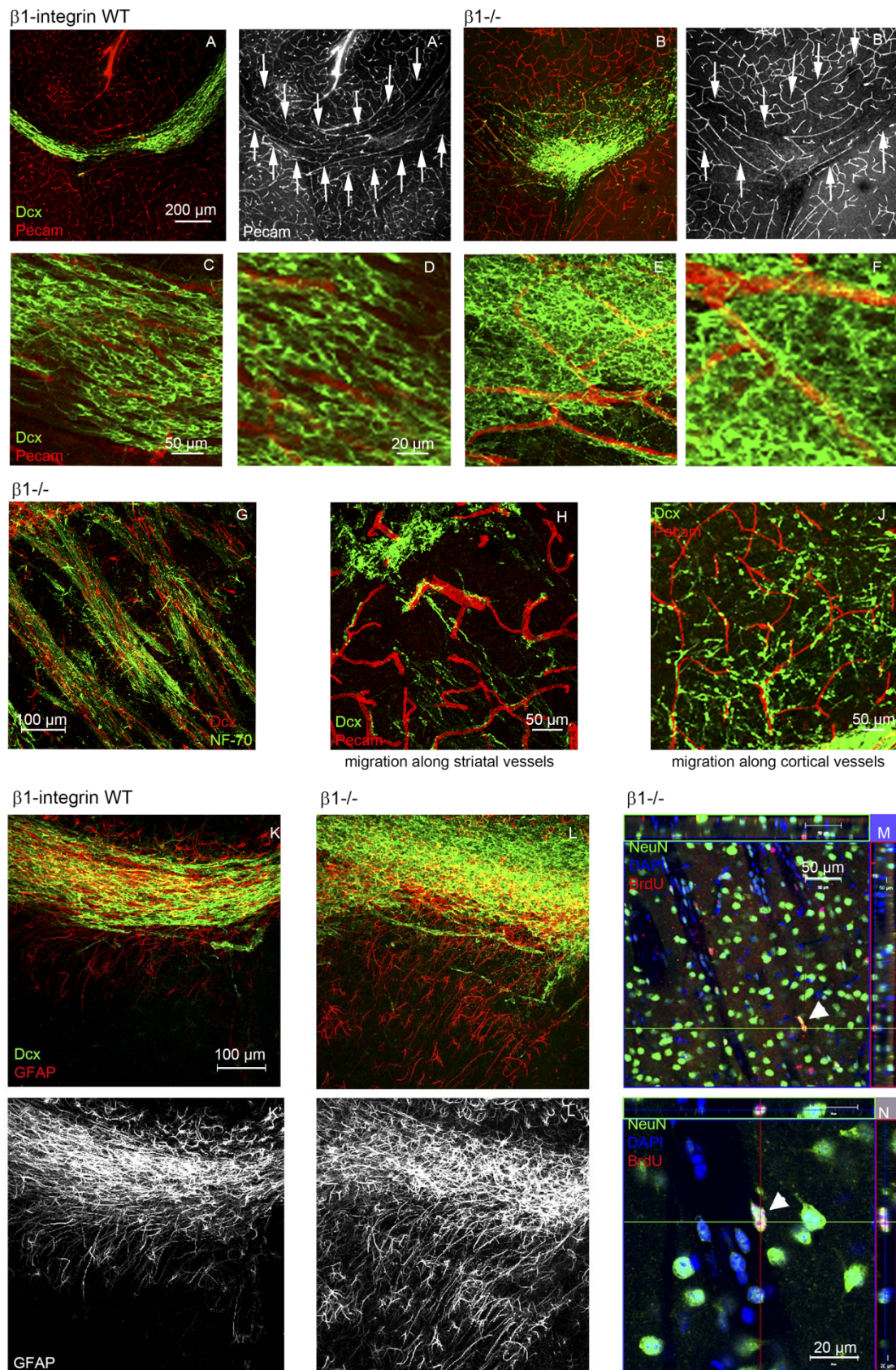
Newly generated neuroblasts, the progeny of the SEZ stem cells, migrate in chains through the RMS towards the OB (Figure 7-15 A, C, D), where they differentiate into interneurons. In WT brains the RMS is a clearly defined path characterized by blood vessels running in parallel (Saghatelyan, 2009; Snapyan et al., 2009) and Figure 7-15 A'), which newborn neurons leave only when they reached the OB. After deletion of  $\beta 1$ -integrins, however, the RMS seemed to be larger containing massive amounts of neuroblasts (Figure 7-15 B, B'). These neuroblasts did not migrate in chains anymore, but in a rather unordered manner (Figure 7-15 B, E, F). Often  $\text{Dcx}^+$  cells leaving the RMS migrated into the striatum along and intermingled with striatal fibers (Figure 7-15 G). Nevertheless, some of them used blood vessels as a substrate (Figure 7-15 H),

as also seen for the neuroblasts migrating towards the cerebral cortex, which were mostly located in lower cortical layers (Figure 7-15 J). Notably, this phenotype was predominant in only one of these regions with migration of neuroblasts either largely into the striatum or the cerebral cortex.

It has been demonstrated that the parallel organization of blood vessels is essential for neuroblast migration within the RMS (Snapyan et al., 2009). Strikingly, the arrangement of RMS blood vessels was disturbed after deletion of  $\beta$ 1-integrins (Figure 7-15 B, B'). As hGFAP-Cre mediated recombination spares endothelial cells, it is tempting to speculate that astrocytes influence the organization of RMS blood vessels during development by  $\beta$ 1-integrins mediated mechanisms.

To investigate the fate of the mismigrating neuroblasts a label retention BrdU pulse was given to mark newly generated cells and allow them to mature. As expected, no overlap between BrdU and NeuN, a marker for mature neurons, could be detected in striatum or cortical gray matter of WT animals. However, the misrouted newborn neurons in the striatum matured to a certain extent, as NeuN BrdU double positive cells were detected in one out of three animals (Figure 7-15 M, N). This was not observed in the cerebral cortex. However, given the variability of this phenotype as described above, many more animals would have to be examined to assert the absence of BrdU/ NeuN positive cells in the cortex. Taking into account the huge number of Doublecortin cells, this analysis clearly shows that only few of them reach the NeuN positive state of neuronal maturity.

**Figure 7-15: Neuroblasts migrate within the rostral migratory stream (RMS) along blood vessels that are arranged in parallel (A, A'). Tangentially migrating neuroblasts formed chains in WT brains (C, D). After loss of  $\beta$ 1-integrins neuroblasts leave the RMS (B), which lost its parallel organization of blood vessels (B'). In addition, the chain migration of neuroblast was lost and neuroblast were unorganized (E, F). Neuroblast that left the RMS migrated into the striatum using striatal fibers (G) or blood vessels (H). Neuroblasts migrating toward the cortical gray matter were observed in close proximity to blood vessels (J). Astrocytes in the RMS were in contrast to surrounding astrocytes fibrous and GFAP-positive clearly outlining the path (K, K'). After deleting  $\beta$ 1-integrin RMS astrocytes became hypertroph and indistinguishable from surrounding astrocytes, which were likewise hypertroph and GFAP-positive (L, L'). Some of the neuroblasts entering the striatum further matured into NeuN positive neurons (arrowheads in M and N).**

Figure 7-15  $\beta 1$ -integrins influence neuroblast migration

### 7.3 Polarity of astrocytes after brain injury

Stem cell astrocytes as well as parenchymal astrocytes of the gray matter are polarized at their basal membrane domain and this special kind of polarity seems to be important for gray matter astrocytes to acquire a mature non-reactive phenotype (see above). After traumatic brain injury, the contact of astrocytes directly at the injury site may be disrupted mechanically, thus interfering with this type of polarity. However, depending on the magnitude of injury astrocytes do not only upregulate IMF and modulate the ECM; in near proximity of the injury site they also change their morphology dramatically towards an elongated shape establishing another kind of polarity (Figure 7-16 A, B and Oberheim et al., 2008) that can be modeled in vitro by using a scratch wound assay. In this assay a monolayer of mouse astrocytes from the postnatal cerebral cortex has been grown to full confluence in standard medium supplemented with 10 % FCS without any further growth factors to allow the acquisition of a relatively mature state. After 3 to 4 weeks in culture cells were mostly of flat morphology and could be labeled with antibodies against the astrocytic proteins S100 $\beta$  and/or GFAP (Figure 7-17 A-A''). Most of the astrocytes were positive for both proteins (arrowheads in Figure 7-17 A-A'') and only some cells were only S100 $\beta$  immunoreactive (stars in Figure 7-17 A-A''). As previously described (Etienne-Manneville, 2006), after injuring the monolayer astrocytes extended a process into the scratch and subsequently migrated, which reduced the scratch size already 24 hours later (Figure 7-17 B-E). Astrocytes adjacent to the scratch extended processes with leading tips mostly filled by tubulin positive fibers and stabilized by the actin cytoskeleton (Figure 7-17 F, G). This protrusion formation was preceded by reorientation of the centrosome (Figure 7-17 H) and the golgi apparatus (Figure 7-17 J) towards the injury site.

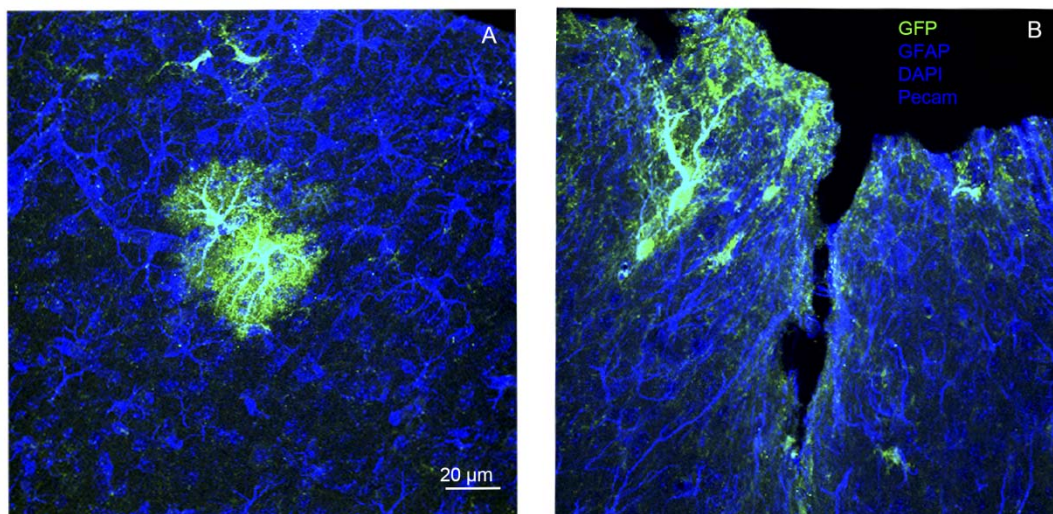


**Figure 7-16 Astrocytes change their morphology after acute injury in vivo**

Astrocytes in the gray matter of the intact cerebral cortex have star like morphology with a few main processes ramifying into thousands of fine branches (A). After stab wound injury astrocytes elongate and extend a few thick processes towards the injury site, whereas branches at the rear of the cell seem to be retracted (B).

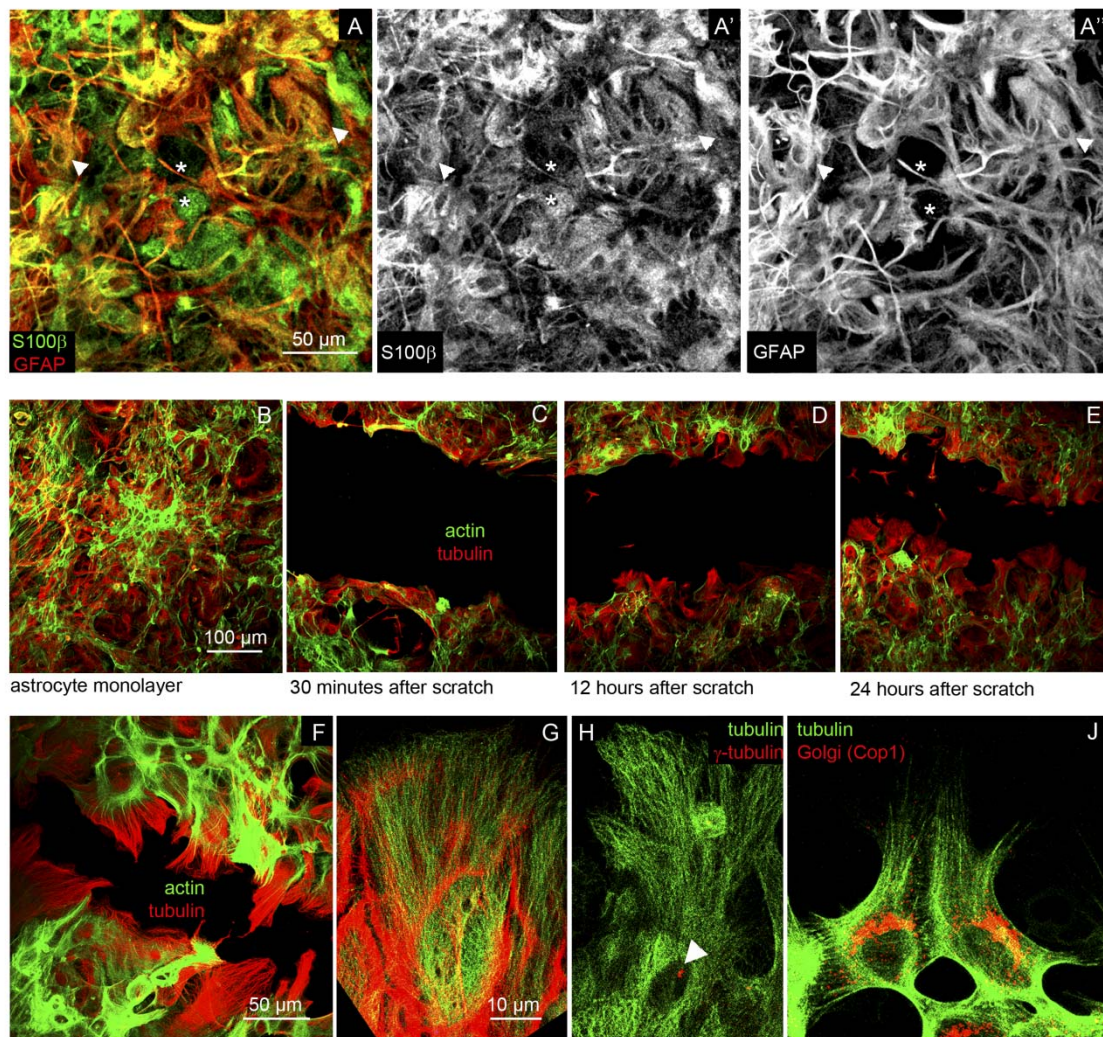


**Figure 7-17 Astrocytes in vitro react to injury by polarization and migration**

Cells of postnatal astrocyte cultures were mainly double-positive for S100 $\beta$  and GFAP (arrowheads in A, A', A''), only few cells were only positive for S100 $\beta$  (stars in A, A', A''). After scratching, cells in the monolayer reacted to the injury and reduced the size of the gap over time (B-E). Astrocytes at the scratch formed an extension into the cell free area (F, G, and H). These protrusions were rich in tubulin and stabilized by the actin cytoskeleton (F, G). Centrosomes (arrowhead in H) or golgi (J) of polarized cells were reoriented facing the injury area.

### 7.3.1 Small RhoGTPases influence astrocyte polarization and migration in vitro

#### Cdc42 is important to polarize cells after injury in vitro

Astrocyte cultures of postnatal C57/Bl6 mice were stained for Cdc42 at different time points after injuring the monolayer (Figure 7-18 A – C'). Shortly after the injury Cdc42 is localized mainly around the nuclei of astrocytes directly at the scratch wound (Figure 7-18 A), whereas the protein is relocalized towards the leading edge of astrocytes facing the scratch 8 hours later (Figure 7-18 B, C). High power magnification revealed that the protein is enriched at the tips of the newly formed processes (Figure 7-18 C').

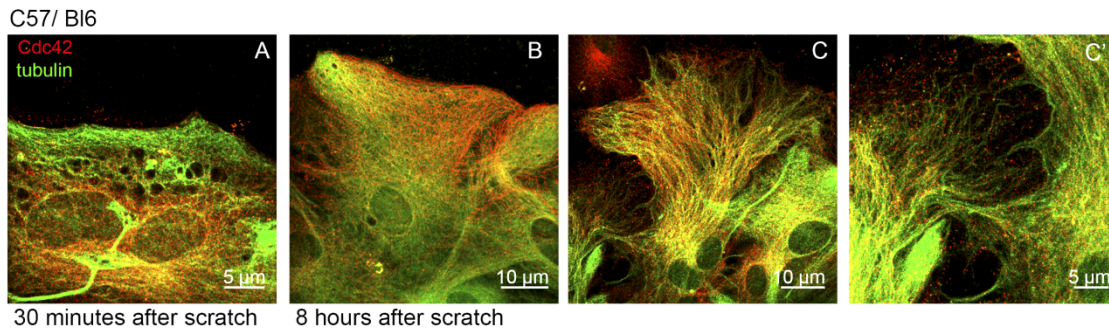


**Figure 7-18 Cdc42 is re-localized after scratch wound in vitro**

**Cdc42 protein is distributed around the nuclei of cells shortly after scratching the monolayer (A). Eight hours later Cdc42 is re-localized towards the leading edge (B) and to the tips of tubulin filaments (C and C').**

To examine the role of Cdc42 in this process, we used a genetic deletion to avoid unspecific side effects of constitutive active and dominant negative constructs (see introduction). Postnatal astrocytes of mice containing the Cdc42 gene flanked by loxP sites (Figure 7-19 A and X. Wu et al., 2006) were cultured and transduced with lentiviruses containing the sequence for either Cre-IRES-GFP/ tomato-IRES-Cre (Cdc42Δ cultures, Figure 7-19 E) or GFP/ tomato alone (control cultures, Figure 7-19 D).

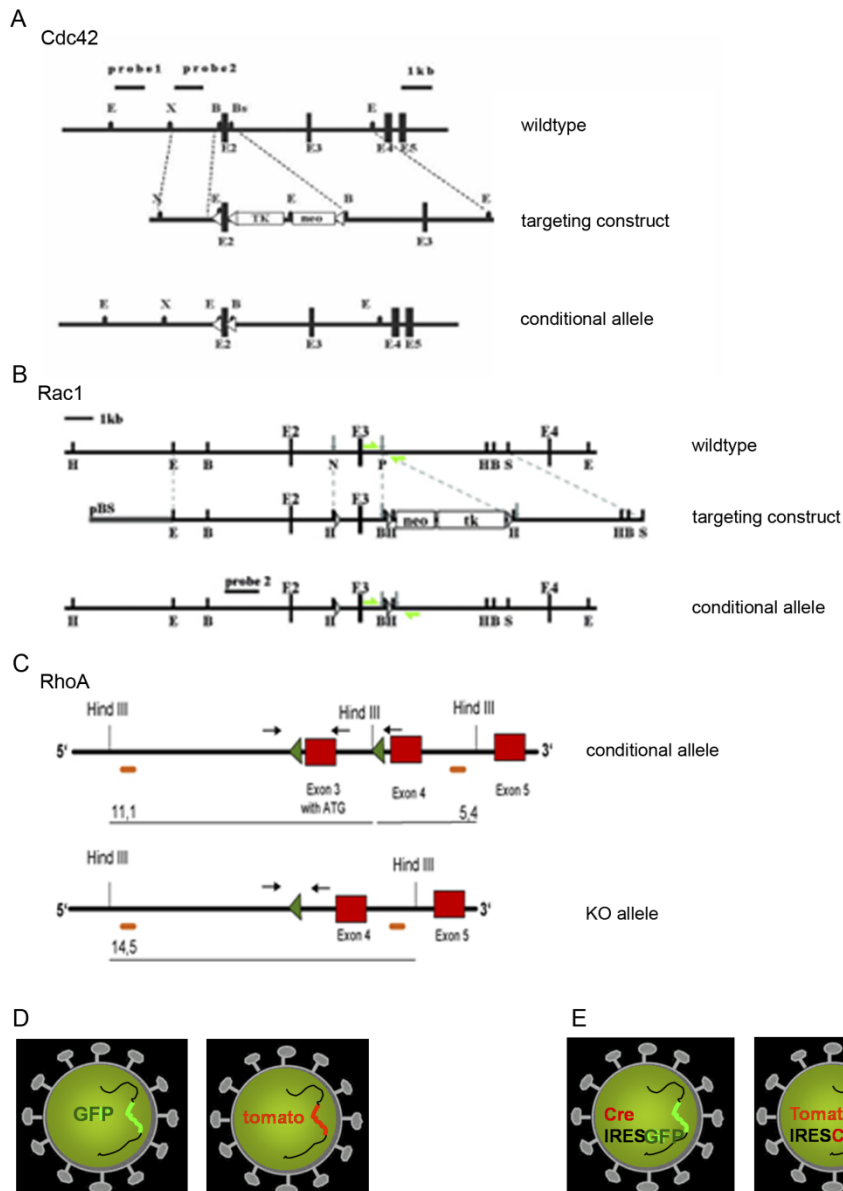


**Figure 7-19** Conditional alleles for Cdc42, Rac1, and RhoA and lentiviral constructs

LoxP sites are inserted into the Cdc42 (A), Rac1 (B) or RhoA (C) gene generating conditional alleles, which can mediate recombination and subsequent gene deletion, when transduced with Cre recombinase containing lentiviruses (E). Control viruses encode fluorescent proteins only (D) and therefore do not recombine conditional alleles.

Drawings of targeting constructs of Cdc42 and Rac1 from Chrostek et al., 2006; X. Wu et al., 2006 and for RhoA provided by Cord Brakebusch.

Two weeks after transduction control and Cdc42 $\Delta$  cultures were stained for Cdc42 (Figure 7-20). Cdc42 was enriched as dots at cell borders and within the cells (Figure 7-20 A, A'), as well as at cell-cell contacts (Figure 7-21 B, B') of

control- and non-transduced cells (Figure 7-20 A'', B'', C''). In contrast, Cdc42 was absent in all these places in tomato-IRES-Cre transduced cells (Figure 7-20 C-D'') confirming that the Cdc42 gene was successfully deleted and Cdc42 protein levels were substantially reduced 2 weeks after lentiviral transduction. Strong red fluorescence around the nuclei of transduced cells could be observed in control and Cdc42 $\Delta$  cultures. This could be due to clustering of the tomato protein or even to a fixation or staining artifact as it has been seen only after enhancement with antibody stainings, but never in timelapse imaging using the intrinsic tomato fluorescence.

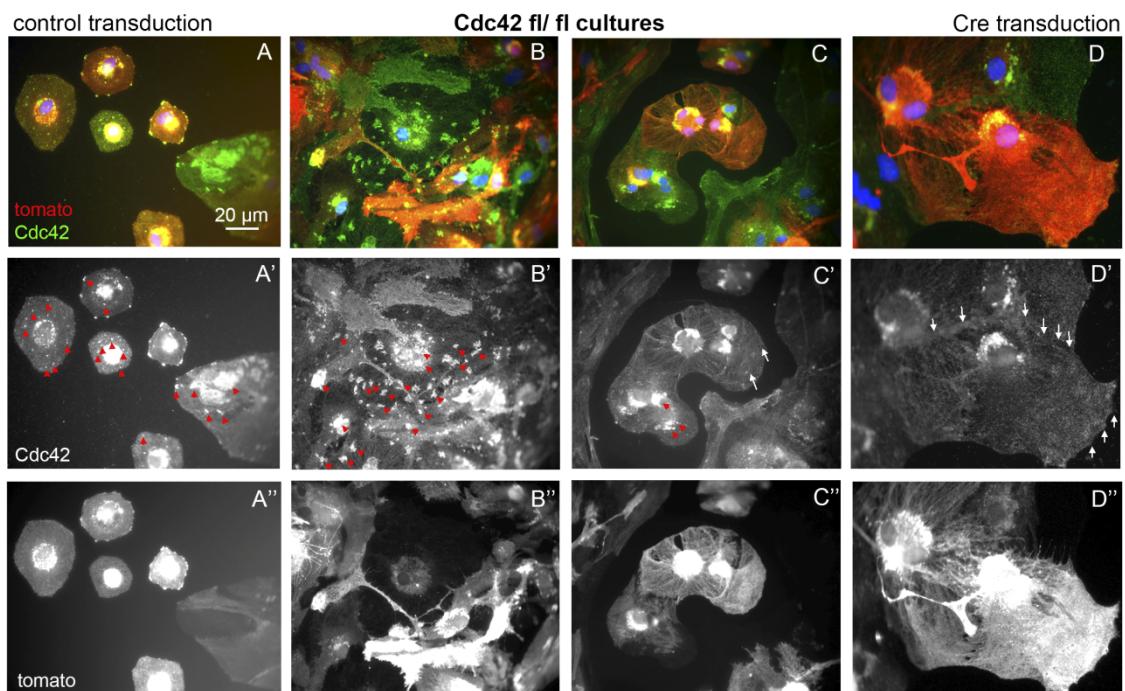


**Figure 7-20 Loss of Cdc42 protein after deletion of the gene**

In a culture transduced with control virus Cdc42 was enriched in dotty structures within the cell and at sites of cell-cell contact (red arrows, A-B''), but vanished in cells transduced with Cre virus (white arrows, C-D'').

After wounding a confluent astrocyte monolayer the reaction of the astrocytes was followed over time in control and Cdc42 $\Delta$  cultures. As expected the majority of first row astrocytes directly at the scratch formed long protrusions, defined as extensions at least 3 times longer than wide into the cell free area 48 hours after starting the experiment in control cultures (Figure 7-21 A, A'). In

Cdc42 $\Delta$  cultures transduced astrocytes in the first row appeared less organized and were largely lacking an obvious polarization towards the scratch (Figure 7-21 B, B'). To investigate whether already initiation of polarization is disturbed the reorientation of the centrosome (microtubule organization center, MTOC) towards the site of injury was determined in transduced cells of control and Cdc42 $\Delta$  cultures. Therefore, the space was separated into 4 equal quadrants joining in the center of the nucleus of interest and placed so that one quadrant was facing the scratch (the median of each 90° angle being either perpendicular or parallel to the scratch). In non-oriented cells, the centrosome is located randomly around the nucleus with equal chance (25 %) to be localized in any of the 4 quadrants. Centrosomes were scored as reoriented, when they were located in the quadrant facing the scratch.

As a starting point the orientation of the centrosome was quantified 30 minutes after wounding the monolayer. By then the fringe of astrocytes directly at the scratch re-attached to the coverslip. In control cultures MTOCs were facing the scratch in a more or less random manner 30 minutes after the scratch ( $30.3 \pm 1.6$  %). As soon as 4 hours post injury (HPI) some of the transduced first row astrocytes started to reorient their MTOC towards the scratch ( $39.9 \pm 1.9$  %). These numbers further increased to around  $53.6 \pm 1.7$  % 24 HPI (Figure 7-21 C, D). Comparable to control cultures Cdc42 $\Delta$  MTOCs were facing the scratch area in a rather random manner at the beginning of the experiment ( $35.4 \pm 1.7$  %). However, even 24 HPI the number of reoriented MTOCs did not increase further in astrocytes with Cdc42 deletion ( $36.9 \pm 1.2$  % and Figure 7-21 C, D), implicating that Cdc42 is necessary to reorient the centrosome towards the wounded area thereby initiating polarization towards the site of injury. To further investigate the influence of Cdc42 on astrocyte polarity the number of protrusion forming cells was quantified at different time points after the scratch wound injury. In control and Cdc42 $\Delta$  cultures a small percentage of the transduced cells had an extension 3 times longer than wide oriented into the scratch wound injury 30 minutes after the start of the experiment ( $7.0 \pm 0.9$  % in control,  $7.9 \pm 1.7$  % in Cdc42 $\Delta$  cultures and Figure 7-21 E, F). This is most likely due to already existing processes that were not removed by scratching the monolayer.

Over time an increasing number of transduced cells built a protrusion into the cell free area (Figure 7-21 E) and 24 HPI more than half of the cells were clearly polarized and elongated towards the injury site in control cultures ( $55.2 \pm 2.4$  % and Figure 7-21 F). In contrast, a significantly lower number of transduced cells formed protrusions into the scratch in Cdc42 $\Delta$  cultures 24 HPI ( $21.6 \pm 3.0$  %,  $n = 6$ ,  $p \leq 0.0022$ ; Figure 7-21 E, F). Taken together, after injury cytosolic Cdc42 is redistributed towards the membrane domain facing the insult to initiate polarization of the cell by mediating MTOC reorientation and protrusion formation.

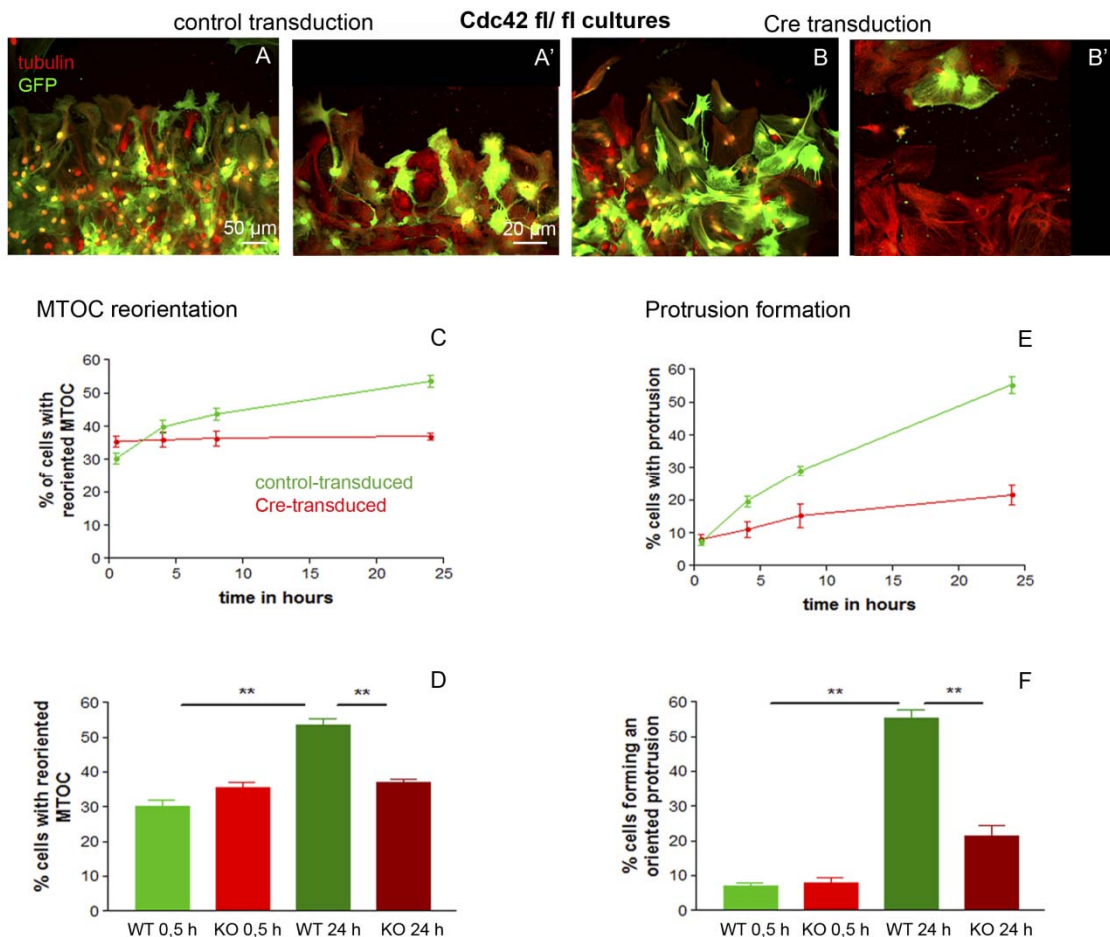


**Figure 7-21 Cdc42 is involved in establishment of astrocyte polarity after injury in vitro**

In control cultures astrocytes formed a protrusion into the scratch (A, A'); whereas Cre-transduced cells partially lack an oriented protrusion (B, B'). The MTOC reorientation (C) and protrusion formation (E) was quantified at different time points. 24 h after scratch statistics show a significant reduction in MTOC reorientation (D) and protrusion formation (F) upon deletion of Cdc42.

### Loss of Rac1 impairs the orientation of formed protrusions after injury in vitro

To examine the specificity of this effect, I also examined cells deficient for Rac1 and RhoA using again a genetic approach (Figure 7-19 B, C and Chrostek et al., 2006). Loss of Rac1 protein could not be confirmed by immunofluorescent staining as no specific antibodies were available. However, defects observed only in Rac1 fl/fl astrocyte cultures transduced with Cre lentivirus, but not with control virus, are indicative for efficient loss of Rac1 protein 2 weeks after transduction. Two days after wounding a monolayer of astrocytes control-transduced cells formed a long protrusion into the cell-free area (Figure 7-22 A). Cre-transduced astrocytes were forming a protrusion, which was, however, often not oriented into the scratch (Figure 7-22 B). As this phenotype seemed to be different from the deletion of Cdc42, again reorientation of the MTOC and protrusion formation of the transduced astrocytes was analyzed at different time points after wounding the astrocyte monolayer to address which steps in polarization of first row cells would be affected. As described before for the deletion of Cdc42, in the beginning of the experiment a random number of transduced cells had their MTOC facing the scratch in control ( $29.0\% \pm 1.3\%$ ,  $n = 8$ ) and Rac1 $\Delta$  ( $26.3\% \pm 1.4\%$ ,  $n = 8$ ) astrocytes (Figure 7-22 C, D). In control-transduced astrocytes the number of cells with reoriented MTOC increased over time reaching a plateau 24 hours after the scratch (Figure 7-22 C). After loss of Rac1 a significant number of cells had reoriented MTOCs 24 hours after wounding the monolayer (Figure 7-22 D). Nevertheless, this number was reduced when compared to control-transduced astrocytes ( $38.9\% \pm 2.0\%$ ,  $n = 8$  Rac1 $\Delta$  versus  $47.0\% \pm 1.7\%$ ,  $n = 6$  control-transduced,  $p \leq 0.083$  and Figure 7-22 D). The number of cells with reoriented MTOC did not increase further, even 48 HPI (Figure 7-22 C). Interestingly, this correlates with a reduced number of protrusions oriented into the scratch area after loss of Rac1 ( $31.4\% \pm 1.1\%$ ,  $n = 6$ ) when compared with control-transduced cultures ( $61.6\% \pm 2.5\%$ ,  $n = 8$ ) 24 HPI (Figure 7-22 E, F). In contrast to deletion of Cdc42, loss of Rac1 does not seem to interfere with the initiation of protrusion formation as a comparable number of cells started to form a protrusion 8 HPI (Figure 7-22

E). However, the orientation of most of the cell towards the site of injury seems to be impaired at later time points (Figure 7-22 C, E, F).

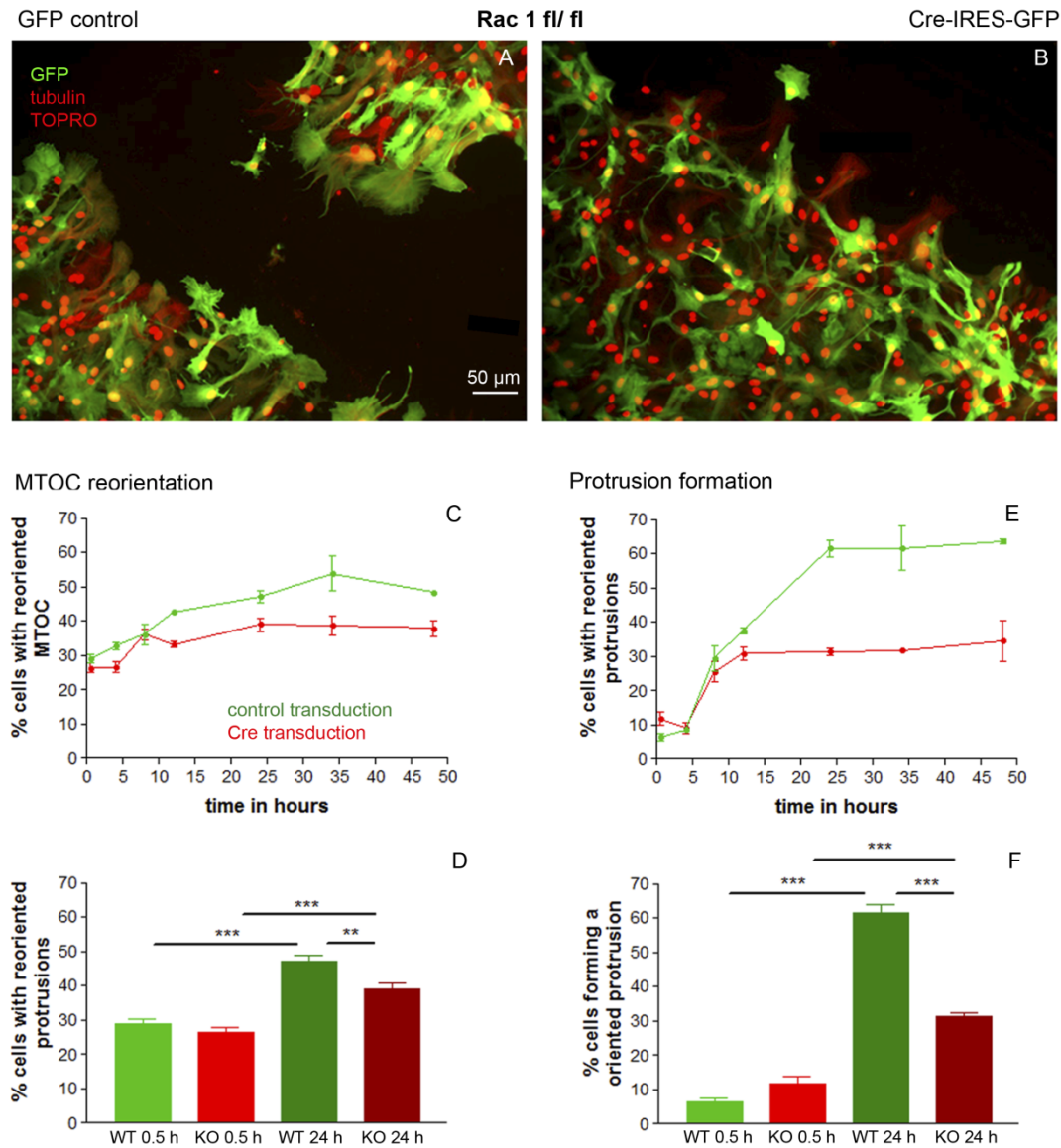


**Figure 7-22** The role of Rac1 after scratch wound injury in vitro

In contrast to control-transduced cells (A), Cre-transduced astrocytes formed protrusions, which were randomly oriented around the cell body (B). MTOC reorientation (C) and oriented protrusion formation (E) were quantified at different time points. Statistical analysis was performed at 24 hours after injury when the number of cells reorienting their MTOC and forming a protrusion reached a plateau (D, F).

RhoA is dispensable for MTOC reorientation and protrusion formation in astrocytes after scratch wound injury in vitro

The third small RhoGTPase important for cytoskeletal rearrangements in astrocytes, RhoA, has been analysed as described above using again a genetic approach (Figure 7-19 C). Despite the clear loss of RhoA in Cre-transduced cells 2 weeks after transduction, control and RhoA $\Delta$  astrocytes were comparable 48 hpi (Figure 7-23 A, B). Accordingly, detailed analysis of MTOC reorientation and protrusion forming at different timepoints after scratch wound injury showed that loss of RhoA did not interfere with any of these parameters (Figure 7-23 C-F).

Taken together, Cdc42 was necessary for orientation of the cell towards the injury as well as for initializing cytoskeletal re-arrangements leading to protrusion formation, whereas Rac1 rather seemed to be important for orientation of these protrusions. On the contrary, RhoA was dispensable for both of these processes showing also that the Cre recombinase encoded by the lentiviral construct acts specific and is not toxic in this experimental setup.

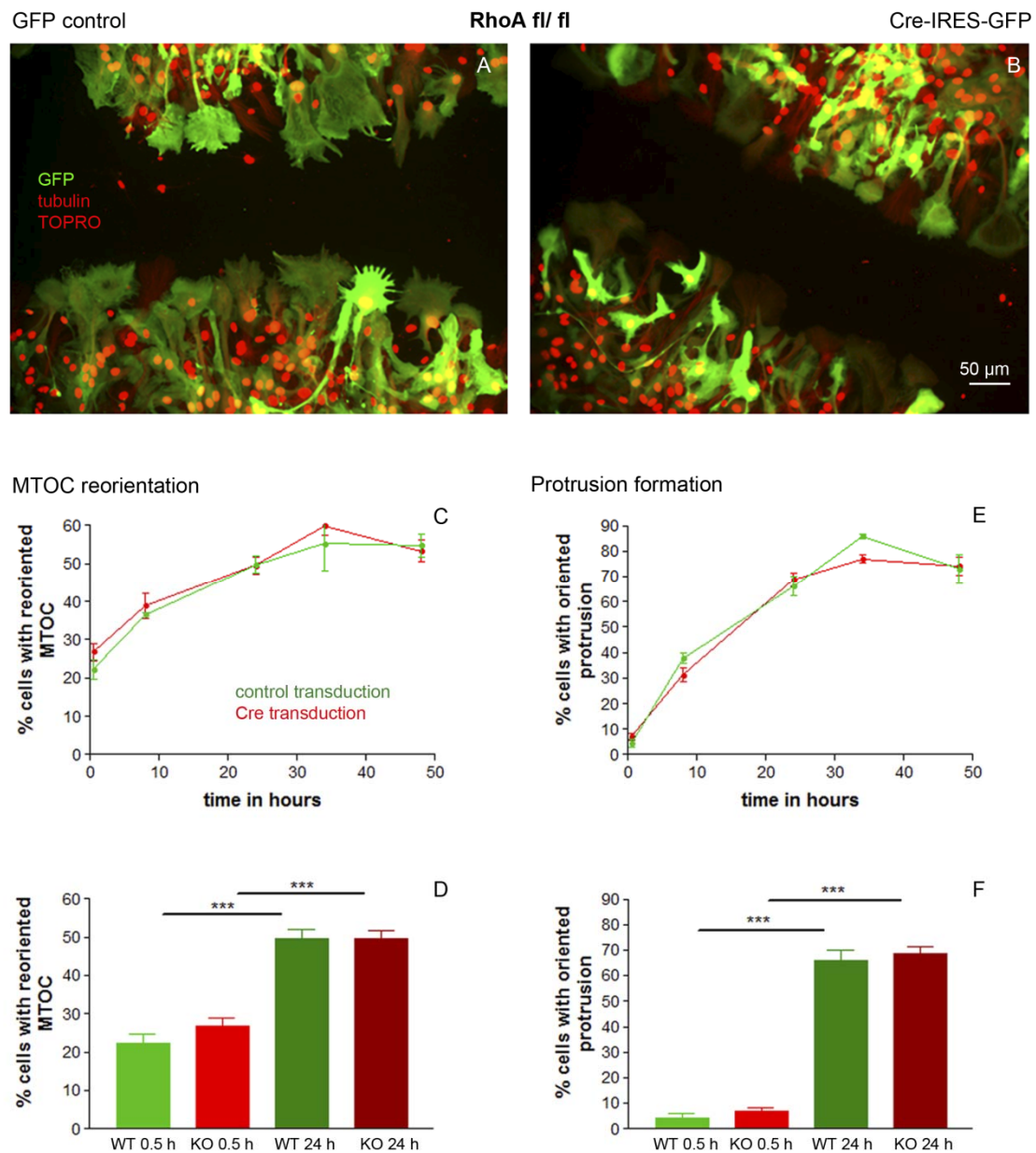


**Figure 7-23** The role of RhoA after scratch wound injury in vitro

No difference in protrusion formation was noted when comparing immunofluorescent stainings of control transduced astrocytes (A) and Cre-transduced astrocytes (B) 48 hours after scratch wounding. Quantification of MTOC reorientation (C, D) and oriented protrusion formation (E, F) confirmed that deletion of RhoA had no effect on these parameters.

### **7.3.2 Astrocyte polarization upon injury leads to their subsequent migration in vitro**

The orientation of fewer cell processes towards the scratch after deletion of Cdc42 and Rac1 could result from a total loss of protrusion formation, random generation of processes or higher protrusion turnover. To investigate the consequences of impaired centrosome reorientation and the cause for a reduced number of oriented processes after deletion of Cdc42 and Rac1 by following single cells over several days, timelapse imaging has been established. In order to do so, an Axioobserver Z.1 microscope with motorized stage from Zeiss was equipped with an incubation chamber (Zeiss XL S1) connected to the TempModul S1 for keeping the cultures at 37°C. Furthermore, the CO<sub>2</sub> Module S1 connected to the CO<sub>2</sub> lid (Zeiss PM S1) allowed controlling CO<sub>2</sub> concentrations and was obligatory for healthy cultures during longer imaging periods (more than 12hours). An additional heating module for the 24-well plates (Zeiss M24 S1) turned out to be absolute essential to keep cultures in focus during imaging. In addition, not all 24-well plates were suited to either fit into the heating unit or to be steady despite small variations in temperature. The best results were achieved using BD Falcon™ 24-well multiwall plates (BD Falcon™ 353047). The microscope was further connected to a high resolution camera (AxioCam HRc Rev.3) allowing rapid time lapse sequences despite a high image resolution. Microscope, heating and CO<sub>2</sub> modules, as well as the camera were controlled by the AxioVision Software from Zeiss.

For timelapse imaging, astrocytes were transduced with lentiviruses and seeded into PLO-coated BD Falcon™ 24-well plates after growing them in T75 cell culture flasks as described above. Two weeks after transduction the astrocyte monolayer was scratched using a pipette tip, thereby taking care that the plastic was not scraped as otherwise cells would stop there.

In the beginning, bright field and fluorescent images were taken each 10 minutes. The exposure time in the fluorescent channel had to be relatively long to detect the comparatively lower GFP levels in LV-Cre-IRES-GFP-transduced cells. Higher GFP levels in control-transduced astrocytes were due to expression of the GFP gene directly behind the CMV promoter, whereas GFP in

LV-Cre-IRES-GFP had to be translated from an internal ribosomal entry site resulting in lower efficiency. However, those cells expressing higher levels of GFP were observed to die more frequently than astrocytes with lower levels of the fluorescent dye, most likely due to phototoxicity (movie 1). Phototoxicity could be minimized by taking only one or two fluorescent images per hour, whereas bright field pictures were still taken every 10 minutes to assure high time resolution of the movies. At this point fluorescent images were needed only to identify transduced cells, whereas bright field images served to follow cellular movements. To further circumvent phototoxicity and different levels of the fluorescent dye in control and Cre-transduced cultures, the gene encoding the red fluorescent dye tomato was cloned behind the CMV promoter resulting in the control lentiviral construct LV-tomato. A second construct was designed with IRES-Cre behind the tomato gene (LV-tomato-IRES-Cre). Transduction of astrocytes with LV-tomato (movie 2) and LV-tomato-IRES-Cre (movie 3) resulted in comparable levels of the fluorescent dye, which allowed reducing the exposure time and therefore phototoxicity allowing imaging over several days.

In movies of Cdc42 fl/ fl astrocytes transduced with LV-tomato cells, as well as non-transduced cells reacted to the injury as described above by extending a long protrusion into the scratch. Subsequently, cells started to migrate into the cell-free area (movie 2 and 4). Interestingly, cell divisions were observed regularly at the injury border (movie 4). Migration as well as proliferation were, nevertheless, notably slower compared to HEK (movie 5) or 3T3 (movie 5) cell lines. After transduction with LV-tomato-IRES-Cre Cdc42 fl/ fl astrocytes sometimes started to form a protrusion, but often did not relocate their cell body thereupon. Meanwhile, non-transduced astrocytes in Cdc42 $\Delta$  cultures passed by leaving the Cdc42 $\Delta$  cells behind (movie 3). In general, cell divisions were also seen in Cdc42 $\Delta$  astrocytes. Taken together, the timelapse imaging showed that some Cdc42 $\Delta$  astrocytes were initially able to form a protrusion, but often failed to migrate efficiently into the scratch. I attempted then to clarify, whether the effect of Cdc42 on the polarity and migratory behavior of astrocytes is also of relevance after brain injury in vivo.

### **7.3.3 Conditional Cdc42 deletion influences morphology changes of astrocytes after cortical stab wound injury**

As Cdc42 had an important role in astrocyte polarity after scratch wound injury in vitro, the relevance of this small RhoGTPase for the reaction of astrocytes to an acute brain injury in vivo was investigated. To investigate the role of Cdc42 in adult NSCs, the gene was conditionally deleted in astrocytes including the NSCs of adult animals taking advantage of the *Glast::CreERT2* mouse line, which was mated to a mouse line with loxP sites flanking exon2 of the *Cdc42* gene. Recombination was achieved by administration of the estrogen analogue Tamoxifen (Figure 7-27 A) in 2-3 month old mice heterozygous for *Glast::CreERT2*, positive for a GFP-reporter and homo- (herein after referred to as *Cdc42Δ*) or heterozygous (WT or control) for the *Cdc42* allele flanked by loxP sites. Four weeks later, a stab wound was placed in the gray matter of the cerebral cortex (Figure 7-24 A). From the in vitro analysis (Figure 7-21), I conclude that recombined cells are deficient of Cdc42 protein at that time point. In the uninjured hemisphere no obvious differences in terms of astrocyte size or morphology have been observed after deletion of Cdc42. Similar to the analysis in vitro, the number of cells, which had formed a protrusion, was quantified. A protrusion was defined as an elongated process clearly longer than wide oriented in the direction of the stab wound injury (Figure 7-24 B). In WT brains 39.2 % ± 1.7 % (n = 3) of the cells in the palisading zone, which is the region where astrocytes elongate their shape, formed a protrusion oriented towards the injury (Figure 7-24 C). Surprisingly, this number was significantly enhanced after loss of Cdc42 (68.4 % ± 3.6 %, n = 4, p ≤ 0.001, Figure 7-24 D, E). This was in contrast to the results achieved in vitro, where less astrocytes formed a protrusion oriented towards scratch wound (see discussion). Although the protrusion length itself or the length of the retracting end was not different between WT and *Cdc42Δ* cells, a significant increase in total cell length was noted (Figure 7-24 D, F) due to *Cdc42Δ* cells being larger in general after stab wound injury (Figure 7-24 G, H).

The measurements of the cell length and width were done together with Sophia Bardehle (Institute of Stem Cell Research, HelmholtzZentrum München).

Quantifying the number of cells per mm<sup>2</sup> revealed a strong tendency towards a reduced number of cells in the palisading zone in Cdc42Δ compared to WT injured brains (209.7 ± 61.4 cells per mm<sup>2</sup> in WT, n = 3 versus 95.5 ± 9.2 in Cdc42Δ, n = 4, p = 0.0571, (Figure 7-24 J). As the number of recombined cells per area in the contralateral uninjured hemispheres were comparable between WT and Cdc42Δ the reduction in cell numbers close to the injury site could be due to a migration defect as observed in vitro. Alternatively, the proliferation of astrocytes at the injury site could be affected. To test this, BrdU was administered for 3 days via the drinking water after stab wounding the animals. Astrocytes that had been incorporated BrdU were counted at day 3 after the stab wound injury. In WT brains 14.8 ± 0.7 % (n = 2) of the recombined cells at the injury site incorporated BrdU. In contrast, this population was reduced by 50 % after deletion of Cdc42 3 DPL (7.8 ± 3 % GFP BrdU+ cells in Cdc42Δ, n = 4, p ≤ 0.0376) showing that deletion of Cdc42 interferes with the proliferation capacity of astrocytes after stab wound injury.

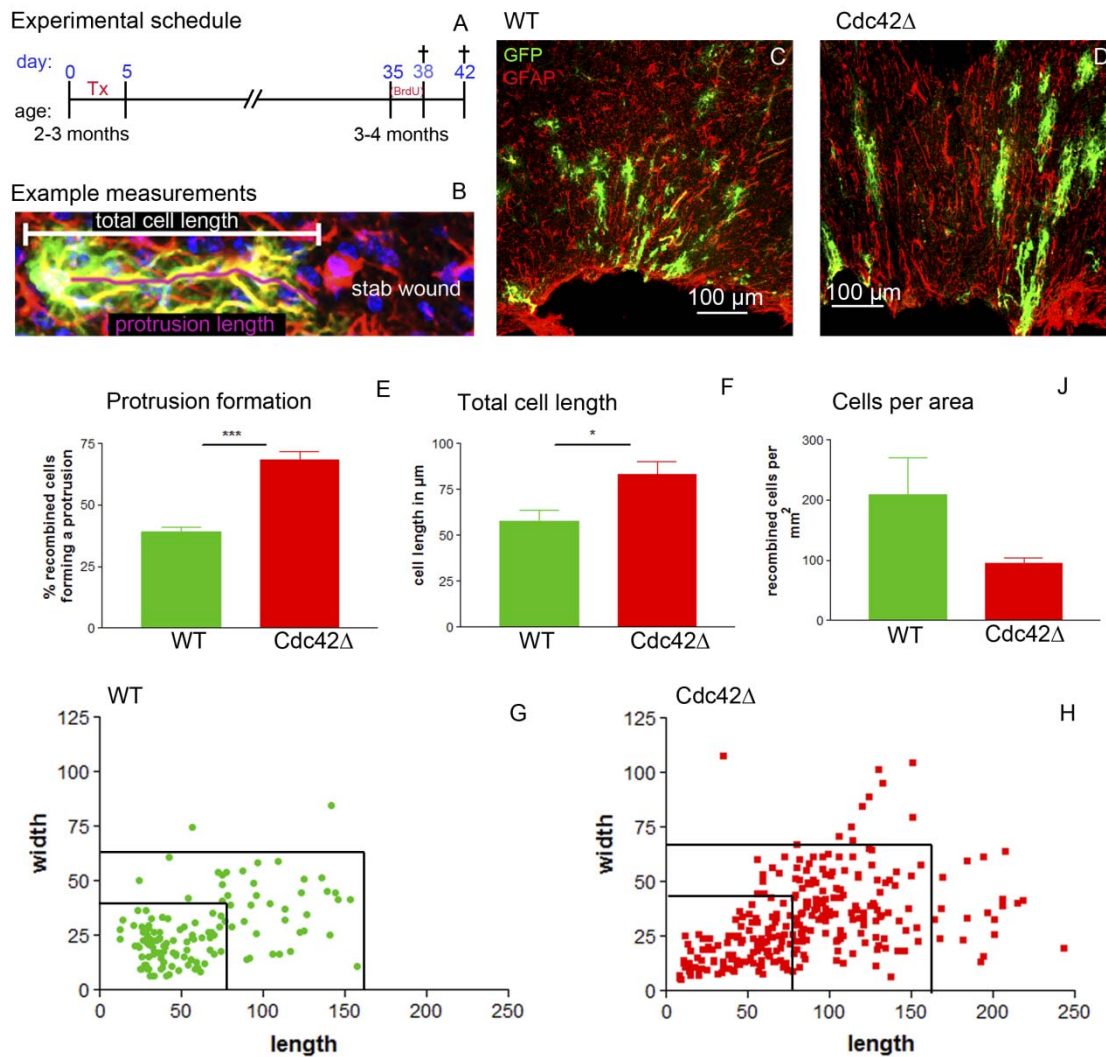


**Figure 7-24** The role of Cdc42 for the reaction of astrocytes to injury in vivo

Genetic recombination was induced in 2-3 months old animals, which were stab wound injured 4 weeks later and sacrificed 3 or 7 days post lesion following the protocol in A. The measurements of cell length and protrusion length in recombined cells were done as shown in B. Recombined astrocytes positive for GFP and counterstained with GFAP were increased in size in Cdc42Δ (D) compared to WT (C) brains. The number of astrocytes forming a protrusion was increased after loss of Cdc42, as well as the total cell length (D). Cell width in relation to cell length is plotted for WT (G) and Cdc42Δ (H) showing a group of larger cells after deletion of Cdc42. The number of recombined astrocytes per area is reduced after Cdc42 deletion (J).

#### **7.3.4 Deletion of Cdc42 in virtually all astrocytes lead to an increased injury size after stab wound injury in vivo**

Deletion of Cdc42 from astrocytes in the adult brain seemed to interfere with their reaction to an acute brain insult in a cell-autonomous way as only a subset of astrocytes was recombined. Whether this would be of functional consequence for the wound healing, was tested by deletion of Cdc42 in virtually all astrocytes using hGFAP-Cre. hGFAP-Cre<sup>+</sup>, Cdc42 fl/ fl animals (referred to as KO) survived into adult stages, when backcrossed to the C57Bl/6 genetic background. KO and WT (negative for hGFAP-Cre) animals were injured at the age of 2-3months and analyzed 3 days later. To judge whether reactivity of microglia and inflammation overall was changed, the area covered by hypertroph Iba1-positive microglia was measured. In WT ( $430800 \pm 89460 \mu\text{m}^2$ ) and KO ( $548500 \pm 202300 \mu\text{m}^2$ ) injured hemispheres a comparable area was covered by hypertroph microglia ( $n = 3$ ,  $p = 0.5581$ ). Likewise, upregulation of GFAP in astrocytes of the injured hemisphere was not significantly changed after deletion of Cdc42 ( $55.9 \pm 1.1 \%$  of the total area measured in WT,  $n = 6$  and  $71.5 \pm 17.1 \%$ ,  $n = 2$  in KO,  $p = 0.1089$ ). As the cells that upregulated GFAP sometimes even exceeded the image section, the area covered by GFAP was displayed as % of the total area measured. As readout for immediate neuronal damage, the transient downregulation of NeuN has been assessed. In WT animals, neurons downregulated NeuN in a defined region around the injury site ( $395000 \pm 149200 \mu\text{m}^2$ ,  $n = 5$ ). Although the mean area was increased in KO brains ( $655900 \pm 362500 \mu\text{m}^2$ ,  $n = 3$ ,  $p = 0.3385$ ), variations from animal to animal were high, not allowing a clear-cut conclusion from this analysis parameter. The actual injury size was determined by measuring the DAPI-free area within the gray matter of the cerebral cortex, where the injury was placed. There was a considerable variation in WT animals as there were brains without any or very little tissue loss (Figure 7-25 A), the mean DAPI-free area was  $40980 \pm 17470 \mu\text{m}^2$  ( $n = 6$ ) in WT brains. KO ipsilateral hemispheres appeared to have pronounced tissue loss (Figure 7-25 B) and a 3 times larger mean injury size of  $120200 \pm 28040 \mu\text{m}^2$  ( $n = 3$ ,  $p \leq 0.0398$  and Figure 7-25 C) suggesting

that Cdc42 in astrocytes is important either to preserve injured brains from tissue loss or for wound closure.

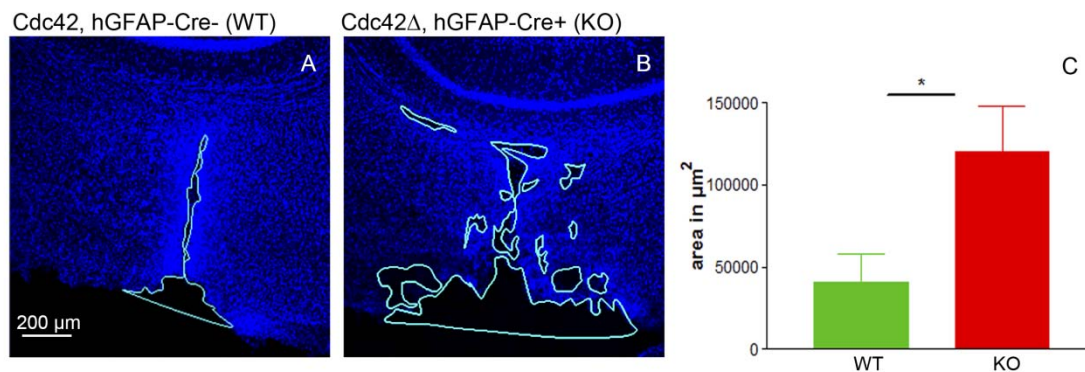


**Figure 7-25 Consequences of Cdc42 deletion in virtually all astrocytes**

After stab wound injury in WT normally almost no tissue is lost (A). After deletion of Cdc42, the injury size was larger (B). The area of tissue loss (= DAPI nuclei free) was quantified per animal in C.

### **7.3.5 Are astrocytes migrating after acute brain trauma in vivo?**

The impaired proliferation capacity of astrocytes after loss of Cdc42 certainly accounts for the reduced astrocyte numbers at the injury size (see above). Deletion of Cdc42 in vitro suggests, however, that impairment in astrocyte migration possibly adds to this phenotype. To address whether migration of astrocytes after an acute brain trauma is part of their reactive response in vivo, astrocytes in the adult mouse cerebral cortex were labeled injecting a lentivirus encoding GFP (LV-GFP, Figure 7-26 A). As the very thin glass needle used for injecting the virus created a small injury itself, the stab wound was done 4 weeks later or even before injecting the virus (Figure 7-26 B) making sure that astrocytes at the needle track were not reactive anymore or attractant molecules from the stab wound site had a “head start”. The stab wound was placed 3 mm distant from the injection site following the protocol of (Auguste et al., 2007 and Figure 7-26 B). The depth of the injection was maximal 1 mm to restrict the labeling to astrocytes in the gray matter. Lentiviral injections were done in both hemispheres, whereas only one hemisphere was stab wounded

(Figure 7-26 B) and the other contralateral (CL) one served as control (Figure 7-26 A). The virus diffused dependent on the quality of the injections up to 850  $\mu\text{m}$  into the tissue in CL hemispheres. Despite strong GFAP-upregulation around the lesion site GFP-positive astrocytes were not seen to be farther away from the injection site independent of the distance of the stab wound injury (Figure 7-26 A and B). Whether astrocytes closer than 1 mm from the injury site would migrate there could not be judged by this indirect method due to the widespread diffusion of the virus. That is why I attempted then to directly follow astrocytes by life imaging in vivo.

2-photon imaging allows to image fluorescent labeled cells and structures like blood vessels intravital, in the living animal. As the animals can be repeatedly analyzed one might hope that it would be possible to ascertain whether astrocytes indeed migrate towards a site of injury. To investigate whether it is possible to follow astrocytes by this technique, some pilot experiments were done in collaboration with Frank Kirchhoff (Max Planck Institute for Experimental Medicine Göttingen). A transgenic mouse expressing GFP under the human GFAP promoter was anaesthetized, the skull was thinned and the mouse was fixed in a stereotactic frame underneath the microscope. Then, a high molecular Dextran-TexasRed was injected into the tail vein to display the vascular structure of the brain for orientation. First, a low resolution bright field picture of the meningeal vessels was taken to be able to determine roughly in which region pictures were taken, which was important for later imaging sessions. Z-stacks of GFP positive astrocytes and TexasRed-labeled blood vessels were collected in the intact gray matter of the cerebral cortex up to a depth of 600  $\mu\text{m}$  (Figure 7-26 C). Then, the laser power was increased and focused to the wall of a blood vessel and tissue surrounded by GFP-positive astrocytes to observe their reaction towards this comparable small laser lesion (Figure 7-26 D). During the imaging period of 2 more hours no reaction of nearby astrocytes in regard to movement or process motility could be observed. When the same animal was imaged again 3 days later astrocytes surrounding the laser lesion changed their morphology towards an elongated shape with processes extended in the direction of the injury (Figure 7-26 E). However, it

was difficult to follow single cells, especially as hGFAP-eGFP transgenic animals upregulate GFP after injury resulting in more labeled cells at day 4 (Figure 7-26 E) than had been seen at day 1 (Figure 7-26 C, D). To overcome this limitation astrocytes were stably labeled before the start of the experiment by the use of adult *Glast::CreERT2* mice (Mori et al., 2006) mated to a GFP-reporter line (Nakamura et al., 2006). The mice were induced with tamoxifen following the above mentioned protocol and were imaged two weeks later to assure that the tamoxifen has been cleared from the system and no new recombination events would occur anymore. Although the astrocytes labeled by the GFP-reporter were clearly not as bright as the ones labeled in the hGFAP-eGFP transgenic line, the signal was sufficient for imaging (Figure 7-26 F-H). Before the lesion, cell bodies were seen as a bright spots surrounded by diffuse and less GFP-intensive signal of their processes (Figure 7-26 F). Immediately after the laser lesion, larger nearby blood vessels dilated in response to the injury, but again no immediate reaction of astrocytes was observed (Figure 7-26 G). The same animal was imaged again two days later showing two astrocytes, which extended a long process towards the injury (Figure 7-26 H, cells1 and 2). Overall the intensity of labeled astrocytes seemed to be higher, maybe due to the retraction of the finer branches. Taken together, following astrocytes by 2-photon microscopy in vivo is feasible. However, with these time intervals I could not determine, whether the increase in astrocyte numbers was due to cell migration.

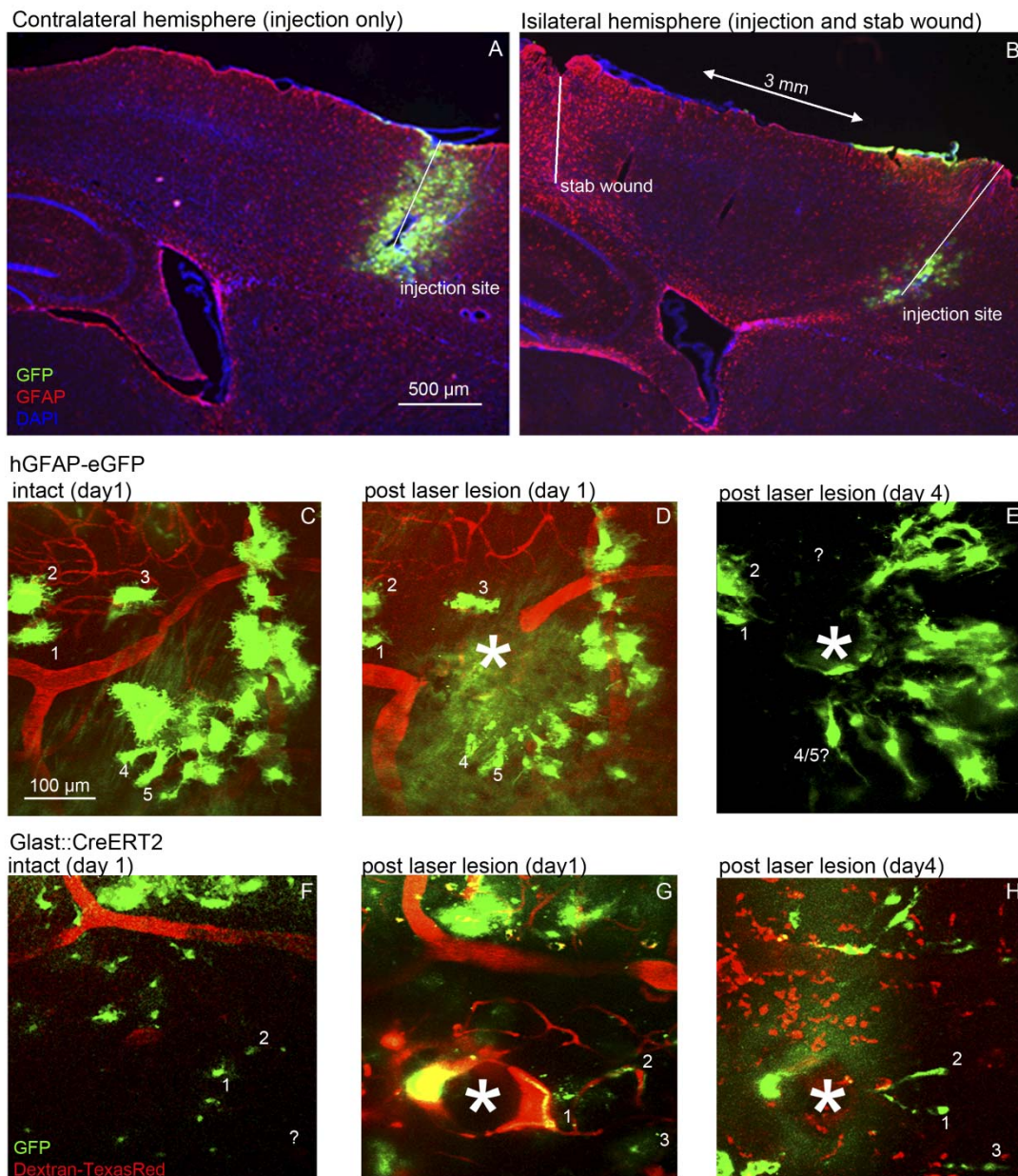


**Figure 7-26** Intravital imaging of astrocytes after an injury

To assess whether astrocytes migrate large distances towards a site of injury, they were labeled using a GFP-Lentivirus (A, B) and a stab wound injury was placed 3 mm away. This led to upregulation of GFAP in the injury site, but not to migration of labeled astrocytes (B). Repeated 2-photon imaging of astrocytes in hGFAP-eGFP mice before (C) and after laser lesion (G, laser lesion indicated by a star), as well as 3 days later (E). Stable labeling of astrocytes in Glax::CreERT2 GFP reporter mice allowed following astrocytes (F) directly after laser lesion (G) and 2 days later (H). Astrocytes that could be followed were indicated with numbers.

## 7.4 The influence of Cdc42 on astroglial-like stem cells and their progeny

SEZ stem cells in the adult brain bear clear morphological resemblance to their RG precursors, the SVZ stem cells of the developing forebrain. A hallmark of the appearance of both, RG cells and adult NSCs is their bipolar shape with a basal membrane domain (see chapters 2.2.3, 2.4.1 and 7.2) and an apical membrane domain where they face the ventricle (see chapters 2.2.3 and 2.4.2). During development the small RhoGTPase Cdc42 has been shown to be a major player in establishing apical polarity as loss of Cdc42 in RG leads to absence of normally apically localized members of the Par complex like Par3 and aPKC, as well as adherens junctions accompanied by failure of apically directed interkinetic nuclear migration. This consequently leads to a premature depletion of apical progenitors and thus switches cell fate possibly due to the loss of apical polarity in RG (Cappello et al., 2006). To investigate the role of Cdc42 in adult NSCs, the gene was conditionally deleted in astrocytes including the NSCs of adult animals by the use of *Glast::CreERT2* (see above and Figure 7-27 A). Four weeks after recombination astroglial-like stem cells were marked using a label retaining BrdU pulse and the glia marker GFAP (Figure 7-27 A). Roughly, one fourth of all reporter positive cells kept the BrdU label in the SEZ of *Glast::CreERT2/ Cdc42 fl/ wt* further referred to as WT (22.3 %  $\pm$  3.5 %), and *Glast::CreERT2/ Cdc42 fl/ fl*, herein after termed as KO (24.6 %  $\pm$  3.9 %). Counter labeling of the reporter-positive BrdU cells with GFAP revealed comparable numbers of adult SEZ NSCs in WT (6.7 %  $\pm$  1.7 %; Figure 7-27 B, C) and KO (6.6 %  $\pm$  2.0 % Figure 7-27 B, C) brains. The number of label retaining *Dcx*<sup>+</sup> progeny of SEZ NSCs, however, was significantly increased after tamoxifen application in *Cdc42* animals homozygous for the floxed allele (6.3 %  $\pm$  2.3 % in WT and 18.9  $\pm$  2.5 in KO;  $n = 3$ ,  $p \leq 0.0195$ ; Figure 7-27 B, D - E'). In the WT SEZ neuroblasts are organized in several layers of chains along the lateral ventricle and no *Dcx*<sup>+</sup> cells are localized within the neighboring striatum (Figure 7-27 D, D'). Overall, this organization seemed to be disturbed with some of the *Dcx*<sup>+</sup> neuroblasts even being localized within the striatum of KO brains

(Figure 7-27 E, E'). Given the fact that the number of NSCs is not changed after deletion of Cdc42, it has to be tested whether higher number of neuroblasts are due to enhanced proliferation of transit amplifying precursors (TAPs) or to impaired migration and subsequent accumulation of Dcx+ cells in the SEZ. Interestingly, this phenotype is similar to the phenotype after  $\beta$ 1-integrin deletion.

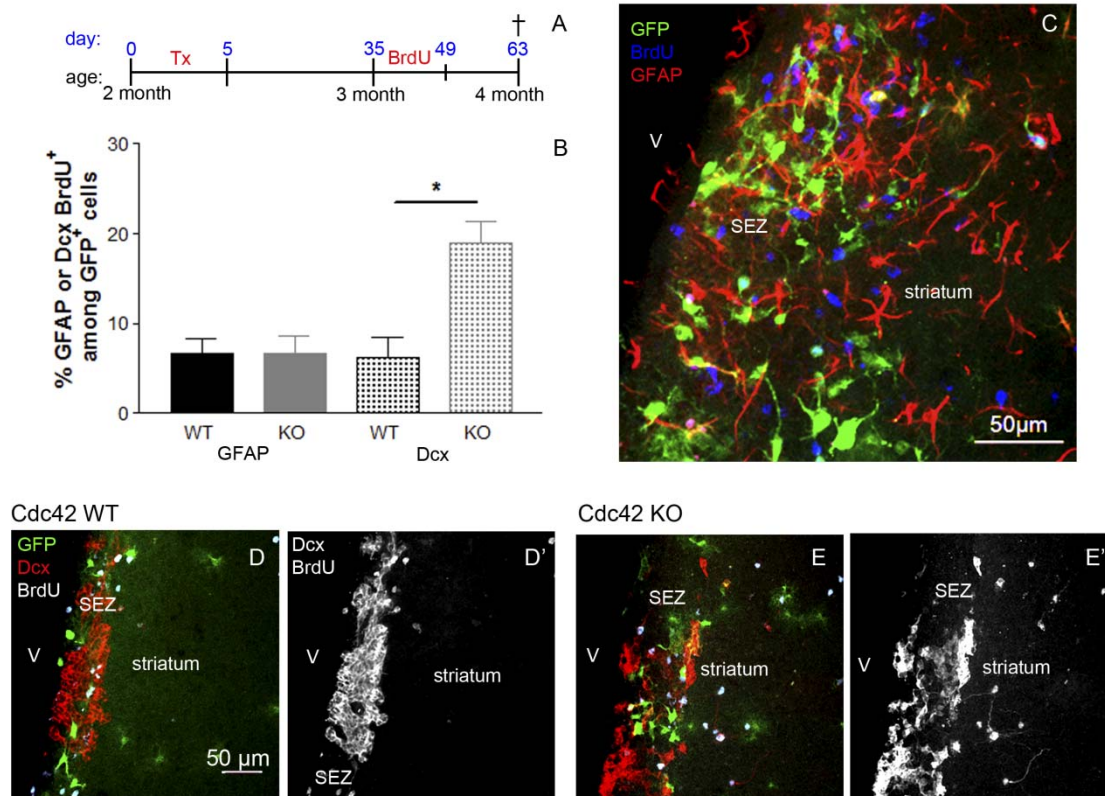


**Figure 7-27 The role of Cdc42 in SEZ stem cells and their progeny**

The experimental schedule is shown in (A). The number of BrdU and GFAP double-positive cells within the pool of recombined GFP-positive cells was unchanged between WT and Cdc42 deleted animals (B, C). Whereas Dcx-positive neuroblasts were restricted to the SEZ in WT brains (D, D'), these cells were rather unorganized after deleting Cdc42 and even entered the striatum (E, E'). Quantifying the number of label retaining neuroblasts revealed a significant increase of these cells in the adult SEZ (B).



## 8 Discussion

### 8.1 $\beta$ 1-Integrin functions in astroglial cells

Although the role of  $\beta$ 1-integrins in radial glial cells during development has been well studied (Beggs et al., 2003; Belvindrah et al., 2007a; Georges-Labouesse et al., 1998; Haubst et al., 2006; Herms et al., 2004; Schroder et al., 2007), still very little is known about the interaction between astrocytes and the leptomeningeal and vascular BMs in the postnatal and adult brain. Here the postnatal role of  $\beta$ 1-integrins was studied by the use of hGFAP-driven Cre recombinase. Although recombination in the cortex starts around E13 in this mouse line (Malatesta et al., 2003) and most proteins have disappeared within few days after recombination (Cappello et al., 2006; Moore et al., 2002), stability of the integrin proteins resulted in persistence of  $\beta$ 1-integrin for about one week after recombination. Indeed, the disruption of the glia limitans and BM at the pial surface and neuronal ectopias mostly in cortical layer I, phenotypes observed after earlier deletion of  $\beta$ 1-integrin, were not observed in this study after deletion with hGFAP-Cre. The absence of developmental malformations therefore allowed to clarify the role of  $\beta$ 1-integrins in the postnatal brain and to elucidate the etiology and nature of the major phenotype elicited at this later stage, namely the partial reactive gliosis. Notably, GFAP upregulation has been described in previous reports after early deletion of  $\beta$ 1-integrin (Belvindrah et al., 2007a), focal adhesion kinase (Beggs et al., 2003) or Cdc42 (Cappello et al., 2006), but this phenotype had neither been examined more closely nor was its cause identifiable given the profound developmental aberrations. From the described data one can conclude that the reactive gliosis phenotype is due to an important role of  $\beta$ 1-integrin associated complexes in postnatal astroglial cells. First, the gliosis phenotype occurred within the first postnatal weeks at a time when no other abnormalities were observed. Second, genetic evidence using different Cre lines, such as the Nex::Cre line, clearly demonstrated that deletion of  $\beta$ 1-integrins only in neurons does not cause a reactive gliosis phenotype. The onset of Cre expression in the Nex locus occurs at very early

stages in neurons as soon as they are born (Goebbels et al., 2006; Wu et al., 2005) in contrast to previous neuron specific deletion of  $\beta$ 1-integrin by CAM-Kinase-Cre in the forebrain, where only mature pyramidal neurons at postnatal stages were affected (Huang et al., 2006). After hGFAP-Cre-mediated  $\beta$ 1-integrin deletion, no obvious defects in oligodendrocytes were observed consistent with data obtained by oligodendrocyte specific  $\beta$ 1-integrins deletion (CNP::Cre; Benninger et al., 2006). Thus, the reactive gliosis phenotype does not correlate with oligodendrocyte defects. On the basis of these results and the absence of gliosis in mice with Nex::Cre mediated  $\beta$ 1-integrin deletion, we conclude that gliosis is unlikely to be influenced by the presence or absence of  $\beta$ 1-integrin in oligodendrocytes and neurons. Conversely,  $\beta$ 1-integrin mediated signaling is required within astrocytes to promote the acquisition of a mature non-reactive phenotype. Interestingly, glial reactivity was not restricted to astrocytes, but also included a partial activation of microglial cells. As confirmed by reporter analysis, hGFAP-Cre-mediated recombination does not occur in microglial cells, indicating that non-cell-autonomous aspects account for this activation. For example, astrocytes can signal to microglia by ATP or cytokine release (Schipke et al., 2002). These data therefore suggest that activation of astrocytes is further communicated to activate microglia. Interestingly, these signals also seem not to be sufficient to elicit a profound proliferation of microglia cells. Only at later stages, when BM irregularities occur, the increased number of microglia could also be a consequence of T-cell recruitment. T-cells, which are also labeled with microglia markers, have been shown to be able to adhere to and transmigrate over BMs containing the endothelial laminin 8, but are only able to enter the second barrier, the parenchymal BM produced by astrocytes, at sites of irregularities (Sixt et al., 2001).

## 8.2 $\beta$ 1-integrins in reactive gliosis

Notably, the phenotype elicited in astrocytes after the loss of  $\beta$ 1-integrin containing heterodimers recapitulates many aspects of reactive gliosis as observed after traumatic brain injury or ischemic insult, except the reversion to a

proliferative progenitor/ stem cell state (Buffo et al., 2008). Given the multitude of changes after acute or chronic injury (Pekny and Nilsson, 2005; Ridet et al., 1997), it is striking to see that removal of a single protein,  $\beta$ 1-integrin, at the time when astrocytes differentiate is sufficient to elicit most of these changes. Upon loss of  $\beta$ 1-integrins astrocytes not only up-regulate GFAP and Vimentin, but also Tenascin-C, and the 473HD-epitope. Further on, lack of  $\beta$ 1-integrin containing subunits in the postnatal cortex resulted in not only in hypertrophy of astrocytes but also in the loss of endfeet polarity, including defects in deposition of the laminin isoforms  $\alpha$ 1 and  $\alpha$ 2, both synthesized by astrocytes (data acquired by Tetsuji Mori, see also Robel et al., 2009). Interestingly, virtually all of the changes characteristic for reactive astrocytes occur rather early (within 1–2 weeks) after loss of  $\beta$ 1-integrin containing proteins. This implies  $\beta$ 1-integrin mediated signaling as a key pathway for astrocytes to acquire a normal, mature and nonreactive state. As  $\beta$ 1-integrin protein levels are reduced already at postnatal stages, astrocytes may require these signals during development to achieve a mature state. Due to the low turnover of  $\beta$ 1-integrins, it was not possible to analyze the effects of  $\beta$ 1-integrin deletion at adult stages by the use of *Glast::CreERT2*, because protein levels were not reduced within a reasonable time frame. However, it is important to bear in mind that integrin expression is also rapidly down-regulated by endothelial and astroglial cells after focal cerebral ischemia (Wagner et al., 1997) even though integrin upregulation has also been observed after other types of injury (Fasen et al., 2003; Kloss et al., 1999). Also,  $\beta$ 1-integrin ligands, such as laminin, CollagenIV, fibronectin and perlecan are down-regulated after injury (del Zoppo and Milner, 2006). These data would be consistent with the model that the reduction of integrin-mediated signaling at the astrocyte-BM interface after injury may trigger the reactive gliosis with the exception of the proliferation response.

### 8.3 Deletion of $\beta 1$ -Integrins in astrocytes leads to polarity defects

Indeed, we also detected defects in the localization of proteins of the DAG-complex, as well as Aqp4 to the astrocyte endfeet. Interestingly, aquaporins are involved in water homeostasis and the reduction of Aqp4 levels have been implicated in mediating cell swelling and hypertrophy after injury (Saadoun et al., 2008; Verkman et al., 2006). Moreover, the DAG, and in particular Agrin, has been shown to be necessary for proper targeting of Aqp4 to the endfeet of astroglia (Bragg et al., 2006; Noell et al., 2009; Wolburg et al., 2009b). Thus, initial disturbances in astrocyte polarity, as indicated by defects in targeting or maintenance of DGC at the endfeet-BM junction, may then lead to further defects at this interface illustrated by the partial disruptions of Aqp4 location. Careful analysis of the gliosis phenotype after  $\beta 1$ - integrin deletion revealed the alterations in astrocyte polarity as one of the earliest phenotypes in these mice, suggesting that further changes may well be downstream of these initial alterations in integrin-mediated signaling at the astrocyte endfeet-BM interface. Already within the first two postnatal weeks, the targeted deposition of laminin  $\alpha 1$  and  $\alpha 2$  from astroglial cells is affected suggesting early aberrations at the astroglia-BM interface (Robel et al., 2009). Conversely, the  $\alpha 4$  and  $\alpha 5$  laminin isoforms derived from endothelial cells are still normally deposited. Notably, astrocytes and endothelial cells not only produce different types of laminins, but also exhibit a distinct laminin receptor composition: endothelial cells express mainly the integrin receptor  $\alpha 6\beta 4$  binding to laminin  $\alpha 5$ , whereas astrocytes additionally have  $\alpha 1\beta 1$ , a receptor for laminin  $\alpha 1$  (Wagner et al., 1997). Missing the latter receptor in mutant animals could possibly account for the disrupted staining pattern of the correlated ligands due to the failure of their clustering. It is also possible that targeted secretion at this interface may fail because of early defects in astrocyte polarity. These accumulating defects at the astrocyte-BM interface may ultimately result in the phenotype of partial reactive gliosis comprising astrocyte hypertrophy and upregulation of GFAP, Vimentin and Tenascin-C.

## 8.4 Basement membrane defects occur only secondary to reactive gliosis phenotype

It has been demonstrated that  $\beta$ 1-integrins, as well as the cell surface receptor dystroglycan, are important for cell surface laminin organization and ECM and BM assembly during early development (Fassler and Meyer, 1995; Fassler et al., 1995; Graus-Porta et al., 2001; Henry et al., 2001). In this regard it is important to consider that the BM is only mildly affected even after several months lacking  $\beta$ 1 containing integrins. At the light microscopy level, analyzed by pan-laminin, fibronectin or CollagenIV immunostaining, no aberrations in localization and protein deposition in the BM along the meninges or vessels could be observed for several months after birth, despite the almost complete loss of  $\beta$ 1-integrin within the first two postnatal weeks. This is the case although we could observe very early alterations in the deposition of both astrocytic laminin isoforms containing the  $\alpha$ 1 and  $\alpha$ 2 chains. This implies that the partial lack of the astrocytic laminins did not affect the overall structure and maintenance of the BM. Moreover, the presence and regular localization of many other main BM components and associated proteins, such as CollagenIV, fibronectin and other laminins allows the conclusion that the aberrant DGC location is not resulting from the lack of ligand binding for this complex. Furthermore, the proper localization of Dystroglycan and the presence of  $\beta$ 1-integrins, which are both critical for BM formation during early development (Williamson et al., 1997; Graus-Porta et al., 2001), are dispensable for integrity of the BM at postnatal stages. The lack of a strong and early BM phenotype in mice with hGFAP-Cre-mediated deletion of  $\beta$ 1-integrins as observed after earlier interference with either  $\beta$ 1-integrin itself (Fassler and Meyer, 1995; Fassler et al., 1995; Graus-Porta et al., 2001), or down-stream signaling components such as FAK (Beggs et al., 2003), or dystroglycan (Moore et al., 2002), highlights the different importance of the signaling complex at the glial endfeet during development in radial glial cells and at postnatal stages in astrocytes. Although impairment of either integrin- or DGC-mediated signaling already in radial glial cells results in disruptions of the leptomeningeal BM within few days (Moore et al., 2002), such failures apparently take much longer and

never reach such a severity, when  $\beta$ 1-integrin protein is only deleted at postnatal stages. This may be due to a decrease in the role of  $\beta$ 1-integrin during development and possibly a converse increase in expression of other integrin subunits. The integrin subunits  $\beta$ 3 (Hermosilla et al., 2008) and  $\beta$ 4 (Wagner et al., 1997) have been described to be expressed in astrocytes. The integrin-subunit  $\beta$ 3 forms a functional receptor with  $\alpha$ v and  $\beta$ 4 dimerizes with  $\alpha$ 6. Astrocytes have been shown to express these integrin subunits,  $\alpha$ v, as well as  $\alpha$ 1-6 (Fasen et al., 2003). Thus, it is well conceivable that  $\beta$ 3 or  $\beta$ 4-containing integrins may partially compensate for the loss of  $\beta$ 1-integrin. In any case, alterations in the BM occur after the onset of the gliosis phenotype. We therefore conclude that alterations in the BM are not the cause for the partial reactive gliosis upon loss of  $\beta$ 1-integrins, but rather develop secondary to the alterations in astroglial polarity.

## **8.5 The BBB is not affected by loss of $\beta$ 1-Integrins from astrocytes at postnatal stages**

Given the profound astroglial alterations at postnatal stages in the cortical gray matter of  $\beta$ 1-/- mice, it was surprising to observe a fully functional intact BBB. However, the role of astrocytes in BBB formation and maintenance is still controversial, also in light of the early appearance of some BBB characteristics in brain endothelial cells prior to astrocyte differentiation (Engelhardt, 2003). Nonetheless, development of the BBB and maturation of astrocytes as defined by the polarization of astrocytes, seem to be closely correlated during development. Thus, precise and complete localization of Aqp4 towards astrocyte endfeet parallels tight junction formation in chick embryonic development (Nico et al., 2001). Furthermore, in autoimmune encephalomyelitis loss of astrocyte polarity is correlated with BBB disruptions (Wolburg-Buchholz et al., 2009). Here the authors postulated that loss of  $\beta$ -dystroglycan mediated astrocyte foot anchoring results in redistribution of the water channel Aqp4 and subsequently in edema formation in EAE. However, another study demonstrated that after Aqp4 gene deletion the BBB was fully functional and

intact (Saadoun et al., 2009). Based on the results of this study, one can only conclude that  $\beta$ 1-integrins on astrocytes (and neurons) are not required for BBB formation and/ or maintenance, at least not after the first postnatal week. Of course the lack of a BBB phenotype in the conditional  $\beta$ 1<sup>-/-</sup> mice may also be due to compensation by other integrin subunits, such as  $\alpha$ 6 $\beta$ 4 that has also been located in astrocyte endfeet (Su et al., 2008). However, given the gaps in the DAG and Aqp4 staining along the blood vessels  $\alpha$ 6 $\beta$ 4 is obviously not able to achieve the appropriate location of these molecules in the absence of  $\beta$ 1-integrins.

## 8.6 Loss of $\beta$ 1-integrins caused misrouting of neuroblasts

After deletion of  $\beta$ 1-integrins many newly generated neuroblasts left their path towards the OB and enter either the striatum or the cortical white and gray matter. A widely accepted model is that neuroblasts are guided through the RMS towards the OB by chemoattractive and chemorepulsive gradients, as well as guidance molecules (for review see Hagg, 2005). For example, the CSF flow generated by beating cilia of ependymal cells lining the ventricles produces a gradient of Slit proteins, which directs and repulses migrating neurons away from the SEZ towards the OB (W. Wu et al., 1999; Sawamoto et al., 2006). The chemoattractant Sonic hedgehog (Shh) is present in the adult SEZ and the Shh receptor patched is expressed on migrating neuroblasts in the SEZ and RMS. Negative regulation of Shh levels in the SEZ has been proposed to be a mechanism of defining the numbers of neuroblasts released into the RMS (Angot et al., 2008). Shh is released from reactive astrocytes after acute brain injury (Amankulor et al., 2009 and Pratibha Tripathi, unpublished observations). Under some pathological conditions including stroke adult neurogenesis is even enhanced and SEZ precursors are recruited into the injury sites (Massouh and Saghatelian, 2010; Arvidsson et al., 2002; Kokaia and Lindvall, 2003). But also a comparatively small lesion due to noninvasive targeted cell death of cortical projection neurons (Macklis, 1993; Madison and Macklis, 1993) resulted in

redirecting SEZ-neuroblasts towards the cortical gray matter (Brill et al., 2009). It is tempting to speculate that reactive astrocytes in  $\beta 1^{-/-}$  brains would release Shh and thus lure neuroblasts towards striatum and/ or cortex.

Besides the influence of diffusible molecules, neuronal precursor migration through the RMS in the adult brain depends on a specialized parallel organization of blood vessels, which are used as physical substrates by migrating neuroblasts (Saghatelian, 2009; Snayyan et al., 2009). Surprisingly, this blood vessel organization was disturbed after deletion of  $\beta 1$ -integrins, although hGFAP-Cre-mediated recombination does not occur in endothelial cells (Zhuo et al., 2001; Malatesta et al., 2003). However, it is well known that astrocytes are important for angiogenesis during development and after brain injury as they secrete angiogenic factors (Lee et al., 2009). Whether loss of  $\beta 1$ -integrins at postnatal stages may interfere with RMS angiogenesis leading to disturbed blood vessel arrangements, which consequently deprive neuroblasts of their usual substrate for migration, remains to be investigated in more detail.

A further candidate for guiding migrating neuroblasts into the cortex and striatum may be TenascinC and the 473HD epitope. Interestingly, an increase of extracellular Tenascin C and the epitope 473HD was observed in the cerebral cortex of  $\beta 1^{-/-}$  mice, similar to what has been observed after brain injury (Laywell et al., 1992; Garwood et al., 2001; Dobbertin et al., 2003; Sirko et al., 2009). Under physiological conditions WT brains are devoid of these ECM proteins, except in embryonic and adult neurogenic niches, as well as a very restricted expression within the RMS (Sirko et al., 2010; Sirko et al., 2007 and Svetlana Sirko, unpublished observations) suggesting that these ECM molecules could act as guidance cues for neuroblasts. Distribution of Tenascin C and the 473HD epitope all over the ECM of the  $\beta 1^{-/-}$  cortical gray matter could be a cause for neuroblast mismigration in these mutants.

Besides these non cell-autonomous mechanisms one can also think of a cell-autonomous defect in neuroblasts, because Cre expression from the hGFAP-Cre promoter recombines astroglia-like stem cells and consequently their progeny. The integrin  $\alpha 6\beta 1$  is expressed on neuroblasts and serves as a

laminin receptor guiding newborn neurons through the RMS towards the OB. Injection of antibodies against  $\alpha$ 6 or  $\beta$ 1 led to loss of the cohesive structure of the RMS (Emsley and Hagg, 2003). Therefore, one can speculate that due to the loss of  $\beta$ 1-integrin containing ECM receptors neuroblasts would be unable to recognize the spatial different ECM composition in RMS. This is also the case in homozygous ES cells ( $\beta$ 1 null), which lack adhesiveness for laminin and fibronectin and do not migrate towards chemoattractants in fibroblast medium. Furthermore, they have fewer cell-cell junctions (Fassler et al., 1995), which has also been observed in the  $\beta$ 1<sup>-/-</sup> neuroblasts, where tangentially chain migration is lost (Belvindrah et al., 2007a). Nonetheless, the exact ECM composition in the RMS has not been analyzed so far. Therefore it is difficult to judge, whether a cell autonomous effect could contribute to the mismigration. Transplantation of mutant neuroblasts in the WT RMS and vice versa could answer this question.

## 8.7 Misrouted neuroblasts mature in the striatum after loss of $\beta$ 1-integrins

After deletion of  $\beta$ 1-integrins in the striatum, misrouted neuroblasts survived and matured to a certain degree recapitulating what has been reported for de-routed neuroblasts after injury (R. L. Zhang et al., 2001; Ohab et al., 2006). However, after massive tissue disruption caused by stroke, as well as after targeted cell death of projection neurons without inflammatory response and necrotic tissue loss, only a tiny proportion of newborn neurons matured to a certain degree in the injured area (Arvidsson et al., 2002; Brill et al., 2009) suggesting that not only a hostile inflammatory environment impedes efficient maturation. Interestingly, also after de-routing of neuroblasts in the forebrain of  $\beta$ 1<sup>-/-</sup> mice, where massive amounts of newborn neurons entered the striatum, also very few newborn NeuN-positive neurons could be observed. These neurons matured despite the fact that in the  $\beta$ 1<sup>-/-</sup> forebrain no cell death was observed, suggesting that the trigger for neuroblasts to mature is not neuronal cell loss per se, but rather the glial reaction or cell intrinsic mechanisms. Nevertheless, also

in the  $\beta$ 1-integrin mutant many neuroblasts did not mature. This is possibly due to changed characteristics of the astrocytes including the upregulation of ECM components TenascinC and 473HD. These molecules are important for progenitor proliferation in neurogenic niches (Sirko et al., 2010; Sirko et al., 2007) and may interfere with neuronal maturation.

## **8.8 The role of polarity cues in astrocytes and their stem cell potential**

### **8.8.1 Basal polarity mediated by $\beta$ 1-integrins**

Notably,  $\beta$ 1-integrin deficient astrocytes recapitulated many, but not all aspects of reactive gliosis. After a stab wound injury, about half of all astrocytes resume proliferation (Buffo et al., 2008) and some of these also readopt neural stem cell properties (Buffo et al., 2008). Although the proportion of BrdU-incorporating astrocytes varies between different types of trauma and is related to the severity of injury (Buffo et al., 2005; Myer et al., 2006; Buffo et al., 2008; Sirko et al., 2009), such a proliferative response is not elicited by conditional  $\beta$ 1-integrin deletion as even after 2 weeks of continuous BrdU application only few of the GFAP- or S100 $\beta$ -positive astrocytes had incorporated BrdU in the  $\beta$ 1-/- cortex and their number was not significantly different from the control. These data therefore imply other signals as potential regulators of this aspect of the proliferation response of astrogliosis. For example, FGF, EGF, and endothelin-mediated signaling is strongly increased after brain injury (W. E. Clarke et al., 2001; G. M. Smith and Strunz, 2005; Gadea et al., 2008). Interestingly, FGF and EGF also affect radial glial cells, the closest relatives of adult astrocytes, during development (Vaccharino et al., 2001; K. M. Smith et al., 2006; Sirko et al., 2007). Likewise purinergic signaling via ATP release is one of the first reactions to tissue damage and well known to stimulate astrocyte proliferation (Neary and Kang, 2005). Notably, many of these signaling pathways have also been implicated in the regulation of proliferation in the neural stem cell niches in the forebrain (Kuhn et al., 1997; Doetsch et al., 2002; Braun et al., 2003; Shukla et al., 2005). As the adult NSCs in the neurogenic niches have been identified

as astrocyte-like cells (Doetsch et al., 1997; Alvarez-Buylla et al., 2001), these pathways may well be involved in the regulation of astrocyte/stem cell division as well as in the reinstruction of proliferation and stem cell features in astrocytes after injury.

From the mutant analysis one can add that  $\beta$ 1-integrins are needed for neurosphere formation after stab wound injury, maybe via the well-known interaction between integrins and growth factor receptors (see e.g. Colognato et al., 2002). On the other hand,  $\beta$ 1-integrins are important for cell-cell adhesion (Fassler et al., 1995; Brakebusch and Fassler, 2005; Shen et al., 2008). It is commonly known that formation of neurospheres is based on cell division of a single clone. This results in formation of cell colonies consisting of daughter cells that adhere to each other. Therefore, it cannot be excluded that impaired adhesion between  $\beta$ 1-integrin deficient cells led to the decrease of neurosphere numbers, because newly formed cells cannot attach to each other to form a sphere.

Apparently,  $\beta$ 1-integrins are not needed to mediate growth factor signaling in SEZ astroglia, as proliferation of stem cells in this region was not affected in the hGFAP-Cre,  $\beta$ 1<sup>-/-</sup> mice. However, the overall size of the RMS appeared increased in the mutant forebrain and although large numbers of neuroblasts left the RMS, the size of the OB seemed to be unchanged, suggesting that a sufficient number of neuroblasts arrived in the OB still. While these effects were not quantified, it appeared as larger numbers of neuroblasts are present in  $\beta$ 1<sup>-/-</sup> RMS compared to the control. If the proliferation of the stem cells is not changed, their progeny, the transit amplifying precursors could account for increased generation of neuroblasts. Indeed, infusion of an antibody against  $\alpha$ 6-integrin, which forms dimers with  $\beta$ 1-integrin and is expressed in progenitors labeled with LewisX in the SEZ and in neurospheres (Shen et al., 2008), leads to an increase in fast proliferating SEZ cells (Shen et al., 2008).

In conclusion, deletion of  $\beta$ 1-integrins in the SEZ did not change the capacity of stem cells to proliferate, but seems to affect the generation of transit amplifying precursors. Notably,  $\beta$ 1-integrin function in the SEZ may also be compensated

by other integrins or  $\beta$ -dystroglycan, another ECM receptor strongly expressed in the adult SEZ (Adorjan and Kalman, 2009 and Stefanie Robel, unpublished observations). Conversely, signaling via  $\beta$ 1-integrins is critical for reactive astrocytes after injury to regain their proliferative capacity given the reduced number of neurospheres in  $\beta$ 1-/- brains.

### **8.8.2 Apical polarity mediated by Cdc42**

Besides the clear polarity of astrocytes towards the basal side, astroglial-like SEZ stem cells at the lateral wall of the lateral ventricle possess another specialized membrane domain, where they face the ventricle. As the basal membrane domain, the apical side is characterized by enrichment of certain proteins responsible for establishing cell polarity and cell contact/ junctions including catenin, cadherins, proteins of the Par complex and the small RhoGTPase Cdc42 (Cappello et al., 2006; Costa et al., 2008). Although Cdc42 is a major player in keeping RG in the VZ in a self-renewing state and preventing premature neurogenic differentiation during development (Cappello et al., 2006), I showed here that Cdc42 is dispensable for proliferation of adult SEZ stem cells. Provided that the apical polarity of VZ stem cells is a precondition for proper regulation of the self renewing capacity (Machon et al., 2003; Costa et al., 2008; Ghosh et al., 2008), it is possible that the effect of Cdc42 deletion during development is secondary and due to the failure of establishment of apical polarity assessed by staining for the apical markers  $\beta$ -catenin, aPKC $\lambda$  and Par3 (Cappello et al., 2006; Chen et al., 2006). In addition, the ventricle is lined exclusively by Radial glia (RG) that are coupled by adherens junctions during development (Gotz and Huttner, 2005). Recombination in RG with Emx1::Cre or hGFAP-Cre leads subsequently to the loss of Cdc42 and thus apical polarity at the entire ventricular surface. This may lead to the loss of a key feature of the stem cell niche and therefore impaired self-renewal at the apical surface. In the adult neurogenic niche the cell body of the stem cells are localized above the ependymal layer in the SEZ. They form a thin process protruding between the ependymal layer towards the ventricle and this apical membrane is the central point of a “pinwheel” surrounded by

ependymal cells, which line the ventricular surface (Mirzadeh et al., 2008). The ependymal cells are coupled by junctions among each other and with the apical process of the stem cell astrocytes. At the time point of gene deletion in this study, polarity was already established in adult SEZ stem cells, only a subset of this population was recombined and ependymal cells were excluded from recombination. Therefore, the niche is affected if at all on a small scale and the apicobasal polarity of Cdc42-deficient stem cells may be remained by surrounding not recombined cells.

## **8.9 Polarity of astrocytes after injury and their dedifferentiation**

One may speculate that - inter alia - the lack of apical polarity in mature astrocytes correlates with their quiescent, non-proliferative state under physiological conditions. However, after injury they change their morphology towards an elongated shape, which is then similar to the bipolar shape of stem cell astrocytes. This can be observed in an in vitro wound healing assay where cultured astrocytes reorienting their centrosome and, intriguingly, establishment of an apical cell polarity where they face the scratch. In this experimental paradigm, Cdc42 in primary astrocytes was essential to induce formation of this front-rear axis. Genetic deletion of this small RhoGTPase interfered with centrosome reorientation, protrusion formation and subsequent migration (Figure 7-21 and Sophia Bardehle, unpublished observations). In vivo, astrocytes change their morphology dramatically directly at the injury border giving up their non-overlapping organization by building a long protrusion towards the injury site, thereby violating neighboring domains (Figure 7-16 and Oberheim et al., 2008). Some astrocytes extended a process already 3 days post lesion and one third of them bear a protrusion one week after the injury. Interestingly, this correlates with an increase in proliferating astrocytes after stab wound injury up to 50 % of the entire astrocyte population 7 days upon injury (Christiane Simon, unpublished observations). It is tempting to speculate

that establishment of an apicobasal polarity, similar to stem cell astrocytes residing in the SEZ, is necessary to allow proliferation.

Also in the second neurogenic niche of the adult forebrain, the dentate gyrus of the hippocampus stem cells have a radial glia-like bipolar morphology and are located in close proximity to the vasculature (for review see Ehninger and Kempermann, 2008). Although direct evidence of an apical membrane domain in stem cells of the dentate gyrus is lacking, polarity cues like ephrins are important for their proliferation (Chumley et al., 2007). Ephrins have been reported to regulate cell-cell junctions through the Par complex (Lee et al., 2008) and play a role in asymmetric cell division at least in the tunicate *Ciona* (Picco et al., 2007). Thus, polarity mediated by the Par complex may be a general prerequisite for cells to acquire or maintain an immature state. I showed here, that after deletion of *Cdc42*, a protein activating the Par complex in cultured astrocytes (Etienne-Manneville and Hall, 2001; Etienne-Manneville et al., 2005), the number of astrocytes at the injury site was reduced. Quantification of the proliferating astrocytes shortly after injury revealed that deletion of *Cdc42* interferes with their capacity to re-enter the cell cycle. A possible mechanism activating *Cdc42* after injury is the EGF-R pathway. *Cdc42* is activated upon EGF stimulation, interacts with MEK1 and 2 and activates the JNK pathway in several cell lines (Fanger et al., 1997; Frost et al., 1997; Bishop and Hall, 2000). Deletion of *Cdc42* in late but not early neural crest stem cells results in a decreased self renewing capacity due to the lack of EGF-responsiveness (Fuchs et al., 2009). Moreover, activation of JNK was reduced, even though not significant, in wounded *Cdc42*-deficient fibroblasts cultures (Czuchra et al., 2005). This pathway could also explain the reduced proliferation observed here in *Cdc42*-deficient reactive astrocytes, as upregulation of the EGF-R and EGF-R signaling is important for proliferation of astrocytes after injury (Nieto-Sampedro et al., 1988; Weickert and Blum, 1995; Rabchevsky et al., 1998; Levison et al., 2000; Liu and Neufeld, 2004; G. M. Smith and Strunz, 2005; Liu et al., 2006; Sharif et al., 2006; Liu and Neufeld, 2007; White et al., 2008). Notably, even adult NSC seem to acquire an enhanced responsiveness to EGF in response to injury (Alagappan et al., 2009). In this regard it is also

interesting to note that integrins and the Rho family of GTPases share some signaling networks with integrins regulating RhoGTPases and vice versa (for review see (Schwartz and Shattil, 2000). As the proliferation of astrocytes from the injured cerebral cortex was also reduced after deletion of  $\beta$ 1-integrins, a possible cascade could involve initially an interaction between the EGF-R and integrins that then would activate Cdc42.

Although deletion of Cdc42 in astrocytes interfered with their ability to orient their protrusions in vitro, this effect was not seen in vivo. One possible explanation is that several redundant factors released in the injury site attract astrocyte processes, while no such signals exist in the scratch assay in vitro. The 3D environment of brain tissue may provide cells with a multitude of factors triggering alternative pathways to mediate reorganization of the cytoskeleton, whereas culturing astrocytes in a monolayer on poly-L-ornithine as the only substrate, is a rather reduced model. In future experiments, this could be clarified by performing the scratch assay in Cdc42-deficient astrocytes cultured on different ECM substrates. The enlarged cell size after Cdc42 deletion in vivo may, nevertheless, hint to a misregulation of cytoskeletal rearrangements similar to what has been shown in Cdc42-deficient fibroblasts (Czuchra et al., 2005).

## **8.10 The role of Cdc42 in astrocyte migration and wound healing**

It has been widely assumed that after injury astrocytes increase in density not only because of their proliferation, but also because they migrate towards the insult. However, whether astrocytes in the brain parenchyma have indeed the ability to migrate had been impossible to study so far. Results from this study revealed, that integrated mature gray matter astrocytes labeled 1-3 mm away from the stab wound injury were not attracted towards the injury site. On the contrary, perinatal astrocytes cultured to confluency prior to their transplantation into the striatum migrated towards an injury (Auguste et al., 2007). Nonetheless, this study does not resemble the situation after trauma in the adult brain, as

postnatal astrocytes may display a different migratory behavior than mature astrocytes and these cells are not integrated into the tissue. Mature astrocytes would need to entirely retract their processes from synapses and blood vessels during a migration process. This involves complex remodeling of the tissue surrounding an injury area, which may explain why astrocyte processes, in contrast to microglia (Nimmerjahn et al., 2005), are not motile immediately after injury (Figure 7-26). Timelapse imaging of primary astrocyte cultures allowed investigating the influence of Cdc42 on astrocyte migration. Whereas astrocytes normally migrate straight into the scratch area, Cdc42-deficient astrocytes were impaired in their directionality remaining behind WT cells, although their migration speed was not reduced (Sophia Bardehle, unpublished observations).

### **8.11 The impact of astrocytes for brain repair**

Deletion of Cdc42 in almost all astrocytes by the use of hGFAP-Cre caused an enlargement of the injury size. Assuming that astrocytes *in vivo* migrate, the deletion of Cdc42 could reduce the number of astrocytes at the injury site by both interfering with proliferation and migration. Thus, Cdc42 in astrocytes is important for wound healing after injury highlighting thereby the importance of reactive astrogliosis. Reactive astrocytes have long been considered detrimental for repair after brain injury, because they form tight scars that are non-permissive for axonal regeneration. However, this reaction does not only provide protection of the brain from further damage, but may even serve for brain repair. Given the fact that upon injury astrocytes re-enter the cell cycle and dedifferentiate towards a state that allows them to self-renew and give rise to all three neural cell types *in vitro* (Buffo et al., 2008), this dedifferentiation implies a stem cell response. As the efficiency of generating neurons can be strongly enhanced by forced expression of neurogenic transcription factors (Buffo et al., 2005; Berninger et al., 2007; Heinrich et al., *in press*), they might be a powerful local source for brain repair. Nonetheless, the exact mechanism of dedifferentiation of reactive astrocytes is not clear. Establishment of a polarity with an apical membrane domain by activating Cdc42 and the Par complex may

play a role, as loss of Cdc42 is accompanied by a reduction in proliferation and thus possibly impairment of dedifferentiation. Whether polarization of astrocytes and their capacity to proliferate, or even give rise to an astrocyte-like stem cell, are directly correlated, remains to be investigated. Therefore, on the one hand, brain injury triggers astrocyte dedifferentiation and is therefore beneficial; on the other hand the environment is inhospitable for efficient neuronal genesis and maturation. This is partly due to the physical barrier formed by astrocytes and the factors they secrete upon injury. Therefore, discriminating between the different responses of astrocytes towards injury would be beneficial. This study gained further insights in the complex mechanisms involved in astrocyte reactivity showing that signaling from the basement membrane via integrin receptors is important in astrocytes to acquire a quiescent non-reactive phenotype, as well as the action of the polarity protein Cdc42, which play a role in the dedifferentiation of astrocytes after injury.



## 9 References

- Abbott NJ, Ronnback L, Hansson E (2006) Astrocyte-endothelial interactions at the blood-brain barrier. *Nat Rev Neurosci* 7:41-53.
- Adorjan I, Kalman M (2009) Distribution of beta-dystroglycan immunopositive globules in the subventricular zone of rat brain. *Glia* 57:657-666.
- Alagappan D, Lazzarino DA, Felling RJ, Balan M, Kotenko SV, Levison SW (2009) Brain injury expands the numbers of neural stem cells and progenitors in the SVZ by enhancing their responsiveness to EGF. *ASN Neuro* 1.
- Altman J (1969) Autoradiographic and histological studies of postnatal neurogenesis. IV. Cell proliferation and migration in the anterior forebrain, with special reference to persisting neurogenesis in the olfactory bulb. *J Comp Neurol* 137:433-457.
- Altman J, Das GD (1965) Autoradiographic and histological evidence of postnatal hippocampal neurogenesis in rats. *J Comp Neurol* 124:319-335.
- Alvarez-Buylla A, Garcia-Verdugo JM, Tramontin AD (2001) A unified hypothesis on the lineage of neural stem cells. *Nat Rev Neurosci* 2:287-293.
- Amankulor NM, Hambardzumyan D, Pyonteck SM, Becher OJ, Joyce JA, Holland EC (2009) Sonic hedgehog pathway activation is induced by acute brain injury and regulated by injury-related inflammation. *J Neurosci* 29:10299-10308.
- Angot E, Loulier K, Nguyen-Ba-Charvet KT, Gadeau AP, Ruat M, Traiffort E (2008) Chemoattractive activity of sonic hedgehog in the adult subventricular zone modulates the number of neural precursors reaching the olfactory bulb. *Stem Cells* 26:2311-2320.
- Arvidsson A, Collin T, Kirik D, Kokaia Z, Lindvall O (2002) Neuronal replacement from endogenous precursors in the adult brain after stroke. *Nat Med* 8:963-970.
- Auguste KI, Jin S, Uchida K, Yan D, Manley GT, Papadopoulos MC, Verkman AS (2007) Greatly impaired migration of implanted aquaporin-4-deficient astroglial cells in mouse brain toward a site of injury. *FASEB J* 21:108-116.
- Baba A (1998) Role of endothelin B receptor signals in reactive astrocytes. *Life Sci* 62:1711-1715.
- Barnes K, Turner AJ (1997) The endothelin system and endothelin-converting enzyme in the brain: molecular and cellular studies. *Neurochem Res* 22:1033-1040.
- Barry D, McDermott K (2005) Differentiation of radial glia from radial precursor cells and transformation into astrocytes in the developing rat spinal cord. *Glia* 50:187-197.
- Beggs HE, Schahin-Reed D, Zang K, Goebbels S, Nave KA, Gorski J, Jones KR, Sretavan D, Reichardt LF (2003) FAK deficiency in cells contributing

- to the basal lamina results in cortical abnormalities resembling congenital muscular dystrophies. *Neuron* 40:501-514.
- Belvindrah R, Hankel S, Walker J, Patton BL, Muller U (2007a) Beta1 integrins control the formation of cell chains in the adult rostral migratory stream. *J Neurosci* 27:2704-2717.
- Belvindrah R, Graus-Porta D, Goebbels S, Nave KA, Muller U (2007b) Beta1 integrins in radial glia but not in migrating neurons are essential for the formation of cell layers in the cerebral cortex. *J Neurosci* 27:13854-13865.
- Belvindrah R, Nalbant P, Ding S, Wu C, Bokoch GM, Muller U (2006) Integrin-linked kinase regulates Bergmann glial differentiation during cerebellar development. *Mol Cell Neurosci* 33:109-125.
- Berninger B, Costa MR, Koch U, Schroeder T, Sutor B, Grothe B, Gotz M (2007) Functional properties of neurons derived from in vitro reprogrammed postnatal astroglia. *J Neurosci* 27:8654-8664.
- Bianco F, Ceruti S, Colombo A, Fumagalli M, Ferrari D, Pizzirani C, Matteoli M, Di Virgilio F, Abbracchio MP, Verderio C (2006) A role for P2X7 in microglial proliferation. *J Neurochem* 99:745-758.
- Bishop AL, Hall A (2000) Rho GTPases and their effector proteins. *Biochem J* 348 Pt 2:241-255.
- Blaess S, Graus-Porta D, Belvindrah R, Radakovits R, Pons S, Littlewood-Evans A, Senften M, Guo H, Li Y, Miner JH, Reichardt LF, Muller U (2004) Beta1-integrins are critical for cerebellar granule cell precursor proliferation. *J Neurosci* 24:3402-3412.
- Bonni A, Sun Y, Nadal-Vicens M, Bhatt A, Frank DA, Rozovsky I, Stahl N, Yancopoulos GD, Greenberg ME (1997) Regulation of gliogenesis in the central nervous system by the JAK-STAT signaling pathway. *Science* 278:477-483.
- Bragg AD, Amiry-Moghaddam M, Ottersen OP, Adams ME, Froehner SC (2006) Assembly of a perivascular astrocyte protein scaffold at the mammalian blood-brain barrier is dependent on alpha-syntrophin. *Glia* 53:879-890.
- Brakebusch C, Fassler R (2005) beta 1 integrin function in vivo: adhesion, migration and more. *Cancer Metastasis Rev* 24:403-411.
- Brakebusch C, Grose R, Quondamatteo F, Ramirez A, Jorcano JL, Pirro A, Svensson M, Herken R, Sasaki T, Timpl R, Werner S, Fassler R (2000) Skin and hair follicle integrity is crucially dependent on beta 1 integrin expression on keratinocytes. *Embo J* 19:3990-4003.
- Brambilla R, Neary JT, Cattabeni F, Cottini L, D'Ippolito G, Schiller PC, Abbracchio MP (2002) Induction of COX-2 and reactive gliosis by P2Y receptors in rat cortical astrocytes is dependent on ERK1/2 but independent of calcium signalling. *J Neurochem* 83:1285-1296.
- Braun N, Sevigny J, Mishra SK, Robson SC, Barth SW, Gerstberger R, Hammer K, Zimmermann H (2003) Expression of the ecto-ATPase NTPDase2 in the germinal zones of the developing and adult rat brain. *Eur J Neurosci* 17:1355-1364.
- Brightman MW (1968) The intracerebral movement of proteins injected into blood and cerebrospinal fluid of mice. *Prog Brain Res* 29:19-40.

- Brightman MW, Kaya M (2000) Permeable endothelium and the interstitial space of brain. *Cell Mol Neurobiol* 20:111-130.
- Brill MS, Ninkovic J, Winpenny E, Hodge RD, Ozen I, Yang R, Lepier A, Gascon S, Erdelyi F, Szabo G, Parras C, Guillemot F, Frotscher M, Berninger B, Hevner RF, Raineteau O, Gotz M (2009) Adult generation of glutamatergic olfactory bulb interneurons. *Nat Neurosci* 12:1524-1533.
- Buffo A, Rolando C, Ceruti S (2010) Astrocytes in the damaged brain: molecular and cellular insights into their reactive response and healing potential. *Biochem Pharmacol* 79:77-89.
- Buffo A, Vosko MR, Erturk D, Hamann GF, Jucker M, Rowitch D, Gotz M (2005) Expression pattern of the transcription factor Olig2 in response to brain injuries: implications for neuronal repair. *Proc Natl Acad Sci U S A* 102:18183-18188.
- Buffo A, Rite I, Tripathi P, Lepier A, Colak D, Horn AP, Mori T, Gotz M (2008) Origin and progeny of reactive gliosis: A source of multipotent cells in the injured brain. *Proc Natl Acad Sci U S A* 105:3581-3586.
- Buisson A, Lesne S, Docagne F, Ali C, Nicole O, MacKenzie ET, Vivien D (2003) Transforming growth factor-beta and ischemic brain injury. *Cell Mol Neurobiol* 23:539-550.
- Bushong EA, Martone ME, Jones YZ, Ellisman MH (2002) Protoplasmic astrocytes in CA1 stratum radiatum occupy separate anatomical domains. *J Neurosci* 22:183-192.
- Cappello S, Attardo A, Wu X, Iwasato T, Itohara S, Wilsch-Brauninger M, Eilken HM, Rieger MA, Schroeder TT, Huttner WB, Brakebusch C, Gotz M (2006) The Rho-GTPase cdc42 regulates neural progenitor fate at the apical surface. *Nat Neurosci* 9:1099-1107.
- Carbonell WS, Mandell JW (2003) Transient neuronal but persistent astroglial activation of ERK/MAP kinase after focal brain injury in mice. *J Neurotrauma* 20:327-336.
- Cau J, Hall A (2005) Cdc42 controls the polarity of the actin and microtubule cytoskeletons through two distinct signal transduction pathways. *J Cell Sci* 118:2579-2587.
- Chan-Palay V, Palay SL (1972) The form of velate astrocytes in the cerebellar cortex of monkey and rat: high voltage electron microscopy of rapid Golgi preparations. *Z Anat Entwicklungsgesch* 138:1-19.
- Chan WY, Kohsaka S, Rezaie P (2007) The origin and cell lineage of microglia: new concepts. *Brain Res Rev* 53:344-354.
- Chen L, Liao G, Yang L, Campbell K, Nakafuku M, Kuan CY, Zheng Y (2006) Cdc42 deficiency causes Sonic hedgehog-independent holoprosencephaly. *Proc Natl Acad Sci U S A* 103:16520-16525.
- Chiang GG, Abraham RT (2007) Targeting the mTOR signaling network in cancer. *Trends Mol Med* 13:433-442.
- Chrostek A, Wu X, Quondamatteo F, Hu R, Sanecka A, Niemann C, Langbein L, Haase I, Brakebusch C (2006) Rac1 is crucial for hair follicle integrity but is not essential for maintenance of the epidermis. *Mol Cell Biol* 26:6957-6970.

- Chumley MJ, Catchpole T, Silvany RE, Kernie SG, Henkemeyer M (2007) EphB receptors regulate stem/progenitor cell proliferation, migration, and polarity during hippocampal neurogenesis. *J Neurosci* 27:13481-13490.
- Clarke E, O'Malley CD (1996) *The Human Brain and Spinal Cord: A Historical Study Illustrated by Writings from Antiquity to the Twentieth Century*, Second Edition Edition: Norman Publishing, U.S.
- Clarke WE, Berry M, Smith C, Kent A, Logan A (2001) Coordination of fibroblast growth factor receptor 1 (FGFR1) and fibroblast growth factor-2 (FGF-2) trafficking to nuclei of reactive astrocytes around cerebral lesions in adult rats. *Mol Cell Neurosci* 17:17-30.
- Codeluppi S, Svensson CI, Hefferan MP, Valencia F, Silldorff MD, Oshiro M, Marsala M, Pasquale EB (2009) The Rheb-mTOR pathway is upregulated in reactive astrocytes of the injured spinal cord. *J Neurosci* 29:1093-1104.
- Colucci-Guyon E, Portier MM, Dunia I, Paulin D, Pournin S, Babinet C (1994) Mice lacking vimentin develop and reproduce without an obvious phenotype. *Cell* 79:679-694.
- Costa MR, Gotz M, Berninger B What determines neurogenic competence in glia? *Brain Res Rev*.
- Costa MR, Wen G, Lepier A, Schroeder T, Gotz M (2008) Par-complex proteins promote proliferative progenitor divisions in the developing mouse cerebral cortex. *Development* 135:11-22.
- Cotrina ML, Nedergaard M (2009) Physiological and pathological functions of P2X7 receptor in the spinal cord. *Purinergic Signal* 5:223-232.
- Czuchra A, Wu X, Meyer H, van Hengel J, Schroeder T, Geffers R, Rottner K, Brakebusch C (2005) Cdc42 is not essential for filopodium formation, directed migration, cell polarization, and mitosis in fibroblastoid cells. *Mol Biol Cell* 16:4473-4484.
- de Bilbao F, Arsenijevic D, Moll T, Garcia-Gabay I, Vallet P, Langhans W, Giannakopoulos P (2009) In vivo over-expression of interleukin-10 increases resistance to focal brain ischemia in mice. *J Neurochem* 110:12-22.
- del Zoppo GJ, Milner R (2006) Integrin-matrix interactions in the cerebral microvasculature. *Arterioscler Thromb Vasc Biol* 26:1966-1975.
- Di Santo E, Alonzi T, Fattori E, Poli V, Ciliberto G, Sironi M, Gnocchi P, Ricciardi-Castagnoli P, Ghezzi P (1996) Overexpression of interleukin-6 in the central nervous system of transgenic mice increases central but not systemic proinflammatory cytokine production. *Brain Res* 740:239-244.
- Di Virgilio F (2007) Liaisons dangereuses: P2X(7) and the inflammasome. *Trends Pharmacol Sci* 28:465-472.
- Di Virgilio F, Ceruti S, Bramanti P, Abbracchio MP (2009) Purinergic signalling in inflammation of the central nervous system. *Trends Neurosci* 32:79-87.
- Dimou L, Simon C, Kirchhoff F, Takebayashi H, Gotz M (2008) Progeny of Olig2-expressing progenitors in the gray and white matter of the adult mouse cerebral cortex. *J Neurosci* 28:10434-10442.

- Discher DE, Mooney DJ, Zandstra PW (2009) Growth factors, matrices, and forces combine and control stem cells. *Science* 324:1673-1677.
- Dobbertin A, Rhodes KE, Garwood J, Properzi F, Heck N, Rogers JH, Fawcett JW, Faissner A (2003) Regulation of RPTPbeta/phosphacan expression and glycosaminoglycan epitopes in injured brain and cytokine-treated glia. *Mol Cell Neurosci* 24:951-971.
- Doetsch F, Garcia-Verdugo JM, Alvarez-Buylla A (1997) Cellular composition and three-dimensional organization of the subventricular germinal zone in the adult mammalian brain. *J Neurosci* 17:5046-5061.
- Doetsch F, Caille I, Lim DA, Garcia-Verdugo JM, Alvarez-Buylla A (1999) Subventricular zone astrocytes are neural stem cells in the adult mammalian brain. *Cell* 97:703-716.
- Doetsch F, Petreanu L, Caille I, Garcia-Verdugo JM, Alvarez-Buylla A (2002) EGF converts transit-amplifying neurogenic precursors in the adult brain into multipotent stem cells. *Neuron* 36:1021-1034.
- Ebadi M, Bashir RM, Heidrick ML, Hamada FM, Refaey HE, Hamed A, Helal G, Baxi MD, Cerutis DR, Lassi NK (1997) Neurotrophins and their receptors in nerve injury and repair. *Neurochem Int* 30:347-374.
- Ehninger D, Kempermann G (2008) Neurogenesis in the adult hippocampus. *Cell Tissue Res* 331:243-250.
- Emsley JG, Hagg T (2003) alpha6beta1 integrin directs migration of neuronal precursors in adult mouse forebrain. *Exp Neurol* 183:273-285.
- Eriksson PS, Perfilieva E, Bjork-Eriksson T, Alborn AM, Nordborg C, Peterson DA, Gage FH (1998) Neurogenesis in the adult human hippocampus. *Nat Med* 4:1313-1317.
- Etienne-Manneville S (2006) In vitro assay of primary astrocyte migration as a tool to study Rho GTPase function in cell polarization. *Methods Enzymol* 406:565-578.
- Etienne-Manneville S (2008) Polarity proteins in migration and invasion. *Oncogene* 27:6970-6980.
- Etienne-Manneville S, Hall A (2001) Integrin-mediated activation of Cdc42 controls cell polarity in migrating astrocytes through PKCzeta. *Cell* 106:489-498.
- Etienne-Manneville S, Hall A (2003) Cdc42 regulates GSK-3beta and adenomatous polyposis coli to control cell polarity. *Nature* 421:753-756.
- Etienne-Manneville S, Manneville JB, Nicholls S, Ferenczi MA, Hall A (2005) Cdc42 and Par6-PKCzeta regulate the spatially localized association of Dlg1 and APC to control cell polarization. *J Cell Biol* 170:895-901.
- Fanger GR, Johnson NL, Johnson GL (1997) MEK kinases are regulated by EGF and selectively interact with Rac/Cdc42. *EMBO J* 16:4961-4972.
- Farina C, Aloisi F, Meinl E (2007) Astrocytes are active players in cerebral innate immunity. *Trends Immunol* 28:138-145.
- Fassler R, Meyer M (1995) Consequences of lack of beta 1 integrin gene expression in mice. *Genes Dev* 9:1896-1908.
- Fassler R, Pfaff M, Murphy J, Noegel AA, Johansson S, Timpl R, Albrecht R (1995) Lack of beta 1 integrin gene in embryonic stem cells affects morphology, adhesion, and migration but not integration into the inner cell mass of blastocysts. *J Cell Biol* 128:979-988.

- Fattori E, Lazzaro D, Musiani P, Modesti A, Alonzi T, Ciliberto G (1995) IL-6 expression in neurons of transgenic mice causes reactive astrocytosis and increase in ramified microglial cells but no neuronal damage. *Eur J Neurosci* 7:2441-2449.
- Franke H, Krugel U, Schmidt R, Grosche J, Reichenbach A, Illes P (2001) P2 receptor-types involved in astrogliosis in vivo. *Br J Pharmacol* 134:1180-1189.
- Fraser MM, Zhu X, Kwon CH, Uhlmann EJ, Gutmann DH, Baker SJ (2004) Pten loss causes hypertrophy and increased proliferation of astrocytes in vivo. *Cancer Res* 64:7773-7779.
- Frost JA, Steen H, Shapiro P, Lewis T, Ahn N, Shaw PE, Cobb MH (1997) Cross-cascade activation of ERKs and ternary complex factors by Rho family proteins. *EMBO J* 16:6426-6438.
- Fuchs S, Herzog D, Sumara G, Buchmann-Moller S, Civenni G, Wu X, Chrostek-Grashoff A, Suter U, Ricci R, Relvas JB, Brakebusch C, Sommer L (2009) Stage-specific control of neural crest stem cell proliferation by the small rho GTPases Cdc42 and Rac1. *Cell Stem Cell* 4:236-247.
- Fumagalli M, Brambilla R, D'Ambrosi N, Volonte C, Matteoli M, Verderio C, Abbracchio MP (2003) Nucleotide-mediated calcium signaling in rat cortical astrocytes: Role of P2X and P2Y receptors. *Glia* 43:218-203.
- Gadea A, Schinelli S, Gallo V (2008) Endothelin-1 regulates astrocyte proliferation and reactive gliosis via a JNK/c-Jun signaling pathway. *J Neurosci* 28:2394-2408.
- Gaiano N (2008) Strange bedfellows: Reelin and Notch signaling interact to regulate cell migration in the developing neocortex. *Neuron* 60:189-191.
- Garwood J, Rigato F, Heck N, Faissner A (2001) Tenascin glycoproteins and the complementary ligand DSD-1-PG/ phosphacan--structuring the neural extracellular matrix during development and repair. *Restor Neurol Neurosci* 19:51-64.
- Ghosh S, Marquardt T, Thaler JP, Carter N, Andrews SE, Pfaff SL, Hunter T (2008) Instructive role of aPKCzeta subcellular localization in the assembly of adherens junctions in neural progenitors. *Proc Natl Acad Sci U S A* 105:335-340.
- Goebbels S, Bormuth I, Bode U, Hermanson O, Schwab MH, Nave KA (2006) Genetic targeting of principal neurons in neocortex and hippocampus of NEX-Cre mice. *Genesis* 44:611-621.
- Gotz M, Huttner WB (2005) The cell biology of neurogenesis. *Nat Rev Mol Cell Biol* 6:777-788.
- Graus-Porta D, Blaess S, Senften M, Littlewood-Evans A, Damsky C, Huang Z, Orban P, Klein R, Schittny JC, Muller U (2001) Beta1-class integrins regulate the development of laminae and folia in the cerebral and cerebellar cortex. *Neuron* 31:367-379.
- Hagg T (2005) Molecular regulation of adult CNS neurogenesis: an integrated view. *Trends Neurosci* 28:589-595.
- Hall A (2005) Rho GTPases and the control of cell behaviour. *Biochem Soc Trans* 33:891-895.

- Hallmann R, Horn N, Selg M, Wendler O, Pausch F, Sorokin LM (2005) Expression and function of laminins in the embryonic and mature vasculature. *Physiol Rev* 85:979-1000.
- Hampton DW, Asher RA, Kondo T, Steeves JD, Ramer MS, Fawcett JW (2007) A potential role for bone morphogenetic protein signalling in glial cell fate determination following adult central nervous system injury in vivo. *Eur J Neurosci* 26:3024-3035.
- Hartfuss E, Galli R, Heins N, Gotz M (2001) Characterization of CNS precursor subtypes and radial glia. *Dev Biol* 229:15-30.
- Hauwel M, Furon E, Canova C, Griffiths M, Neal J, Gasque P (2005) Innate (inherent) control of brain infection, brain inflammation and brain repair: the role of microglia, astrocytes, "protective" glial stem cells and stromal endependymal cells. *Brain Res Brain Res Rev* 48:220-233.
- Haydon PG (2001) GLIA: listening and talking to the synapse. *Nat Rev Neurosci* 2:185-193.
- He F, Ge W, Martinowich K, Becker-Catania S, Coskun V, Zhu W, Wu H, Castro D, Guillemot F, Fan G, de Vellis J, Sun YE (2005) A positive autoregulatory loop of Jak-STAT signaling controls the onset of astrogliogenesis. *Nat Neurosci* 8:616-625.
- Heasman SJ, Ridley AJ (2008) Mammalian Rho GTPases: new insights into their functions from in vivo studies. *Nat Rev Mol Cell Biol* 9:690-701.
- Heinrich C, Blum R, Tripathi P, Sánchez R, Götz M, Berninger B (in press) Directing Astroglia from the Cerebral Cortex into Subtype Specific Functional Neurons. *PLOS Biology*
- Henry MD, Satz JS, Brakebusch C, Costell M, Gustafsson E, Fassler R, Campbell KP (2001) Distinct roles for dystroglycan, beta1 integrin and perlecan in cell surface laminin organization. *J Cell Sci* 114:1137-1144.
- Herrmann JE, Imura T, Song B, Qi J, Ao Y, Nguyen TK, Korsak RA, Takeda K, Akira S, Sofroniew MV (2008) STAT3 is a critical regulator of astrogliosis and scar formation after spinal cord injury. *J Neurosci* 28:7231-7243.
- Herx LM, Yong VW (2001) Interleukin-1 beta is required for the early evolution of reactive astrogliosis following CNS lesion. *J Neuropathol Exp Neurol* 60:961-971.
- Huang Z, Shimazu K, Woo NH, Zang K, Muller U, Lu B, Reichardt LF (2006) Distinct roles of the beta 1-class integrins at the developing and the mature hippocampal excitatory synapse. *J Neurosci* 26:11208-11219.
- Iadecola C, Nedergaard M (2007) Glial regulation of the cerebral microvasculature. *Nat Neurosci* 10:1369-1376.
- Iandiev I, Pannicke T, Biedermann B, Wiedemann P, Reichenbach A, Bringmann A (2006) Ischemia-reperfusion alters the immunolocalization of glial aquaporins in rat retina. *Neurosci Lett* 408:108-112.
- Ihrie RA, Alvarez-Buylla A (2008) Cells in the astroglial lineage are neural stem cells. *Cell Tissue Res* 331:179-191.
- Irving EA, Bamford M (2002) Role of mitogen- and stress-activated kinases in ischemic injury. *J Cereb Blood Flow Metab* 22:631-647.
- Ito M, Natsume A, Takeuchi H, Shimato S, Ohno M, Wakabayashi T, Yoshida J (2009) Type I interferon inhibits astrocytic gliosis and promotes functional

- recovery after spinal cord injury by deactivation of the MEK/ERK pathway. *J Neurotrauma* 26:41-53.
- Itoh S, Itoh F, Goumans MJ, Ten Dijke P (2000) Signaling of transforming growth factor-beta family members through Smad proteins. *Eur J Biochem* 267:6954-6967.
- Jing R, Wilhelmsson U, Goodwill W, Li L, Pan Y, Pekny M, Skalli O (2007) Synemin is expressed in reactive astrocytes in neurotrauma and interacts differentially with vimentin and GFAP intermediate filament networks. *J Cell Sci* 120:1267-1277.
- Joester A, Faissner A (2001) The structure and function of tenascins in the nervous system. *Matrix Biol* 20:13-22.
- Johansson CB, Momma S, Clarke DL, Risling M, Lendahl U, Frisen J (1999) Identification of a neural stem cell in the adult mammalian central nervous system. *Cell* 96:25-34.
- Kagami S, Kondo S (2004) Beta1-integrins and glomerular injury. *J Med Invest* 51:1-13.
- Kahn MA, Ellison JA, Speight GJ, de Vellis J (1995) CNTF regulation of astrogliosis and the activation of microglia in the developing rat central nervous system. *Brain Res* 685:55-67.
- Kahn MA, Huang CJ, Caruso A, Barresi V, Nazarian R, Condorelli DF, de Vellis J (1997) Ciliary neurotrophic factor activates JAK/Stat signal transduction cascade and induces transcriptional expression of glial fibrillary acidic protein in glial cells. *J Neurochem* 68:1413-1423.
- Kessarlis N, Pringle N, Richardson WD (2008) Specification of CNS glia from neural stem cells in the embryonic neuroepithelium. *Philos Trans R Soc Lond B Biol Sci* 363:71-85.
- Kettenmann H, Ransom BR (2005) *Neuroglia*, 2nd Edition. Oxford: Oxford University Press.
- Kim SU, de Vellis J (2005) Microglia in health and disease. *J Neurosci Res* 81:302-313.
- Klein MA, Moller JC, Jones LL, Bluethmann H, Kreutzberg GW, Raivich G (1997) Impaired neuroglial activation in interleukin-6 deficient mice. *Glia* 19:227-233.
- Kokaia Z, Lindvall O (2003) Neurogenesis after ischaemic brain insults. *Curr Opin Neurobiol* 13:127-132.
- Kordek R, Nerurkar VR, Liberski PP, Isaacson S, Yanagihara R, Gajdusek DC (1996) Heightened expression of tumor necrosis factor alpha, interleukin 1 alpha, and glial fibrillary acidic protein in experimental Creutzfeldt-Jakob disease in mice. *Proc Natl Acad Sci U S A* 93:9754-9758.
- Kreda SM, Seminario-Vidal L, Heusden C, Lazarowski ER (2008) Thrombin-promoted release of UDP-glucose from human astrocytoma cells. *Br J Pharmacol* 153:1528-1537.
- Krueger M, Bechmann I (2010) CNS pericytes: concepts, misconceptions, and a way out. *Glia* 58:1-10.
- Krum JM, Mani N, Rosenstein JM (2008) Roles of the endogenous VEGF receptors flt-1 and flk-1 in astroglial and vascular remodeling after brain injury. *Exp Neurol* 212:108-117.

- Kuhn HG, Winkler J, Kempermann G, Thal LJ, Gage FH (1997) Epidermal growth factor and fibroblast growth factor-2 have different effects on neural progenitors in the adult rat brain. *J Neurosci* 17:5820-5829.
- Lauffenburger DA, Horwitz AF (1996) Cell migration: a physically integrated molecular process. *Cell* 84:359-369.
- Laywell ED, Dorries U, Bartsch U, Faissner A, Schachner M, Steindler DA (1992) Enhanced expression of the developmentally regulated extracellular matrix molecule tenascin following adult brain injury. *Proc Natl Acad Sci U S A* 89:2634-2638.
- Leadbeater WE, Gonzalez AM, Logaras N, Berry M, Turnbull JE, Logan A (2006) Intracellular trafficking in neurones and glia of fibroblast growth factor-2, fibroblast growth factor receptor 1 and heparan sulphate proteoglycans in the injured adult rat cerebral cortex. *J Neurochem* 96:1189-1200.
- Lecca D, Ceruti S (2008) Uracil nucleotides: from metabolic intermediates to neuroprotection and neuroinflammation. *Biochem Pharmacol* 75:1869-1881.
- Lee HS, Han J, Bai HJ, Kim KW (2009) Brain angiogenesis in developmental and pathological processes: regulation, molecular and cellular communication at the neurovascular interface. *FEBS J* 276:4622-4635.
- Lee HS, Nishanian TG, Mood K, Bong YS, Daar IO (2008) EphrinB1 controls cell-cell junctions through the Par polarity complex. *Nat Cell Biol* 10:979-986.
- Lenhossék M (1893) *Der feinere Bau des Nervensystems im Lichte neuester Forschung*. Berlin: Fischer's Medicinische Buchhandlung H. Kornfeld.
- Levison SW, Goldman JE (1993) Both oligodendrocytes and astrocytes develop from progenitors in the subventricular zone of postnatal rat forebrain. *Neuron* 10:201-212.
- Levison SW, Chuang C, Abramson BJ, Goldman JE (1993) The migrational patterns and developmental fates of glial precursors in the rat subventricular zone are temporally regulated. *Development* 119:611-622.
- Levison SW, Jiang FJ, Stoltzfus OK, Ducceschi MH (2000) IL-6-type cytokines enhance epidermal growth factor-stimulated astrocyte proliferation. *Glia* 32:328-337.
- Levy DE, Darnell JE, Jr. (2002) Stats: transcriptional control and biological impact. *Nat Rev Mol Cell Biol* 3:651-662.
- Lin HW, Basu A, Druckman C, Cicchese M, Krady JK, Levison SW (2006) Astroglialosis is delayed in type 1 interleukin-1 receptor-null mice following a penetrating brain injury. *J Neuroinflammation* 3:15.
- Lindvall O, Kokaia Z (2004) Recovery and rehabilitation in stroke: stem cells. *Stroke* 35:2691-2694.
- Lindvall O, Kokaia Z, Martinez-Serrano A (2004) Stem cell therapy for human neurodegenerative disorders-how to make it work. *Nat Med* 10 Suppl:S42-50.
- Liu B, Neufeld AH (2004) Activation of epidermal growth factor receptor causes astrocytes to form cribriform structures. *Glia* 46:153-168.

- Liu B, Neufeld AH (2007) Activation of epidermal growth factor receptors in astrocytes: from development to neural injury. *J Neurosci Res* 85:3523-3529.
- Liu B, Chen H, Johns TG, Neufeld AH (2006) Epidermal growth factor receptor activation: an upstream signal for transition of quiescent astrocytes into reactive astrocytes after neural injury. *J Neurosci* 26:7532-7540.
- Lledo PM, Alonso M, Grubb MS (2006) Adult neurogenesis and functional plasticity in neuronal circuits. *Nat Rev Neurosci* 7:179-193.
- Ma XM, Blenis J (2009) Molecular mechanisms of mTOR-mediated translational control. *Nat Rev Mol Cell Biol* 10:307-318.
- Machon O, van den Bout CJ, Backman M, Kemler R, Krauss S (2003) Role of beta-catenin in the developing cortical and hippocampal neuroepithelium. *Neuroscience* 122:129-143.
- Macklis JD (1993) Transplanted neocortical neurons migrate selectively into regions of neuronal degeneration produced by chromophore-targeted laser photolysis. *J Neurosci* 13:3848-3863.
- Madison RD, Macklis JD (1993) Noninvasively induced degeneration of neocortical pyramidal neurons in vivo: selective targeting by laser activation of retrogradely transported photolytic chromophore. *Exp Neurol* 121:153-159.
- Malatesta P, Hartfuss E, Gotz M (2000) Isolation of radial glial cells by fluorescent-activated cell sorting reveals a neuronal lineage. *Development* 127:5253-5263.
- Malatesta P, Hack MA, Hartfuss E, Kettenmann H, Klinkert W, Kirchhoff F, Gotz M (2003) Neuronal or glial progeny: regional differences in radial glia fate. *Neuron* 37:751-764.
- Massouh M, Saghatelian A De-routing neuronal precursors in the adult brain to sites of injury: role of the vasculature. *Neuropharmacology* 58:877-883.
- Mathewson AJ, Berry M (1985) Observations on the astrocyte response to a cerebral stab wound in adult rats. *Brain Res* 327:61-69.
- McKeon RJ, Jurynek MJ, Buck CR (1999) The chondroitin sulfate proteoglycans neurocan and phosphacan are expressed by reactive astrocytes in the chronic CNS glial scar. *J Neurosci* 19:10778-10788.
- McMahon SS, McDermott KW (2007) Developmental potential of radial glia investigated by transplantation into the developing rat ventricular system in utero. *Exp Neurol* 203:128-136.
- Melani A, Turchi D, Vannucchi MG, Cipriani S, Gianfriddo M, Pedata F (2005) ATP extracellular concentrations are increased in the rat striatum during in vivo ischemia. *Neurochem Int* 47:442-448.
- Mirzadeh Z, Merkle FT, Soriano-Navarro M, Garcia-Verdugo JM, Alvarez-Buylla A (2008) Neural stem cells confer unique pinwheel architecture to the ventricular surface in neurogenic regions of the adult brain. *Cell Stem Cell* 3:265-278.
- Miyazono K (2000) Positive and negative regulation of TGF-beta signaling. *J Cell Sci* 113 ( Pt 7):1101-1109.
- Moore SA, Saito F, Chen J, Michele DE, Henry MD, Messing A, Cohn RD, Ross-Barta SE, Westra S, Williamson RA, Hoshi T, Campbell KP (2002)

- Deletion of brain dystroglycan recapitulates aspects of congenital muscular dystrophy. *Nature* 418:422-425.
- Mori T, Buffo A, Gotz M (2005) The novel roles of glial cells revisited: the contribution of radial glia and astrocytes to neurogenesis. *Curr Top Dev Biol* 69:67-99.
- Mori T, Tanaka K, Buffo A, Wurst W, Kuhn R, Gotz M (2006) Inducible gene deletion in astroglia and radial glia--a valuable tool for functional and lineage analysis. *Glia* 54:21-34.
- Myer DJ, Gurkoff GG, Lee SM, Hovda DA, Sofroniew MV (2006) Essential protective roles of reactive astrocytes in traumatic brain injury. *Brain* 129:2761-2772.
- Nakamura T, Colbert MC, Robbins J (2006) Neural crest cells retain multipotential characteristics in the developing valves and label the cardiac conduction system. *Circ Res* 98:1547-1554.
- Namihira M, Nakashima K, Taga T (2004) Developmental stage dependent regulation of DNA methylation and chromatin modification in a immature astrocyte specific gene promoter. *FEBS Lett* 572:184-188.
- Neary JT, Kang Y (2005) Signaling from P2 nucleotide receptors to protein kinase cascades induced by CNS injury: implications for reactive gliosis and neurodegeneration. *Mol Neurobiol* 31:95-103.
- Neary JT, Kang Y, Shi YF (2004) Signaling from nucleotide receptors to protein kinase cascades in astrocytes. *Neurochem Res* 29:2037-2042.
- Neary JT, Baker L, Jorgensen SL, Norenberg MD (1994) Extracellular ATP induces stellation and increases glial fibrillary acidic protein content and DNA synthesis in primary astrocyte cultures. *Acta Neuropathol* 87:8-13.
- Neary JT, Shi YF, Kang Y, Tran MD (2008) Opposing effects of P2X(7) and P2Y purine/pyrimidine-preferring receptors on proliferation of astrocytes induced by fibroblast growth factor-2: implications for CNS development, injury, and repair. *J Neurosci Res* 86:3096-3105.
- Nedergaard M, Ransom B, Goldman SA (2003) New roles for astrocytes: redefining the functional architecture of the brain. *Trends Neurosci* 26:523-530.
- Nelson WJ (2003) Adaptation of core mechanisms to generate cell polarity. *Nature* 422:766-774.
- Nesic O, Lee J, Ye Z, Unabia GC, Rafati D, Hulsebosch CE, Perez-Polo JR (2006) Acute and chronic changes in aquaporin 4 expression after spinal cord injury. *Neuroscience* 143:779-792.
- Newman EA (2003) New roles for astrocytes: regulation of synaptic transmission. *Trends Neurosci* 26:536-542.
- Nico B, Frigeri A, Nicchia GP, Quondamatteo F, Herken R, Errede M, Ribatti D, Svelto M, Roncali L (2001) Role of aquaporin-4 water channel in the development and integrity of the blood-brain barrier. *J Cell Sci* 114:1297-1307.
- Nie XJ, Olsson Y (1996) Endothelin peptides in brain diseases. *Rev Neurosci* 7:177-186.
- Nieto-Sampedro M (1988) Astrocyte mitogen inhibitor related to epidermal growth factor receptor. *Science* 240:1784-1786.

- Nieto-Sampedro M, Gomez-Pinilla F, Knauer DJ, Broderick JT (1988) Epidermal growth factor receptor immunoreactivity in rat brain astrocytes. Response to injury. *Neurosci Lett* 91:276-282.
- Nimmerjahn A, Kirchhoff F, Helmchen F (2005) Resting microglial cells are highly dynamic surveillants of brain parenchyma in vivo. *Science* 308:1314-1318.
- Noell S, Fallier-Becker P, Deutsch U, Mack AF, Wolburg H (2009) Agrin defines polarized distribution of orthogonal arrays of particles in astrocytes. *Cell Tissue Res* 337:185-195.
- Nolte C, Matyash M, Pivneva T, Schipke CG, Ohlemeyer C, Hanisch UK, Kirchhoff F, Kettenmann H (2001) GFAP promoter-controlled EGFP-expressing transgenic mice: a tool to visualize astrocytes and astrogliosis in living brain tissue. *Glia* 33:72-86.
- Novak A, Guo C, Yang W, Nagy A, Lobe CG (2000) Z/EG, a double reporter mouse line that expresses enhanced green fluorescent protein upon Cre-mediated excision. *Genesis* 28:147-155.
- Oberheim NA, Wang X, Goldman S, Nedergaard M (2006) Astrocytic complexity distinguishes the human brain. *Trends Neurosci* 29:547-553.
- Oberheim NA, Tian GF, Han X, Peng W, Takano T, Ransom B, Nedergaard M (2008) Loss of astrocytic domain organization in the epileptic brain. *J Neurosci* 28:3264-3276.
- Oberheim NA, Takano T, Han X, He W, Lin JH, Wang F, Xu Q, Wyatt JD, Pilcher W, Ojemann JG, Ransom BR, Goldman SA, Nedergaard M (2009) Uniquely hominid features of adult human astrocytes. *J Neurosci* 29:3276-3287.
- Oh Y (1997) Ion channels in neuroglial cells. *Kaohsiung J Med Sci* 13:1-9.
- Ohab JJ, Fleming S, Blesch A, Carmichael ST (2006) A neurovascular niche for neurogenesis after stroke. *J Neurosci* 26:13007-13016.
- Ojeda SR, Ma YJ, Lee BJ, Prevot V (2000) Glia-to-neuron signaling and the neuroendocrine control of female puberty. *Recent Prog Horm Res* 55:197-223; discussion 223-194.
- Okada S, Nakamura M, Mikami Y, Shimazaki T, Mihara M, Ohsugi Y, Iwamoto Y, Yoshizaki K, Kishimoto T, Toyama Y, Okano H (2004) Blockade of interleukin-6 receptor suppresses reactive astrogliosis and ameliorates functional recovery in experimental spinal cord injury. *J Neurosci Res* 76:265-276.
- Okada S, Nakamura M, Katoh H, Miyao T, Shimazaki T, Ishii K, Yamane J, Yoshimura A, Iwamoto Y, Toyama Y, Okano H (2006) Conditional ablation of Stat3 or Socs3 discloses a dual role for reactive astrocytes after spinal cord injury. *Nat Med* 12:829-834.
- Pearson G, Robinson F, Beers Gibson T, Xu BE, Karandikar M, Berman K, Cobb MH (2001) Mitogen-activated protein (MAP) kinase pathways: regulation and physiological functions. *Endocr Rev* 22:153-183.
- Pegtel DM, Ellenbroek SI, Mertens AE, van der Kammen RA, de Rooij J, Collard JG (2007) The Par-Tiam1 complex controls persistent migration by stabilizing microtubule-dependent front-rear polarity. *Curr Biol* 17:1623-1634.

- Pekny M, Wilhelmsson U, Bogestal YR, Pekna M (2007) The role of astrocytes and complement system in neural plasticity. *Int Rev Neurobiol* 82:95-111.
- Pekny M, Leveen P, Pekna M, Eliasson C, Berthold CH, Westermark B, Betsholtz C (1995) Mice lacking glial fibrillary acidic protein display astrocytes devoid of intermediate filaments but develop and reproduce normally. *EMBO J* 14:1590-1598.
- Peng W, Cotrina ML, Han X, Yu H, Bekar L, Blum L, Takano T, Tian GF, Goldman SA, Nedergaard M (2009) Systemic administration of an antagonist of the ATP-sensitive receptor P2X7 improves recovery after spinal cord injury. *Proc Natl Acad Sci U S A* 106:12489-12493.
- Peters CM, Rogers SD, Pomonis JD, Egnaczyk GF, Keyser CP, Schmidt JA, Ghilardi JR, Maggio JE, Mantyh PW (2003) Endothelin receptor expression in the normal and injured spinal cord: potential involvement in injury-induced ischemia and gliosis. *Exp Neurol* 180:1-13.
- Pfeifer A, Brandon EP, Kootstra N, Gage FH, Verma IM (2001) Delivery of the Cre recombinase by a self-deleting lentiviral vector: efficient gene targeting in vivo. *Proc Natl Acad Sci U S A* 98:11450-11455.
- Picco V, Hudson C, Yasuo H (2007) Ephrin-Eph signalling drives the asymmetric division of notochord/neural precursors in *Ciona* embryos. *Development* 134:1491-1497.
- Pinto L, Gotz M (2007) Radial glial cell heterogeneity--the source of diverse progeny in the CNS. *Prog Neurobiol* 83:2-23.
- Pinto L, Mader MT, Irmeler M, Gentilini M, Santoni F, Drechsel D, Blum R, Stahl R, Bulfone A, Malatesta P, Beckers J, Gotz M (2008) Prospective isolation of functionally distinct radial glial subtypes--lineage and transcriptome analysis. *Mol Cell Neurosci* 38:15-42.
- Potocnik AJ, Brakebusch C, Fassler R (2000) Fetal and adult hematopoietic stem cells require beta1 integrin function for colonizing fetal liver, spleen, and bone marrow. *Immunity* 12:653-663.
- Puklin-Faucher E, Sheetz MP (2009) The mechanical integrin cycle. *J Cell Sci* 122:179-186.
- Rabchevsky AG, Weinitz JM, Coulpier M, Fages C, Tinel M, Junier MP (1998) A role for transforming growth factor alpha as an inducer of astrogliosis. *J Neurosci* 18:10541-10552.
- Reichardt LF, Tomaselli KJ (1991) Extracellular matrix molecules and their receptors: functions in neural development. *Annu Rev Neurosci* 14:531-570.
- Reuss B, Dono R, Unsicker K (2003) Functions of fibroblast growth factor (FGF)-2 and FGF-5 in astroglial differentiation and blood-brain barrier permeability: evidence from mouse mutants. *J Neurosci* 23:6404-6412.
- Reynolds BA, Weiss S (1992) Generation of neurons and astrocytes from isolated cells of the adult mammalian central nervous system. *Science* 255:1707-1710.
- Ridley AJ, Schwartz MA, Burridge K, Firtel RA, Ginsberg MH, Borisy G, Parsons JT, Horwitz AR (2003) Cell migration: integrating signals from front to back. *Science* 302:1704-1709.
- Ritchie JM (1992) Voltage-gated ion channels in Schwann cells and glia. *Trends Neurosci* 15:345-351.

- Robel S, Mori T, Zoubaa S, Schlegel J, Sirko S, Faissner A, Goebbels S, Dimou L, Gotz M (2009) Conditional deletion of beta1-integrin in astroglia causes partial reactive gliosis. *Glia* 57:1630-1647.
- Rogers SD, Peters CM, Pomonis JD, Hagiwara H, Ghilardi JR, Mantyh PW (2003) Endothelin B receptors are expressed by astrocytes and regulate astrocyte hypertrophy in the normal and injured CNS. *Glia* 41:180-190.
- Rosenberg GA (2009) Matrix metalloproteinases and their multiple roles in neurodegenerative diseases. *Lancet Neurol* 8:205-216.
- Saadoun S, Tait MJ, Reza A, Davies DC, Bell BA, Verkman AS, Papadopoulos MC (2009) AQP4 gene deletion in mice does not alter blood-brain barrier integrity or brain morphology. *Neuroscience* 161:764-772.
- Sabo JK, Kilpatrick TJ, Cate HS (2009) Effects of bone morphogenic proteins on neural precursor cells and regulation during central nervous system injury. *Neurosignals* 17:255-264.
- Saghatelian A (2009) Role of blood vessels in the neuronal migration. *Semin Cell Dev Biol* 20:744-750.
- Sahni V, Mukhopadhyay A, Tysseling V, Hebert A, Birch D, McGuire TL, Stupp SI, Kessler JA (2010) BMPR1a and BMPR1b signaling exert opposing effects on gliosis after spinal cord injury. *J Neurosci* 30:1839-1855.
- Sawamoto K, Wichterle H, Gonzalez-Perez O, Cholfin JA, Yamada M, Spassky N, Murcia NS, Garcia-Verdugo JM, Marin O, Rubenstein JL, Tessier-Lavigne M, Okano H, Alvarez-Buylla A (2006) New neurons follow the flow of cerebrospinal fluid in the adult brain. *Science* 311:629-632.
- Schinelli S (2006) Pharmacology and physiopathology of the brain endothelin system: an overview. *Curr Med Chem* 13:627-638.
- Schinelli S, Zanassi P, Paolillo M, Wang H, Feliciello A, Gallo V (2001) Stimulation of endothelin B receptors in astrocytes induces cAMP response element-binding protein phosphorylation and c-fos expression via multiple mitogen-activated protein kinase signaling pathways. *J Neurosci* 21:8842-8853.
- Schwab MH, Druffel-Augustin S, Gass P, Jung M, Klugmann M, Bartholomae A, Rossner MJ, Nave KA (1998) Neuronal basic helix-loop-helix proteins (NEX, neuroD, NDRF): spatiotemporal expression and targeted disruption of the NEX gene in transgenic mice. *J Neurosci* 18:1408-1418.
- Schwartz MA, Shattil SJ (2000) Signaling networks linking integrins and rho family GTPases. *Trends Biochem Sci* 25:388-391.
- Setoguchi T, Yone K, Matsuoka E, Takenouchi H, Nakashima K, Sakou T, Komiya S, Izumo S (2001) Traumatic injury-induced BMP7 expression in the adult rat spinal cord. *Brain Res* 921:219-225.
- Shapiro SD (1998) Matrix metalloproteinase degradation of extracellular matrix: biological consequences. *Curr Opin Cell Biol* 10:602-608.
- Sharif A, Prevot V, Renault-Mihara F, Allet C, Studler JM, Canton B, Chneiweiss H, Junier MP (2006) Transforming growth factor alpha acts as a gliotrophin for mouse and human astrocytes. *Oncogene* 25:4076-4085.
- Shen Q, Wang Y, Kokovay E, Lin G, Chuang SM, Goderie SK, Roysam B, Temple S (2008) Adult SVZ stem cells lie in a vascular niche: a

- quantitative analysis of niche cell-cell interactions. *Cell Stem Cell* 3:289-300.
- Shin JJ, Fricker-Gates RA, Perez FA, Leavitt BR, Zurakowski D, Macklis JD (2000) Transplanted neuroblasts differentiate appropriately into projection neurons with correct neurotransmitter and receptor phenotype in neocortex undergoing targeted projection neuron degeneration. *J Neurosci* 20:7404-7416.
- Shukla V, Zimmermann H, Wang L, Kettenmann H, Raab S, Hammer K, Sevigny J, Robson SC, Braun N (2005) Functional expression of the ecto-ATPase NTPDase2 and of nucleotide receptors by neuronal progenitor cells in the adult murine hippocampus. *J Neurosci Res* 80:600-610.
- Sibilia M, Steinbach JP, Stingl L, Aguzzi A, Wagner EF (1998) A strain-independent postnatal neurodegeneration in mice lacking the EGF receptor. *EMBO J* 17:719-731.
- Sievers J, Pehlemann FW, Gude S, Berry M (1994a) A time course study of the alterations in the development of the hamster cerebellar cortex after destruction of the overlying meningeal cells with 6-hydroxydopamine on the day of birth. *J Neurocytol* 23:117-134.
- Sievers J, Pehlemann FW, Gude S, Berry M (1994b) Meningeal cells organize the superficial glia limitans of the cerebellum and produce components of both the interstitial matrix and the basement membrane. *J Neurocytol* 23:135-149.
- Sirko S, von Holst A, Wizenmann A, Gotz M, Faissner A (2007) Chondroitin sulfate glycosaminoglycans control proliferation, radial glia cell differentiation and neurogenesis in neural stem/progenitor cells. *Development* 134:2727-2738.
- Sirko S, von Holst A, Weber A, Wizenmann A, Theocharidis U, Gotz M, Faissner A (2010) Chondroitin Sulfates are Required for FGF-2-dependent Proliferation and Maintenance in Neural Stem Cells and for EGF-dependent Migration of Their Progeny. *Stem Cells*.
- Sirko S, Neitz A, Mittmann T, Horvat-Brocker A, von Holst A, Eysel UT, Faissner A (2009) Focal laser-lesions activate an endogenous population of neural stem/progenitor cells in the adult visual cortex. *Brain* 132:2252-2264.
- Sixt M, Engelhardt B, Pausch F, Hallmann R, Wendler O, Sorokin LM (2001) Endothelial cell laminin isoforms, laminins 8 and 10, play decisive roles in T cell recruitment across the blood-brain barrier in experimental autoimmune encephalomyelitis. *J Cell Biol* 153:933-946.
- Smith GM, Strunz C (2005) Growth factor and cytokine regulation of chondroitin sulfate proteoglycans by astrocytes. *Glia* 52:209-218.
- Smith KM, Ohkubo Y, Maragnoli ME, Rasin MR, Schwartz ML, Sestan N, Vaccarino FM (2006) Midline radial glia translocation and corpus callosum formation require FGF signaling. *Nat Neurosci* 9:787-797.
- Snapyan M, Lemasson M, Brill MS, Blais M, Massouh M, Ninkovic J, Gravel C, Berthod F, Gotz M, Barker PA, Parent A, Saghatelian A (2009) Vasculature guides migrating neuronal precursors in the adult

- mammalian forebrain via brain-derived neurotrophic factor signaling. *J Neurosci* 29:4172-4188.
- Sofroniew MV (2009) Molecular dissection of reactive astrogliosis and glial scar formation. *Trends Neurosci* 32:638-647.
- Sofroniew MV, Vinters HV Astrocytes: biology and pathology. *Acta Neuropathol* 119:7-35.
- Somjen GG (1988) Nervenkitz: notes on the history of the concept of neuroglia. *Glia* 1:2-9.
- Sriram K, Benkovic SA, Hebert MA, Miller DB, O'Callaghan JP (2004) Induction of gp130-related cytokines and activation of JAK2/STAT3 pathway in astrocytes precedes up-regulation of glial fibrillary acidic protein in the 1-methyl-4-phenyl-1,2,3,6-tetrahydropyridine model of neurodegeneration: key signaling pathway for astrogliosis in vivo? *J Biol Chem* 279:19936-19947.
- Stahl N, Boulton TG, Farruggella T, Ip NY, Davis S, Witthuhn BA, Quelle FW, Silvennoinen O, Barbieri G, Pellegrini S, et al. (1994) Association and activation of Jak-Tyk kinases by CNTF-LIF-OSM-IL-6 beta receptor components. *Science* 263:92-95.
- Stupack DG (2005) Integrins as a distinct subtype of dependence receptors. *Cell Death Differ* 12:1021-1030.
- Sun D, Bullock R, Altememi N, Zhou Z, Hagood S, Rolfe A, McGinn M, Hamm RJ (2010) The effect of epidermal growth factor in the injured brain following trauma in rats. *J Neurotrauma*.
- Sundaram MV (2006) RTK/Ras/MAPK signaling. *WormBook*:1-19.
- Swartz KR, Liu F, Sewell D, Schochet T, Campbell I, Sandor M, Fabry Z (2001) Interleukin-6 promotes post-traumatic healing in the central nervous system. *Brain Res* 896:86-95.
- Taga T, Kishimoto T (1997) Gp130 and the interleukin-6 family of cytokines. *Annu Rev Immunol* 15:797-819.
- Takada Y, Ye X, Simon S (2007) The integrins. *Genome Biol* 8:215.
- Tavazoie M, Van der Veken L, Silva-Vargas V, Louissaint M, Colonna L, Zaidi B, Garcia-Verdugo JM, Doetsch F (2008) A specialized vascular niche for adult neural stem cells. *Cell Stem Cell* 3:279-288.
- Tran KT, Griffith L, Wells A (2004) Extracellular matrix signaling through growth factor receptors during wound healing. *Wound Repair Regen* 12:262-268.
- Tripathi P, Beckervordersandforth-Bonk R, Ninkovic J, Bayam E, Lepier A, Kirchhoff F, Hirrlinger J, Haslinger A, Lie D, Beckers J, Irmeler M, Gotz M (2010) The transcriptome of prospectively isolated adult neural stem cells reveals unique features as well as similarities to astrocytes and ependymal cells. submitted.
- Tripathi RB, McTigue DM (2008) Chronically increased ciliary neurotrophic factor and fibroblast growth factor-2 expression after spinal contusion in rats. *J Comp Neurol* 510:129-144.
- Ulbricht E, Pannicke T, Hollborn M, Raap M, Goczalik I, Iandiev I, Hartig W, Uhlmann S, Wiedemann P, Reichenbach A, Bringmann A, Francke M (2008) Proliferative gliosis causes mislocation and inactivation of

- inwardly rectifying K(+) (Kir) channels in rabbit retinal glial cells. *Exp Eye Res* 86:305-313.
- Vaccarino FM, Ganat Y, Zhang Y, Zheng W (2001) Stem cells in neurodevelopment and plasticity. *Neuropsychopharmacology* 25:805-815.
- Valverde F, Lopez-Mascaraque L (1991) Neuroglial arrangements in the olfactory glomeruli of the hedgehog. *J Comp Neurol* 307:658-674.
- Virchow R (1856) *Gesammelte Abhandlungen zur wissenschaftlichen Medizin*. Frankfurt: Verlag von Meidinger Sohn & Comp.
- Virchow R (1858) *Die Cellular pathologie in ihrer Begründung auf physiologische und pathologische Gewebelehre*. Berlin: Verlag von August Hirschwald.
- Vitellaro-Zuccarello L, Mazzetti S, Madaschi L, Bosisio P, Fontana E, Gorio A, De Biasi S (2008) Chronic erythropoietin-mediated effects on the expression of astrocyte markers in a rat model of contusive spinal cord injury. *Neuroscience* 151:452-466.
- Vivien D, Ali C (2006) Transforming growth factor-beta signalling in brain disorders. *Cytokine Growth Factor Rev* 17:121-128.
- Volterra A, Magistretti PJ, Haydon PG (2002) *The tripartite synapse : glia in synaptic transmission*. Oxford: Oxford University Press.
- Wang DD, Bordey A (2008) The astrocyte odyssey. *Prog Neurobiol* 86:342-367.
- Wang Y, Moges H, Bharucha Y, Symes A (2007) Smad3 null mice display more rapid wound closure and reduced scar formation after a stab wound to the cerebral cortex. *Exp Neurol* 203:168-184.
- Washburn KB, Neary JT (2006) P2 purinergic receptors signal to STAT3 in astrocytes: Difference in STAT3 responses to P2Y and P2X receptor activation. *Neuroscience* 142:411-423.
- Weickert CS, Blum M (1995) Striatal TGF-alpha: postnatal developmental expression and evidence for a role in the proliferation of subependymal cells. *Brain Res Dev Brain Res* 86:203-216.
- White RE, Yin FQ, Jakeman LB (2008) TGF-alpha increases astrocyte invasion and promotes axonal growth into the lesion following spinal cord injury in mice. *Exp Neurol*.
- Williamson RA, Henry MD, Daniels KJ, Hrstka RF, Lee JC, Sunada Y, Ibraghimov-Beskrovnaya O, Campbell KP (1997) Dystroglycan is essential for early embryonic development: disruption of Reichert's membrane in Dag1-null mice. *Hum Mol Genet* 6:831-841.
- Wolburg-Buchholz K, Mack AF, Steiner E, Pfeiffer F, Engelhardt B, Wolburg H (2009) Loss of astrocyte polarity marks blood-brain barrier impairment during experimental autoimmune encephalomyelitis. *Acta Neuropathol* 118:219-233.
- Wolburg H, Noell S, Mack A, Wolburg-Buchholz K, Fallier-Becker P (2009a) Brain endothelial cells and the glio-vascular complex. *Cell Tissue Res* 335:75-96.
- Wolburg H, Noell S, Wolburg-Buchholz K, Mack A, Fallier-Becker P (2009b) Agrin, aquaporin-4, and astrocyte polarity as an important feature of the blood-brain barrier. *Neuroscientist* 15:180-193.

- Wolburg H, Neuhaus J, Kniesel U, Krauss B, Schmid EM, Ocalan M, Farrell C, Risau W (1994) Modulation of tight junction structure in blood-brain barrier endothelial cells. Effects of tissue culture, second messengers and cocultured astrocytes. *J Cell Sci* 107 ( Pt 5):1347-1357.
- Wolburg H, Wolburg-Buchholz K, Kraus J, Rascher-Eggstein G, Liebner S, Hamm S, Duffner F, Grote EH, Risau W, Engelhardt B (2003) Localization of claudin-3 in tight junctions of the blood-brain barrier is selectively lost during experimental autoimmune encephalomyelitis and human glioblastoma multiforme. *Acta Neuropathol* 105:586-592.
- Wu SX, Goebbels S, Nakamura K, Nakamura K, Kometani K, Minato N, Kaneko T, Nave KA, Tamamaki N (2005) Pyramidal neurons of upper cortical layers generated by NEX-positive progenitor cells in the subventricular zone. *Proc Natl Acad Sci U S A* 102:17172-17177.
- Wu W, Wong K, Chen J, Jiang Z, Dupuis S, Wu JY, Rao Y (1999) Directional guidance of neuronal migration in the olfactory system by the protein Slit. *Nature* 400:331-336.
- Wu X, Quondamatteo F, Lefever T, Czuchra A, Meyer H, Chrostek A, Paus R, Langbein L, Brakebusch C (2006) Cdc42 controls progenitor cell differentiation and beta-catenin turnover in skin. *Genes Dev* 20:571-585.
- Yang L, Wang L, Kalfa TA, Cancelas JA, Shang X, Pushkaran S, Mo J, Williams DA, Zheng Y (2007) Cdc42 critically regulates the balance between myelopoiesis and erythropoiesis. *Blood* 110:3853-3861.
- Yong VW, Krekoski CA, Forsyth PA, Bell R, Edwards DR (1998) Matrix metalloproteinases and diseases of the CNS. *Trends Neurosci* 21:75-80.
- Yoshimura S, Teramoto T, Whalen MJ, Irizarry MC, Takagi Y, Qiu J, Harada J, Waeber C, Breakefield XO, Moskowitz MA (2003) FGF-2 regulates neurogenesis and degeneration in the dentate gyrus after traumatic brain injury in mice. *J Clin Invest* 112:1202-1210.
- Zhang RL, Zhang ZG, Zhang L, Chopp M (2001) Proliferation and differentiation of progenitor cells in the cortex and the subventricular zone in the adult rat after focal cerebral ischemia. *Neuroscience* 105:33-41.
- Zhang Z, Trautmann K, Artelt M, Burnet M, Schluesener HJ (2006) Bone morphogenetic protein-6 is expressed early by activated astrocytes in lesions of rat traumatic brain injury. *Neuroscience* 138:47-53.
- Zhuo L, Theis M, Alvarez-Maya I, Brenner M, Willecke K, Messing A (2001) hGFAP-cre transgenic mice for manipulation of glial and neuronal function in vivo. *Genesis* 31:85-94.

## 10 Acknowledgments

First and foremost, I would like to thank Magdalena Götz for her continuous support and advice during my time in her laboratory. Her enthusiasm and passion for science have been very inspiring. She taught me that science is about exploring ideas, asking questions and discussing data besides working at the bench. She showed me how to approach a research problem and the need to be persistent to accomplish any goal. She has been a great mentor!

Special thanks go to Leda, who has been a priceless colleague and friend. She was always there to discuss scientific or other issues and to listen to my complaints and frustrations during the dissertation writing odyssey. I highly appreciated her advice and encouragement.

I like to thank Gabi Jäger, Simone Bauer, Rebecca Krebs, Andrea Steiner-Mezzadri, Tatiana Simon-Ebert and Angelika Waiser for sharing their expertise with me and for excellent technical assistance.

I am grateful to our animal caretakers, especially to Susi and Petra, who helped me to manage my various mouse lines.

Let me also say 'thank you' to Gwen for the fun we had during working hours and beyond, Lana for preventing mental breakdowns, for insightful discussions and the reassurance during writing this thesis, Sophia for taking over the exciting imaging projects I could not further pursue due to a lack of time; thanks also to the folks in our lab for interesting discussions, the exchange of experience and for creating a pleasant lab environment.

Last, but not least, I like to thank my family: Yan, for all the joy we share, my sister, Jenny, for being there for me and for believing in me, and my parents, Renée and Jan, for giving me a carefree childhood, for initially interesting me in nature and science, and, above all, for their unconditional support, for having confidence in me, when I doubted myself and for the encouragement to pursue my interests.



## 11 Curriculum vitae

Name: Stefanie Robel

Address: Schillerstraße 30  
80336 Munich  
Germany

Telephone: 0049 – 89 – 218075580  
Email: [stefanie.robel@lrz.uni-muenchen.de](mailto:stefanie.robel@lrz.uni-muenchen.de)

Date of birth: May 10, 1981  
Nationality: German

### SCIENTIFIC CAREER

Since May 2006

PhD thesis: “Diverse Functions of Astroglial Cells – The Role of Molecular Pathways Regulating Polarity”

Supervisor: Prof. Dr. Magdalena Götz

Institute for Stem Cell Research, Helmholtz Zentrum München and

Institute for Physiological Genomics, Ludwig-Maximilians University, Munich

April 2005 – April 2006

Research assistant in the Department of Psychiatry, Molecular and Clinical Neurobiology, Ludwig-Maximilians University, Munich

### EDUCATION

March 2005

Diploma degree in Biology at the Humboldt University Berlin (grade 1.6)

April 2004 – March 2005

Diploma thesis: „Generation and Characterisation of Transgenic *Drosophila melanogaster* Lines for the

Gene *Optic Atrophy 1 (OPA1)* Mutated in Human  
Autosomal Dominant Optic Atrophy“

Supervisor: Dr. Christiane Alexander

Referees: Prof. Dr. Gerd Kempermann (grade 1.3)

Prof. Dr. Harald Saumweber (grade 1.7)

Max Delbrück Center for Molecular Medicine, Berlin

October 2002 – February 2004 Undergraduate studies in Biology, Specialization:  
Molecular Biology and Genetics; Humboldt University  
Berlin

October 2000 – September 2002 Undergraduate studies in Biology, Potsdam University

September 1993 - July 2000 Upper Secondary School, Berlin, Germany

## MEETINGS

September 2009 EdU Glia Kick off Meeting, Leipzig

September 2009 9<sup>th</sup> European Meeting on Glial Cells in Health and  
Disease, Paris, poster presentation

March 2009 Gordon Research Conference Glial Biology:  
Functional Interactions among Glia & Neurons,  
Ventura, poster presentation

June 2008 Gordon Research Conference Basement Membranes,  
New England, poster presentation

September 2007 8<sup>th</sup> European Glial Cell Meeting: Glial Cells in Health  
and Disease, London, poster presentation

September 2007 17<sup>th</sup> Neuro DoWo (Workshop for PhD students in  
Neuroscience), Konstanz, poster presentation

- October 2005                      24<sup>th</sup> Symposium of the AGNP (Consortium for Neuropsychopharmacology and Pharmacopsychiatry), Munich, poster presentation
- April 2005                          13<sup>th</sup> Conference of the Association of European Psychiatrists: "European Psychiatry: The interface between biological and social factors", Munich

### STIPENDS

- September 2009                      GLIA stipend to cover travel expenses to the 9<sup>th</sup> European Meeting on Glial Cells in Health and Disease, Paris

### COURSES / TRAININGS

- September 2007                      Training on care and use of laboratory animals, Federation of European Laboratory Animal Science Association, Category C, certified by the Society of Laboratory Animal Science
- December 2005                      Training for project leaders and representatives of biological safety in accordance with § 15 para 4 sentence 1 GenTSV (German Genetic Engineering Act)

### PUBLICATIONS

Benninghoff J., Gritti A., Rizzi M., LaMorte G., Schloesser J., Schmitt A, **Robel S**, Genius J, Moessner R, Riederer P, Manji HK., Grunze H, Rujescu D, Moeller HJ, Lesch KP, Vescovi AL. "Serotonin Depletion Hampers Survival and Proliferation in Neurospheres Derived from Adult Neural Stem Cells." *Neuropsychopharmacology*, 2010 Mar; 35(4): 893-903

**Robel S.**, Tetsuji M., Zoubaa S., Schlegel J., Sirko S., Faissner A., Goebbels S., Dimou L., and Götz M. (2009). "Conditional Deletion of  $\beta$ 1-Integrin in Astroglia Causes Partial Reactive Gliosis." *GLIA*, 57: 1630-1647